



University
of Glasgow

France, Liam John (2011) *Characterisation of carbonaceous species formed over mordenite*. PhD thesis.

<http://theses.gla.ac.uk/2921/>

Copyright and moral rights for this thesis are retained by the author

A copy can be downloaded for personal non-commercial research or study, without prior permission or charge

This thesis cannot be reproduced or quoted extensively from without first obtaining permission in writing from the Author

The content must not be changed in any way or sold commercially in any format or medium without the formal permission of the Author

When referring to this work, full bibliographic details including the author, title, awarding institution and date of the thesis must be given

Characterisation of carbonaceous species formed over mordenite

Liam John France

**Submitted in partial fulfilment of the requirements for the degree of
Doctor of Philosophy**



School of Chemistry

College of Science and Engineering

University of Glasgow

Abstract

The halide free carbonylation of methanol is a reaction of industrial relevance. A process based upon the use of a proton-form mordenite catalyst, which cokes during reaction, is currently under investigation. This study explores the carbonaceous deposits formed upon mordenite from various methanol and dimethylcarbonate containing feedstreams. Dimethylcarbonate was investigated because it generates dimethylether upon decomposition.

^{13}C CP MAS NMR spectroscopic studies demonstrate that the carbonaceous deposits formed over mordenite from methanol containing feedstreams contained very similar compounds (poly-methylated aromatics and polycyclic species). A combination of elemental analysis and ^{13}C CP MAS NMR spectroscopy demonstrated that under a methanol-only feedstream for 5 minutes at 300°C , samples contained approximately 5.8 wt% carbon (which was around 45% of the 12.3 wt% observed at 300 minutes) and a distribution of species (methylated aromatics and polycyclic compounds) similar to that observed at longer times on stream (60, 180, 300 and 420 minutes). This is in contrast to the observations made after 2 minutes on stream where 3.3 wt% carbon and a relatively small amount of aromatic species were deposited. The species formed from a methanol/ CO/H_2 feedstream were found to be similar.

Similar species were evident in coked samples generated from both dimethylcarbonate and dimethylcarbonate/ CO/H_2 . However the carbon content for samples generated with dimethylcarbonate-only was found to be lower (9.5 wt%) for samples generated at 250°C for 300 minutes compared to those generated with methanol-only under equivalent conditions. The sample coked at 300°C displayed similar carbon contents, whereas the coked mordenite sample generated at 500°C displayed an increase in the carbon content (18.3 wt%) compared to (17.6 wt%) samples generated with methanol-only. Although similar carbon contents were observed for syn-gas containing feedstreams, the ^{13}C CP MAS NMR studies evidenced acetic acid for samples generated at 300°C for 300 minutes with a dimethylcarbonate/ CO/H_2 feedstream, whereas this was not observed employing a methanol/ CO/H_2 feedstream at equivalent conditions. Samples generated at 250°C exhibited similar species (methylated aromatics) regardless of the presence of syn-gas. This was also true for samples generated at 500°C which exhibited polycyclic species. The sample generated at 150°C exhibited only adsorbed methanol under methanol/ CO/H_2 , whereas under a dimethylcarbonate feedstream species indicative of methanol, dimethylether, dimethylcarbonate and zeolite bound methoxy groups were observed.

Contents

Abstract.....	i
List of Tables.....	vi
List of Figures.....	ix
List of Reaction Schemes and Equations.....	xix
Acknowledgements.....	xx
Author's declaration.....	xxi
1 Introduction.....	1
1.1 General background.....	1
1.1.1 Coking.....	1
1.1.2 Common methods of coke analysis.....	2
1.2 Zeolites.....	2
1.2.1 Zeolites - natural and synthetic.....	5
1.2.2 Mordenite.....	5
1.2.3 Zeolites as solid acid catalysts.....	7
1.3 Coking on zeolites.....	9
1.3.1 Inhibiting and beneficial coke.....	10
1.3.2 Regeneration.....	11
1.4 Scope of the thesis.....	12
References.....	13
2 Experimental.....	17
2.1 Materials.....	17
2.2 Material characterisation.....	17

2.2.1 Elemental analysis.....	17
2.2.2 Nitrogen adsorption isotherms.....	17
2.2.3 Powder x-ray diffraction.....	18
2.2.4 Thermogravimetric analysis.....	18
2.2.5 Thermogravimetric analysis coupled with mass spectrometry.....	18
2.2.6 Thermal volatilisation analysis and Sub-ambient thermal volatilisation analysis.....	18
2.2.7 MAS NMR spectroscopy.....	20
2.3 Material coking and coke removal.....	23
2.3.1 Methanol-only reactor specification.....	23
2.3.2 Methanol-only and dimethylcarbonate-only reactions.....	24
2.3.3 Carbonylation reactor specification.....	25
2.3.4 Methanol and dimethylcarbonate carbonylation reactions.....	26
2.3.5 Ageing effects.....	26
2.3.6 Steaming reactor specification.....	27
2.3.7 Steaming coked materials generated with a methanol-only feedstream.....	28
3 Carbonaceous species deposited from methanol-only feedstreams.....	29
3.1 Introduction.....	29
3.2 Results and discussion.....	35
3.2.1 Temperature dependence on the form of carbonaceous species deposited.....	35
3.2.2 Time dependence on the form of carbonaceous species deposited.....	63
3.2.3 Ethanol impurity effects upon the nature of the carbonaceous species generated.....	73
3.2.4 Methyl acetate impurity effects upon the nature of the carbonaceous species generated.....	80

3.2.5 The influence of activation time upon the nature of the carbonaceous species deposited.....	85
3.2.6 Carbonaceous species generated by reaction of methanol with some materials other than mordenite.....	90
3.3 Conclusions.....	98
References.....	102
4 Carbonaceous species deposited from methanol carbonylation.....	105
4.1 Introduction.....	105
4.2 Results and discussion.....	107
4.2.1 Temperature dependence of the carbonaceous species deposited during carbonylation.....	107
4.2.2 Time on stream dependence of the carbonaceous species deposited during carbonylation.....	121
4.3 Conclusions.....	127
References.....	129
5 Carbonaceous species deposited from dimethylcarbonate and dimethylcarbonate carbon monoxide and hydrogen feedstreams.....	131
5.1 Introduction.....	131
5.2 Results and discussion.....	132
5.2.1 Dimethylcarbonate carbonylation (using a γ -alumina pre-bed) temperature dependence.....	132
5.2.2 Dimethylcarbonate carbonylation (with no γ -alumina pre-bed) temperature dependence.....	145
5.2.3 Temperature dependence of the carbonaceous species deposited during dimethylcarbonate-only reactions.....	151

5.3 Conclusions.....	156
References.....	158
6 Conclusions.....	159
6.1 Comparative conclusions.....	159
6.2 Preliminary further work.....	173
6.2.1 Steaming of coked mordenite.....	173
6.2.2 TGA employing dilute H ₂ and H ₂ /CO atmospheres.....	174
6.3 Future work.....	175
References.....	176
7 Appendices.....	177

List of Tables

Table 1.2.1: Some zeolites and their pore dimensions.....	4
Table 3.2.1: Evolved gas mass spectrometry under 2% O ₂ /Ar of coked mordenite generated with methanol at 150, 200, 250 and 300°C for 300 minutes (products have been identified by examining unique fragments and fragment patterns).....	45
Table 3.2.2: Evolved gas mass spectrometry under 2% O ₂ /Ar of coked mordenite generated with methanol at 350, 400, 450 and 500°C for 300 minutes (products have been identified by examining unique masses and mass patterns).....	46
Table 3.2.3: Evolved gas mass spectrometry under Ar of coked mordenite generated with methanol at 150, 200, 250 and 300°C for 300 minutes (products have been identified by examining unique masses and mass patterns).....	48
Table 3.2.4: Evolved gas mass spectrometry under Ar of coked mordenite generated with methanol at 350, 400, 450 and 500°C for 300 minutes (products have been identified by examining unique masses and mass patterns).....	49
Table 3.2.5: BET and single point surface areas and isotherm types for NH ₄ MOR20 and of coked mordenite generated with methanol at different reaction temperatures for 300 minutes.....	58
Table 3.2.6: BET and single point surface areas and isotherm types for coked mordenite generated with methanol at 300°C for different reaction times.....	71
Table 3.2.7: BET and single point surface areas and isotherm types for coked mordenite generated with methanol containing different percentages of ethanol “impurity” at 300°C for 300 minutes.....	78
Table 3.2.8: BET and single point surface areas and isotherm types for coked mordenite unactivated and activated at 500°C for different activation times, generated with methanol at 300°C for 300 minutes.....	89
Table 3.2.9: Carbon content and atomic H:C ratio of materials and coked materials generated with methanol at 300°C for 300 minutes (Not corrected for the influence of adsorbed water).....	91

Table 4.2.1: Evolved gas mass spectrometry under 2% O ₂ /Ar for coked mordenite generated with methanol at 150, 250, 300 and 500°C for 300 minutes (products have been identified by examining unique fragments and fragment patterns).....	114
Table 4.2.2: Evolved gas mass spectrometry under Ar for coked mordenite generated with methanol at 150, 250, 300 and 500°C for 300 minutes (products have been identified by examining unique fragments and fragment patterns).....	117
Table 4.2.3: BET and single point surface areas and isotherm types for coked mordenite generated with methanol at different reaction temperatures for 300 minutes.....	120
Table 4.2.4: BET and single point surface areas and isotherm types for coked mordenite generated with methanol at 300°C for different reaction times.....	126
Table 5.2.1: Evolved gas mass spectrometry under 2% O ₂ /Ar for coked mordenite generated with dimethylcarbonate using a pre-bed at 150, 250, 300 and 500°C for 300 minutes (products have been identified by examining unique fragments and fragment patterns).....	139
Table 5.2.2: Evolved gas mass spectrometry under Ar for coked mordenite generated with dimethylcarbonate using a pre-bed at 150, 250, 300 and 500°C for 300 minutes (products have been identified by examining unique fragments and fragment patterns).....	142
Table 5.2.3: BET and single point surface areas and isotherm types for coked mordenite generated with dimethylcarbonate using a pre-bed at different reaction temperatures for 300 minutes.....	143
Table 5.2.4: BET and single point surface areas and isotherm types for coked mordenite generated with dimethylcarbonate at different reaction temperatures for 300 minutes.....	150
Table 5.2.5: BET and single point surface areas and isotherm types for coked mordenite generated with dimethylcarbonate at different reaction temperatures for 300 minutes.....	155
Table 6.1.1: Carbon contents and H:C ratios of coked mordenite generated with different feedstreams at 250°C for 300 minutes.....	162

Table 6.1.2: Carbon contents and H:C ratios of coked mordenite generated with different feedstreams at 300°C for 300 minutes.....	165
Table 6.1.3: Carbon contents and H:C ratios of coked mordenite generated with methanol containing feedstreams at 300°C for 60 minutes.....	167
Table 6.1.4: Carbon contents and H:C ratios of coked mordenite generated with methanol containing feedstreams at 300°C for 180 minutes.....	169
Table 6.1.5: Carbon contents and H:C ratios of coked mordenite generated with methanol containing feedstreams at 300°C for 420 minutes.....	170
Table 6.1.6: Carbon contents and H:C ratios of coked mordenite generated with methanol containing feedstreams at 300°C for 600 minutes.....	172
Table 6.2.1: Carbon contents of coked mordenite generated with methanol at 300°C for 300 minutes prior to and post-steaming at different temperatures for 18 hours.....	173

List of Figures

Figure 1.2.1: Common secondary building units found in zeolites.....	3
Figure 1.2.2: BEA (polymorph A), MFI and FAU framework structures.....	4
Figure 1.2.3: Mordenite framework structure.....	6
Figure 1.2.4: Framework representation of the 8 and 12 MR pores in mordenite.....	6
Figure 1.2.5: The processes required for generating Brønsted or Lewis acid sites in zeolites.....	8
Figure 1.2.6: Shape selectivity induced by the zeolite upon (a) reactant, (b) product and (c) transition state.....	9
Figure 2.2.1: A simplified diagram of the TVA system.....	19
Figure 2.3.1 A simplified diagram of the atmospheric micro reactor.....	24
Figure 2.3.2 A simplified diagram of the atmospheric pressure carbonylation micro reactor.....	25
Figure 2.3.3 A simplified diagram of the steaming regeneration reactor.....	27
Figure 3.2.1: ^{13}C DP MAS NMR spectrum of coked mordenite generated with 25% ^{13}C enriched methanol at different reaction temperatures for 300 minutes.....	36
Figure 3.2.2: First derivative TGA profile attained under air of coked mordenite generated with methanol at different reaction temperatures for 300 minutes.....	38
Figure 3.2.3: ^{13}C CP MAS NMR spectrum of coked mordenite generated with methanol at different temperatures for 300 minutes.....	39
Figure 3.2.4: Carbon content of coked mordenite generated with methanol at different reaction temperatures for 300 minutes.....	40
Figure 3.2.5: H:C atomic ratios of coked mordenite generated with methanol at different reaction temperatures for 300 minutes (not corrected for the influence of adsorbed water).....	41

Figure 3.2.6: First derivative TGA profiles attained under air of coked mordenite generated with methanol at different reaction temperatures for 300 minutes.....	42
Figure 3.2.17: First derivative TGA profiles attained under 2% O ₂ /Ar of coked mordenite generated with methanol at different reaction temperatures for 300 minutes.....	43
Figure 3.2.8: First derivative TGA profiles attained under argon of coked mordenite generated with methanol at different reaction temperatures for 300 minutes.....	47
Figure 3.2.9: First derivative TGA profiles attained under air of post Ar TGA of coked mordenite generated with methanol at different reaction temperatures for 300 minutes.....	50
Figure 3.2.10: Thermal volatilisation analysis of coked mordenite generated with methanol at 300°C for 300 minutes. The trace shows total volatiles and non-liquid N ₂ condensable products.....	52
Figure 3.2.11: Sub-ambient thermal volatilisation analysis (SATVA) of coked mordenite generated with methanol at 300°C for 300 minutes. Trace shows products evolved by heating of collected volatiles trap from -196 to 30°C.....	53
Figure 3.2.12: GCMS analysis of the liquid fraction collected from SATVA of coked mordenite generated with methanol at 300°C for 300 minutes.....	54
Figure 3.2.13: Thermal volatilisation analysis of coked mordenite generated with methanol at 500°C for 300 minutes. The trace shows total volatiles and non- liquid N ₂ condensable products in liquid nitrogen.....	55
Figure 3.2.14: Sub-ambient thermal volatilisation analysis of coked mordenite generated with methanol at 500°C for 300 minutes. Trace shows products evolved by heating of the liquid nitrogen trap.....	56
Figure 3.2.15: Nitrogen adsorption-desorption isotherm of NH ₄ MOR20.....	57
Figure 3.2.16: Nitrogen adsorption isotherms of coked mordenite generated with methanol at different reaction temperatures for 300 minutes.....	57
Figure 3.2.17: XRD patterns of NH ₄ MOR20 and coked mordenite generated with methanol at different reaction temperatures for 300 minutes.....	59

Figure 3.2.18: ^{27}Al DP MAS NMR spectra of $\text{NH}_4\text{MOR20}$, and coked mordenite generated with 25% ^{13}C enriched methanol at 300°C and 500°C for 300 minutes (spinning side bands not removed).....	60
Figure 3.2.19: ^{29}Si DP MAS NMR spectrum of $\text{NH}_4\text{MOR20}$, and coked mordenite generated with 25% ^{13}C enriched methanol at 300°C and 500°C for 300 minutes.....	60
Figure 3.2.20: ^{29}Si DP MAS NMR spectrum of $\text{NH}_4\text{MOR20}$ (deconvoluted and integrated).....	61
Figure 3.2.21: ^{29}Si DP MAS NMR of coked mordenite generated with 25% ^{13}C enriched methanol at 300°C for 300 minutes (deconvoluted and integrated).....	62
Figure 3.2.22: ^{29}Si DP MAS NMR of coked mordenite generated with 25% ^{13}C enriched methanol at 500°C for 300 minutes (deconvoluted and integrated).....	62
Figure 3.2.23: ^{13}C DP MAS NMR spectrum of coked mordenite generated with 25% ^{13}C enriched methanol at 300°C for different reaction times.....	65
Figure 3.2.24: ^{13}C CP MAS NMR spectrum of coked mordenite generated with methanol at 300°C for different reaction times.....	66
Figure 3.2.25: Carbon content of coked mordenite generated with methanol at 300°C for different reaction times.....	67
Figure 3.2.26: H:C atomic ratios of coked mordenite generated with methanol at 300°C for different reaction times (not corrected for the influence of adsorbed water).....	68
Figure 3.2.27: First derivative TGA profiles attained under air of coked mordenite generated with methanol at 300°C for different reaction times.....	70
Figure 3.2.28: Nitrogen adsorption isotherms of coked mordenite generated with methanol at 300°C for different reaction times.....	70
Figure 3.2.29: XRD patterns of coked mordenite generated with methanol at 300°C for different reaction times.....	72
Figure 3.2.30: Carbon content of coked mordenite generated with methanol containing different percentages of ethanol “impurity” at 300°C for 300 minutes.....	74

Figure 3.2.31: Atomic H:C ratio of coked mordenite generated with methanol containing different percentages of ethanol “impurity” at 300°C for 300 minutes (not corrected for the influence of adsorbed water).....	74
Figure 3.2.32: First derivative TGA profiles attained under air of coked mordenite generated with methanol containing different percentages of ethanol “impurity” at 300°C for 300 minutes.....	75
Figure 3.2.33: Nitrogen adsorption isotherms of coked mordenite generated with methanol containing different percentages of ethanol “impurity” at 300°C for 300 minutes.....	77
Figure 3.2.34: XRD patterns of coked mordenite generated with methanol containing different percentages of ethanol “impurity” at 300°C for 300 minutes.....	79
Figure 3.2.35: Carbon content of coked mordenite generated with methanol containing a 2.0% methyl acetate “impurity” at different reaction temperatures for 300 minutes.....	80
Figure 3.2.36: Atomic H:C ratio of coked mordenite generated with methanol containing a 2.0% methyl acetate “impurity” at different reaction temperatures for 300 minutes (not corrected for the influence of adsorbed water).....	81
Figure 3.2.37: First derivative TGA profiles attained under air of coked mordenite generated with methanol containing a 2.0% methyl acetate “impurity” at different reaction temperatures for 300 minutes.....	82
Figure 3.2.38: Nitrogen adsorption isotherms of MTH catalysts coked at 2.0% methyl acetate impurity at different reaction temperatures.....	83
Figure 3.2.39: XRD patterns of coked mordenite generated with methanol containing a 2.0% methyl acetate “impurity” at different reaction temperatures for 300 minutes.....	84
Figure 3.2.40: Carbon content of coked mordenite unactivated and activated at 500°C for different activation times, generated with methanol at 300°C for 300 minutes.....	85
Figure 3.2.41: Atomic H:C ratio of coked mordenite unactivated and activated at 500°C for different activation times, generated with methanol at 300°C for 300 minutes (not corrected for the influence of adsorbed water).....	86

Figure 3.2.42: First derivative TGA profile attained under air of non-reacted NH ₄ MOR ₂₀	87
Figure 3.2.43: First derivative TGA profiles attained under air of coked mordenite unactivated and activated at 500°C for different activation times, generated with methanol at 300°C for 300 minutes.....	88
Figure 3.2.44: Nitrogen adsorption isotherms of coked mordenite unactivated and activated at 500°C for different activation times, generated with methanol at 300°C for 300 minutes.....	88
Figure 3.2.45: XRD patterns of coked mordenite unactivated and activated at 500°C for different activation times, generated with methanol at 300°C for 300 minutes.....	90
Figure 3.2.46: First derivative TGA profiles attained under air of Cu(55)MOR ₂₀ and coked Cu(55)MOR ₂₀ generated with methanol at 300°C for 300 minutes.....	92
Figure 3.2.47: First derivative TGA profiles attained under air of MCM-41 and coked MCM-41 generated with methanol at 300°C for 300 minutes.....	93
Figure 3.2.48: First derivative TGA profiles attained under air of γ -alumina and coked γ -alumina generated with methanol at 300°C for 300 minutes.....	94
Figure 3.2.49: Nitrogen adsorption isotherms of Cu(55)MOR ₂₀ and coked Cu(55)MOR ₂₀ generated with methanol at 300°C for 300 minutes.....	95
Figure 3.2.50: Nitrogen adsorption isotherms of MCM-41 and coked MCM-41 generated with methanol at 300°C for 300 minutes.....	95
Figure 3.2.51: Nitrogen adsorption isotherms of γ -alumina and coked γ -alumina generated with methanol at 300°C for 300 minutes.....	96
Figure 3.2.52: XRD patterns of Cu(55)MOR ₂₀ and coked Cu(55)MOR ₂₀ generated with methanol at 300°C for 300 minutes.....	96
Figure 3.2.53: XRD patterns of MCM-41 and coked MCM-41 generated with methanol at 300°C for 300 minutes.....	97
Figure 3.2.54: XRD patterns of γ -alumina and coked γ -alumina generated with methanol at 300°C for 300 minutes.....	98

Figure 4.2.1: ^{13}C CP MAS NMR spectrum of coked mordenite generated with methanol at different reaction temperatures for 300 minutes.....	108
Figure 4.2.2: Carbon content of coked mordenite generated with methanol at different reaction temperatures for 300 minutes.....	110
Figure 4.2.3: H:C atomic ratios of coked mordenite generated with methanol at different reaction temperatures for 300 minutes (not corrected for the influence of adsorbed water). The H:C ratio for the sample generated at 150°C should be measured against the left hand Y-axis, whereas 250, 300 and 500°C should be measured against the right Y-axis.....	111
Figure 4.2.4: First derivative TGA profiles attained under air of coked mordenite generated with methanol at different reaction temperatures for 300 minutes.....	112
Figure 4.2.5: First derivative TGA profiles attained under 2% O_2/Ar of coked mordenite generated with methanol at different reaction temperatures for 300 minutes.....	113
Figure 4.2.6: First derivative TGA profiles attained under argon of coked mordenite generated with methanol at different reaction temperatures for 300 minutes.....	116
Figure 4.2.7: First derivative TGA profiles attained under air of post TGA argon of coked mordenite generated with methanol at different reaction temperatures for 300 minutes.....	119
Figure 4.2.8: Nitrogen adsorption isotherms of coked mordenite generated with methanol at different reaction temperatures for 300 minutes.....	119
Figure 4.2.9: XRD patterns of coked mordenite generated with methanol at different reaction temperatures for 300 minutes.....	121
Figure 4.2.10: ^{13}C CP MAS NMR spectrum of coked mordenite generated with methanol at 300°C for different reaction times.....	122
Figure 4.2.11: Carbon content of coked mordenite generated with methanol at 300°C for different reaction times.....	123
Figure 4.2.12: Atomic H:C ratio of coked mordenite generated with methanol at 300°C for different reaction times (not corrected for the effects of adsorbed water).....	124
Figure 4.2.13: First derivative TGA profiles attained under air of coked mordenite generated with methanol at 300°C for different reaction times.....	125

Figure 4.2.14: Nitrogen adsorption isotherms of coked mordenite generated with methanol at 300°C for different reaction times.....	126
Figure 4.2.15: XRD patterns of coked mordenite generated with methanol at 300°C for different reaction times.....	127
Figure 5.2.1: ¹³ C CP MAS NMR spectrum of coked mordenite generated with dimethylcarbonate using a pre-bed at different reaction temperatures for 300 minutes.....	133
Figure 5.2.2: Carbon content of coked mordenite generated with dimethylcarbonate using a pre-bed at different reaction temperatures for 300 minutes.....	135
Figure 5.2.3: H:C atomic ratios of coked mordenite generated with dimethylcarbonate using a pre-bed at different reaction temperatures for 300 minutes (not corrected for the influence of adsorbed water).....	136
Figure 5.2.4: First derivative TGA profiles attained under air of coked mordenite generated with dimethylcarbonate using a pre-bed at different reaction temperatures for 300 minutes.....	137
Figure 5.2.5: First derivative TGA profiles attained under 2% O ₂ /Ar of coked mordenite generated with dimethylcarbonate using a pre-bed at different reaction temperatures for 300 minutes.....	138
Figure 5.2.6: First derivative TGA profiles attained under argon of coked mordenite generated with dimethylcarbonate using a pre-bed at different reaction temperatures for 300 minutes.....	140
Figure 5.2.7: Nitrogen adsorption isotherms of coked mordenite generated with dimethylcarbonate using a pre-bed at different reaction temperatures for 300 minutes.....	143
Figure 5.2.8: XRD patterns of coked mordenite generated with dimethylcarbonate using a pre-bed at different reaction temperatures for 300 minutes.....	144
Figure 5.2.9: ¹³ C CP MAS NMR spectrum of coked mordenite generated with dimethylcarbonate at different reaction temperatures for 300 minutes.....	145
Figure 5.2.10: Carbon content of coked mordenite generated with dimethylcarbonate at different reaction temperatures for 300 minutes.....	147

Figure 5.2.11: H:C atomic ratios of coked mordenite generated with dimethylcarbonate at different reaction temperatures for 300 minutes (not corrected for the influence of adsorbed water).....	148
Figure 5.2.12: First derivative TGA profiles attained under air of coked mordenite generated with dimethylcarbonate at different reaction temperatures for 300 minutes.....	149
Figure 5.2.13: Nitrogen adsorption isotherms of coked mordenite generated with dimethylcarbonate at different reaction temperatures for 300 minutes.....	150
Figure 5.2.14: XRD patterns of coked mordenite generated with dimethylcarbonate at different reaction temperatures for 300 minutes.....	151
Figure 5.2.15: Carbon content of coked mordenite generated from dimethylcarbonate at different reaction temperatures for 300 minutes.....	151
Figure 5.2.16: Atomic H:C ratio of coked mordenite generated from dimethylcarbonate at different reaction temperatures for 300 minutes (not corrected for the influence of adsorbed water).....	152
Figure 5.2.17: First derivative TGA profiles attained under air of coked mordenite generated with dimethylcarbonate at different reaction temperatures for 300 minutes.....	153
Figure 5.2.18: Nitrogen adsorption isotherms of coked mordenite generated with dimethylcarbonate at different reaction temperatures for 300 minutes (The isotherm for the sample generated at 300°C is problematic after approximately 0.4 P/P ⁰ but is used to illustrate the relative pressure range used in the BET method. It was not possible to rerun this isotherm because a problem developed on the system).....	154
Figure 5.2.19: XRD patterns of coked mordenite generated at different reaction temperatures for 300 minutes.....	155
Figure 6.1.1: ¹³ C CP MAS NMR spectra of coked mordenite generated with different feedstreams at 250°C for 300 minutes.....	162
Figure 6.1.2: First derivative TGA profiles attained under air of coked mordenite generated with different feedstreams at 250°C for 300 minutes.....	163

Figure 6.1.3: First derivative TGA profiles attained under 2% O ₂ /Ar of coked mordenite generated with different feedstreams at different 250°C for 300 minutes.....	163
Figure 6.1.4: First derivative TGA profiles attained under argon of coked mordenite generated with different feedstreams at 250°C for 300 minutes.....	164
Figure 6.1.5: ¹³ C CP MAS NMR spectra of coked mordenite generated with different feedstreams at 300°C for 300 minutes.....	164
Figure 6.1.6: First derivative TGA profiles attained under air of coked mordenite generated with different feedstreams at 300°C for 300 minutes.....	165
Figure 6.1.7: First derivative TGA profiles attained under 2% O ₂ /Ar of coked mordenite generated with different feedstreams at different 300°C for 300 minutes.....	166
Figure 6.1.8: First derivative TGA profiles attained under argon of coked mordenite generated with different feedstreams at 300°C for 300 minutes.....	166
Figure 6.1.9: ¹³ C CP MAS NMR spectrum of coked mordenite generated with methanol containing feedstreams at 300°C for 60 minutes.....	167
Figure 6.1.10: First derivative TGA profiles attained under air of coked mordenite generated with methanol containing feedstreams at 300°C for 60 minutes.....	168
Figure 6.1.11: ¹³ C CP MAS NMR spectrum of coked mordenite generated with methanol containing feedstreams at 300°C for 180 minutes.....	168
Figure 6.1.12: First derivative TGA profiles attained under air of coked mordenite generated with methanol containing feedstreams at 300°C for 180 minutes.....	169
Figure 6.1.13: ¹³ C CP MAS NMR spectrum of coked mordenite generated with methanol containing feedstreams at 300°C for 420 minutes.....	170
Figure 6.1.14: First derivative TGA profiles attained under air of coked mordenite generated with methanol containing feedstreams at 300°C for 420 minutes.....	171
Figure 6.1.15: ¹³ C CP MAS NMR spectrum of coked mordenite generated with methanol containing feedstreams.....	171

Figure 6.1.16: First derivative TGA profiles attained under air of coked mordenite generated with methanol containing feedstreams at 300°C for 600 minutes.....172

Figure 6.2.1: XRD patterns of coked mordenite generated with methanol at 300°C for 300 minutes post-steaming at different temperatures for 18 hours.....173

Figure 6.2.2: First derivative TGA profiles attained under 2% syn gas and 5% hydrogen of coked mordenite generated with methanol containing feedstreams at 300°C for 300 minutes.....174

Figure 7.3.1: Variable temperature XRD analysis from 30°C - 900°C (10°C min⁻¹ ramp rate) under 2% O₂/Ar of coked mordenite generated under methanol carbonylation conditions at 300°C for 360 minutes reaction time.....178

List of Reaction Schemes and Equations

Reaction Scheme 3.1.1: The main reaction steps involved in MTH chemistry.....	30
Reaction Scheme 3.1.2: Product spectrum produced from methanol over CuO/ZnO ZSM-5 at 400°C and atmospheric pressure.....	31
Reaction Scheme 3.1.3: Product spectrum produced from methanol over MOR mixed with kaolinite at 530°C and 1 bar pressure.....	31
Reaction Scheme 3.1.4: The first description of the hydrocarbon pool mechanism.....	32
Reaction scheme 3.1.5: The proposed hydrocarbon pool mechanism for the production of C ₄ olefinic products from lower order methyl benzenes.....	33
Reaction scheme 3.1.6: Side chain methylation route for hexa-methyl benzene to hexamethylmethylenecyclohexadiene through a carbocation transition state.....	34
Reaction Scheme 4.1.1: The BASF methanol carbonylation process.....	105
Reaction Scheme 4.1.2: The Monsanto methanol carbonylation process.....	106
Reaction Scheme 5.1.1: Proposed mechanism for the carbonylation of dimethylether.....	131
Equation 3.2.1: Determination of the framework Si/Al ratio from integrated silicon signals in deconvoluted ²⁹ Si MAS NMR spectra.....	63

Acknowledgements

First and foremost I would like to thank my supervisor Justin Hargreaves for all of his guidance and support during the course of my PhD. His vast reserves of knowledge are indeed legendary! It was all truly appreciated, especially the trip to the IZC 2010 conference.

I would like to acknowledge my industrial supervisor Evert Ditzel for all of his efforts in organising two month long trips down to BP Chemicals to undertake the work employing carbon monoxide.

Thanks to David Apperley for allowing me to spend time at the University of Durham undertaking solid state NMR spectroscopy, John Liggat, Deborah Todd and James Lewicki for all of their help and support with the TVA experiments, Mrs Kim Wilson for performing elemental analysis on my many samples and performing duplicates when required.

I would like to thank my parents for their emotional support during the course of this work, my mum who listened to my-self doubts and told me I could do it and my dad who after three hours got the printer working for me.

I would like to acknowledge my fiancée Vicky, who although in China has supported me during my PhD more than she knows.

I would like to thank the catalysis research group, particularly Anne-Marie, Fiona and Lynsey who were great friends and colleagues and will be greatly missed. Stuart and Mark who helped me adapt to Glasgow living and helped me out greatly during my first few months, Andy for all of his sage like wisdom and his every increasing knowledge and application of anything TGA, Jim for always having the time to stop and have a chat. Finally everyone else both past and present you know who you are!

Author's declaration

The work contained within this thesis, submitted for the degree of doctor of philosophy, is my own original work, except where due reference is made to others. No material within has been previously submitted for a degree at this or any other university.

1 Introduction

1.1 General background

The requirements of a good catalyst are high activity, favourable selectivity of desired products and stability over an extended reaction time. Deactivation of the catalyst (decrease in activity and/or selectivity) is inevitable; the period of time over which the material deactivates has a large impact on process and reactor design [1]. As such, understanding the process of catalyst deactivation has not only scientific but also economic value. Deactivation of catalysts may be caused by a number of different effects; sintering of ionic metal species [2] and thermal instability [3] etc; however the most frequently discussed pathway for acid catalysed hydrocarbon reactions is the formation of coke [4]. Coke characterisation studies had been undertaken on many traditional catalytic systems prior to the emergence of zeolitic materials. Some examples include the original cracking catalysts, amorphous silica/alumina [1] and traditional supported metal catalysts [4]. At the advent of zeolite catalysed processes, however, very little attention was paid to the formation of coke [4] and this continued until the late 1970's when efforts were redirected to these relatively novel systems [4, 5]. As such the research on these systems by industry and academia has intensified significantly [6]. Given the current state of the economic climate and ever increasing demands on industry to reduce costs this is not at all surprising.

1.1.1 Coking

Coking (deposition of carbonaceous species) is often envisaged as being a problem when in fact it may not necessarily be the case. Carbonaceous species deposited on catalysts may be split into three distinct groups; inhibiting (adversely affects the process) [1, 7], beneficial (aids the process) [1, 7, 8] and benign (often referred to as spectator coke has no effect on the process) [9, 10]. A general definition of coke was given by Karge in 2001 [4] as “coke consists of carbonaceous deposits which are mainly deficient in hydrogen compared with the coke-forming reactant molecule(s)”. This is rather biased and not completely correct. As such an amendment was made by Bauer and Karge in 2006 [1] where the definition of coke was altered to include the qualifier “and which are responsible for catalyst deactivation”.

1.1.2 Common methods of coke analysis

To elucidate the nature of carbonaceous materials deposited on catalysts, a wide range of spectroscopic techniques are currently available which include, infrared spectroscopy (IR) [11], Raman spectroscopy [12, 13], ultra-violet/visible spectroscopy (UV/Vis) [14, 15], and X-ray photoelectron spectroscopy (XPS) [16, 17]. Thermal analysis techniques can also be employed, which include; elemental analysis [18, 19] as well as thermogravimetric analysis (TGA) [20, 21] under a variety of different atmospheres. Extraction methods such as Soxhlet extraction [22, 23] may be used to remove soluble fractions of the residue with subsequent analysis being undertaken. More extreme extraction methods may be employed whereby the catalyst is dissolved in hydrofluoric acid (HF) [24, 25] and the remaining carbonaceous species are collected and analysed. Finally methods examining the location and effect of coking on catalysts may be undertaken. Adsorption studies using different adsorbates may be undertaken on pre- and post-reaction zeolites [26, 27], especially in determining the location of the carbonaceous deposits through physisorption isotherm analysis. X-ray diffraction (XRD) may be used to identify deformations of the zeolite framework which may indicate the presence of carbonaceous species within the crystallites [28, 29]. Finally, NMR spectroscopy can be used to examine the aluminium and silicon species within the zeolite and determine if the reaction and/or coking had any detriment on the framework [30, 31] (i.e. formation of extra framework aluminium species and/or silanol groups). However in respect to the latter quantitative analysis would be necessary as the Si-OH and Si-1Al silicon peaks are indistinguishable [32]. It is also possible to employ ^{13}C and ^1H MAS NMR techniques to directly probe the carbonaceous species themselves [18, 33].

1.2 Zeolites

The following section has been included to give a very brief overview on zeolites. The material used for the bulk of the work undertaken within this thesis is the zeolite mordenite ($\text{NH}_4\text{MOR20}$), which in its proton form (HMOR20) is currently under investigation by BP Chemicals for its capacity in the carbonylation of methanol, and more recently dimethylether, to yield acetic acid/ methyl acetate. Therefore detailed information shall be provided about zeolites in general and aspects of mordenite will be specifically described.

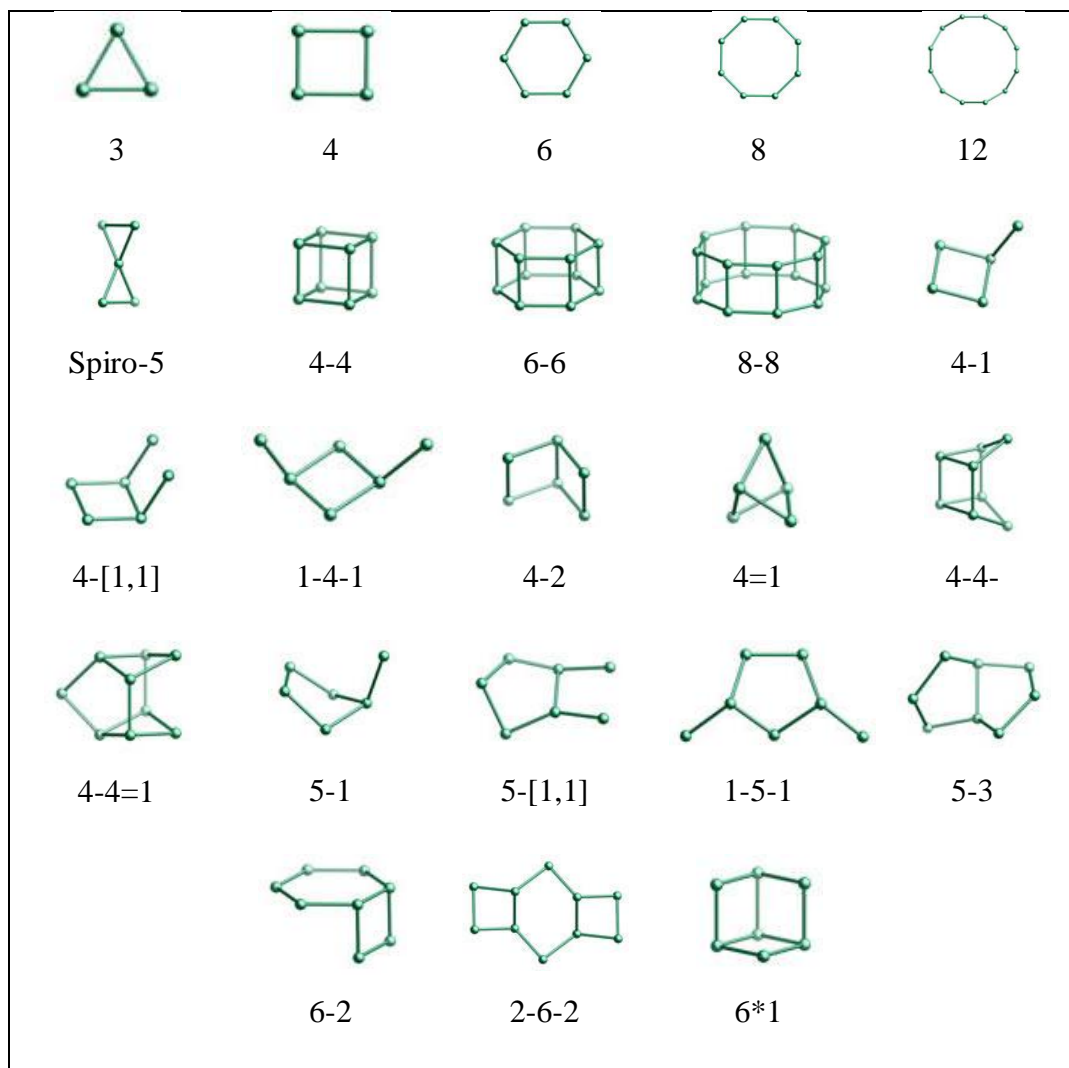


Figure 1.2.1: Common secondary building units found in zeolites [36].

Zeolites are microporous crystalline aluminosilicate solids with well defined structures. They consist primarily of aluminium, silicon and oxygen in their framework (though it is well known that ZSM-5 type frameworks can be synthesised substituting aluminium for titanium [34] iron or boron) and water, cationic species and/or other molecules within their pores. They are complex inorganic structures, consisting of an extended 3-dimensional tetrahedrally coordinated framework comprised of AlO_4^- and SiO_4 tetrahedra linked via shared (bridging) oxygen atoms. As has been indicated, aluminium containing tetrahedra have a net negative charge, which is balanced by a cationic species. The primary constituents of the framework (AlO_4^- and SiO_4) combine to form a wide variety of cages and rings called secondary

building units (SBU) [35]. Common SBUs found in zeolite structures are given in Figure 1.2.1 which has been taken from [36].

The final zeolite framework consists of grouped SBUs. The way in which the SBUs combine dictates the framework type produced (currently as many as 197 framework types are recognised by the International Zeolite Association [37]). The framework structure of zeolites with framework types BEA (beta), MFI (ZSM-5) and FAU (faujasite) are presented in Figure 1.2.2, from [38].

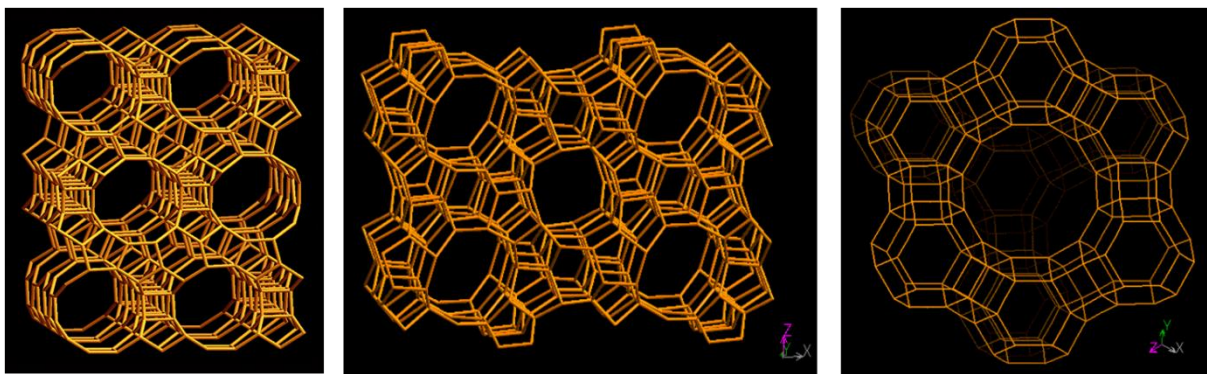


Figure 1.2.2: BEA (polymorph A), MFI and FAU framework structures [38].

Zeolite	Pore dimensions (Å)
Beta	6.6 x 6.7, 5.6 x 5.6
ZSM-5	5.1 x 5.5, 5.3 x 5.6
Faujasite	7.4 x 7.4
Linde type A	4.1 x 4.1
Mordenite	7.0 x 6.5, 5.7 x 2.6

Table 1.2.1: Some zeolites and their pore dimensions [38].

The zeolite framework contains channels and pores with molecular dimensions. In general the pore sizes range from approximately 3-8 Å and subsequently zeolites are classified in

accordance with their dimensions. The dimensions found in five of the most well known zeolites are presented in Table 1.2.1 (adapted from [38]).

Due to the presence of the pores, of molecular-scale dimensions, zeolites have found numerous applications in the chemistry field such as; ion exchange, desiccants, gas filtration, air separation, cracking for the production of gasoline based products and shape selective catalysis. Zeolites have also found use in agriculture and construction [39].

Zeolite classification is made according to pore dimension based upon the number of oxygen atoms in the pore mouth, though further classification can be made depending in their Si/Al ratio (or $\text{SiO}_4/\text{Al}_2\text{O}_3$ (SAR)). It has been found that with an increasing Si/Al ratio the crystal framework stabilises to a greater degree. In acidic media, a zeolite with a large Si/Al is more stable than when in the presence of basic media. The reverse is also true for materials with a low Si/Al ratio [38, 39].

1.2.1 Zeolites – natural and synthetic

Two further classes of zeolite are observed. The first are zeolites which are found in nature as minerals. Natural zeolites possess numerous applications, for example in gas adsorption, ion exchange and water treatment. Clinoptilolite, formed from the devitrification of volcanic ash in water sources millions of years ago, has channel sizes (3.1 x 7.5, 4.6 x 3.6 and 2.8 x 4.7 Å) which enable it to act as a molecular sieve and remove ammonia from sewage waste streams and remove nitrogen from air [40]. The second class are synthetic zeolites, which include ZSM-5 which was developed by Mobil in the early 1970s [41] Interestingly “natural” zeolites such as faujasite and mordenite can fit into both classes as they can be produced synthetically for use as shape selective catalysts in hydrocarbon based reactions.

1.2.2 Mordenite

While many different zeolite and zeotype based structures exist, one of the most abundant and most used is mordenite. The tetrahedra combine to form rings consisting of four, five and six oxygen atoms. These building units result in a lattice structure arranged in eight and

twelve rings, with a unit cell composition of $[(\text{NH}_4^+)_8 (\text{H}_2\text{O})_{24} | \text{Al}_8\text{Si}_{40}\text{O}_{96}]$. The mordenite framework structure is depicted below in Figure 1.2.3 [38].

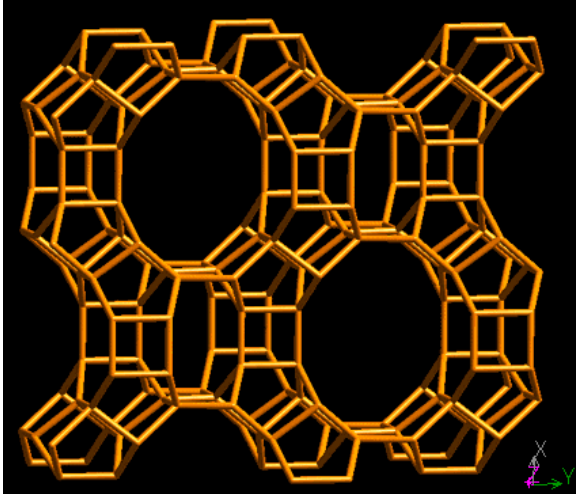


Figure 1.2.3: Mordenite framework structure [38].

The pore structure of mordenite is shown in Figure 1.2.4 [38]. It comprises of a set of linear 8 and 12-membered ring (MR) pores having diameters of 7.0×6.5 and $5.7 \times 2.6 \text{ \AA}$ respectively which have interconnecting side windows ($5.7 \times 2.6 \text{ \AA}$) from the 8 MR pore to the 12 MR pore.

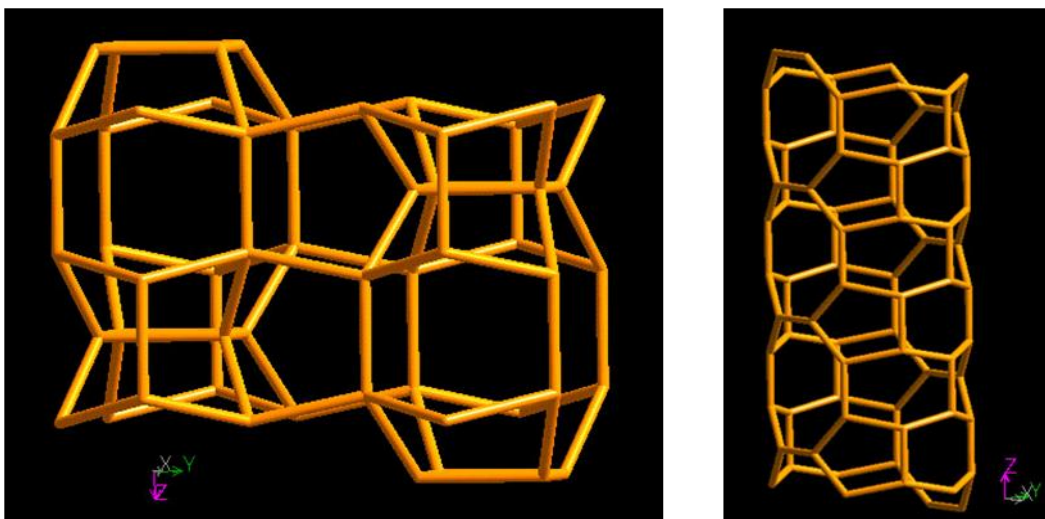


Figure 1.2.4: Framework representation of the 8 and 12 MR pores in mordenite [38].

1.2.3 Zeolites as solid acid catalysts

Currently a large amount of interest has been directed towards the use of zeolitic materials as solid acid catalysts. Zeolites possess significant advantages as catalysts due to the high density of catalytic sites and relatively high thermal stability, with decomposition temperatures ranging from 700 to 1300°C.

One of the most beneficial properties of zeolites as catalysts is their acidic properties. The observed catalytic activity of activated zeolites (removal of framework charge balancing cationic species) is attributed to the acid sites formed due to the AlO_4 tetrahedral units in the framework. These sites can either be of Brønsted or Lewis type. Zeolites are commonly synthesised in the presence of sodium ions (normally originating with the aluminium source) which act as framework charge balancing ions. These, however, can be readily exchanged for either protons or ammonium ions. Proton exchange can be achieved by employing a technique known as acid washing, which results in the formation of surface hydroxyl groups (Brønsted acid sites). If the framework is not particularly stable in acidic environments, ammonium ion exchange is favoured. The acidic form may then be generated prior to reaction by applying heat, which decomposes the ammonium ion generating ammonia and the proton form (acidic form) of the zeolite. Further heating at somewhat higher temperatures (generally above 500°C) results in dehydration of the Brønsted acid sites, which results in the formation of framework Lewis acid sites and also extra-framework aluminium which also acts as a Lewis acid. Extra-framework aluminium may also be formed via steaming of the zeolite at temperatures above 500°C. A schematic (Figure 1.2.5) has been adapted and modified from reference [42] which details the routes of formation of these sites. Therefore the zeolite can display either Brønsted or Lewis acid sites (both framework and/or extra-framework), or a mixture of both depending on the preparation of the zeolite [42].

Some of the most important and as such most often studied reactions in which zeolites act as catalysts are acid catalysed cracking, isomerisation and hydrocarbon synthesis. Acidic catalysed processes however are not the only reactions in which zeolites may be used. They can support a large range of reactions including acid-base, metal induced, oxidative and reductive processes. As mentioned previously, one of the more remarkable traits of a zeolite is its molecular scale microporous network, which enables the materials to act as shape selective catalysts. This type of reaction involves the steric influence wrought by the

microporous network, which is often selected based upon specific pore shape and size. These types of reactions occur within the confines of the internal cavities of the zeolite [43].

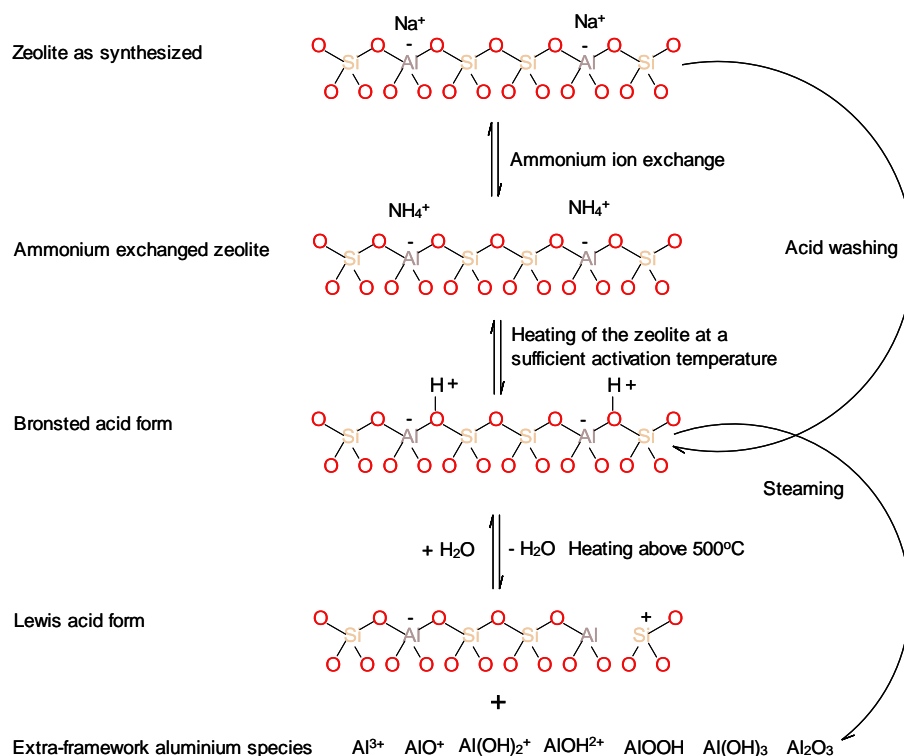


Figure 1.2.5: The processes required for generating Brønsted or Lewis acid sites in zeolites [42].

Three distinct types of shape selectivity are induced by the steric constraints of the pores, namely reactant selectivity, product selectivity and transition state selectivity. Reactant selectivity occurs at the pore mouth of the zeolite, where molecules with dimensions less than a defined critical size may enter the porous network and access internal active sites. Product selectivity occurs in the vicinity of the active site, whereby products of a certain dimension may leave the area of the active site and diffuse unhindered out through the channels. The final type of selectivity also occurs in the area around active sites whereby potential side reactions may be avoided if the transition state of the unwanted reaction requires more space than is available within the cavity. These three types of shape selectivity are represented

schematically in Figure 1.2.6 which has been reproduced from [43]. It was observed by Sugi [44] that mordenite exhibits shape selective formation (induced by the 12 MR pore system) of the least bulky products (4, 4' diisopropylbiphenyl and 2, 6 diisopropylnaphthalene) during isopropylation of biphenyl and naphthalene.

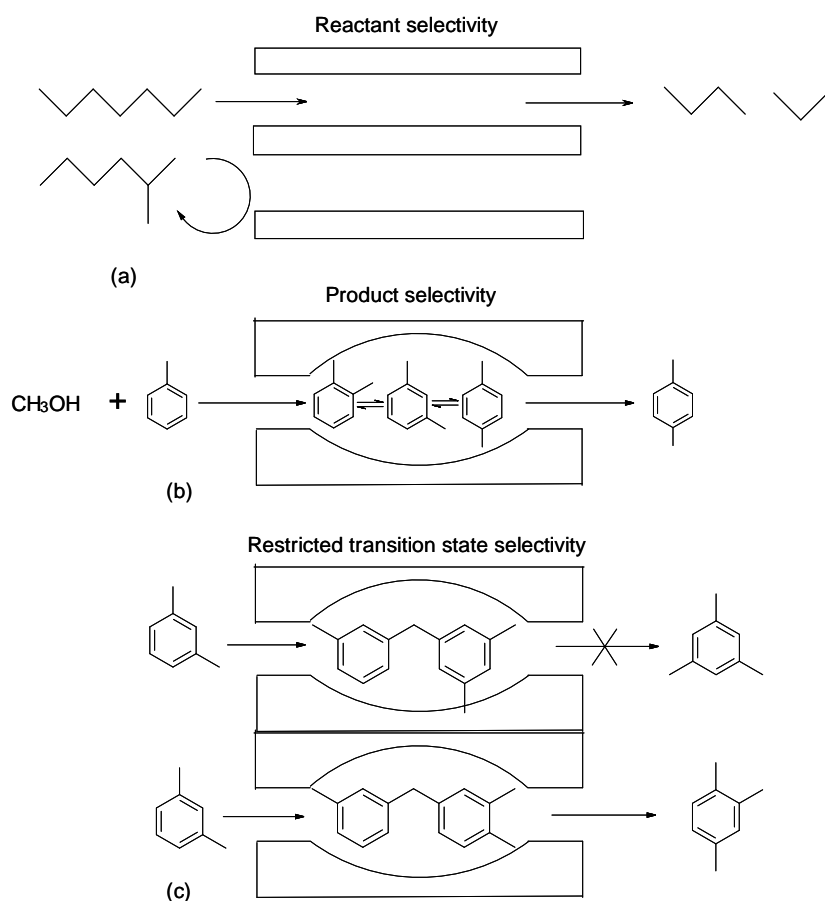


Figure 1.2.6: Shape selectivity induced by the zeolite upon (a) reactant, (b) product and (c) transition state [43].

1.3 Coking on zeolites

As has been briefly mentioned previously, three types of “coke” exist which can be defined as inhibiting, beneficial and benign coke. Interestingly the latter may also be in part either inhibiting or beneficial as well depending upon its location on the catalyst. Within this

section inhibiting and beneficial types of coke will be briefly discussed with reference to zeolite systems.

1.3.1 Inhibiting and beneficial coke

Coke can be extremely harmful to the activity of zeolite catalysts in several ways such as poisoning the active sites as a result of the presence of heavy by-products which are very difficult to remove. The pores can also become blocked which will reduce the surface area of the catalyst significantly. Many different types of hydrocarbon processing reactions undergo deactivation due to the formation of coke [45]. Subsequent regeneration procedures are required which, in most instances, are oxidative treatments resulting in exotherms. This can have detrimental effects on the zeolite catalyst such as dealumination, degradation of the framework and possible sintering of supported metals [45]. Studies undertaken by Huang *et al.* [46] comparing zeolites ZSM-5 and Y (faujasite), led to the conclusion that the acidity and pore size of the zeolite had a dramatic effect on the formation of coke. It was observed that the faujasite at lower reaction temperatures displayed a relatively clean reaction with very little by-product observed, whereas ZSM-5 exhibited copious quantities of coke (formed by ethylbenzene dealkylation which proceeded at lower temperatures) were attributed to the rapid deactivation observed.

The fluid catalytic cracking (FCC) process is perhaps the most industrially important process that zeolites are currently used in on a commercial scale. It employs faujasite dispersed in an amorphous matrix [47], which deactivates due to the interaction of carbonaceous deposits with active sites [48]. It was observed that these deposits form uniform layers on the walls of the pores [48]. These materials may be regenerated; this is performed under air at temperatures as high as 750°C [49]. However, this results in a massive exothermic response; some of the generated heat is absorbed by the catalyst. The remainder can in turn be utilised for vaporisation of the feedstock and endothermic cracking processes. In this way the catalyst is cycled through reaction and regeneration procedures to not only regenerate the material but supply energy for the process.

As suggested previously there are instances where coking can be beneficial, for example by improving selectivity to desired products by decreasing the size of the pores with controlled pre-coking. This is a rather popular route employed commercially for generating preferential

para product selectivity in disproportionation reactions [50] though passivation of surface acid sites can also be employed in conjunction with pre-coking.

Another example is the methanol to hydrocarbon process where the so called coke acts as a hydrocarbon pool facilitating the formation of olefinic species. Many studies have been directed towards elucidating the nature of the active hydrocarbon pool. A recent study by Bjorgen *et al.* [24] examining the carbonaceous species built up on zeolite beta, SAPO-34 and mordenite, showed that all catalysts displayed striking similarities in composition and reaction patterns of the retained carbonaceous species. Coke precursor species were found to be bicyclic compounds, whereas highly substituted polymethylbenzenes were found to act as reaction intermediates in the hydrocarbon pool mechanism for the three zeolites tested. Smaller pore zeolites (e.g. ZSM-5) were examined by Schulz *et al.* in 1987 [19] prior to the proposal of the hydrocarbon pool mechanism. It was found that two ring aromatics were the favoured coke species present in their pores. It has been suggested by Seiler *et al.* [51] that for zeolites with relatively small pores, the hydrocarbon pool may occur as olefinic species as opposed to methylated aromatic species. This suggestion is also in accordance with the suggestions made by Dahl and Kolboe [52] who first suggested the presence of such a pool. Indirectly, this work has parallels with proposals made by Thomson and Webb [53] who examined olefin hydrogenation on metal catalysts. They proposed a model whereby, hydrogen transfer occurs between an adsorbed hydrocarbon and the adsorbed olefin and examined it against information from previous studies which found that the model was successful. This certainly seems to suggest the presence of an active hydrocarbon co-catalytic species and in a manner describes a fundamental hydrocarbon pool (or in this case a pool of hydrogen). A similar effect is observed for the hydrogenation of alkynes where atomic carbon and hydrogen are deposited on the palladium catalyst [54]. Although a review by Bond [55] states that the model proposed by Thomson and Webb has never been experimentally justified.

1.3.2 Regeneration

Common regeneration methods normally employ air or oxygen to completely remove carbonaceous species (as discussed previously for the fluid catalytic cracking catalyst). This also presents problems with respect to generated exotherms which, in some instances, may

irreparably damage the zeolite framework. Therefore the use of alternative methods is required.

In a study performed by Benamar *et al.* [56] examining deactivation and regeneration of an ultra-stable Y (faujasite) during the transformation of m-xylene, it was observed that regeneration of the coked materials was partially successful when employing hydrogen and no significant change was observed when treated under nitrogen at 500°C for 16 hours. When using air, however, it was found that nearly complete reactivation was observed. Interestingly some carbonaceous material still remained after the treatment under air, whereas significantly more was found after both of the other treatments.

It was observed by Ivanov *et al.* [57] that the use of nitrous oxide was more effective than oxygen when regenerating a ZSM-5 catalyst used in the benzene to phenol oxidation reaction. It was found that only a fraction of the coke required removal to fully regenerate the catalyst under nitrous oxide 30-35% removal was required, whereas with oxygen 60-65% removal was needed.

Work undertaken by Bauer *et al.* [58] examining regeneration procedures of ZSM-5 coked under methanol to gasoline chemistry, employing hydrogen and alkanes as regeneration gases demonstrated that partial reactivation can be achieved and hence increasing the time on stream until combustion of carbonaceous deposits was required to fully reactivate. This suggests due to the increased time on stream and the decrease of coke content, that alkanes are an excellent hydrogen source for hydrocracking of alkylaromatic coke species. Although after the first cycle the spent catalyst was found to have dealuminated, but this was found to have no apparent effect on activity or stability on subsequent cycles.

1.4 Scope of the thesis

The work presented in this thesis is directed towards the characterisation of the carbonaceous species deposited over mordenite from a variety of feedstreams. The aim of this is to understand the similarities and differences between residues formed from methanol-only, methanol/CO/H₂, dimethylcarbonate-only and dimethylcarbonate/CO/H₂ feeds. This work is relevant to methanol conversion processes and also, possibly, deactivation and regeneration in an industrial context. In view of the primary focus of the study, initial attention has been

solely directed towards characterising the establishment of carbonaceous residues under various reaction regimes and determining their reactivity. Whilst it would be anticipated that there would be a relationship between such species and products of methanol conversion, gas-phase product analysis was not undertaken, primarily due to limitations in the sensitivity of the gas chromatograph available. It is recognised that the inter-relationship between the deposited carbonaceous species and the gas-phase products of reaction is an important parameter and future efforts should be directed towards elucidating this.

References

- [1] F. Bauer, H. Karge, *Molecular Sieves* 5 (2007) 249
- [2] D. Haynes, A. Campos, M. Smith, D. Berry, D. Shekhawat, J. Spivey, *Catalysis Today* 154 (2010) 210
- [3] M. Janik, B. Bardin, R. Davis, M. Neurock, *Journal of Physical Chemistry B* 110 (2006) 4170
- [4] H. Karge, *Studies in Surface Science and Catalysis* 137 (2001) 707
- [5] L. Rollmann, *Journal of Catalysis* 47 (1979) 113
- [6] S. Bhatia, J. Beltramini, D. Do, *Catalysis Reviews Science and Engineering* 31 (1990) 431
- [7] J. Haw, W. Song, D. Marcus, J. Nicholas, *Accounts of Chemical Research* 36 (2003) 317
- [8] U. Olsbye, M. Bjorgen, S. Svelle, K. Lillerud, S. Kolboe, *Catalysis Today* 106 (2005) 108
- [9] M. Pareira, J. Orfao, J. Figuerido, *Applied Catalysis A: General* 218 (2001) 307
- [10] M. Bjorgen, S. Svelle, F. Joensen, J. Nerlov, S. Kolboe, F. Bonino, L. Polumbo, S. Bordig, U. Olsbye, *Journal of Catalysis* 249 (2007) 195
- [11] K. Patrilyak, L. Patrilyak, V. Ivanenko, M. Okhrimenko, Y. Voloshina, *Theoretical and Experimental Chemistry* 46 (2010) 256
- [12] Y. Chua, P. Stair, *Journal of Catalysis* 213 (2003) 39

- [13] C. Li, P. Stair, *Catalysis Today* 33 (1997) 353
- [14] D. Mores, J. Kornatowski, U. Olsbye, B. Weckhuysen, *Chemistry-A European Journal* 17 (2011) 2874
- [15] Y. Jiang, J. Huang, V. Reddy Marthala, Y. Ooi, J. Weitkamp, M. Hunger, *Microporous and Mesoporous Materials* 105 (2007) 132
- [16] M. Muhler, R. Schlogl, G. Ertl, *Surface Science* 189 (1987) 69
- [17] B. Sexton, A. Hughes, D. Bibby, *Journal of Catalysis* 109 (1988) 126
- [18] M. Callejas, M. Martinez, T. Blasco, E. Sastre, *Applied Catalysis A: General* 218 (2001) 181
- [19] H. Schulz, Z. Siwei, W. Baumgartner, *Studies in Surface Science* 34 (1987) 479
- [20] B. Barman, L. Skarlos, D. Kushner, *Energy and Fuels* 11 (1997) 593
- [21] B. Li, R. Gonzalez, *Catalysis Letters* 54 (1998) 5
- [22] H. Abdullah, A. Hauser, F. Ali, A. Al-Adwani, *Energy and Fuels* 20 (2006) 320
- [23] J. Afonso, M. Schmal, R. Frety, *Fuel Processing Technology* 41 (1994) 13
- [24] M. Bjorgen, S. Akyalcin, S. Benard, S. Kolboe, S. Svelle, *Journal of Catalysis* 275 (2010) 170
- [25] M. Guisnet, P. Magnoux, *Applied Catalysis* 54 (1989) 1
- [26] M. Uguina, D. Serrano, R. van Grieken, S. Venes, *Applied Catalysis A: General* 99 (1993) 97
- [27] A. de Lucas, P. Canizares, A. Duran, A. Carrero, *Applied Catalysis A: General* 156 (1997) 299
- [28] D. Bibby, N. Milestone, J. Patterson, L. Aldridge, *Journal of Catalysis* 97 (1986) 493
- [29] M. Rozwadowski, J. Wioch, K. Erdmann, J. Kornatowski, *Collection of Czechoslovak Chemical Communications* 57 (1992) 959

- [30] D. Ma, Y. Shu, X. Han, X. Liu, Y. Xu, X. Bao, *Journal of Physical Chemistry B* 105 (2001) 1786
- [31] J. Xia, D. Mao, N. Xu, Q. Chen, Y. Zhang, Y. Tang, *Chemistry Letters* 33 (2004) 1456
- [32] J. Kuhn, J. Gross, J. Jansen, F. Kapleijn, P. Jansens, *From Zeolites to Porous MOF Materials. The 40th anniversary of international zeolite conference.* 170 A (2007) 942.
- [33] S. Campbell, X. Juang, R. Howe, *Microporous and Mesoporous Materials* 29 (1999) 91
- [34] S. Jackson, J. Hargreaves, *Metal Oxide Catalysis* Wiley (2009) 705
- [35] C. Baerlocher, L. McCusker, D. Olsen, *Atlas of Zeolite Framework Types.* (2007) 6
- [36] <http://izasc.ethz.ch/fmi/xsl/iza-sc/sbulist.htm> (accessed on 31/03/2011)
- [37] <http://izasc.mirror.la.asu.edu/fmi/xsl/iza-sc/ft.xml> (accessed on 31/03/2011)
- [38] www.iza-online.org (accessed on 31/03/2011)
- [39] www.bza.org/zeolites.html (accessed on 31/03/2011)
- [40] www.britannica.com/ebchecked/topic/121782/clinoptilolite (accessed on 31/03/2011)
- [41] R. Argauer, G. Candolt, US Patent 3702886 (1972)
- [42] B. Gates, *Catalytic Chemistry*, Wiley (1992) 458
- [43] H. van Bekkum, E. Flannigan, J. Jansen, *Introduction to Zeolite Science and Practice*, Elsevier (1991) 754
- [44] Y. Sugi, *Journal of the Japan Petroleum Institute* 53 (2010) 263
- [45] M. Guisnet, L. Costa, F. Ramoa Ribeiro, *Journal of Molecular Catalysis A: Chemical* 305 (2009) 69
- [46] J. Huang, Y. Jiang, V. Reddy Marthala, A. Bressel, J. Frey, M. Hunger, *Journal of Catalysis* 263 (2009) 277
- [47] P. Venuto, E. Habib Jr. M. Dekker, *Fluid Catalytic Cracking with Zeolite Catalysts* (1979)
- [48] M. Ocelli, J. Olivier, A. Auroux, *Journal of Catalysis.* 209 (2002) 385

- [49] V. Dimitriadis, A. Lappas, I. Vasalos, *Fuel*. 77 (1998) 1377
- [50] T. Tsai, S. Liu, I. Wang, *Applied Catalysis A: General*. 181 (1999) 355
- [51] M. Seiler, U. Schenk, M. Hunger, *Catalysis Letters* 62 (1999) 139-145
- [52] I. Dahl, S. Kolboe, *Journal of Catalysis* 149 (1994) 458
- [53] S. Thompson, G. Webb, *Journal of the Chemical Society Chemical Communications* 13 (1976) 526
- [54] D. Teschner, J. Borsodi, A. Wootsch, Z. Revay, M. Havecker, A. Knop-Genricke, S. Jackson, R. Schlögl, *Science* 320 (2008) 86
- [55] G. Bond, *Catalysis Reviews* 50 (2008) 532
- [56] A. Benamar, Z. Beckhet, Y. Boucheffa, A. Miloudi, *Comptes Rendus Chimie* 12 (2009) 706
- [57] D. Ivanov, V. Sobolev, G. Panov, *Applied Catalysis A: General* 241 (2003) 113
- [58] F. Bauer, H. Ernst, E. Geidel, R. Schudel, *Journal of Catalysis* 164 (1996) 146

2 Experimental

2.1 Materials

The zeolite used for each reaction was 100% ammonium ion exchanged mordenite (supplied by Zeolyst) where the silicon to aluminium ratio was 10. Prior to the methanol or dimethyl carbonate only reactions, 0.3g of the catalyst was activated *in-situ* under 30ml min⁻¹ of argon (BOC, 99.999%) at 500°C for 60 minutes. Prior to carbonylation reactions, 2.6g of the mordenite was activated *in-situ* under 50ml min⁻¹ of nitrogen (BOC, 99.999%) at 500°C for 60 minutes. Pre-treatment (activation) was undertaken to yield the proton form of the zeolite. Reactions were employed investigating different materials which included 55% exchanged (by aluminium content) copper mordenite with a unit cell composition of $[(\text{NH}_4^+)_{3.6} (\text{Cu})_{4.4} (\text{H}_2\text{O})_{24} | \text{Al}_8\text{Si}_{40}\text{O}_{96}]$ (supplied by BP), γ -alumina (supplied by BP) and MCM-41 aluminosilicate (SiO_2 (98.75%) Al_2O_3 (1.25%) (Sigma-Aldrich)).

2.2 Material characterisation

2.2.1 Elemental analysis

The total weight percentage of carbon, hydrogen and nitrogen was determined for fresh and spent catalysts. This was performed via combustion analysis using an Exeter analytical CE-440 analyser. This technique was kindly performed by Mrs Kim Wilson at the University of Glasgow.

2.2.2 Nitrogen adsorption isotherms

Nitrogen physisorption isotherms were measured at liquid nitrogen temperature. The experiments were undertaken on a Micrometrics Gemini BET machine. Prior to analysis, samples were degassed overnight using helium (BOC 99.999%) at 110°C to remove adsorbed moisture and gases. The BET method was applied for surface area determination.

2.2.3 Powder x-ray diffraction

Powder x-ray diffraction patterns were obtained using a Siemens D5000 x-ray diffractometer employing a monochromatised CuK α source (1.5418 Å) operating at 40 kV and 40mA. Scans were run in the range 5-80° 2 θ with a counting time of 1s per step and a step size of 0.02°.

2.2.4 Thermogravimetric analysis

Thermogravimetric analysis (TGA) was undertaken on a TA instruments Q500. The temperature was ramped from 20 to 1000°C at 10°C min⁻¹. Analysis was undertaken under air (BOC). Typically 8 mg of sample was used and the gas flow was set to 50 ml min⁻¹.

2.2.5 Thermogravimetric analysis coupled with mass spectrometry

Experiments were performed on a Thermo Quest SDT Q600 combined TGA/DSC analyser coupled to an ESS evolution mass spectrometer. The temperature was ramped from 20 to 1000°C at 10°C/min. Typically 10 mg of sample was loaded and the gas flow set to 50 ml min⁻¹. For inert atmospheres Ar, (BOC 99.999% purity) was used. 2% O₂ in balance Ar (BOC 99.998% purity) was used for oxidative atmospheres. Mass spectrometry was operated in multiple ion detection mode (MID mode), whereby specific ions were selected prior to analysis and recorded every 7°C up to 1000°C. Ions were generated via electron ionization and filtered accordingly by charge, where anionic species were removed and cationic species were analysed.

2.2.6 Thermal volatilisation and Sub-ambient thermal volatilisation analysis

Thermal volatilisation analysis (TVA) and sub-ambient thermal volatilisation analysis (SATVA) were undertaken on a number of samples.

100mg of sample was pumped to vacuum overnight on the TVA system (Figure 2.2.1) prior to analysis. The purpose for this procedure was the reduction of background levels of carbon

dioxide and water within the system. Initial experiments were undertaken where the samples were heated to 1000°C at 10°C min⁻¹ and held isothermally at 1000°C for twenty minutes with continual cryogenic collection of evolved volatiles. Sub-ambient differential distillation was performed on the collected volatiles by heating the primary cold trap from -195°C to 30°C. The volatiles were collected in four secondary cold traps and transferred to IR and GC-MS sample cells. The separated volatiles were analysed via a combination of MS and GC-MS.

Mass spectrometry was carried out online with a Hiden 1-300 amu VG single quadrupole Q300D mass spectrometer, operating in continual scan mode with a 10% sample split going to the spectrometer.

All GC-MS analyses were carried out using a Finnigan Thermo Quest capillary column trace GC and Finnigan Polaris Quadrupole Mass Spectrometer which scanned an m/z range of 30 to 650. The GC column was programmed with a temperature ramp from 40 to 320°C at a rate of 20°C min⁻¹, with a helium carrier gas. Cold ring fractions were removed from the sample tube and dissolved in chloroform, whilst the higher molar mass products were collected for GC-MS analysis from the primary cold trap.

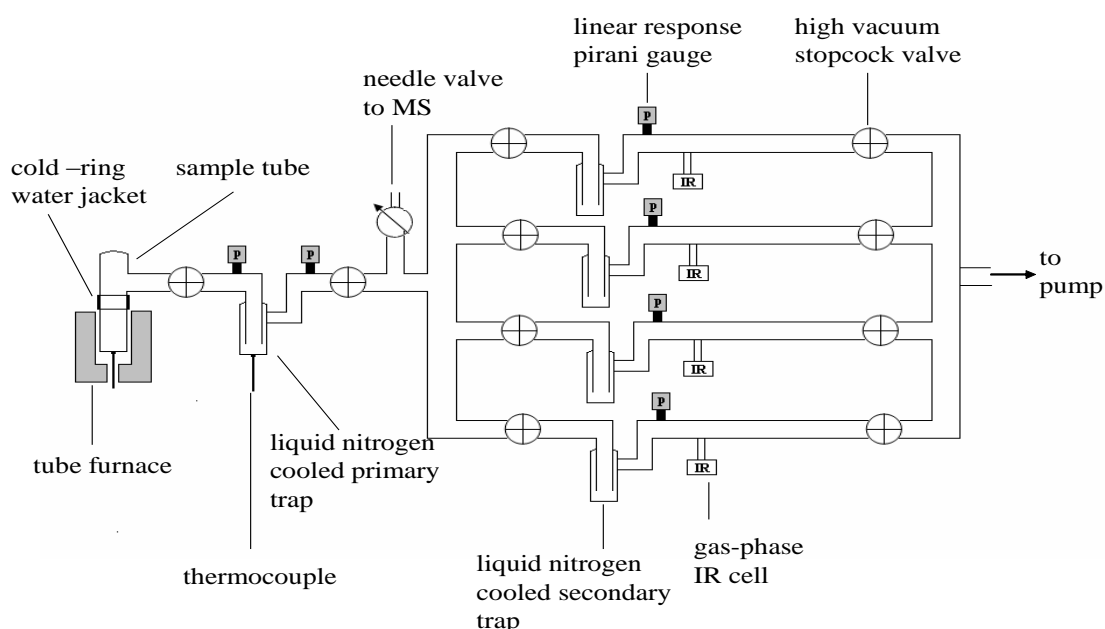


Figure 2.2.1: A simplified diagram of the TVA system.

Other experiments were undertaken to complement the experiments performed above which corresponded to temperatures where evolved non-condensable gases were observed:

1. The samples were ramped from 20°C to 265°C at 10°C min⁻¹ and held isothermally at 265°C for 20 minutes with continual cryogenic collection.
2. The samples were ramped from 20°C to 660°C at 10°C min⁻¹ and held isothermally at 660°C for 20 minutes with cryogenic collection between 265°C and 660°C.
3. The samples were ramped from 20°C to 1000°C at 10°C min⁻¹ and held isothermally at 1000°C for 20 minutes with cryogenic collection between 660°C and 1000°C.

2.2.7 MAS NMR spectroscopy

All solid state NMR spectroscopic investigations were undertaken at the EPSRC service at the University of Durham, ¹³C measurements were carried out using a Varian VNMRS spectrometer equipped with a 9.40 T magnet, operating at 100.56 MHz for ¹³C and 399.88 MHz for ¹H. Spectral referencing was undertaken with respect to neat tetramethylsilane. A 4 mm (rotor outer diameter) magic angle spinning probe was used for ¹³C enriched samples and a 6 mm (rotor outer diameter) magic angle spinning probe for non-enriched samples. Talc was added to samples (1:1) with low hydrogen content to enhance the signals observed in cross polarisation experiments. Due to friction arising from the rotation of the rotor, samples in the 4 mm rotor were at approximately 30°C during analysis and samples in the 6 mm rotor were at 50°C.

Cross polarisation (CP) occurs via the transfer of magnetization from abundant/sensitive nuclei to dilute/less sensitive nuclei (for example ¹H to ¹³C). For this to work however there must be dipolar coupling between the protons and the nuclei of interest (¹³C).

Experimentally, polarisation transfer is achieved by simultaneously applying radiofrequency irradiation to ¹H and ¹³C (for a duration called the contact time). For efficient polarisation transfer the spins of the abundant and dilute nuclei must precess, under irradiation, at the same rate, i.e.

$$\gamma^H B_1^H = \gamma^C B_1^C$$

where γ is the magnetogyric ratio and B_1 is the radiofrequency field strength. This is known as the Hartmann-Hahn matching condition.

The build up of the carbon signal for cross polarisation can be defined as:

$$S(t) = S_0(1 - e^{-t/\tau_c}) e^{-t/T_{1\rho}^H}$$

where:

$S(t)$ = carbon signal intensity with contact time t

S_0 = maximum obtainable signal intensity in the absence of relaxation

τ_c = cross polarisation rate (rate of signal build up) $T_{1\rho}^H$ = proton spin lattice relaxation time in the rotating reference frame

Cross polarisation measurements have two main advantages over direct excitation ones.

In a direct excitation measurement the repetition rate (recycle delay) (NMR spectra result from the co-addition of the results from many repetitions of the NMR pulse) is determined by the relaxation time of the ^{13}C (here) and this can be very long (minutes). In a cross-polarisation measurement the repetition rate is determined by the relaxation of the ^1H and this is usually significantly less than that for ^{13}C . This means more repetitions of the pulse sequence can be made in any given time in a cross polarisation experiment and this yields a higher signal-to-noise ratio in the spectrum.

There is also a signal gain (over direct excitation) using cross polarisation. At best this can be equal to $\gamma^H/\gamma^C \sim 4$. This equates to a sixteen-fold saving in experiment time for cross polarisation over direct excitation.

However, the intensities in cross-polarisation spectra reflect the strength of dipolar coupling between ^1H and ^{13}C . The carbon in a CH or CH_2 unit in a rigid solid (strong coupling) is represented well in a CP spectrum but the same carbon in a mobile/soft solid (weak coupling) will be underrepresented (or even absent altogether). Similarly, carbon remote from a proton (weak coupling) will also be underrepresented (or absent) in a CP spectrum. In a direct-excitation spectrum, with an appropriate (long) delay between repetitions all the carbon in a sample should be visible (with quantitative intensities).

Two key instrument parameters for cross polarisation experiments are:

- Recycle delay: The delay between successive repetitions of excitation/acquisition, which allows the sample to return to its equilibrium state (relaxation). For cross polarisation experiments the delay is dependent upon the relaxation time of the abundant nuclei and is typically a few seconds (In this instance a 1 s delay was used).
- Contact time: The period during which magnetisation is transferred from the abundant nuclei to the dilute nuclei (In this instance a 1 ms contact time was used).

The recycle delay was optimised by performing a series of experiments with different delays. The shortest delay where no saturation (loss of signal) was observed was used to record the spectrum. The contact time was selected to give maximum signal based on a series of measurements with different contact times.

The optimised parameters for each series of experiments are given below:

Cross polarisation spectra of non-enriched samples were obtained using a 1 s delay, a 1 ms contact time, a sample spin rate of 6.8 kHz and 'TOSS' spinning sideband suppression. 1700 to 20000 repetitions were accumulated.

Direct polarisation spectra of ^{13}C enriched samples were obtained following a 90° pulse (4.0 μs duration) with a 120 s recycle delay, at a spin rate of 14.0 kHz. 352 to 3600 repetitions were accumulated.

Solid state NMR ^{27}Al and ^{29}Si experiments were carried out using a Varian Unity Inova spectrometer equipped with a 7.05 T magnet, incorporating a 5 mm rotor o.d. probe, operating at 59.56 MHz for ^{27}Al and 104.20 MHz for ^{29}Si . Spectral referencing was undertaken with respect to 1 molar $\text{AlCl}_3(\text{aq})$ and neat tetramethylsilane. Samples were at approximately 50°C during analysis.

Silicon cross polarisation spectra were obtained using 1 s recycle delay, 3 ms contact time and a sample spin rate of 5.0 kHz. 1314 to 7000 repetitions were accumulated.

Silicon direct polarisation spectra were obtained following a 90° pulse (4.0 μs duration) with a 30 s recycle delay, at a spin rate of 5.0 kHz. 812 to 2000 repetitions were accumulated.

Aluminium direct polarisation spectra were obtained following a 25° pulse (1.0 μ s duration) with a 0.2 s recycle delay at a spin rate 14.0 kHz. 6600 to 18600 repetitions were accumulate

2.3 Material coking and coke removal

2.3.1 Methanol-only reactor specification

Reactions were performed in a fixed bed plug flow reactor operated at ambient pressure. The reactor tube was made of quartz with the dimensions of 12 mm outer diameter, 10 mm internal diameter and which was approximately 220 mm in length. It contained a frit to support the powdered catalyst. All reactor lines were constructed from stainless steel. The quartz reactor tube was connected to the stainless inlet and outlet lines via Ultra Torr O-ring fittings which resulted in an air tight seal. All gas lines contained a pressure regulator and a non-return valve. Argon flow rates were regulated via rotameters and flow rates were calibrated with a bubble meter for accuracy. Liquid methanol (Aldrich, 99.8% purity) or dimethylcarbonate (Sigma, 99% purity) were fed via a Knauer K-501 HPLC pump and vaporised using lines trace heated with heating tape to 150°C. The vapour was subsequently blended with argon to ensure a consistent gas mixture and a smooth flow of methanol or dimethylcarbonate over the catalyst bed. A feed rate of 0.03 ml min⁻¹ liquid methanol or 0.06 ml min⁻¹ liquid dimethylcarbonate was used. The reactor tube was heated using a ceramic tube furnace and the temperature was controlled with a West 4400 temperature control unit and a K-type thermocouple placed in a quartz thermalwell in contact with the reaction bed. A simplified schematic diagram of the reactor is shown in Figure 2.3.1. For safety reasons, a bursting disk was used to ensure that in the event of blockage or regulator failure the quartz tube was not exposed to high pressure. To further protect the reactor tube, a trip thermocouple was utilised to prevent overheating and this was connected to the temperature controller.

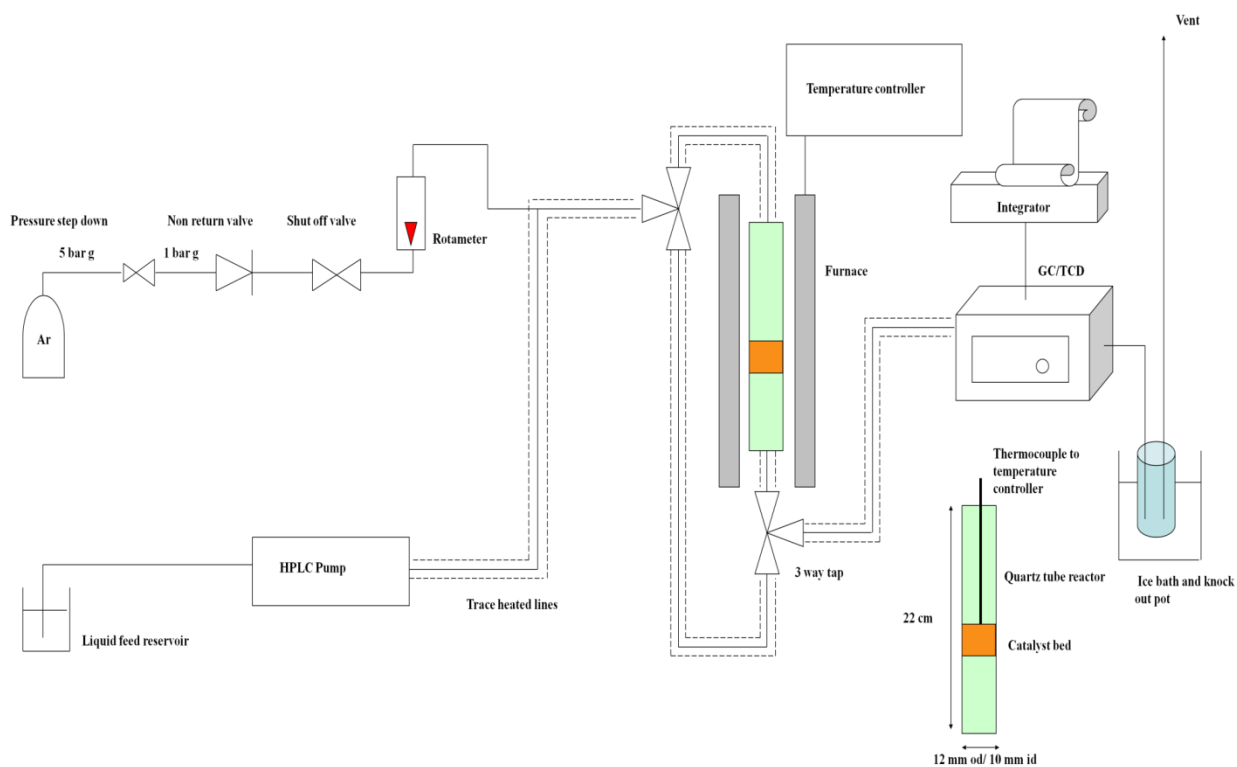


Figure 2.3.1 A simplified diagram of the atmospheric micro reactor.

2.3.2 Methanol-only and dimethylcarbonate-only reactions

The reactor lines were brought up to a temperature of 150°C. The material (0.3g) was loaded and activated in the reactor using the conditions described in the materials section. After activation, the zeolite was allowed to cool to reaction temperature and then isolated employing a by-pass line. The liquid feed was purged through the HPLC pump and the gas/liquid lines. The HPLC pump was then set to 0.03 ml min⁻¹ for methanol (MeOH) or 0.06 ml min⁻¹ for dimethylcarbonate (DMC). This was mixed with 30 ml min⁻¹ of argon (BOC, 99.999%) diluent. After 30 minutes to allow the flow rate to stabilise, the zeolite was exposed to the gaseous feed stream.

The reactor shut down procedure was performed in the following order:

1. The HPLC pump was shut down leaving the zeolite exposed to 30 ml min⁻¹ of argon.
2. The furnace was shut down and the material cooled under the flow of argon.
3. When the temperature of the reactor reached 25°C or below the argon flow was switched off and the coked sample was removed from the reactor tube.

2.3.3 Carbonylation reactor specification

Reactions were performed in an atmospheric pressure fixed bed plug flow carbonylation reactor at BP Chemicals' research laboratory. The reactor tube was made of quartz with dimensions of 23mm outer diameter, 20mm internal diameter and was approximately 700mm in length. It contained a frit to support the powdered catalyst. Gas lines were constructed from rubber tubing. Liquid was fed via a B/Braun Perfusor Compact S syringe drive into the top of the reactor tube. The quartz reactor tube was connected to a glass top piece with a gas inlet and a septum pierced with a long needle connected to the feed syringe. A round bottomed flask was attached to the bottom of the tube and was used to trap condensable liquids and solids. A side arm was attached to allow gases to vent off. Gas flows were regulated via rotameters and checked with a bubble meter for accuracy prior to reaction. Liquid methanol (Aldrich, 99.8%) or dimethylcarbonate (Sigma, 99%) was fed via a syringe drive pump and vaporised at the top of the reactor tube. A feed rate of 0.045ml min^{-1} for liquid methanol or 0.094ml min^{-1} for liquid dimethylcarbonate was used. The reactor tube was heated via a ceramic clamshell tube furnace and the temperature was controlled with a Eurotherm 2416 temperature control unit. A simplified schematic diagram of the reactor is shown in Figure 2.3.2.

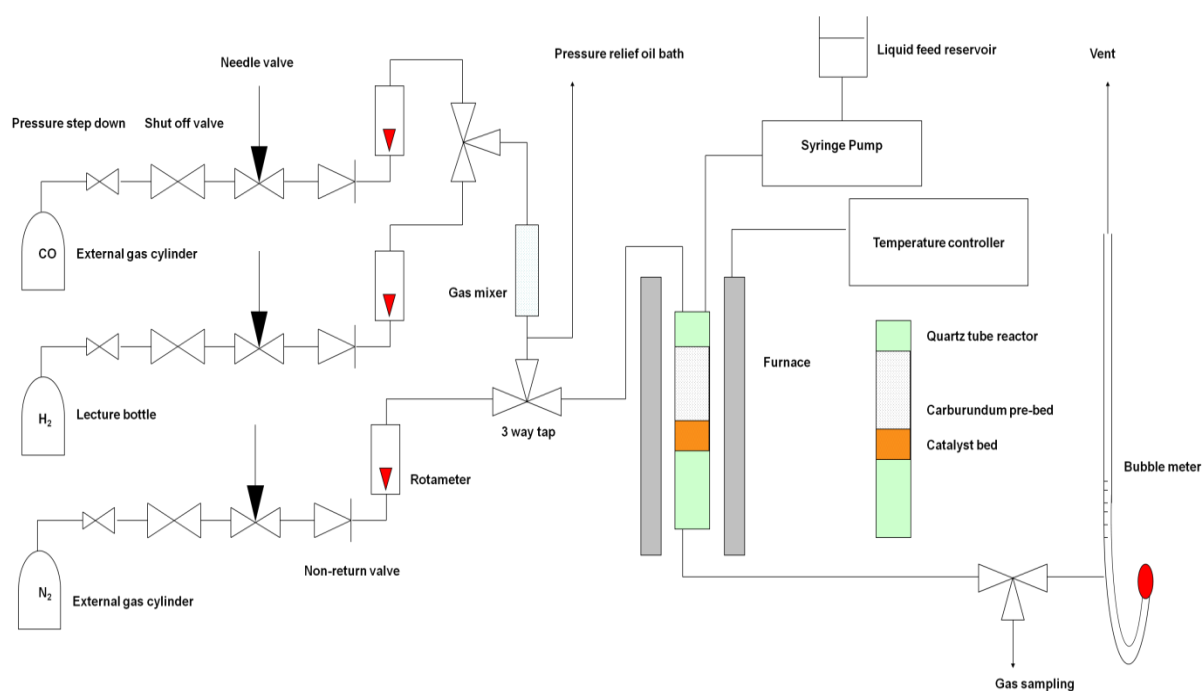


Figure 2.3.2 A simplified diagram of the atmospheric pressure carbonylation micro reactor.

2.3.4 Methanol and dimethylcarbonate carbonylation reactions

The zeolite (2.6g) was loaded with a carborundum (Fischer) pre-bed (90 ml). Mordenite was activated in the reactor using the conditions described in the materials section. After activation, the material was allowed to cool to reaction temperature. The gas stream was switched from 50 ml min⁻¹ of nitrogen (BOC, 99.999%) to 180 ml min⁻¹ of carbon monoxide (BOC, 99.9%) and 45 ml min⁻¹ of hydrogen (BOC, 99.995%). An in-line gas mixer was used to mix the carbon monoxide and hydrogen thoroughly prior to entering the reactor tube. A 60 ml syringe and long needle was filled with liquid feed and attached to the syringe drive. The syringe drive was then set to 0.045 ml min⁻¹ for methanol or 0.094 ml min⁻¹ for dimethylcarbonate. Flow rates were determined for gases using a bubble meter prior to reaction. The syringe drive was primed and started at the prescribed flow rate, exposing the catalyst to the mixed feed stream.

The reactor shut down procedure was performed in the following order:

1. The liquid feed was stopped leaving the sample under flowing carbon monoxide and hydrogen.
2. The heater was immediately turned off and the gas stream was switched to 50 ml min⁻¹ nitrogen.
3. The material was cooled under flowing nitrogen.
4. When the temperature of the reactor reached 25°C or below the nitrogen stream was switched off and the coked sample was removed from the reactor tube.

2.3.5 Ageing effects

In order to eliminate concerns over potential delay between the preparation and analysis of samples, routine re-analysis of select samples was performed periodically over an extended period of approximately one year. No effects of ageing were observed.

2.3.6 Steaming reactor specification

Reactions were carried out in an atmospheric pressure fixed bed plug flow steaming reactor. The reactor tube was made of quartz and had a 12mm outer diameter and 10mm internal diameter and was approximately 400mm in length. Quartz wool was used to support the powdered mordenite. Gas and liquid lines were all constructed from stainless steel. The quartz reactor tube was connected to the inlet and outlet lines via ultra torr O-ring fittings which resulted in an air tight seal.

All connected gas lines contained a pressure regulator and a non-return valve. Gas flows were regulated via a mass flow controller and checked with a digital flow meter and a bubble meter for accuracy. The reactor tube was heated using a Carbolite tube furnace and control unit. A simplified schematic diagram of the reactor is shown in Figure 2.3.3. An ice cooled knock-out pot was used to capture condensables. For safety reasons, a bursting disk was used to ensure that the quartz tube was not exposed to high pressure.

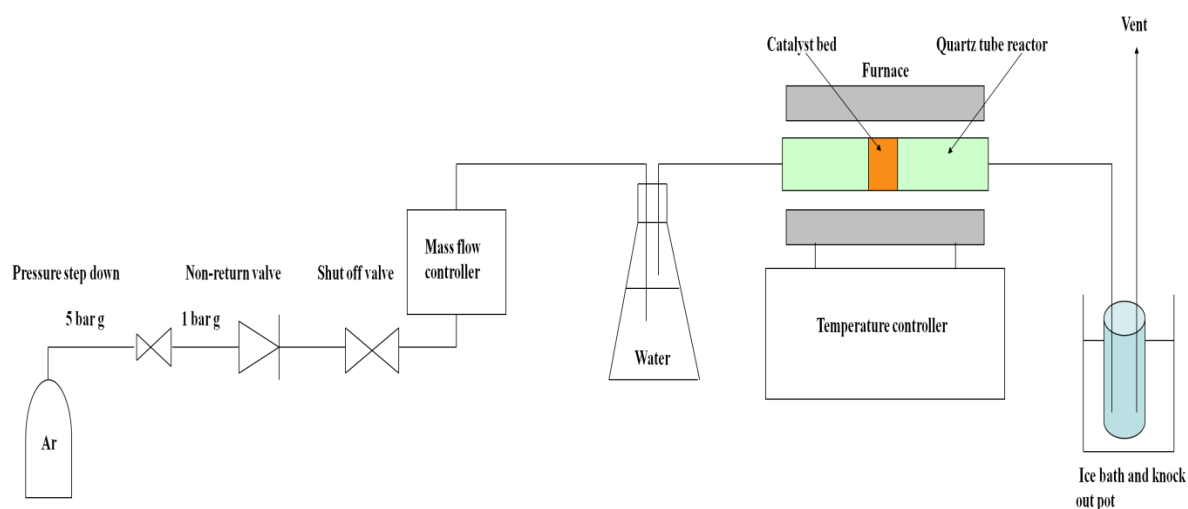


Figure 2.3.3 A simplified diagram of the steaming regeneration reactor.

2.3.7 Steaming coked materials generated with a methanol-only feed

The coked catalyst (0.05g) was loaded and plugged with quartz wool. 60ml min⁻¹ argon (BOC, 99.999%) was bubbled through the water at room temperature and passed over the catalyst bed. The furnace was set to 350°C with a ramp rate of 10°C min⁻¹. The procedure was undertaken for 18 hours. The flow of argon was measured using a bubble meter prior to and after reaction. The liquid was collected in a knock out pot and the pH checked. In some instances the flow rate used was 10 ml min⁻¹, the time on line was 24 hours and the temperature used was 750°C.

3 Carbonaceous species deposited from methanol-only feedstreams

3.1 Introduction

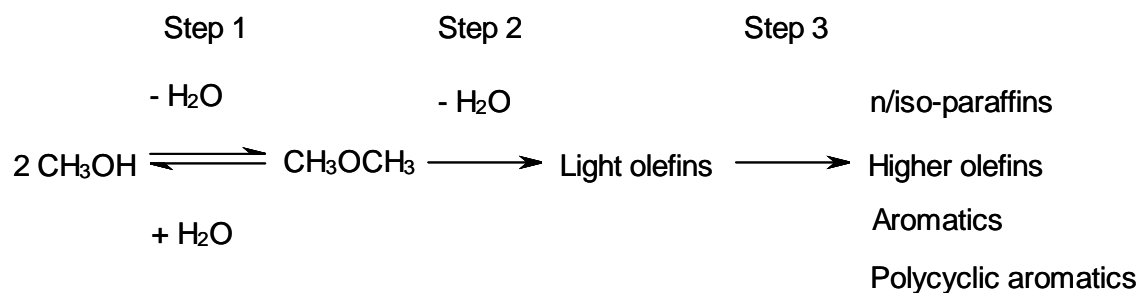
In this chapter, the nature and reactivity of the carbonaceous species generated by reaction of mordenite and other materials with methanol containing feeds is described. This has obvious parallels with the methanol to hydrocarbon reaction studied over zeolites and related systems and, accordingly, some of this literature is briefly summarised.

The methanol to hydrocarbons (MTH) reaction is more commonly known as the methanol to gasoline (MTG) reaction. The discovery of MTG in the early 1970's was accidental and took place at Mobil Central Research Laboratories, while workers were attempting to develop a new process for making high-octane gasoline from methanol and isobutane utilizing Mobil's newly developed zeolite catalyst ZSM-5. Mass balance showed that none of the isobutane was consumed, and that the same products were obtained with a methanol-only route [1]. This discovery was patented in 1975 and disclosed in the literature in 1977 [2].

On the basis of this discovery Mobil commercialized the methanol to gasoline (MTG) process at a plant in New Zealand which ran from 1986 producing 600,000 tonnes a year of gasoline and which supplied approximately one third of the nation's gasoline demand per annum [3, 4]. At a later date the gasoline production section of the plant was closed down due to the decreased cost of gasoline and a subsequent increase in the cost of methanol. The latter led to the methanol production section being retained and it is still currently in operation [4, 5].

A simplified version of the MTG process, as shown in Reaction Scheme 3.1.1 (Overleaf) has three steps where:

- i. methanol is initially dehydrated to dimethyl ether (DME). This results in an equilibrium mixture of methanol, dimethyl ether and water.
- ii. this equilibrium mixture is converted to light olefins in the C_2 - C_4 range.
- iii. the mixture of light olefins is converted to paraffins, aromatics, polycyclic aromatics and higher olefins $> C_4$.



Reaction Scheme 3.1.1: The main reaction steps involved in MTH chemistry (reproduced from [4]).

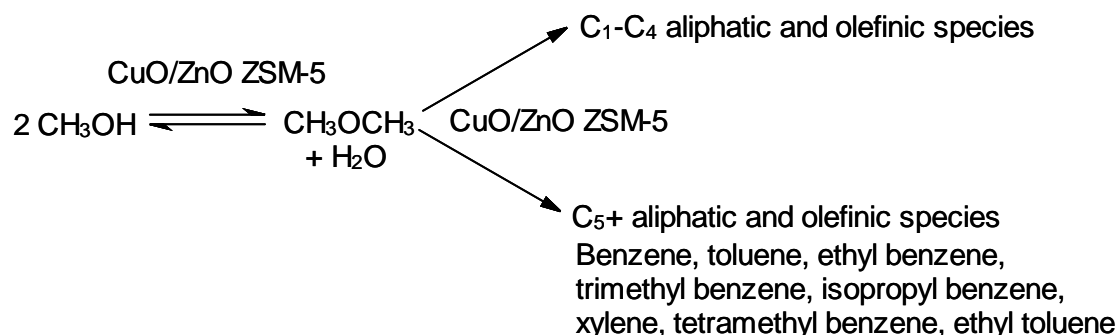
For example Zaidi *et al.* [6] demonstrated a very diverse product distribution (Reaction Scheme 3.1.2) employing a CuO/ZnO containing ZSM-5 catalyst from a methanol containing feedstream at 400°C and atmospheric pressure. It was found that this system under these conditions favoured the formation of aromatic species and longer chain hydrocarbon species (C₅+)

Fougerit *et al.* [7] employed a mordenite system mixed with a kaolinite binder at 530°C and 1 bar total pressure using a mixture of dimethyl ether and water to eliminate the exothermic response caused by the conversion of methanol to these initial products. They observed that at low dimethyl ether conversions C₃-C₆ alkenes are favoured, whereas at higher conversions propylene is the favoured product with ethylene and aromatic species appearing in relatively large quantities. The overall reaction is presented in Reaction Scheme 3.1.3.

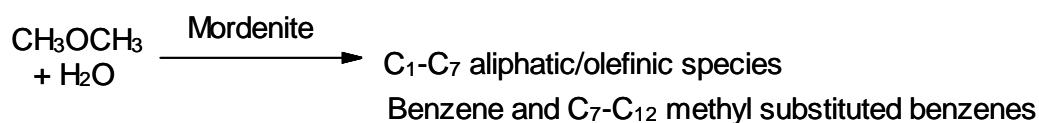
The process may be further simplified by removing the third step from the reaction scheme and collecting the low olefinic products. This is commonly referred to as the methanol to olefins (MTO) process. In general, in this case, ZSM-5 is replaced by SAPO-34 to optimise olefinic yields [8, 9].

The first step “methanol dehydration” in the reaction scheme is very well documented and is observed to readily occur over a wide variety of solid acid catalysts [10]. The initial stage involves dehydration of the methanol at an acid site forming water and a surface bound methoxy intermediate. The intermediate undergoes nucleophilic attack by methanol to regenerate the acid site and produce the product DME [4].

The third step forming a mixture of products proceeds via traditional carbocation mechanisms with concurrent hydrogen transfer [4].



Reaction Scheme 3.1.2: Product spectrum produced from methanol over CuO/ZnO ZSM-5 at 400°C and atmospheric pressure (adapted from [6]).

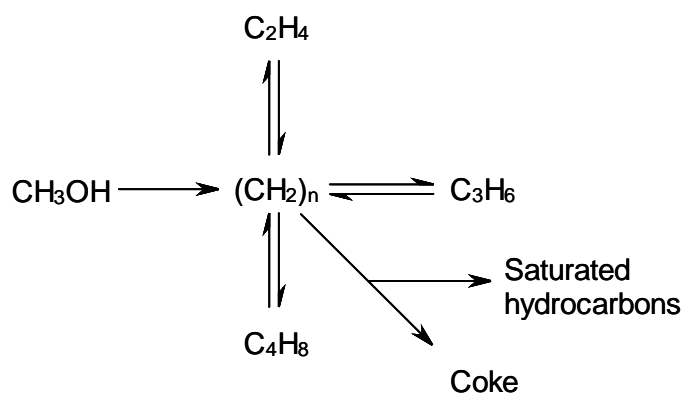


Reaction Scheme 3.1.3: Product spectrum produced from methanol over MOR mixed with kaolinite at 530°C and 1 bar pressure (adapted from [7]).

The formation of the initial carbon to carbon bonds is described in step two and is considered to be significantly more complex in assigning a mechanism than the other two. It has been an area of an immense amount of research resulting in a large number of mechanisms being proposed (at least 20 to date) [1, 4]. Five proposals have dominated the others in terms of the volume of literature and attention that they have previously received [4]:

1. The oxonium ylide mechanism
2. The carbene mechanism
3. The carbocationic mechanism
4. The free radical mechanism
5. The hydrocarbon pool mechanism

The hydrocarbon pool mechanism is a comparatively modern theory first proposed by Dahl and Kolboe in the early nineties, while studying MTH using a SAPO-34 to increase the yield of olefinic products (MTO) [11, 12]. A simplified reaction scheme (Reaction Scheme 3.1.2) was suggested by Dahl and Kolboe [11, 12] which did not take into account the form of the hydrocarbon pool species.

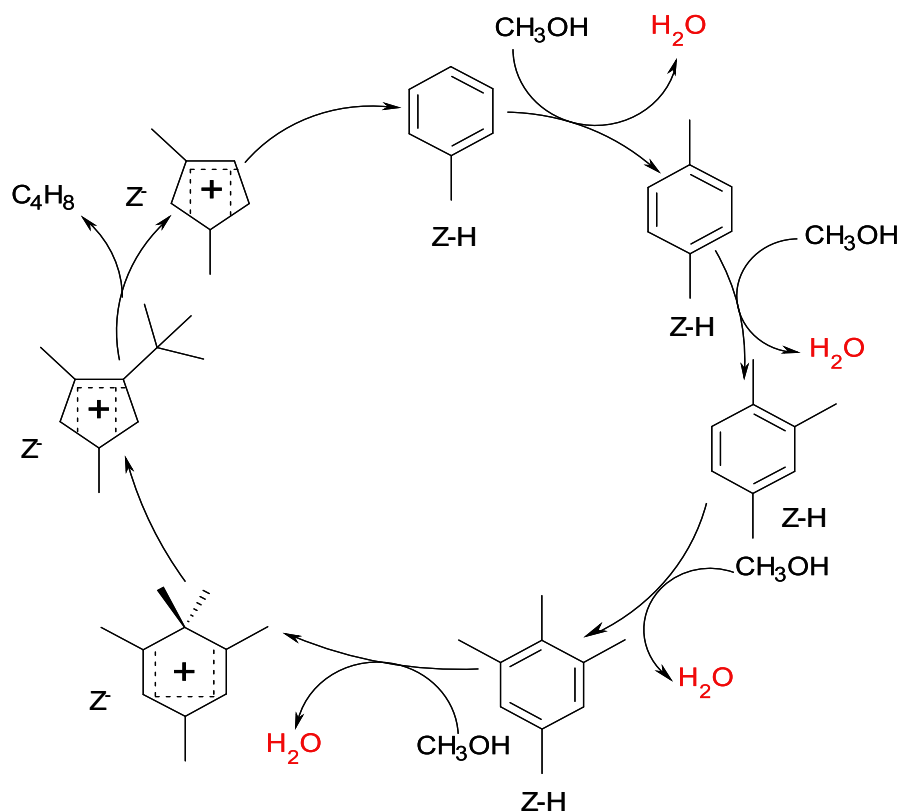


Reaction Scheme 3.1.4: The first description of the hydrocarbon pool mechanism (reproduced from [12]).

Many studies have been undertaken by various research groups in an attempt to elucidate the nature of the hydrocarbon pool. Over the years a consensus has been reached where many authors agree that the species are in the form of poly-methyl benzenes [1, 8, 9, 13]. These studies have concentrated upon the conventional MTH and MTO catalysts ZSM-5 and SAPO-34. Recently Bjorgen *et al.* [14] undertook a study examining a multitude of different framework types, in an attempt at offering a general description of the hydrocarbon species regardless of framework type. They were able to determine by using a methanol and benzene mixed feedstream that zeolite beta, MCM-22 and mordenite exhibit the same hydrocarbon species as those observed in SAPO-34 studies.

By linking experimental results and theoretical studies, Lesthaeghe *et al.* [15] were able to offer a general hydrocarbon pool mechanism (Reaction scheme 3.1.3). They suggested that toluene could undergo multiple methylation and deprotonation stages resulting in the formation of a carbocation. The carbocation could then undergo a ring contraction and eliminate isobutene. The resultant carbocation ring could expand and deprotonate resulting in toluene.

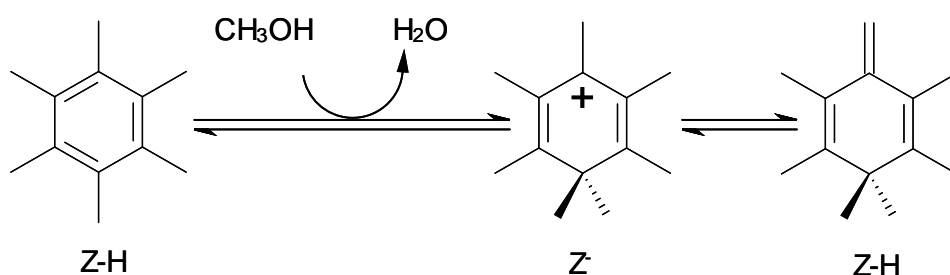
Although the above only describes lower order methyl benzenes, recent research by Kolboe *et al.* has suggested the viability of higher order methyl-benzenes in this process. Penta- and hexa-methyl benzenes may undergo a similar process, where C₂-C₄ products split off through a series of complex rearrangements and dealkylation reactions resulting in lower order methyl substituted aromatic species remaining. This is commonly referred to as the paring route [14, 16, 17].



Reaction scheme 3.1.5: The proposed hydrocarbon pool mechanism for the production of C₄ olefinic products from lower order methyl benzenes (reproduced from [15]).

Another route has been proposed involving a methyl substituted aromatic carbocation species which may deprotonate forming an exocyclic double bond. Methylation of the double bond can then occur, resulting in the formation of alkyl side chains. Elimination of this side chain would produce an olefin (Reaction scheme 3.1.4). This is known as the side chain methylation route [14, 18, 19].

As with most hydrocarbon conversion reactions, the catalyst undergoes deactivation due to coke deposition. Li and Stair observed that in USY, aromatic species (presumably similar to hydrocarbon pool species) aggregate to form pre-graphite in the cages with increasing reaction temperature [20].



Reaction scheme 3.1.6: Side chain methylation route for hexa-methyl benzene to hexamethylmethylenecyclohexadiene through a carbocation transition state (reproduced from [14]).

Park *et al.* observed an increased rate of deactivation for mordenite catalysts with a relatively large acid site density with increasing reaction time. Alkyl aromatics were observed to condense to larger polycyclic aromatic species with larger acid site density mordenites. By decreasing the acid site density by approximately 25x it was observed that a sustained MTH reaction could be achieved with minimal deactivation [21].

Bjorgen and co-workers showed that methylnaphthalenes formed in SAPO-34 cages retain a degree of reactivity in the MTO process, but they have been identified as coke precursors in other studies [9, 22, 23]. It is demonstrated that the formation of bicyclic molecules and the formation of alkenes occur at roughly the same temperature. This suggests that coke formation is directly linked to the formation of the desired olefins [14].

This was also supported by Haw and Marcus who describe the aging of methyl naphthalenes to phenanthrene. They may also age further still to pyrene losing all methyl groups [24]. This is an example of aging in a relatively unrestrained environment resulting in “polycyclic plates”, whereas in more confined conditions such as the pores of ZSM-5, the aging of these species would be expected to proceed in a different manner producing “polycyclic chains” [25].

On basis of the above literature, it can be envisaged that the interaction of methanol with mordenite may result in a range of different deposited carbonaceous species of varying complexity. This has been investigated as both a function of reaction temperature and time on stream. Comparisons have also been drawn with other materials.

3.2 Results and discussion

3.2.1 Temperature dependence of the form of carbonaceous species deposited

In order to determine the effect of reaction temperature on the type, nature and location of the carbonaceous deposits formed from reaction with methanol-only, mordenite was activated at 500°C for 60 minutes under a 30 ml min⁻¹ argon gas stream. They were run for 300 minutes in a 45% methanol feedstream at a GHSV of 3000 hr⁻¹ at reaction temperatures of 300 and 500°C. Spent materials were cooled to room temperature under an argon flow.

Solid state ¹³C MAS NMR spectroscopy using direct polarisation was undertaken in an attempt to elucidate the nature of the carbonaceous residues formed. Two 25% ¹³C enriched samples generated at 300 and 500°C respectively were investigated. The spectra are presented in Figure 3.2.1. The ¹³C NMR spectrum of the sample generated at 300°C shows a very broad distribution of species. Peak assignments can be made upon the basis of previously published literature studies. It is noticeable that all peaks have broadened significantly compared to those observed in liquid NMR spectra indicating restricted mobility of the carbonaceous deposits. The signal at 19 ppm can be assigned to methyl groups associated with aromatic species [1]. The signals at 26 ppm and 35 ppm appear to be consistent with trapped aliphatic hydrocarbons [26]. The signal at 49 ppm is associated with methanol and the signal at 56 ppm with zeolite surface bound methoxy species [27]. The signal present at 129 ppm indicates the presence of alkyl substituted aromatics [1, 28] and, due to the broadening evident in Figure 3.2.1, it can be assumed to be a spectrum of closely related products [29]. The signal at 111 ppm is an artefact of the measurement associated with the Teflon rotor cap used in the experiment. The signal at 26 ppm may also be attributed to methyl groups present on polycyclic aromatic species [29] and a shoulder evident at approximately 138 ppm indicates the presence of polycyclic aromatic species [28]. Undertaking ¹H MAS NMR

results in very broad convoluted signals offering very little information on the proton environments present on the coked mordenite system and so this procedure was not undertaken further.

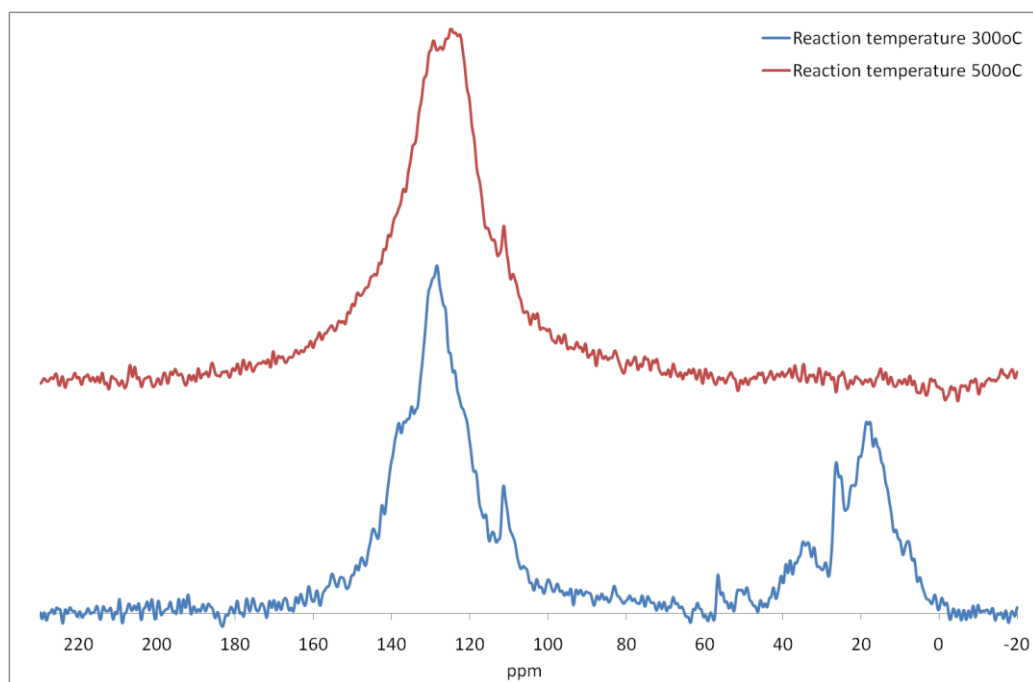


Figure 3.2.1: ^{13}C DP MAS NMR spectrum of coked mordenite generated with 25% ^{13}C enriched methanol at different reaction temperatures for 300 minutes.

The ^{13}C NMR spectrum of the sample generated at 500°C in Figure 3.2.1 is found to be very different than that observed for the sample coked at 300°C . No high field signals are observed associated with methyl species, products or methanol. Only two signals are observed at 111 ppm and 123 ppm. As with the sample generated at 300°C , the signal at 111 ppm is attributed to the Teflon rotor cap. The disappearance of the signals at high field indicates a change in the carbonaceous deposits which suggests they are higher order polycyclic aromatic compounds [30].

The ^{13}C MAS NMR demonstrates that the samples generated at 300 and 500°C have very different speciations of carbonaceous deposits post-reaction. Therefore the amount of carbon and hydrogen present on each spent material was investigated via elemental analysis, in an

attempt to elucidate the effect of reaction temperature on the carbon content and hydrogen deficiency of the carbonaceous residue.

Elemental analysis revealed that the sample generated at 300°C contained 12.3 wt% carbon and had a H:C atomic ratio of approximately 1.2. The sample generated at 500°C had a carbon content of 17.6 wt% and a atomic H:C atomic ratio of approximately 0.4. Samples were analysed within seven days of reaction and no correction for the effects of adsorbed water were performed. It was therefore expected that the corrected H:C ratios would be more hydrogen deficient than those quoted above.

On the basis of the elemental analysis it was observed that the increase in reaction temperature results in an increase in the carbon content of the spent mordenite. The increase in the hydrogen deficiency supports the observations in the ^{13}C solid state NMR spectra.

Thermogravimetric analysis (TGA) was undertaken to probe the differences in the reactivity of the carbonaceous deposits which are anticipated on the basis of the ^{13}C NMR and elemental analysis. Overlaid derivative mass data for 300 and 500°C reaction temperature are presented for air in Figure 3.2.2.

The first derivative TGA profile for the sample generated at 300°C shows four peaks observed centering at 70, 325, 425 and 625°C. The peak at 70°C is attributed to water desorption. The peaks observed at 325, 425 and 625°C are attributed to the removal of carbonaceous species. The feature at 325°C is shown to be real later in this chapter when undertaking TGA with online mass spectrometry.

The first derivative TGA profile for the sample generated at 500°C shows two peaks observed centering at 125 and 625°C. The peak at 125°C is attributed to water desorption. The peak observed at 625°C is attributed to the removal of carbonaceous deposits.

The peak at 125°C in the case of the sample generated at 500°C has shifted with respect to that observed for the 300°C post-reaction sample. This may be as a consequence of the changes in the speciation of the deposits between the two samples observed in solid state NMR.

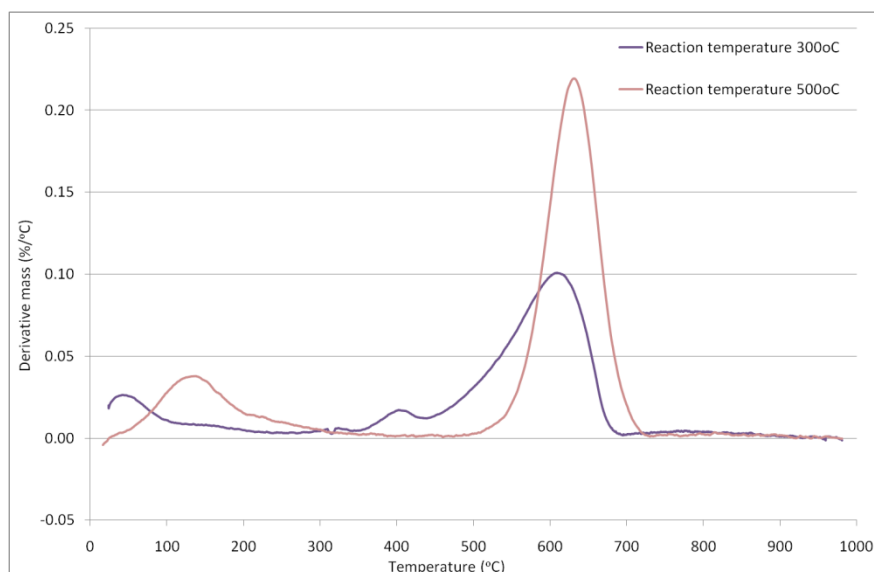


Figure 3.2.2: First derivative TGA profile attained under air of coked mordenite generated with methanol at different reaction temperatures for 300 minutes.

The solid state NMR spectroscopic studies, elemental analysis and TGA under air revealed a stark contrast between the nature of deposits formed at 300 and 500°C under the methanol to hydrocarbon regime. As such, further additional samples were generated at temperatures in the range 150 to 500°C at 50°C intervals in an attempt to develop a thorough understanding of the role of reaction temperature has on the nature of the residue.

Solid state ^{13}C MAS NMR using cross polarisation was undertaken on four non-enriched post-reaction samples generated at 150, 250, 300 and 500°C. In the case of the sample reacted at 500°C due to the lack of hydrogen, an equivalent mass of talc had to be added to the sample to ensure a reasonable signal for cross polarisation. The spectra are presented in Figure 3.2.3.

The ^{13}C CP MAS NMR spectrum of the sample generated at 150°C shows one broad signal present at 126 ppm which is consistent with the formation of aromatics [31]. The spectrum has a low signal to noise ratio due to the relatively small amount of carbon present on the mordenite and hence no other peak assignments have been made, although may possibly be a feature centered at *ca.* 175 ppm present.

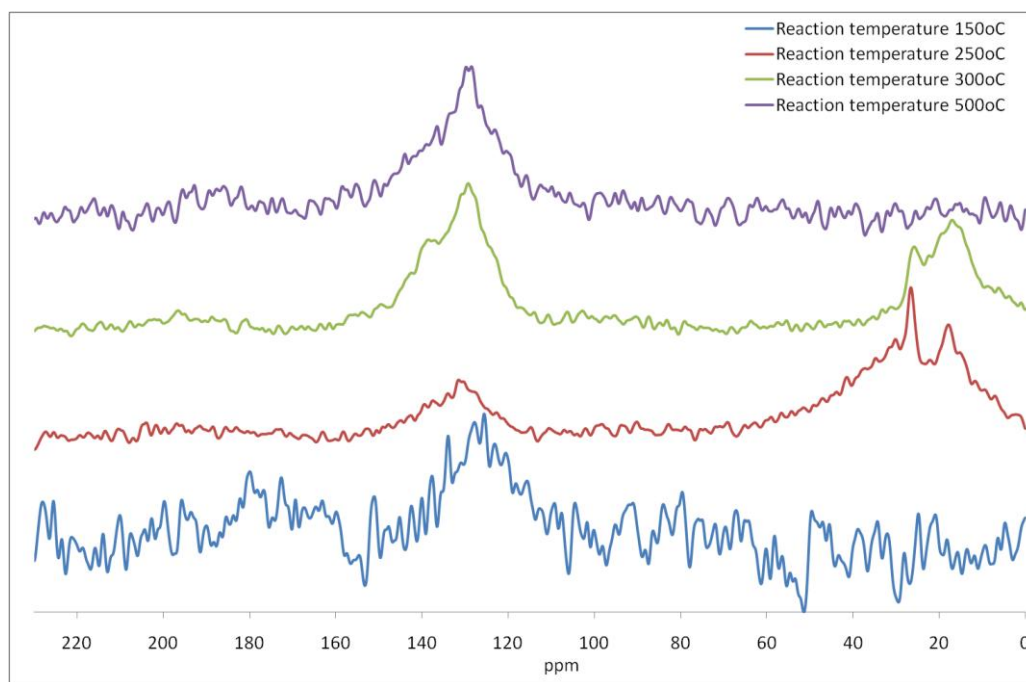


Figure 3.2.3: ^{13}C CP MAS NMR spectrum of coked mordenite generated with methanol at different reaction temperatures for 300 minutes.

The ^{13}C CP MAS NMR spectrum of the sample generated at 250°C shows three signals at *ca.* 18, 26 and 132 ppm. The former two signals are fairly sharp resonances superimposed on a broader background. The high field signal present at 18 ppm is associated with methyl groups present on methylated benzenes. The low field peak at 132 ppm is indicative of methyl substituted benzenes [32]. The peak present at 26 ppm could be an indication of retained alkane hydrocarbons as well as methylated polycyclic species [26, 29].

The ^{13}C CP MAS NMR spectrum of the sample generated at 300°C shows four signals at *ca.* 17, 26, 129 and 136 ppm. The signal seen at 17 ppm can be associated with the methyl groups present on methyl substituted aromatics [28, 32]. A broad signal is observed centering at 129 ppm with a shoulder *ca.* 138 ppm. Both signals represent alkyl substituted aromatics possibly with different degrees of substitution. The peak at 26 ppm is coincident with not only alkanes [26] but also with methyl substituted polycyclic aromatics such as alkyl substituted naphthalene [29]. This is supported by the observed range of aromatic carbon.

There is a significant increase in the relative intensity of the aromatic peak compared to that observed in the instance of 250°C. Due to the nature of the cross polarisation technique and the small increase in the amount of carbon observed via CH analysis it is apparent that the

resultant increase could be due to an increase in the amount of alkyl substituted aromatics. Hence an increase in the amount of hydrogen present would enhance the carbon signals [33].

The ^{13}C CP MAS NMR spectrum of the sample generated at 500°C and mixed 1:1 by wt% with talc shows only a single broad peak present at 129 ppm with a shoulder present at approximately 138 ppm. The addition of talc was undertaken to increase the number of protons present in an attempt to increase the signal for cross polarisation. The NMR data in this instance indicates that the methyl substituted aromatics observed in the samples generated at 250 and 300°C are no longer present due to the lack of signals normally observed between 17 and 19 ppm. It can be speculated that the shifts are also coincident with polycyclic aromatics [29] and the broad peak allows a degree of flexibility with respect to the assignment of the true form of the species. This is in good agreement with the CH data which indicates a large amount of carbon (17.6wt%) present on the post-reaction sample.

Elemental analysis was undertaken to determine the amount of carbon and hydrogen on the materials following reaction. The carbon content and the atomic H:C ratios are presented in Figure 3.2.4 and Figure 3.2.5 for the various reaction temperatures employed.

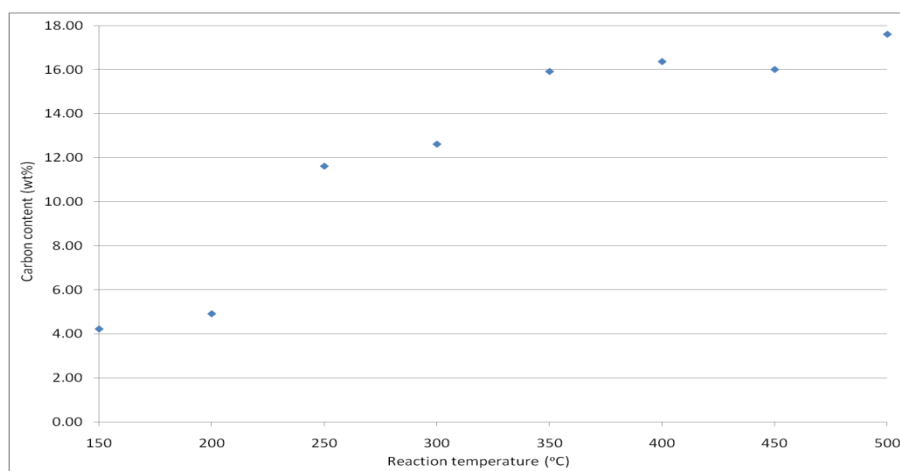


Figure 3.2.4: Carbon content of coked mordenite generated with methanol at different reaction temperatures for 300 minutes.

In Figure 3.2.4 it can be observed that as the reaction temperature increases from 150 to 350°C the quantity of carbon deposited increases from 4.0 to 16.0 wt%. Between 350 and 450°C the carbon content plateaus at approximately 16.0 wt%, from 450 to 500°C the carbon content increases from 16.0 to 17.6 wt%. It was observed that reproducibility of measurements of the carbon content for the samples generated at 150 and 200°C was very poor. This may be in part due to the bed profile observed post-reaction with different degrees of coking occurring along the bed. At higher temperatures, no apparent bed profile was observed and as such the reproducibility of the carbon contents improved significantly.

In Figure 3.2.5 it can be observed that the H:C atomic ratio decreases from approximately 3.5 at 150°C to 1.7 and 1.3 at 250 and 300°C respectively. Thereafter it decreases further to approximately 0.4 at 500°C. The ^{13}C CP MAS NMR demonstrates that the samples contain a relatively large complex spectrum of products and any H:C atomic ratio is going to be an average of all present species. Due to the uncorrected water content of the samples the H:C atomic ratios may be quite far out in terms of the 'real' ratio. But information may still be drawn from this data which suggests that the carbon species become more hydrogen deficient as the reaction temperature is increased, which is confirmed to a degree by the solid state NMR data. It is also the case that the hydrophobicity of the systems may be altered by the difference in nature of the carbonaceous species present.

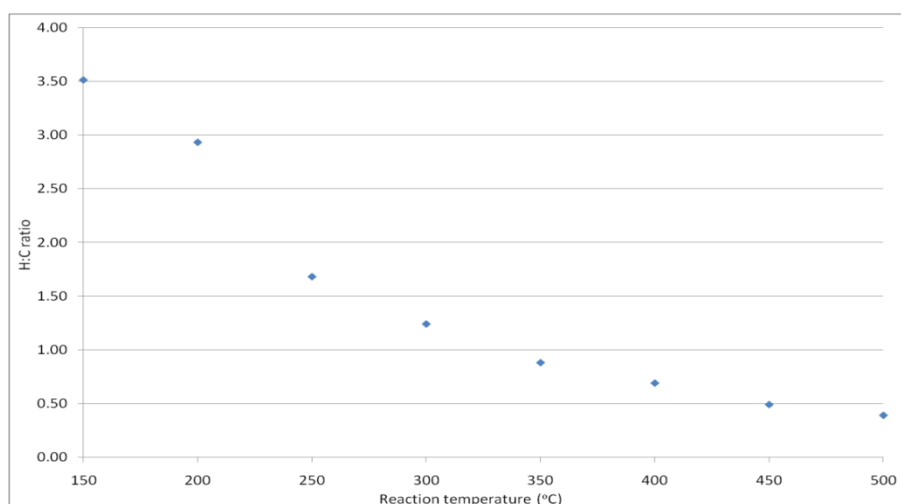


Figure 3.2.5: H:C atomic ratios of coked mordenite generated with methanol at different reaction temperatures for 300 minutes (not corrected for the influence of adsorbed water).

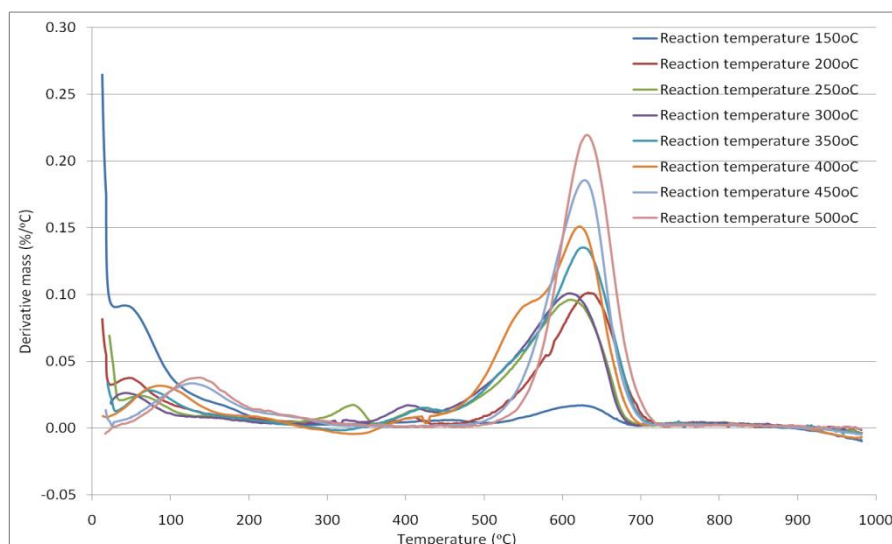


Figure 3.2.6: First derivative TGA profiles attained under air of coked mordenite generated with methanol at different reaction temperatures for 300 minutes.

Thermogravimetric analysis was undertaken to probe the differences in reactivity between the carbonaceous deposits formed at different reaction temperatures. Overlaid first derivative TGA profiles for the various reaction temperatures employed are presented in Figures 3.2.6 (measurements undertaken in air), 3.2.7 (measurements undertaken in 2% O₂/Ar) and 3.2.8 (measurements undertaken in Ar). The same temperature ramp rate (10°C/min) was used in all cases.

In Figure 3.2.6 it can be observed that for post-reaction material generated at reaction temperatures 150 and 200°C a similar first derivative TGA profile under air is observed, displaying a peak at 60°C and a very broad peak centering at approximately 625°C. This indicates that both samples contain water, as well as mixture of aromatic species as assigned in the ¹³C solid state NMR of the sample generated at 150°C.

Samples generated at 250, 300 and 350°C display a very similar first derivative TGA profiles exhibiting peaks centering at 80, 325, 425 and 625°C. The peak at 80°C is attributed to water and the peaks at 325, 425 and 625°C is attributed to the removal of the carbonaceous species present which, according to the ¹³C MAS NMR data for post 250 and 300°C coking, are in the form of aromatic, methyl substituted aromatic, polycyclic and methyl substituted polycyclic species. The peak at 625°C is associated with the bulk of the deposit and is believed to be present in the pores of the zeolite [34].

The post-reaction sample coked at 400°C exhibits a first derivative TGA profile showing peaks centering at 90, 425, 525 and 625°C. The peaks at 90 and 625°C are associated with water and higher order aromatic, polycyclic and their alkyl substituted derivatives trapped in the pores [34]. As a result of the increase in the amount of polycyclic and alkyl substituted polycyclic species, a peak at 525°C becomes visible as a shoulder indicating the presence of higher order polycyclic aromatic species possibly forming on the external surface.

As the reaction temperature is increased further to 450 and 500°C, only two peaks are observed in both instances centering at 125 and 625°C. The peak present at 125°C is attributed to water. The peak at 625°C is associated with the presence of polycyclic aromatic species based upon the assignments made in the solid state NMR spectrum of the sample generated at 500°C.

The peak at 125°C has shifted significantly from that observed at *ca.* 80°C at higher reaction temperatures compared to those at 250-350°C, and this may be as a consequence of the change in the amount and nature of the carbonaceous residues. Currently this trend which is reproducible cannot be readily explained.

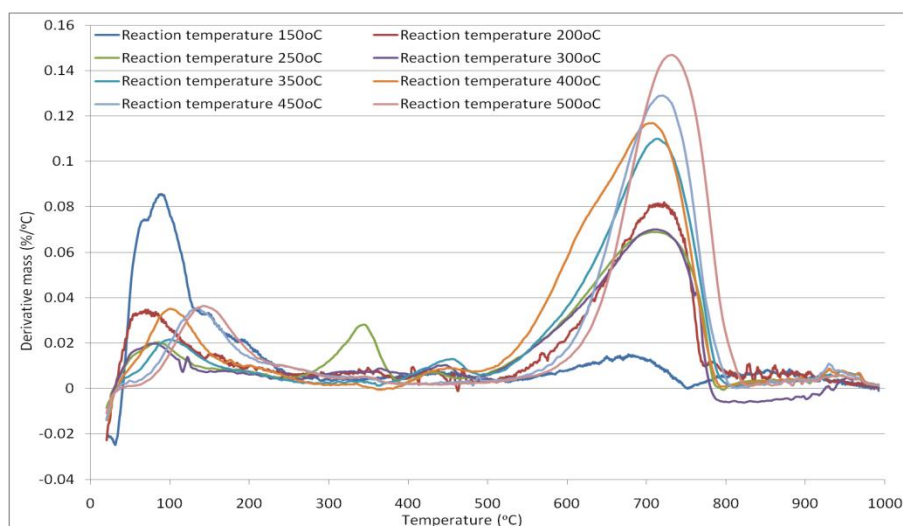


Figure 3.2.7: First derivative TGA profiles attained under 2% O₂/Ar of coked mordenite generated with methanol at different reaction temperatures for 300 minutes.

It can be observed in Figure 3.2.7 that, in all instances, very similar first derivative TGA profiles are observed for all samples under 2% O₂/Ar as under air. The peak associated with water and the peaks previously observed at 325 and 425°C in Figure 3.2.6 have shifted by approximately 25°C. This would appear to be a systematic effect. The peak at 625°C in Figure 3.2.6 has been shifted by 100°C. This is a kinetic effect caused by the change in the oxygen concentration.

Online mass spectrometry was undertaken to determine which gases were evolved from the sample during thermal analysis under different atmospheres. Mass spectrometry data is presented for the various reaction temperatures employed. Tables 3.2.1 and 3.2.2 present data for 2% O₂/Ar. In some cases unique mass to charge ratios were scanned, whereas in others multiple fragments were used for the identification of products.

Given the evolved species observed in Tables 3.2.1 and 3.2.2 arise from the carbonaceous residue on the mordenite, it is apparent that cracking processes as well as combustion are occurring. When looking at the thermal analysis data for both air and the 2% O₂ mixture, the temperature was seen to increase significantly for the higher temperature peak in the 2% O₂ regime. Cracking and combustion products are observed in this region suggesting that the reactivity of the carbonaceous material differs markedly. This may indicate that incomplete combustion occurs and as such leaves a species present that can actively crack to form some of the observed species.

The material coked at 250°C shows a large range of evolved products indicating that at this reaction temperature the carbonaceous residue consists mainly of active hydrocarbon pool species such as toluene, xylenes, tri- and tetra-methyl benzenes. Incomplete and deactivated forms of the hydrocarbon pool may be present at this temperature but not to the same extent as those observed for material generated at other temperatures.

Product	MeOH-only 150	Temp (°C)	MeOH-only 200	Temp (°C)	MeOH-only 250	Temp (°C)	MeOH-only 300	Temp (°C)
Hydrogen	Y	350	Y	450	Y	350	Y	450
Water	Y	100 350 725	Y	150 350 725	Y	125 350 450 725	Y	125 450 725
Carbon monoxide	N	N/A	Y	350 725	Y	350 450 650	Y	450 625
Carbon dioxide	Y	350 725	Y	450 725	Y	350 450 725	Y	450 725
Methane	N	N/A	Y	350	Y	350	Y	350 725
Ethene	N	N/A	N	N/A	Y	350	Y	350
Ethane	N	N/A	Y	450 725	Y	350 450 725	Y	450 725
Propene	N	N/A	N	N/A	Y	350	Y	350
Propane	N	N/A	N	N/A	Y	350	Y	350 450
Butene	N	N/A	Y	350	Y	350	Y	350
Butane	Y	350	Y	725	Y	350	Y	350
Benzene	N	N/A	N	N/A	Y	350	N	N/A

Table 3.2.1: Evolved gas mass spectrometry under 2% O₂/Ar of coked mordenite generated with methanol at 150, 200, 250 and 300°C for 300 minutes (products have been identified by examining unique fragments and fragment patterns).

Product	MeOH-only 350	Temp (°C)	MeOH-only 400	Temp (°C)	MeOH-only 450	Temp (°C)	MeOH-only 500	Temp (°C)
Hydrogen	Y	450	Y	450	N	N/A	N	N/A
Water	Y	125 450 725	Y	125 450 725	Y	150 725	Y	150 750
Carbon monoxide	Y	450 650	Y	450 650	Y	725	Y	675
Carbon dioxide	Y	450 725	Y	450 725	Y	725	Y	750
Methane	Y	350 725	Y	350 725	Y	725	Y	750
Ethene	Y	350 450	Y	350 450	Y	725	Y	675
Ethane	Y	450 725	Y	450 725	Y	675	Y	750
Propene	N	N/A	N	N/A	N	N/A	N	N/A
Propane	N	N/A	N	N/A	N	N/A	N	N/A
Butene	N	N/A	N	N/A	N	N/A	N	N/A
Butane	N	N/A	N	N/A	N	N/A	N	N/A
Benzene	N	N/A	N	N/A	N	N/A	N	N/A

Table 3.2.2: Evolved gas mass spectrometry under 2% O₂/Ar of coked mordenite generated with methanol at 350, 400, 450 and 500°C for 300 minutes (products have been identified by examining unique masses and mass patterns).

An argon atmosphere was used to examine if the residue could be removed in the presence of an “inert” gas. Under the argon atmosphere, as may be expected, the samples exhibit different patterns to those observed under both air and 2% O₂/Ar. The peak associated with water for all reaction temperatures is observed in a similar position as those seen under the 2% O₂/Ar atmosphere. The post-200°C reaction sample exhibits a peak at 325°C. Post 250°C a relatively intense peak is observed at 350°C and a shoulder at 425°C. For the coked mordenite generated at 300°C a very broad peak is seen centering at 400°C. For the sample generated at 350°C, a peak is observed centering at 500°C.

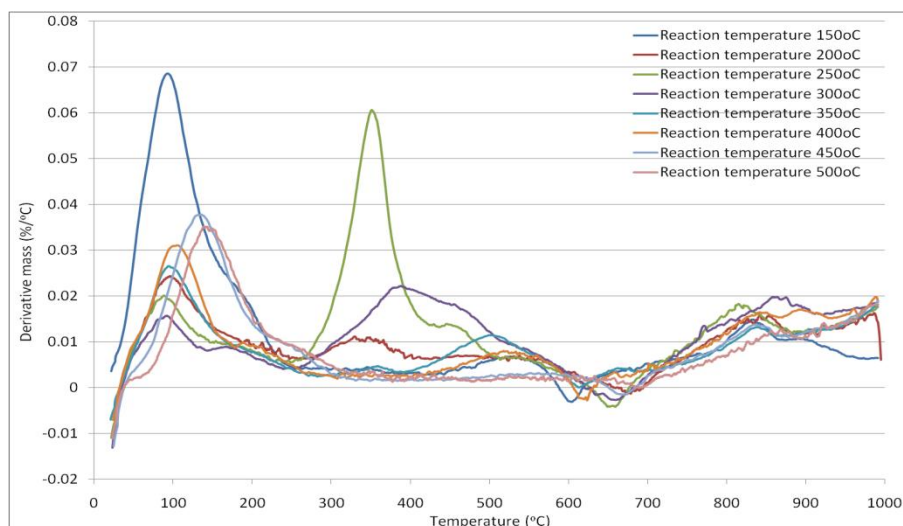


Figure 3.2.8: First derivative TGA profiles attained under argon of coked mordenite generated with methanol at different reaction temperatures for 300 minutes.

In all instances after 600°C a very broad peak is present encompassing the range up to 1000°C. In the case of the sample generated at 150°C a small derivative TGA profile peak is observed at approximately 550°C and the broad peak encompassing the top temperature range starts to plateau around 950°C. It can be observed in Figure 3.2.8 that under argon the mass losses associated with cracking processes occur above the reaction temperature at which they were formed, indicating that they are real and not artefacts formed upon cooling the reactor. At lower reaction temperatures it is apparent that an active form of carbonaceous deposit is present, due to the lower temperature peaks observed for coked mordenite generated at 200, 250, 300 and 350°C respectively. It can be hypothesised that in these instances the active hydrocarbon pool is still present and may undergo further catalysis, involving either lower temperature catalysed cracking reactions, or conversion of the methylated benzene species to a series of olefinic products, methane and a deactivated form of the hydrocarbon pool such as polycyclic aromatic species. At higher temperatures in all instances, a broad first derivative TGA profile peak is observed across a relatively large temperature range. Larger deposits such as polycyclic aromatic species may start to crack to produce hydrogen leaving more hydrogen deficient species present on the mordenite.

Product	MeOH- only 150	Temp (°C)	MeOH- only 200	Temp (°C)	MeOH- only 250	Temp (°C)	MeOH- only 300	Temp (°C)
Hydrogen	Y	600 825	Y	600 825	Y	400 500 825	Y	525 825
Water	Y	125 325	Y	125 325	Y	125	Y	125
Carbon monoxide	N	N/A	N	N/A	N	N/A	N	N/A
Carbon dioxide	N	N/A	N	N/A	N	N/A	N	N/A
Methane	Y	550	Y	325 475	Y	325 475	Y	425
Ethene	N	N/A	Y	325 475	Y	325 475	Y	375 475
Ethane	N	N/A	N	N/A	Y	325	Y	375 525
Propene	N	N/A	Y	350 450	Y	325 475	Y	375
Propane	N	N/A	Y	325	Y	325 450	Y	350
Butene	N	N/A	N	N/A	Y	325	Y	375
Butane	N	N/A	Y	325	Y	325	Y	325
Benzene	N	N/A	N	N/A	Y	350	N	N/A

Table 3.2.3: Evolved gas mass spectrometry under Ar of coked mordenite generated with methanol at 150, 200, 250 and 300°C for 300 minutes (products have been identified by examining unique masses and mass patterns).

Product	MeOH- only 350	Temp (°C)	MeOH- only 400	Temp (°C)	MeOH- only 450	Temp (°C)	MeOH- only 500	Temp (°C)
Hydrogen	Y	575 750	Y	600 750	Y	625 825	Y	825
Water	Y	150	Y	150	Y	175	Y	175
Carbon monoxide	N	N/A	N	N/A	N	N/A	N	N/A
Carbon dioxide	N	N/A	N	N/A	N	N/A	N	N/A
Methane	Y	500	Y	550	Y	550	Y	550
Ethene	Y	500	N	N/A	N	N/A	N	N/A
Ethane	Y	550	N	N/A	N	N/A	N	N/A
Propene	Y	475	N	N/A	N	N/A	N	N/A
Propane	Y	475	N	N/A	N	N/A	N	N/A
Butene	Y	475	N	N/A	N	N/A	N	N/A
Butane	Y	475	N	N/A	N	N/A	N	N/A
Benzene	N	N/A	N	N/A	N	N/A	N	N/A

Table 3.2.4: Evolved gas mass spectrometry under Ar of coked mordenite generated with methanol at 350, 400, 450 and 500°C for 300 minutes (products have been identified by examining unique masses and mass patterns).

The mass spectrometry data presented in Tables 3.2.3 and 3.2.4 corresponds to the thermal analysis data performed under argon. The distribution of products suggests that at reaction temperatures 200, 250, 300 and 350°C the carbonaceous residue is of a form similar to the active hydrocarbon pool detailed in the literature and summarised in the introduction to this chapter, with olefinic products observed in all instances as well as relatively small quantities of benzene present in the instance of 250°C. The materials present crack to form olefinic species from the methylated benzenes, methane from the alkyl groups and hydrogen from aromatic and polycyclic species, leaving largely hydrogen deficient species on the surface of the material. This is in accordance with the species associated with the hydrocarbon pool.

Upon reaction at 150, 400, 450 and 500°C only hydrogen, water and methane were observed as products indicating that at lower temperatures the carbonaceous deposits are not similar to those observed at moderate temperatures. However at higher temperatures the hydrocarbon pool is highly deactivated to the extent where it forms large polycyclic molecules which do not crack completely. The observed methane occurs at the same temperature in all instances (approximately 550°C) indicating that its source is similar. Given that for samples generated at 150 and 500°C respectively no methyl or alkyl groups are observed in the ^{13}C CP MAS NMR spectra, the methane must arise through cracking of the lower order aromatic species.

Samples were retained after performing TGA under argon and reanalysed under air to determine if there were any changes in the materials after the argon treatment. Overlaid first derivative TGA profiles for post Ar TGA treatment determined under air for the 150, 200, 250, 300, 350, 400, 450 and 500°C reaction temperature are presented in Figure 3.2.9.

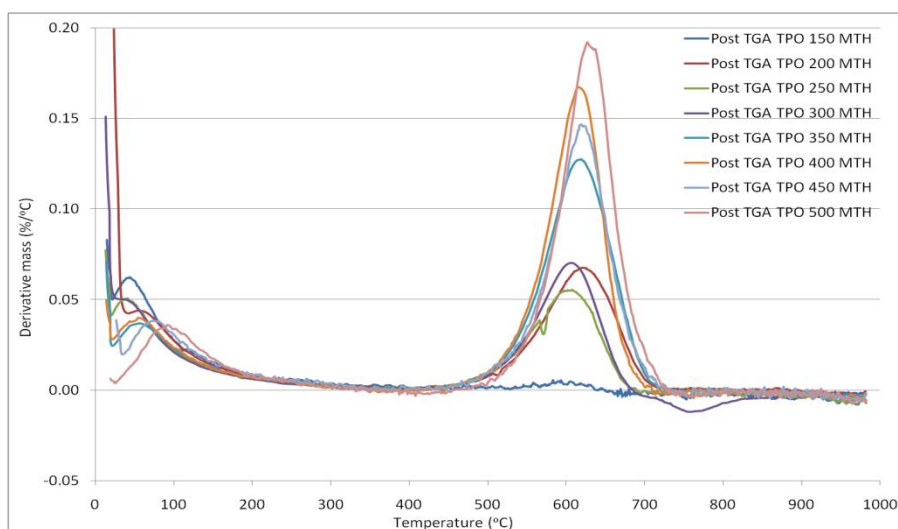


Figure 3.2.9: First derivative TGA profiles attained under air of post Ar TGA of coked mordenite generated with methanol at different reaction temperatures for 300 minutes.

Two peaks are observed for all samples. All other peaks have been lost including the shoulder at 525°C previously observed for the 400°C sample. The sample generated at 300°C exhibits an apparent gain in mass at approximately 750°C which, although reproducible may be an

artefact. In all instances, the observed peaks are attributed to the loss of water and the combustion of carbonaceous deposits. This indicates that the species previously observed at 325, 425 and 525°C, which are no longer present in the first derivative TGA profiles under an air atmosphere, crack readily and which were hence removed under Ar, may still be active as a hydrocarbon pool. This in turn suggests that the higher temperature materials observed at 625°C remain on the whole unchanged due the suspected inactive nature of the residue.

Clearly TGA with online mass spectrometry employing different atmospheres reveals an intricate and detailed picture about the carbonaceous deposits, indicating removal via a variety of processes. Unfortunately very little information can be gleaned about the species deposited on the surface of the mordenite, as the carbonaceous species interact and form different molecules upon heating and through the influence of gases. It was observed under the argon atmosphere that processes such as cracking and/ or volatilisation appear to occur at both lower and higher temperatures.

Thermal volatilisation analysis was undertaken in an attempt to examine the species evolved upon heating the coked mordenite samples generated at 300 and 500°C.

Thermal volatilisation analysis incorporating on-line mass spectrometry and off-line GCMS was utilised as an alternative to TGA to look at products generated thermally from the material under vacuum. Two samples were investigated the first was generated with methanol at 300°C for 300 minutes; the data is presented in Figures 3.2.10 - 3.2.12.

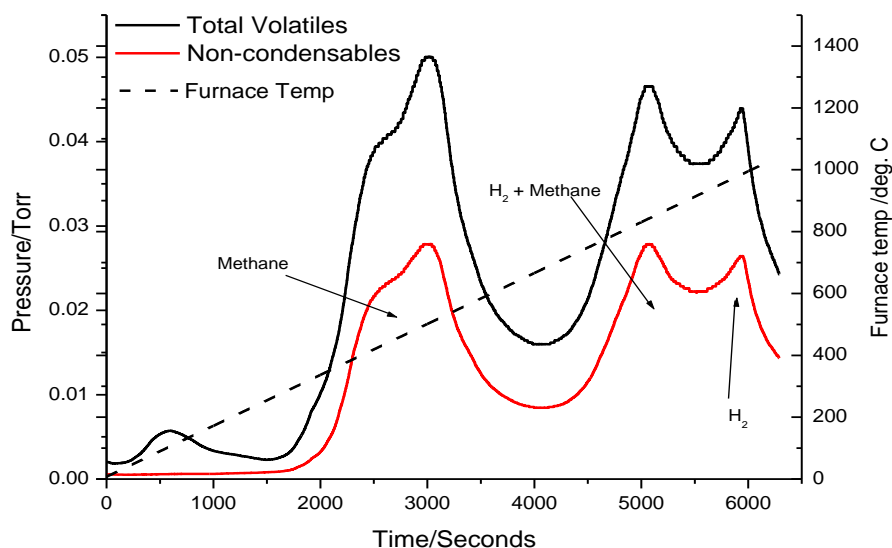


Figure 3.2.10: Thermal volatilisation analysis of coked mordenite generated with methanol at 300°C for 300 minutes. The trace shows total volatiles and non-liquid N₂ condensable products.

The post-reaction sample generated at 300°C shows a significant amount of total volatiles (black trace above) and non-condensable products (shown by red trace above). Non-condensable products have been identified via on-line mass spectrometry as water at *ca.* 100°C, methane in the temperature range 300 to 500°C, methane and hydrogen between 750 to 900°C and hydrogen between 900 to 1000°C.

These products and temperature ranges indicate that three different cracking reactions may be occurring. Between 300 to 500°C it would appear that the methyl groups are cracking off methyl substituted benzenes. From 750 to 900°C methyl groups are cracking from higher order methyl substituted benzenes or polycyclic aromatic materials. The hydrogen can be produced via cracking of the lower order polycyclic aromatics observed in ¹³C CP MAS NMR. At higher temperatures only hydrogen was observed which would be associated with cracking of higher order polycyclic aromatics.

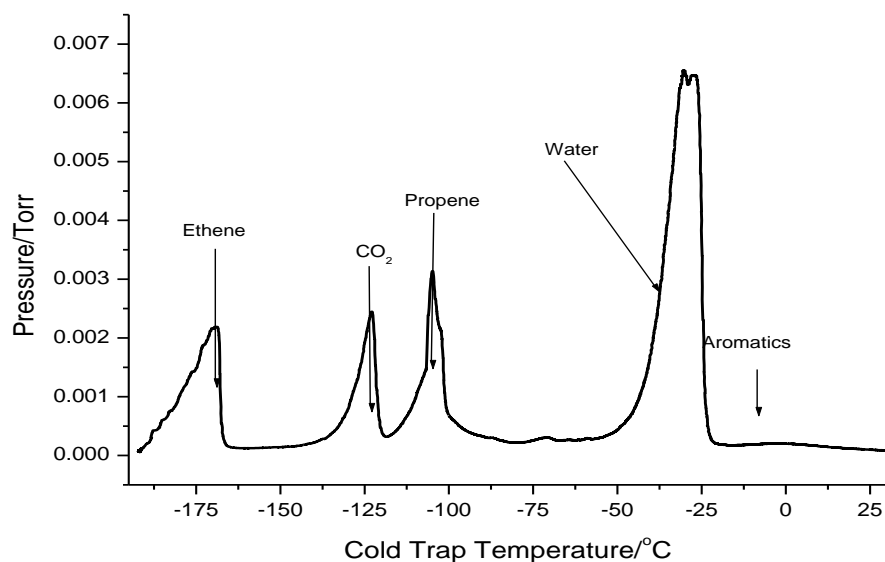


Figure 3.2.11: Sub-ambient thermal volatilisation analysis (SATVA) of coked mordenite generated with methanol at 300°C for 300 minutes. Trace shows products evolved by heating of collected volatiles trap from -196 to 30°C.

Condensable products were determined by mass spectrometry. Due to the nature of SATVA it cannot be determined at which temperature each of the products are formed. The observed condensables include ethene, carbon dioxide, propene, a small quantity of butene, copious amounts of water and a small quantity of aromatics. The observed hydrocarbons are expected products from the cracking of aromatic materials in the presence of hydrogen formed from the cracking of other species. The water is observed due to desorption of water normally seen in zeolite materials. The carbon dioxide may be as a result of the decomposition of oxygenated species such as residual methanol.

The GCMS trace of the liquid fraction shown in Figure 3.2.12 contains a multitude of aromatic and polycyclic products ranging from toluene to methyl naphthalenes. Due to the method applied for the collection of the liquid fraction it cannot be proposed where each of the products are evolved in Figure 3.2.10. But it could be hypothesized that at lower temperatures, products like toluene and lower order methyl benzenes would evolve, due to cracking of methyl groups on products like tri- and tetra-methyl benzenes, whereas at higher temperatures it could be expected that tri- and tetra- methyl benzenes and naphthalenes would evolve.

When looking at the TVA no hydrogen is observed at temperatures from *ca.* 400-500°C, which suggests that the products observed in SATVA and some of the aromatics observed in the GCMS trace of the collected liquid fraction, may occur in this region allowing for complete utilisation of the produced hydrogen.

At temperatures above 700°C a mixture of hydrogen and methane is observed whereas at 900°C only hydrogen is observed. At 700°C formation of higher order products observed in the GCMS trace of the collected liquid fraction is expected, given that methane is observed in the TVA trace indicates the removal of methyl species from substituted aromatic and polycyclic deposits. The presence of hydrogen indicates that either more is produced or the utilisation is not as efficient as at lower temperatures. The presence of hydrogen at 900°C suggests cracking of larger polycyclic aromatic molecules.

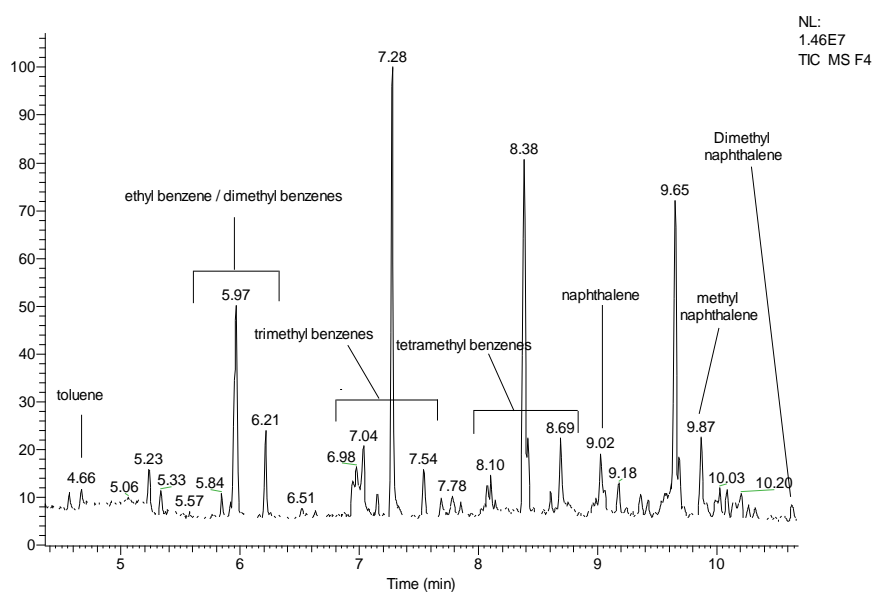


Figure 3.2.12: GCMS analysis of the liquid fraction collected from SATVA of coked mordenite generated with methanol at 300°C for 300 minutes.

The second sample investigated was generated with methanol at 500°C for 300 minutes; the data is presented in Figures 3.2.13 and 3.2.14.

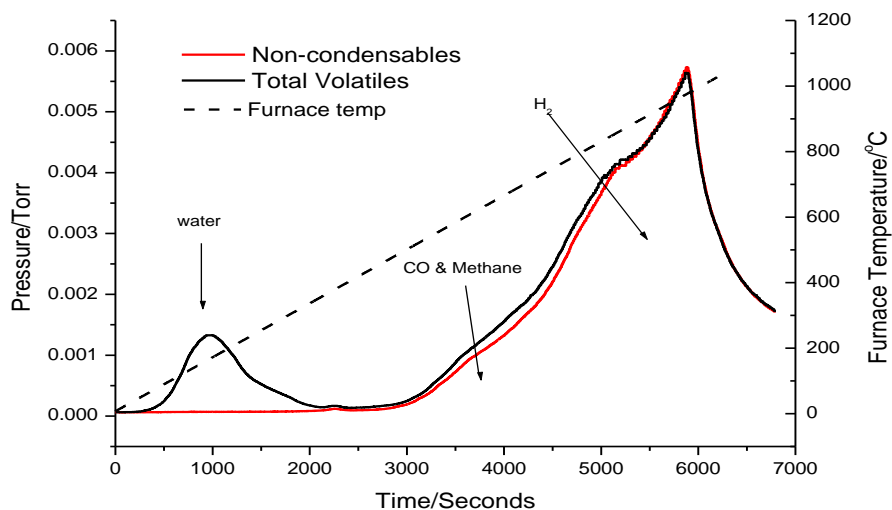


Figure 3.2.13: Thermal volatilisation analysis of coked mordenite generated with methanol at 500°C for 300 minutes. The trace shows total volatiles and non- liquid N₂ condensable products in liquid nitrogen.

The post-reaction material generated at 500°C shows a significant amount of evolved volatiles and non-condensable products (Figure 3.2.13). Non-condensable products have been identified via on-line mass spectrometry as water at *ca.* 200°C, methane and carbon monoxide in the temperature range from 500 to 700°C and hydrogen between 700 and 1000°C.

These products and temperature ranges indicate that three different cracking reactions may be occurring. Between 500 and 700°C it would appear that the methyl groups are cracking off of methyl substituted benzenes or lower order polycyclic aromatics. The carbon monoxide present may be due to a small leak of air over the sample and thus combustion is occurring. At higher temperatures only hydrogen was observed which would be associated with cracking of higher order polycyclic aromatics.

The observed condensables for the post-500°C mordenite sample presented in Figure 3.2.14 are carbon dioxide and water. The carbon dioxide level is similar to that normally observed as a background, although a small contribution may come from the residual amount of air present in the system and hence as a combustion product. The bulk of the water comes from desorption from the zeolite structure and also a contribution from any combustion that occurs.

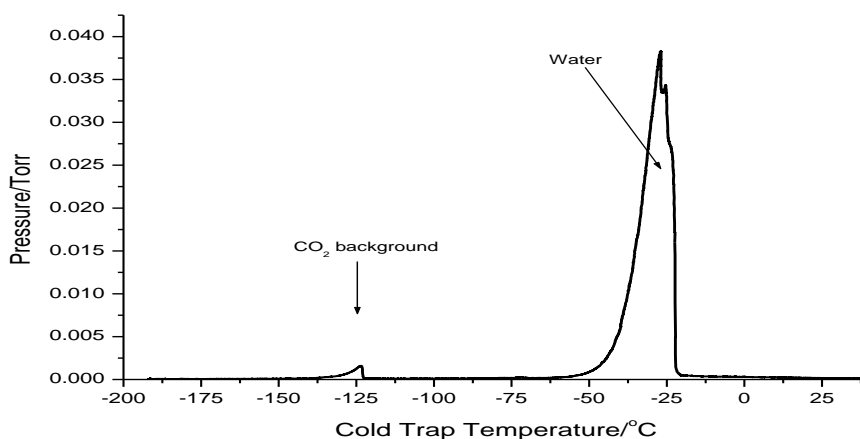


Figure 3.2.14: Sub-ambient thermal volatilisation analysis of coked mordenite generated with methanol at 500°C for 300 minutes. Trace shows products evolved by heating of the liquid nitrogen trap.

Much information has been gathered about the nature and reactivity of the carbonaceous deposits formed from coking of mordenite with a methanol-only feedstream at different temperatures. However, the location of the carbonaceous species and the stability of the framework upon reaction should be established.

Nitrogen adsorption isotherms were examined to determine the location of the coke. Figure 3.2.15 presents the isotherm for non-activated mordenite and Figure 3.2.16 presents the stacked N₂ physisorption isotherms for materials following reaction at various different temperatures.

The ammonium form of mordenite exhibited a type I type IV composite nitrogen adsorption isotherm (Figure 3.2.15) with a BET surface area of 244 m²g⁻¹ +/- 108 m²g⁻¹. This is a very large range which may reflect limitations of the equipment applied. A pore volume of 0.15 cm³ g⁻¹ was determined via the Gurvitsch rule, this pore volume is of the same order as that observed by Park *et al.* [21] (0.14-0.17 cm³ g⁻¹). Although the BET method is not strictly applicable to a type I isotherm, it has been performed for comparative purposes only. Post-reaction nitrogen adsorption isotherms were type IV for samples generated at 150 and 200°C and type II for the other samples in Figure 3.2.16. BET surface area data along with single point surface area determination at $p/p^0 = 0.1$ are listed in Table 3.2.5.

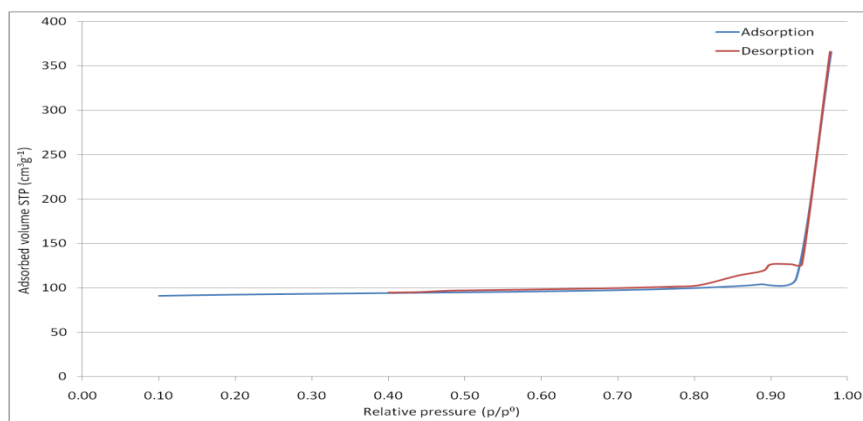


Figure 3.2.15: Nitrogen adsorption-desorption isotherm of NH₄MOR20.

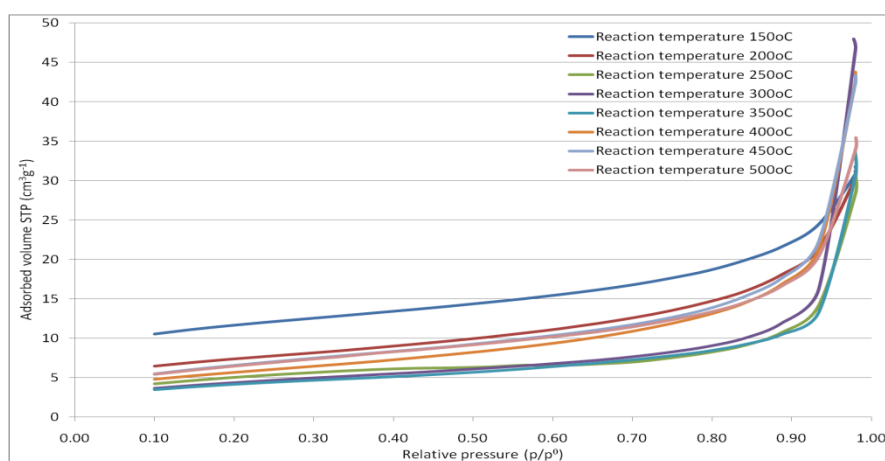


Figure 3.2.16: Nitrogen adsorption isotherms of coked mordenite generated with methanol at different reaction temperatures for 300 minutes.

As the reaction temperature and the nature and content of the carbonaceous residue changes, the surface area decreases and appears to plateau after 200°C at a surface area of approx 20 m²g⁻¹. This corresponds to a change in the isotherm from type IV to type II. This indicates that the micropores are no longer accessible and that further carbon lay down may occur on the external surface of the zeolite at moderate temperatures (250 to 400°C), since beyond which, based upon the studies detailed previously, it appears that methyl substituted aromatics and small polycyclic species condense further to form larger polycyclic aromatics.

Material	BET surface area (m ² g ⁻¹)	Single point surface area at p/p ₀ = 0.1 (m ² g ⁻¹)	Isotherm
NH₄MOR20	244	356	Type I/IV composite
Reaction temperature 150°C	38	41	Type IV
Reaction temperature 200°C	25	25	Type IV
Reaction temperature 250°C	18	16	Type II
Reaction temperature 300°C	16	14	Type II
Reaction temperature 350°C	15	14	Type II
Reaction temperature 400°C	20	19	Type II
Reaction temperature 450°C	24	22	Type II
Reaction temperature 500°C	23	21	Type II

Table 3.2.5: BET and single point surface areas and isotherm types for NH₄MOR20 and of coked mordenite generated with methanol at different reaction temperatures for 300 minutes.

Powder x-ray diffraction investigations were undertaken to determine the influence that the reaction has upon the mordenite. Stacked patterns are presented in Figure 3.2.17 for the various reaction temperatures applied.

In Figure 3.2.17 it can be observed that as the reaction temperature is increased to 200°C and above a shift occurs in the (511) reflection at approximately 28° 2θ which may indicate a deformation of the crystal lattice. Interestingly, no other reflections appear to have shifted. Although other structural changes appear to have taken place to varying degrees above 35° 2θ. In Figure 3.2.4 it was seen that the amount of carbon lay-down increases with increasing reaction temperature which may be the cause of the change in the XRD patterns above 35° 2θ. Figure 3.2.16 showed that the surface area of the zeolite rapidly decreases with increasing reaction temperature. This indicates that the pores are becoming blocked because the bulk of the surface area of a zeolite is internal. Hence, the observed deformation may be as a result of an expansion or strain of the pores due to large aromatic and polycyclic compounds forming internally.

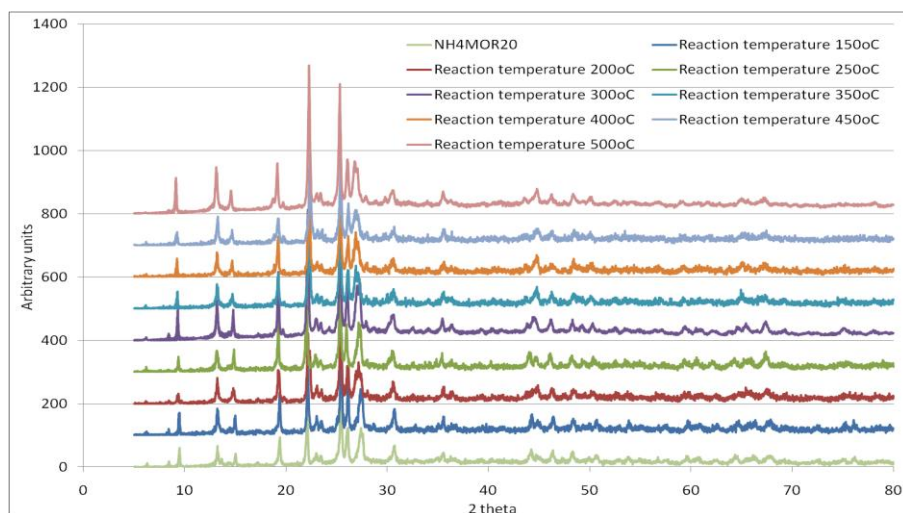


Figure 3.2.17: XRD patterns of NH₄MOR20 and coked mordenite generated with methanol at different reaction temperatures for 300 minutes.

Solid state ²⁷Al and ²⁹Si MAS NMR spectroscopy using direct polarisation was undertaken in an attempt to identify if the bulk structure of the zeolite changes during the reaction. Three samples were investigated, the NH₄MOR20 precursor sample and the two ¹³C enriched coked mordenite samples generated at 300 and 500°C respectively. The ²⁷Al spectra are presented in Figure 3.2.18, the ²⁹Si spectra in Figure 3.2.19 and the fitted ²⁹Si spectra in Figures 3.2.20 – 3.2.22.

It can be observed in Figure 3.2.18 that NH₄MOR20 exhibits primarily tetrahedral aluminium species appearing at approximately 55 ppm and a very small contribution at 0 ppm which is barely discernible indicating the presence of octahedral extra-framework aluminium [35, 36].

It is apparent that the sample generated at 300°C under ¹³C enriched methanol-only conditions exhibits an increase in the amount of octahedral aluminium, indicating partial removal from the framework.

The sample generated at 500°C under ¹³C enriched methanol-only conditions again exhibits an increase in the amount of octahedral aluminium indicating a further removal from the framework.

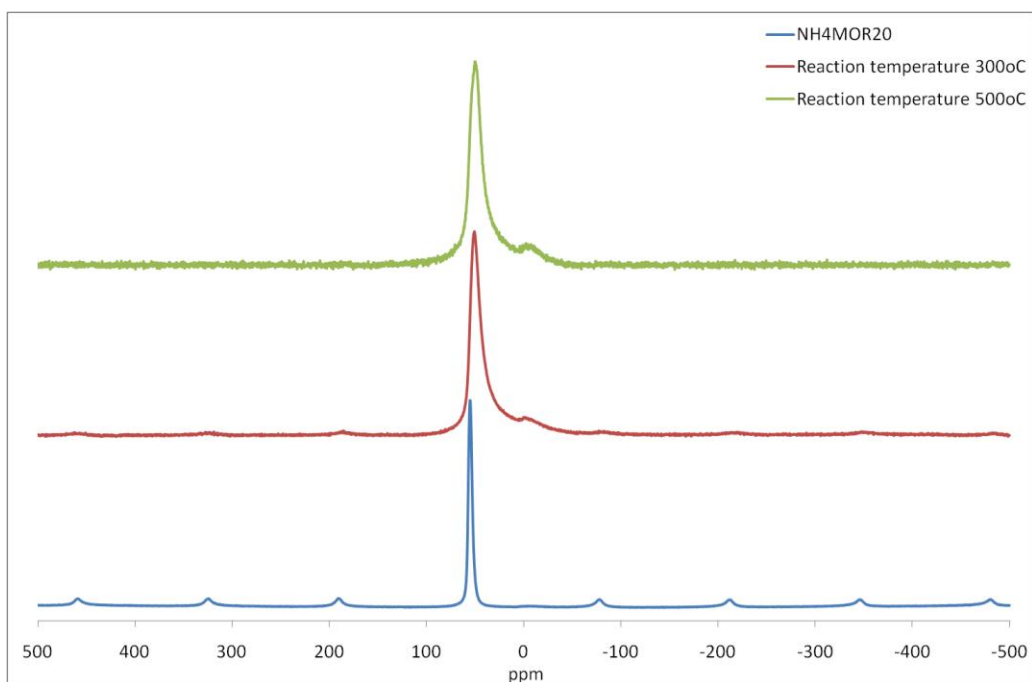


Figure 3.2.18: ^{27}Al DP MAS NMR spectra of $\text{NH}_4\text{MOR20}$, and coked mordenite generated with 25% ^{13}C enriched methanol at 300°C and 500°C for 300 minutes (spinning side bands not removed).

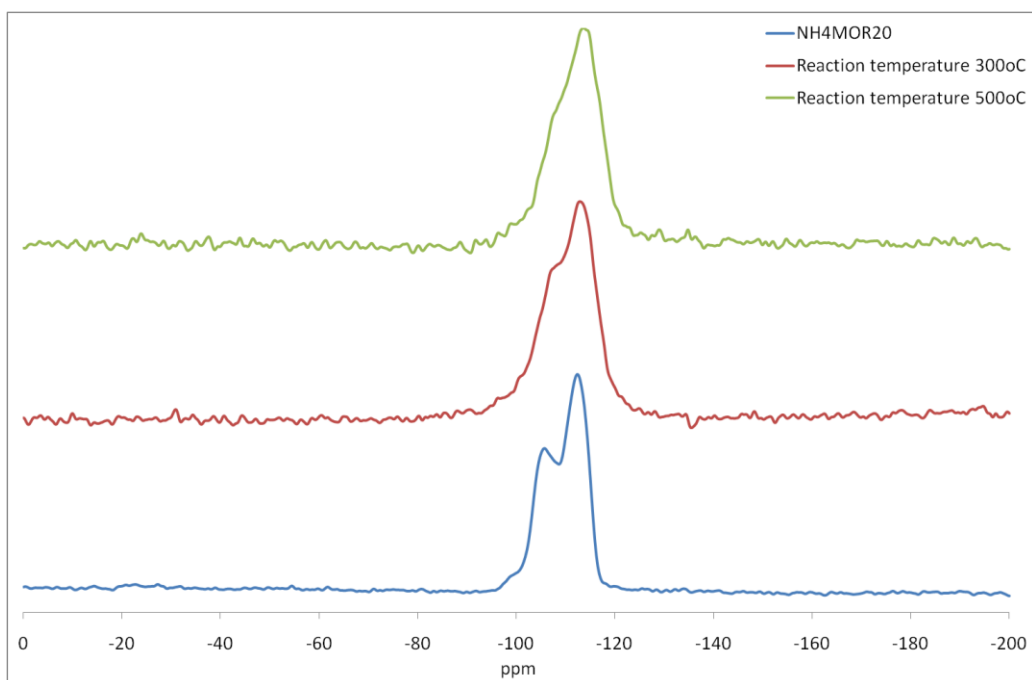


Figure 3.2.19: ^{29}Si DP MAS NMR spectrum of $\text{NH}_4\text{MOR20}$, and coked mordenite generated with 25% ^{13}C enriched methanol at 300°C and 500°C for 300 minutes.

Three silicon signals are present for NH₄MOR20 in Figure 3.2.19. The small shoulder which appears at -99 ppm can be attributed to silicon species with two aluminium atoms in the second coordination sphere (Si-2Al) [36]. The relatively large signal at -112 ppm is consistent with silicon species with no aluminium present in the second coordination sphere (Si-0Al) and the signal at -106 ppm is indicative of silicon species with one aluminium atom (Si-1Al) and also defect silicon hydroxyls (Si-OH) [37].

The sample generated at 300°C exhibits a signal appearing at -113 ppm. The signal at -106 ppm is associated with both Si-1Al and Si-OH and the signal at -99 ppm is indicative of Si-2Al. Given the observed increase in the octahedral aluminium signal seen in Figure 3.2.18, it is apparent that a partial removal of the tetrahedral aluminium has occurred. It is also possible that some of the silanol groups have decomposed during activation of the zeolite [37].

The silicon NMR spectrum shows a slight shift to -114 ppm for the signal previously observed at -112 ppm for the ammonium mordenite. The two other signals previously seen at -99 ppm and -106 ppm are less apparent. The post-500°C sample exhibits a much less significant shoulder at -106 ppm than previously observed in the post-300°C sample indicating a decrease in the amount of Si-1Al which is supported by the aluminium NMR spectra in Figure 3.2.18, and a suspected decrease in the quantity of silanol groups [37].

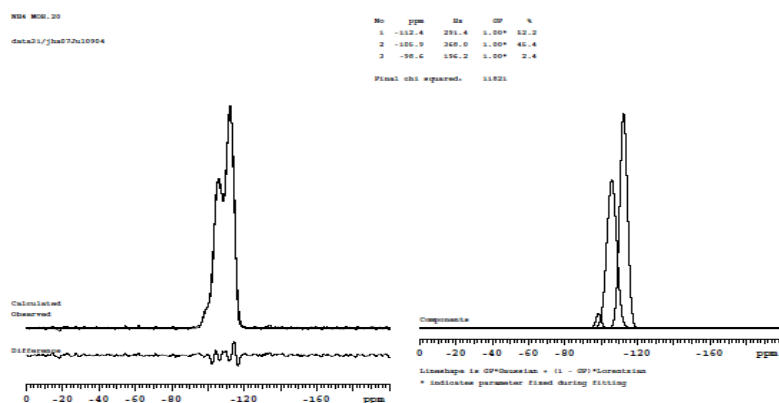


Figure 3.2.20: ²⁹Si DP MAS NMR spectrum of NH₄MOR20 (deconvoluted and integrated).

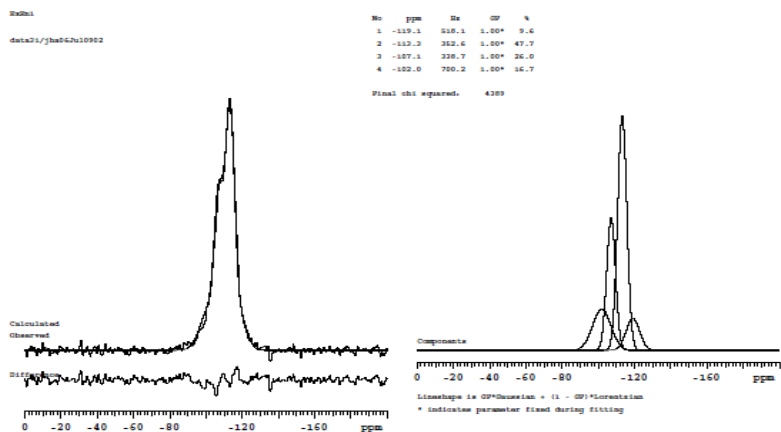


Figure 3.2.21: ^{29}Si DP MAS NMR spectrum of coked mordenite generated with 25% ^{13}C enriched methanol at 300°C for 300 minutes (deconvoluted and integrated).

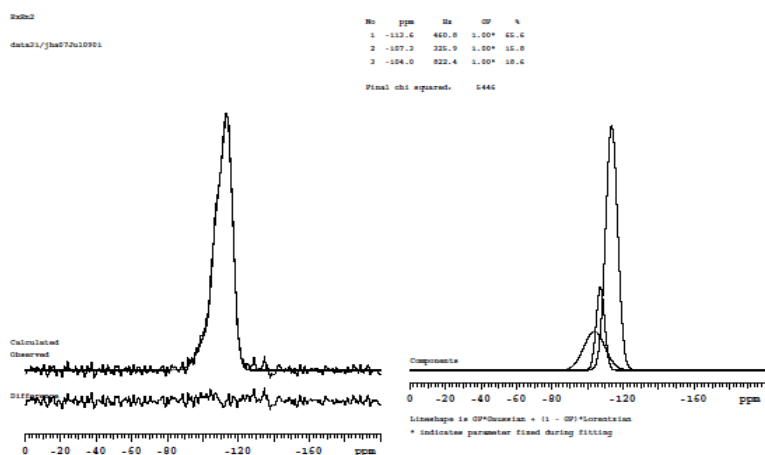


Figure 3.2.22: ^{29}Si DP MAS NMR of coked mordenite generated with 25% ^{13}C enriched methanol at 500°C for 300 minutes (deconvoluted and integrated).

In Figures 3.2.20 - 3.2.22 deconvoluted and integrated silicon NMR spectra are shown for a non-reacted mordenite and the two ^{13}C enriched post-reaction samples generated at 300 and 500°C respectively. From this it is possible to calculate corresponding framework Si/Al ratios using Equation 3.2.1:

$$\frac{Si}{Al} = \frac{\sum_{n=0}^4 I_{Si(nAl)}}{\sum_{n=0}^4 0.25 \cdot n \cdot I_{Si(nAl)}}$$

Equation 3.2.1: Determination of the framework Si/Al ratio from integrated silicon signals in deconvoluted ^{29}Si MAS NMR spectra.

Both the unreacted mordenite and the ^{13}C enriched sample generated at 500°C have a Si/Al of approximately 8 whereas the sample generated at 300°C has a Si/Al of approximately 7. It is apparent that these numbers show a slightly smaller Si/Al than has been suggested by the manufacturers (10:1). This could be related to the larger peak at approximately -106 ppm which, as mentioned previously, is attributed to two different silicon species (Si-1Al and Si-OH respectively). So the above equation does not take account of the contribution of the silanol species.

Scanning and transmission electron microscopies were undertaken on the samples, but due to the limitations of scanning electron microscopy no information regarding the location of the carbonaceous residue could be determined. Transmission electron microscopy resulted in rapid destruction of the samples under the electron beam. No resultant carbon structures were apparent under high resolution indicating the amorphous nature of the material and no information in its whereabouts on the coked mordenite sample could be obtained.

3.2.2 Time on stream dependence on the form of the carbonaceous species deposited

In order to determine the effect of reaction time on the nature of the carbonaceous deposits formed from reaction with methanol, materials were activated at 500°C for 60 minutes under a 30 ml min^{-1} argon gas stream. They were then run at 300°C in a 45% methanol feedstream at a GHSV of 3000 hr^{-1} at reaction times of 2, 5, 30, 60, 120, 180, 240, 300, 360, 420, 480, 540 and 600 minutes. Spent mordenite was cooled to room temperature under argon.

Solid state ^{13}C MAS NMR spectroscopy using direct polarisation was performed in an attempt to elucidate the species formed at short times on stream with a methanol-only feedstream. Two ^{13}C enriched samples were investigated which were generated at 2 and 5 minutes respectively. The data is presented in Figure 3.2.23.

The ^{13}C NMR spectrum for sample generated at 2 minutes in Figure 3.2.23 shows a very broad distribution of species. The peaks are all relatively sharp except the small aromatic signal indicating that the associated species have a significantly smaller distribution compared to those observed in Figure 3.2.1 in the temperature dependence section. At 13 ppm a methyl species is present associated with trapped aliphatic hydrocarbon species [28]. The signals observed at 16 ppm and 24 ppm can be attributed to methyl groups attached to substituted aromatic species such as toluene and xylene isomers and trapped aliphatic species [26, 28]. The signal at 16 ppm may also be attributed to ethyl groups attached to aromatic compounds [28, 31, 38].

The signal at 51 ppm is associated with methanol [31] and the signal at 60 ppm with dimethylether and possibly methanol bound to silanol species [27, 39]. The small signal present at 130 ppm indicates the presence of alkyl substituted aromatics including toluene and the xylene isomers [28, 31]. The signal at 111 ppm is associated with the Teflon rotor cap. Given the relatively short reaction time and the distribution of species present it would appear that the hydrocarbon pool commonly associated with methanol to hydrocarbon chemistry is in its early stages.

The ^{13}C NMR spectrum for the sample generated at 5 minutes shows a very broad distribution of species. The signals have transformed significantly from those previously observed in at 2 minutes. It is apparent from the spectrum that the molecular mobility of the carbon species has been reduced significantly indicating characteristics of a 'real' solid.

Similarities between the samples generated at 2 and 5 minutes are evident. Signals indicating the presence of alkyl groups attached to aromatic and possibly aliphatic species (13 ppm) are still present at *ca.* 16 and 24 ppm. A new signal at approximately 19 ppm has appeared and, based on previous enriched and non-enriched studies performed in the previous section, can be attributed to alkyl species attached to an aromatic centre. The corresponding signal at approximately 131 ppm has increased in intensity relative to the aliphatic peaks indicating an increase in the aromatic component [31, 38, 40]. Signals attributed to methanol [31] and

dimethyl ether or methanol adsorbed on silanol groups [27, 38] are still observed at *ca.* 51 and 60 ppm respectively.

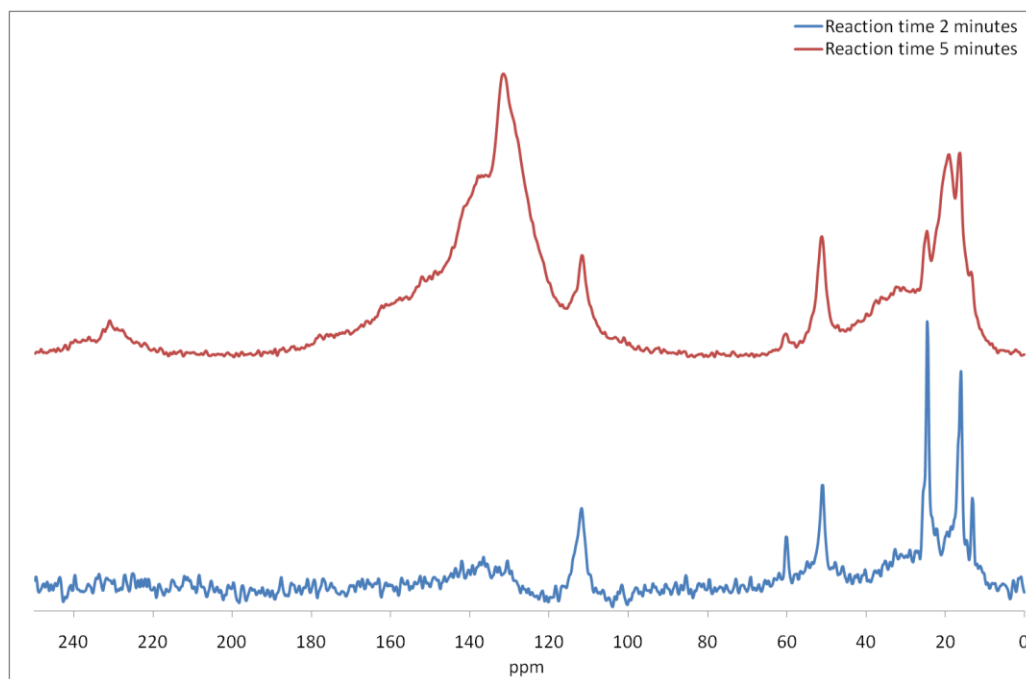


Figure 3.2.23: ^{13}C DP MAS NMR spectrum of coked mordenite generated with 25% ^{13}C enriched methanol at 300°C for different reaction times.

Even though the time difference between the two reactions is only a matter of three minutes, the difference in species is apparent, especially in the aromatic region of the spectrum where a shoulder at approximately 138 ppm is also identifiable. This was previously observed in the initial solid state NMR studies performed with ^{13}C enriched methanol, as well as non-enriched studies, after 300 minutes on stream as described in the previous section and it indicates the presence of polycyclic aromatic species with varying degrees of substitution [29, 32, 41].

Solid state ^{13}C MAS NMR using cross polarisation was undertaken on four non-enriched coked mordenite samples generated at 60, 180, 420 and 600 minutes reaction time. The data is presented in Figure 3.2.24.

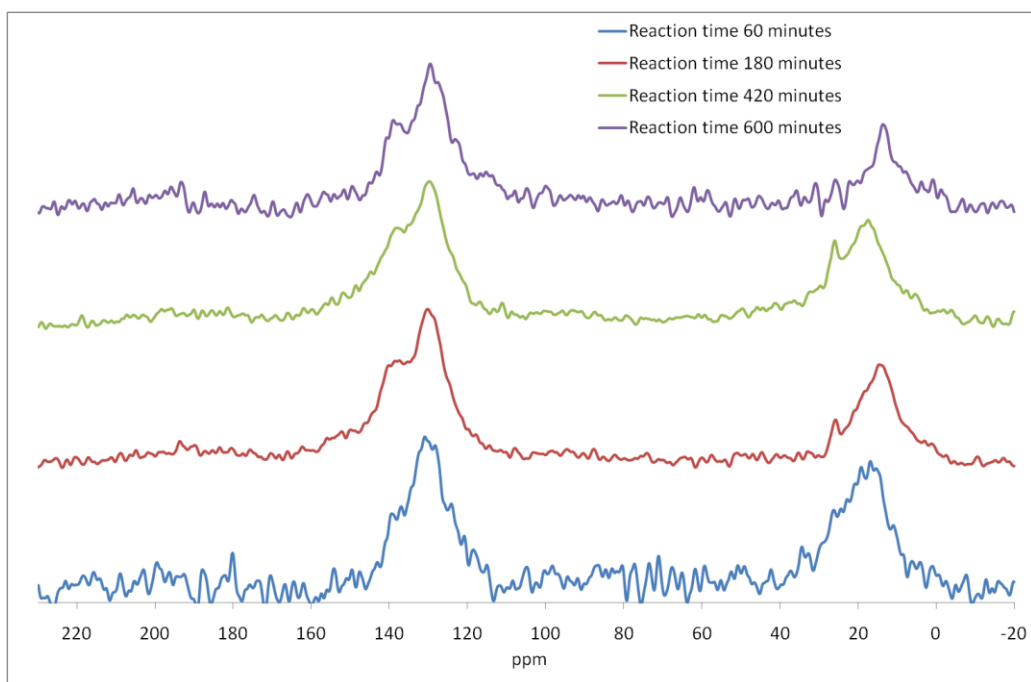


Figure 3.2.24: ^{13}C CP MAS NMR spectra of coked mordenite generated with methanol at 300°C for different reaction times.

After 60 minutes of reaction time the signal shape begins to broaden out indicating that a wider range of species are present in the aliphatic and aromatic regions of the spectrum compared to the previous enriched studies at 2 and 5 minutes. Only two peaks are particularly evident appearing at approximately 17 ppm and 131 ppm associated with methyl substituted aromatics [31, 39], although there do appear to be shoulders present at approximately 26 ppm and 138 ppm associated with alkyl substituted polycyclic aromatic species [29, 31, 40, 41].

180 minutes into the reaction, very little apparent change has taken place. No further broadening has occurred indicating no change in the distribution of species. It can be observed that the shoulders previously suspected after 60 minutes of reaction time are more prominent and appear at 26 ppm as a resolved signal and at 138 ppm as a shoulder on the broad signal observed *ca.* 130 ppm. The new signals suggest that higher order alkyl substituted aromatic species and possibly lower order polycyclic species have formed [29,31, 40, 41].

After 420 minutes of reaction time it would appear that the carbonaceous species have not changed compared previously to those observed after 180 minutes. Comparing both ^{13}C CP MAS NMR spectra for 180 and 420 minutes reaction time to that of the 300°C , 300 minute sample presented in Figure 3.2.3, no difference can be observed between the three. This indicates that during this time period the distribution of species remains similar. This suggests that during this time period the species deposited on the zeolite are in a steady state, whereby further addition of methanol results in no overall change in the species present. This is in line with previously published studies indicating the presence of an active hydrocarbon pool consisting of polymethylbenzenes [42, 43, 44, 45], which are proposed to facilitate the methanol to hydrocarbons reaction [42, 46, 47, 48].

After 600 minutes of reaction the sample appears to have changed in nature. In Figure 3.2.36 three peaks are observed at 14 ppm, 130 ppm and 138 ppm. It is apparent that methyl substituted aromatics are present from the signals at 14 ppm and 130 ppm [31, 39]. Given the broadening of the peaks it is apparent that a range of species is present. The peak at 138 ppm has evolved from the shoulder previously observed at 136 ppm for 60 minutes and 138 ppm for 180 and 420 minutes. The signal is consistent with polycyclic aromatic species [29, 31, 40, 41].

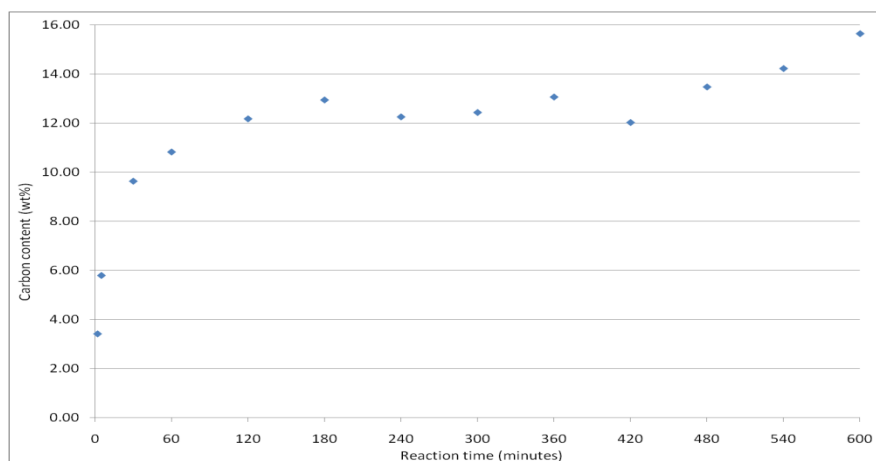


Figure 3.2.25: Carbon content of coked mordenite generated with methanol at 300°C for different reaction times.

The carbon content and the H:C ratios are presented in Figures 3.2.25 and 3.2.26 for the various reaction times investigated. In Figure 3.2.25 it can be seen that as the reaction time increases from 2 to 120 minutes the carbon wt% increases from 3.3 to 12.1 wt%. This indicates the initial formation of hydrocarbon species and the gradual development of the hydrocarbon pool. Thereafter there appears to be a plateau from approximately 120 to 420 minutes on stream at 12.5 wt%. This would appear to be similar to a steady state approximation whereby the net gain of carbon on the hydrocarbon pool is zero. After this the carbon content starts to increase again from 480 to 600 minutes where the carbon content is approximately 15.6 wt%. After an extended reaction time, the hydrocarbon pool could begin to deactivate and form highly methylated aromatics and higher order polycyclic aromatic species [42, 43]. This is supported by the observations made in solid state NMR data presented previously.

Figure 3.2.26 shows that the atomic H:C ratio decreases from aliphatic, alcohol and ether character at 2 minutes to aromatic and alkyl substituted aromatic character at 30 minutes. It decreases further to higher order aromatics and polycyclic aromatics at 120 minutes after which the atomic H:C may plateau up to 480 minutes. Thereafter the H:C atomic ratio possibly begins to decrease very slightly up to 600 minutes where the final H:C atomic ratio is approximately 1.

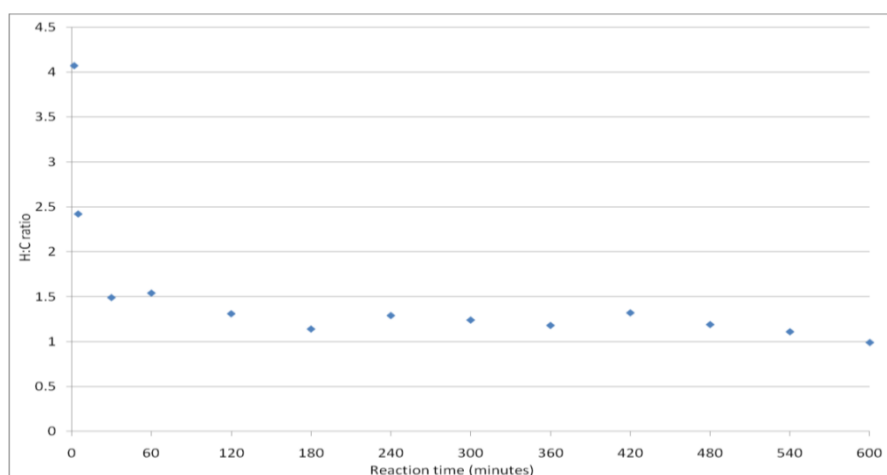


Figure 3.2.38: H:C atomic ratios of coked mordenite generated with methanol at 300°C for different reaction times (not corrected for the influence of adsorbed water).

Overlaid first derivative TGA profiles in an air atmosphere are presented in Figure 3.2.27 for the various reaction times investigated. In Figure 3.2.39 it can be observed that the post-reaction samples generated at 2 and 5 minutes reaction time display two similar first derivative TGA profile peaks displayed centering at 70°C and 180°C. These are associated with the loss of water and adsorbed volatile species such as methanol and dimethyl ether as observed in the ¹³C DP solid state NMR studies respectively. There is also a higher temperature peak centering at 600°C for 2 minutes on stream and 625°C for 5 minutes on stream which coincides with the formation of aromatic species related to the hydrocarbon pool [42, 44, 47], as suggested by the presence of the aromatic signal in the ¹³C solid state NMR investigations.

Three first derivative TGA profile peaks were observed for post-reaction samples generated at 30, 60, 120 and 180 minutes reaction time. The first peak appears centering between 60 and 80°C and is associated with the loss of water. The two other peaks appear centering at 425°C and 625°C associated with the bulk of the deposits removed being in the form of aromatic, polycyclic and their alkyl substituted derivatives [5, 34].

The samples coked at 240, 300 and 420 minutes reaction time exhibit four first derivative TGA profile peaks appearing at 70, 325, 425 and 625°C. The peak at 70°C is associated with water, 325, 425°C and 625°C with the bulk of the carbonaceous deposits being in the form of methyl substituted aromatics and polycyclic species [5, 34]. The bulk speciation observed in the NMR for samples generated at 180, 300 and 420 minutes reaction time suggests no apparent change in the composition of the carbonaceous material. The different temperatures attributed to the oxidation of the carbonaceous deposits are suspected to be an effect of the location of the residue and hence the accessibility of the oxygen to the deposit [49]. The sample coked at 360 minutes on stream exhibits only four peaks at 60, 180, 425 and 625°C and all assignments are the same as those given for 240, 300 and 420 minutes reaction time.

Three first derivative TGA profile peaks centering at 70, 425, 625°C and a shoulder at 525°C were observed for the samples reacted at 480, 540 and 600 minutes reaction time. The peaks can be attributed to water, surface bound aromatic and polycyclic species [49] and a large amount of polycyclic, higher order alkyl substituted aromatic and polycyclic species trapped in the pores [5, 34]. The shoulder at 525°C may be assigned to a smaller quantity of higher order polycyclic aromatic species forming on the external surface [49].

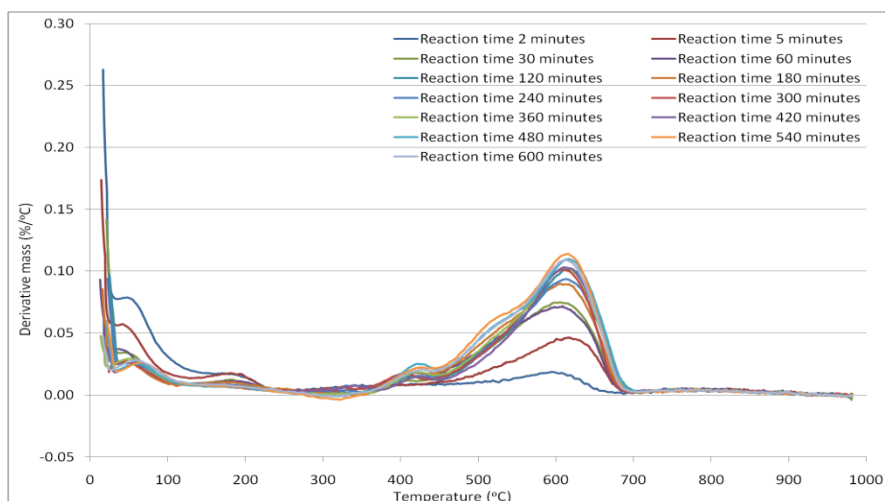


Figure 3.2.27: First derivative TGA profiles attained under air of coked mordenite generated with methanol at 300°C for different reaction times.

Figure 3.2.28 presents the N₂ physisorption isotherms for the various reaction times investigated. Post-reaction nitrogen adsorption isotherms were type IV for 2 and 5 minutes reaction time, all other reaction times exhibited a type II isotherm. BET surface area data along with single point surface area determination at $p/p^0 = 0.1$ are presented in Table 3.2.6.

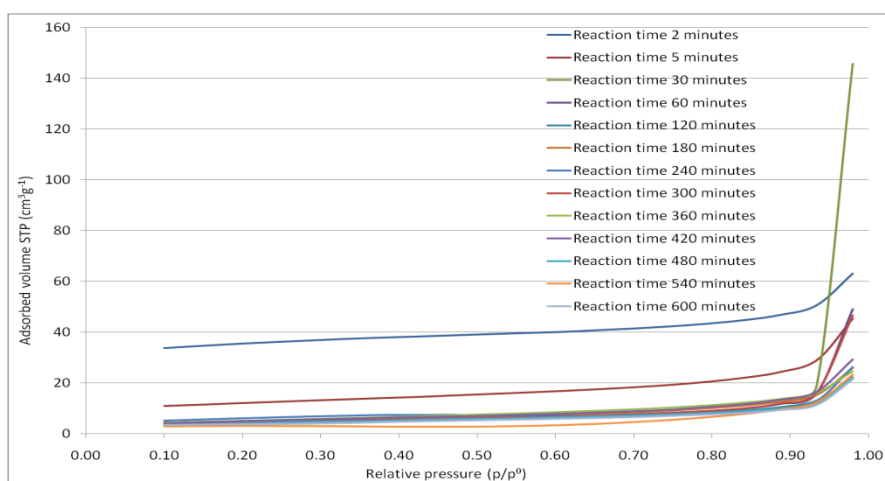


Figure 3.2.28: Nitrogen adsorption isotherms of coked mordenite generated with methanol at 300°C for different reaction times.

As the reaction time and the amount of carbonaceous deposits increase, the surface area subsequently decreases and appears to plateau at approximately $17 \text{ m}^2\text{g}^{-1}$ from 30 minutes to 480 minutes reaction time. It can be observed that the wt% C and H:C ratios plateau at approximately 120 minutes to 420 minutes indicating that further lay-down from 30 to 120 minutes has no effect on the surface area suggesting that at 30 minutes the zeolite pores are blocked. After 420 minutes further carbon lay-down is observed, sample mass will be increasing but there is still no further change in the surface area. After 480 minutes, the surface area decreases further still to approximately $10 \text{ m}^2\text{g}^{-1}$, where it appears to plateau which may indicate that the species present in the pores are beginning to condense into larger polycyclic species reducing further any available surface area in the pore openings.

Material	BET surface area (m^2g^{-1})	Single point surface area at $p/p_0 = 0.1$ (m^2g^{-1})	Isotherm
Reaction time 2 minutes	109	131	Type IV
Reaction time 5 minutes	40	42	Type IV
Reaction time 30 minutes	18	17	Type II
Reaction time 60 minutes	16	14	Type II
Reaction time 120 minutes	16	14	Type II
Reaction time 180 minutes	16	13	Type II
Reaction time 240 minutes	21	20	Type II
Reaction time 300 minutes	16	14	Type II
Reaction time 360 minutes	19	17	Type II
Reaction time 420 minutes	18	16	Type II
Reaction time 480 minutes	15	12	Type II
Reaction time 540 minutes	9	11	Type II
Reaction time 600 minutes	12	14	Type II

Table 3.2.6: BET and single point surface areas and isotherm types for coked mordenite generated with methanol at 300°C for different reaction times.

Stacked XRD patterns are presented in Figure 3.2.29 for the various times on stream investigated. In Figure 3.2.29 it can be observed that as the reaction time is increased to 5 minutes and above a shift in the (511) reflection observed at approximately $28^\circ 2\theta$ (as observed in the previous section) occurs which suggests possible deformation of the crystal lattice. In Figure 3.2.34 it was seen that the amount of carbon lay-down increases with increasing reaction time to 120 minutes whereby it plateaus to 420 minutes, after which it increases further still.

Table 3.2.6 showed that the surface area of the mordenite rapidly decreased with increasing reaction time and plateaus from 30 to 480 minutes. This indicates that the micropores are becoming blocked because the bulk of the surface area of a zeolite is internal. Hence the observed deformation may be as a result of an expansion or strain of the pores due to large aromatic and polycyclic compounds forming internally.

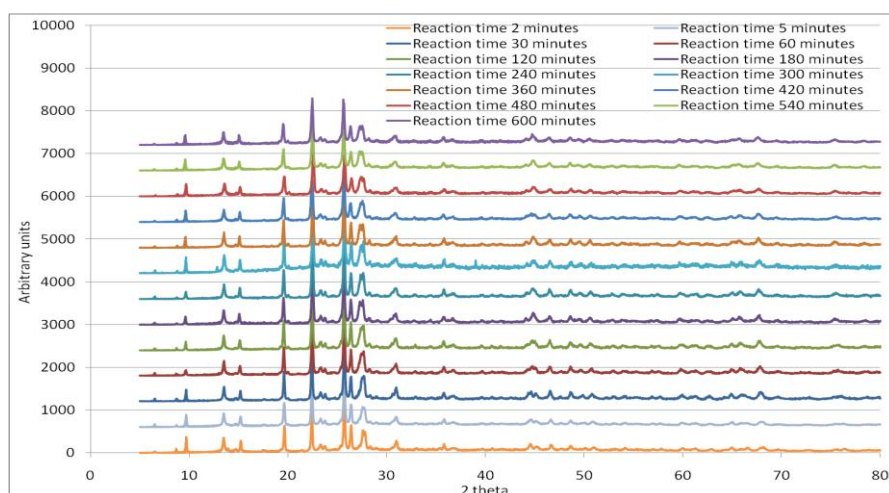


Figure 3.2.29: XRD patterns of coked mordenite generated with methanol at 300°C for different reaction times.

3.2.3 Ethanol impurity effects upon the nature of the carbonaceous species generated

As previously mentioned in the temperature and time dependence sections, it appears that the so called “coke” on the post-reaction mordenite is in a form similar to that observed in other literature studies and commonly referred to as a hydrocarbon pool. It is considered to act as a co-catalyst for the MTH reaction in conjunction with the zeolite giving an organic/inorganic hybrid supra-molecular system [50]. It still remains unclear as to how the hydrocarbon pool compounds are initially formed. It has been suggested that there could be three potential formation routes for this; (i) incomplete calcination of templating agents (mordenite is not templated); (ii) impurities in the methanol feed stream or (iii) primary reaction products such as ethene and propene [1, 50, 51].

In order to determine the effect of ethanol impurity on the type, nature and location of the carbonaceous deposits formed from impure methanol feedstreams. Mordenite was activated at 500°C for 60 minutes under a 30 ml min⁻¹ argon gas stream.

The reaction temperature was decided previously as a standard test temperature due to the level of information obtained for it in the temperature dependence summary. The reaction time study demonstrated that between 180 to 420 minutes a steady state in the amount and nature of the carbon was reached, therefore an intermediate reaction time was decided upon at 300 minutes.

Samples were then run with impure methanol feedstreams at 300°C for 300 minutes in a 45% methanol feedstream containing a known impurity of ethanol 0.1, 0.2, 0.3, 0.4, 0.5, 0.6, 0.7, 0.8, 0.9, 1.0, 1.1, 1.2, 1.3, 1.4, 1.5, 1.6, 1.7, 1.8, 1.9 and 2.0 mol% with respect to methanol, at a GHSV of 3000 hr⁻¹. Coked materials were cooled to room temperature under argon.

The carbon content and the H:C ratios are presented in Figures 3.2.30 and 3.2.31 for the various ethanol impurities investigated.

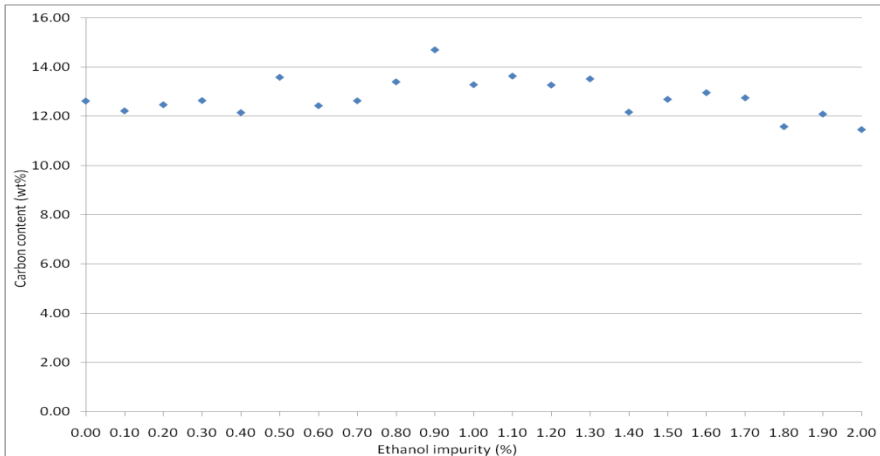


Figure 3.2.30: Carbon content of coked mordenite generated with methanol containing different percentages of ethanol “impurity” at 300°C for 300 minutes.

In Figure 3.2.30 it can be observed that initially the amount of carbon lay down is similar until 0.8 mol% where there appears to be a possible small increase at 0.9 mol% where the carbon content reaches a maximum at approximately 14.7 wt%. Thereafter in general there is a decrease in the wt% C beyond 0.9 mol% and up to 2.0 mol% “impurity”. At 0.5 mol% there is an apparent increase in the carbon content. Reproduction of the data demonstrates that this was not a real increase and was an artefact.

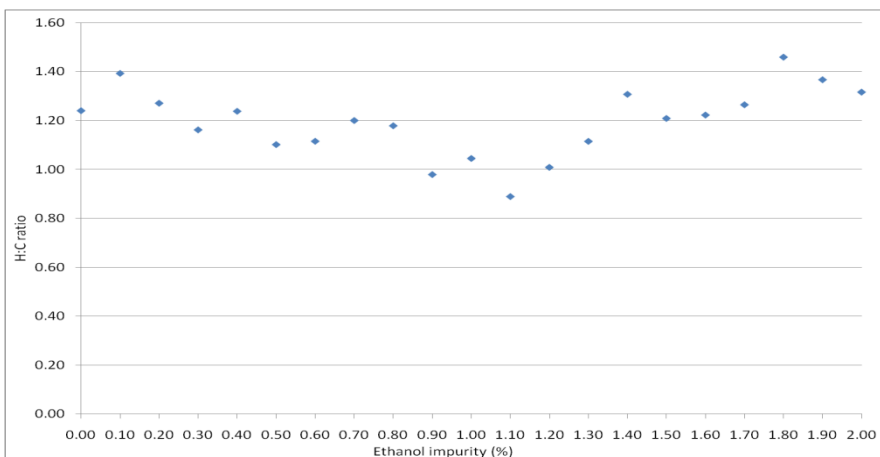


Figure 3.2.31: Atomic H:C ratio of coked mordenite generated with methanol containing different percentages of ethanol “impurity” at 300°C for 300 minutes (not corrected for the influence of adsorbed water).

It can be observed in Figure 3.2.31 that in general the atomic H:C ratio decreases from approximately 1.2 to approximately 0.9 as the ethanol content changes from 0.0 to 1.1%. After 1.1 mol% impurity the atomic H:C ratio begins to increase until 2.0 mol% where it is approximately 1.3. Overall, the reproducibility of the H:C ratio was rather poor.

Overlaid derivative mass data for mordenite coked under the various ethanol containing feed-streams are presented for air in Figure 3.2.32. It can be observed that post-reaction samples generated with ethanol “impurities” all have similar first derivative TGA profiles with the exception of samples generated with 1.10 and 1.30 mol% ethanol impurities. Comparing them to the sample examined under standard methanol-only coking conditions (300°C for 300 minutes) previously discussed, shows a degree of comparability between the samples, which in turn suggests that the carbonaceous deposits are of a similar nature in all instances.

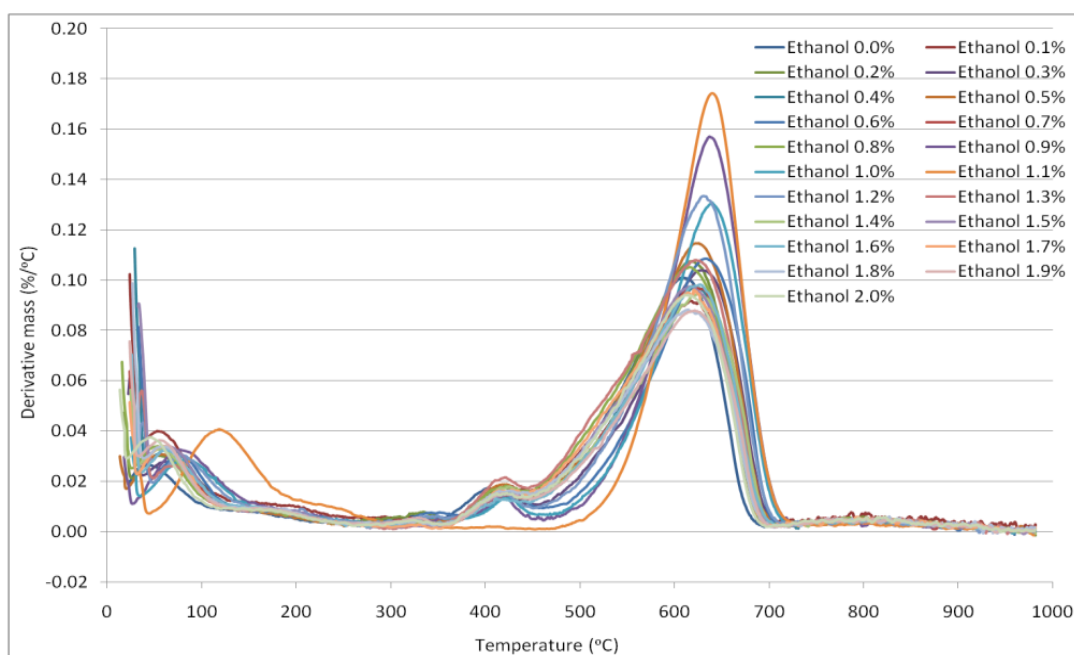


Figure 3.2.32: First derivative TGA profiles attained under air of coked mordenite generated with methanol containing different percentages of ethanol “impurity” at 300°C for 300 minutes.

The sample generated with 1.1 mol% ethanol impurity displays two first derivative TGA profile peaks centering at 125°C, attributed to adsorbed water, and 625°C associated with higher order alkyl substituted aromatic and polycyclic species [5, 34, 49]. This particular sample exhibits a first derivative TGA profile similar to that exhibited for higher temperature reactions performed at 450 or 500°C.

The sample generated with a 1.3 mol% impurity displays three first derivative TGA profile peaks centering at 70, 425, 625°C. The first derivative TGA profile peak centering around 70°C is associated with adsorbed water. The peak at 425°C is assigned to surface bound species such as alkylated aromatic and polycyclic species or species with a moderate combustion temperature [34, 49]. The large first derivative TGA profile peak observed at 625°C is associated with the bulk of the carbonaceous deposits believed to be trapped in the pores of the zeolite in the form of alkylated aromatic and polycyclic species [5, 49].

The first derivative mass TGA profiles suggest that the samples generated from 0.0 to 1.0 mol% ethanol impurity are similar and produce a very similar hydrocarbon pool. At 1.1 mol% impurity the first derivative mass data is different suggesting that a different type of chemistry predominates and produces more condensed carbonaceous deposits similar to those deposited at higher temperatures with a “pure” methanol-only feedstream. Thereafter, in general, the first derivative TGA profile adopts characteristics exhibited by typical materials run under standard conditions. This is interesting because if the ethanol to hydrocarbon reaction was to take place, the hydrocarbon pool species would be expected to change from methylated aromatic to ethylated aromatic species [51] and possibly exhibit a different first derivative TGA profile.

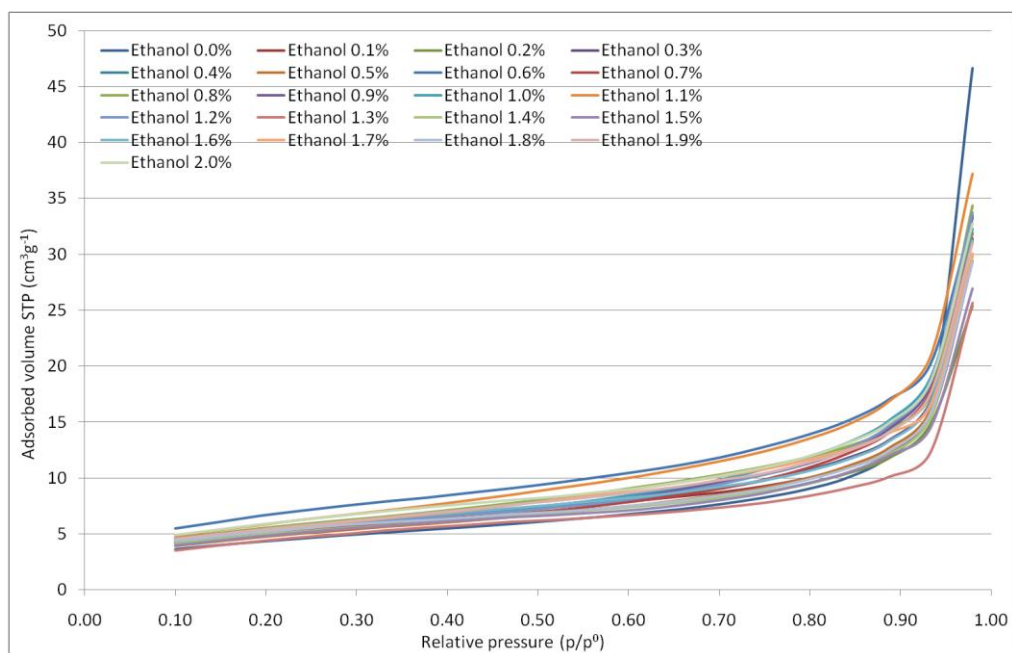


Figure 3.2.33: Nitrogen adsorption isotherms of coked mordenite generated with methanol containing different percentages of ethanol “impurity” at 300°C for 300 minutes

Figure 3.2.33 presents stacked N₂ physisorption isotherms for the range of ethanol impurities employed in this study. Post-reaction nitrogen adsorption isotherms were type II for all coked samples and are all shown in Figure 3.2.33. BET surface area data along with single point surface area determination at $p/p^0 = 0.1$ are presented in Table 3.2.7. No significant change is observed in surface area regardless of ethanol impurity. The surface area appears to plateau at approximately $18\text{m}^2\text{g}^{-1}$ indicating that the micropores are completely blocked. The presence of a type II isotherm in all instances supports this.

Material	BET surface area (m ² g ⁻¹)	Single point surface area at p/p ₀ = 0.1 (m ² g ⁻¹)	Isotherm
Ethanol 0.0 mol%	16	14	Type II
Ethanol 0.1 mol%	19	16	Type II
Ethanol 0.2 mol%	18	16	Type II
Ethanol 0.3 mol%	19	16	Type II
Ethanol 0.4 mol%	20	18	Type II
Ethanol 0.5 mol%	17	15	Type II
Ethanol 0.6 mol%	24	22	Type II
Ethanol 0.7 mol%	18	16	Type II
Ethanol 0.8 mol%	20	18	Type II
Ethanol 0.9 mol%	19	18	Type II
Ethanol 1.0 mol%	19	18	Type II
Ethanol 1.1 mol%	22	19	Type II
Ethanol 1.2 mol%	19	17	Type II
Ethanol 1.3 mol%	16	14	Type II
Ethanol 1.4 mol%	18	17	Type II
Ethanol 1.5 mol%	18	16	Type II
Ethanol 1.6 mol%	20	17	Type II
Ethanol 1.7 mol%	20	17	Type II
Ethanol 1.8 mol%	18	17	Type II
Ethanol 1.9 mol%	19	18	Type II
Ethanol 2.0 mol%	21	19	Type II

Table 3.2.7: BET and single point surface areas and isotherm types for coked mordenite generated with methanol containing different percentages of ethanol “impurity” at 300°C for 300 minutes.

Stacked XRD patterns are presented in Figure 3.2.34 for the various ethanol impurities employed.

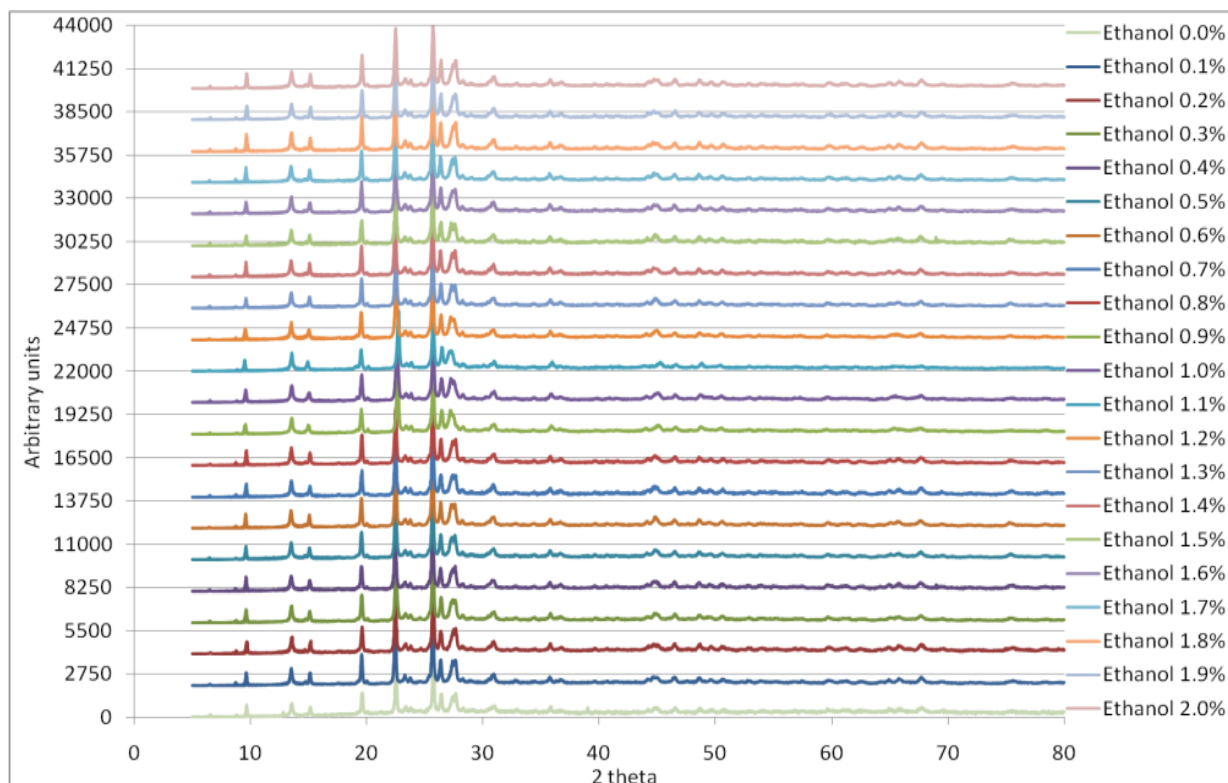


Figure 3.2.34: XRD patterns of coked mordenite generated with methanol containing different percentages of ethanol “impurity” at 300°C for 300 minutes.

In Figure 3.2.34 it can be observed that as the ethanol impurity percentage is increased no apparent shifts are observed. This indicates that no further deformation of the crystal lattice occurs due to the influence of ethanol impurity. This is supported by the isotherms presented in Figure 3.2.33 which suggest no change in the surface area with increasing ethanol impurity.

3.2.4 Methyl acetate impurity effects upon the nature of the carbonaceous species generated

The carbonylation of methanol or dimethylether leads to formation of methyl acetate or acetic acid as the desired products [52, 53, 54]. But in these cases, the MTH reaction is known to be the dominant process during the initial period of the reaction. Even during this stage of the process carbonylation is suspected to proceed concurrently with the MTH reaction [55]. This therefore results in the presence of methyl acetate/ acetic acid over the zeolite during MTH chemistry.

Hence an attempt at simulating these conditions was undertaken using a methyl acetate “impurity” in the methanol feed-stream. Methyl acetate was chosen due to incompatibility issues between acetic acid and the seals and O-rings of the HPLC pump used and due to the fact that is the product of esterification of acetic acid with methanol.

In order to determine the effect of methyl acetate impurity on the type, nature and location of the carbonaceous deposits formed, mordenite was activated at 500°C for 60 minutes under a 30 ml min⁻¹ argon gas stream. They were then run at 250, 300 and 500°C for 300 minutes in a 45% methanol feedstream containing a 2.0 mol% impurity of methyl acetate with respect to the methanol, at a GHSV of 3000 hr⁻¹. Spent samples were cooled to room temperature under argon.

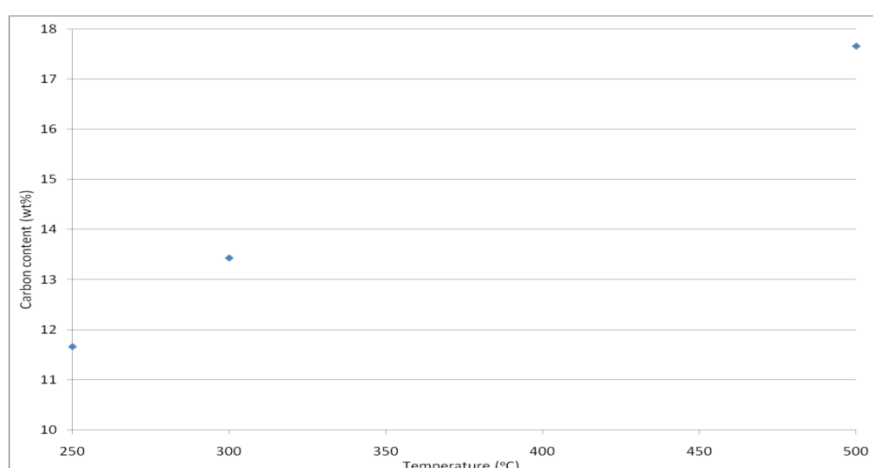


Figure 3.2.35: Carbon content of coked mordenite generated with methanol containing a 2.0% methyl acetate “impurity” at different reaction temperatures for 300 minutes.

The carbon content and the H:C ratios are presented in Figures 3.2.35 and 3.2.36 at the various reaction temperatures employed. In Figure 3.2.35 it can be observed that with increasing temperature the carbon content increases. The sample generated at 250°C had a carbon content of approximately 11.7 wt%, thereafter increasing the temperature to 300°C resulted in a carbon content of approximately 13.4 wt%. The final increase in temperature resulted in a carbon content of approximately 17.7 wt%.

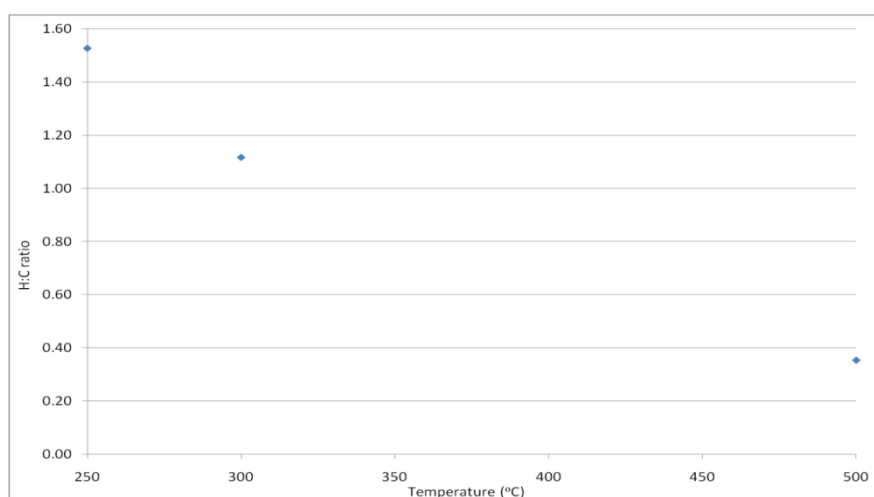


Figure 3.2.36: Atomic H:C ratio of coked mordenite generated with methanol containing a 2.0% methyl acetate “impurity” at different reaction temperatures for 300 minutes (not corrected for the influence of adsorbed water).

Figure 3.2.36 shows that the hydrogen deficiency of the samples increases with increasing reaction temperature. The sample coked at 250°C exhibited a H:C ratio of approximately 1.5. Increasing the reaction temperature to 300°C gave a H:C ratio of 1.1. A H:C of 0.4 is observed for the post-500°C sample.

When compared to the data presented for temperature dependence studies, it is apparent that with a 2.0% methyl acetate impurity no appreciable difference is observed in either the carbon content or H:C ratio. This is based upon the reproducibility of coked samples generated at each reaction temperature (reproducibility based upon two runs, 250°C: C wt% 97% and H:C 88%, 300°C: C wt% 94% and H:C 86%, and 500°C: C wt% 94% and H:C 85%).

Overlaid first derivative TGA profiles are presented in Figure 3.2.37 for 2.0% methyl acetate impurity with the series of reaction temperatures employed. In Figure 3.2.37 it can be observed that the sample reacted at 250°C displays four first derivative TGA profile peaks at 60, 325, 425 and 625°C. The peak at 60°C is attributed to adsorbed water. The peaks at 325 and 425°C are suspected of being associated with surface bound species such as alkylated aromatic and polycyclic species. The species associated with peak observed centering around 625°C are the bulk of the deposits believed to reside in the pores of the zeolite on the form of alkylated aromatics and polycyclic species.

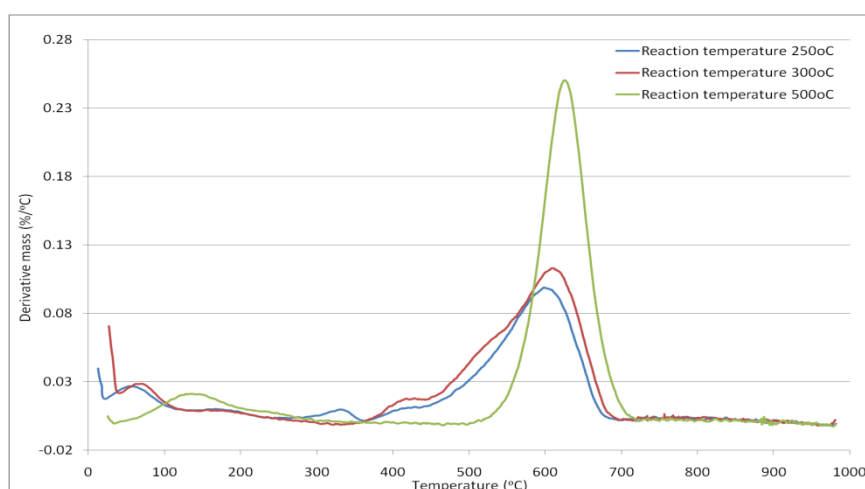


Figure 3.2.37: First derivative TGA profiles attained under air of coked mordenite generated with methanol containing a 2.0% methyl acetate “impurity” at different reaction temperatures for 300 minutes.

The sample generated at 300°C displays three first derivative TGA profile peaks at 70, 425 and 625°C. The peak observed at 70°C is attributed to adsorbed water. The peak at 425°C is indicative of either surface bound species such as alkylated aromatic and polycyclic species or species which have a moderate combustion temperature. The relatively large peak observed at 625°C indicates alkylated aromatics and polycyclic species trapped in the pores of the zeolite.

Only two first derivative TGA profile peaks are observed for the sample coked at 500°C. These occur at 125°C and 625°C. The peak at 125°C is attributed to adsorbed water, whereas

the peak at 625°C is associated with the carbonaceous species believed to reside in the pores of the zeolite.

Very little difference is observed between the samples generated with a 2.0% methyl acetate impurity presented in Figure 3.2.37 and the data presented for the samples generated in the temperature dependence study. Given the similarity of first derivative mass data it can be suggested that the addition of the 2.0% methyl acetate impurity has no apparent effect on the carbonaceous residue with respect to combustion temperature.

Figure 3.2.38 presents stacked N₂ physisorption isotherms for 2.0% methyl acetate impurity at 250, 300 and 500°C. Post-reaction nitrogen adsorption isotherms were type II for all coked catalysts and are all observed in Figure 3.2.50 with a BET surface area of 15m²g⁻¹ (single point surface area at p/p⁰ = 0.1 of 13 m²g⁻¹) for 2.0% methyl acetate impurity post 250°C reaction, 17m²g⁻¹ (single point surface area at p/p⁰ = 0.1 of 15 m²g⁻¹) post 300°C reaction and 23m²g⁻¹ (single point surface area at p/p⁰ = 0.1 of 21 m²g⁻¹) post 500°C reaction. The surface area is fairly consistent at approximately 18m²g⁻¹ regardless of reaction temperature with a methyl acetate impurity level of 2.0%.

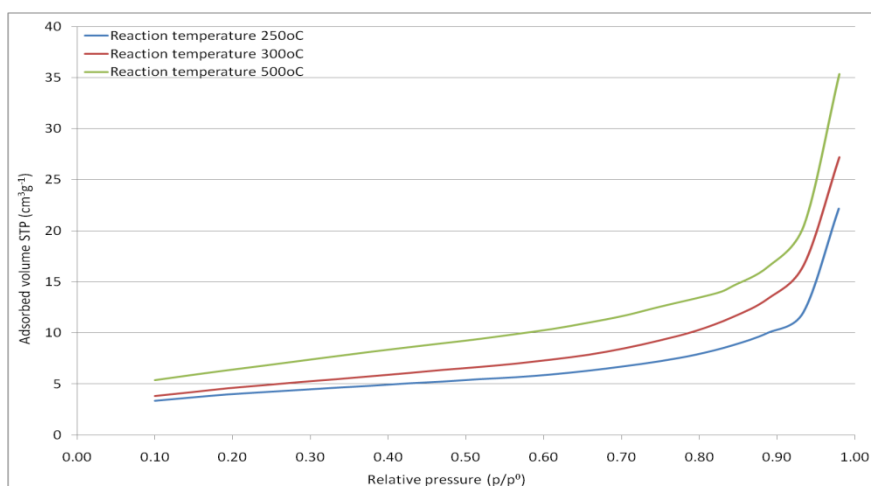


Figure 3.2.38: Nitrogen adsorption isotherms of MTH catalysts coked at 2.0% methyl acetate impurity at different reaction temperatures.

Very little difference is observed between the samples generated with a 2.0% methyl acetate impurity presented in Figure 3.2.38 and the data presented for the samples generated in the temperature dependence study. The surface area measurements support the conclusion that there is no appreciable difference between the two sets of samples.

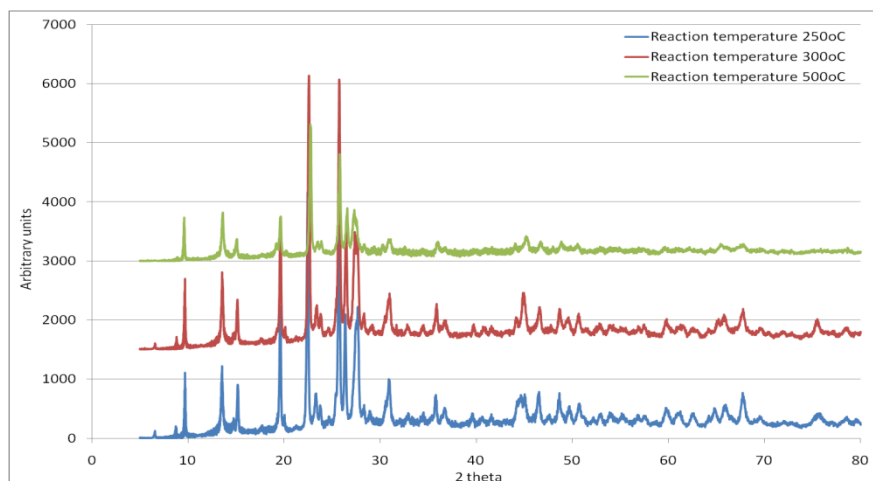


Figure 3.2.39: XRD patterns of coked mordenite generated with methanol containing a 2.0% methyl acetate “impurity” at different reaction temperatures for 300 minutes.

Stacked XRD patterns are presented in Figure 3.2.39 for 2.0% methyl acetate impurity at the different of temperatures employed. In Figure 3.2.39 it can be observed that as the reaction temperature is increased no apparent shifts are observed. This confirms that no further deformation of the crystal lattice occurs with increasing reaction temperature and a 2.0% methyl acetate impurity. This is supported by the isotherms presented in Figure 3.2.38 which suggest that no increase in surface area is observed with increasing reaction temperature. But slight changes in the crystal structure are observed which may be attributed to the deposition of carbon over the catalyst.

Samples generated with a 2.0% methyl acetate impurity show a similar post-reaction XRD patterns to those observed in the temperature dependence section, comparing peak position reveals that no additional shifts are caused by the addition of a methyl acetate impurity.

3.2.5 The influence of activation time upon the nature of the carbonaceous species deposited

In order to determine the effect of activation time the zeolite was activated at 500°C for 60, 120 and 180 minutes under a 30ml min⁻¹ argon gas stream. An unactivated sample was also used. They were then at 300°C for 300 minutes in a 45% methanol feedstream at a GHSV of 3000hr⁻¹. Coked mordenite samples were allowed to cool to room temperature under argon.

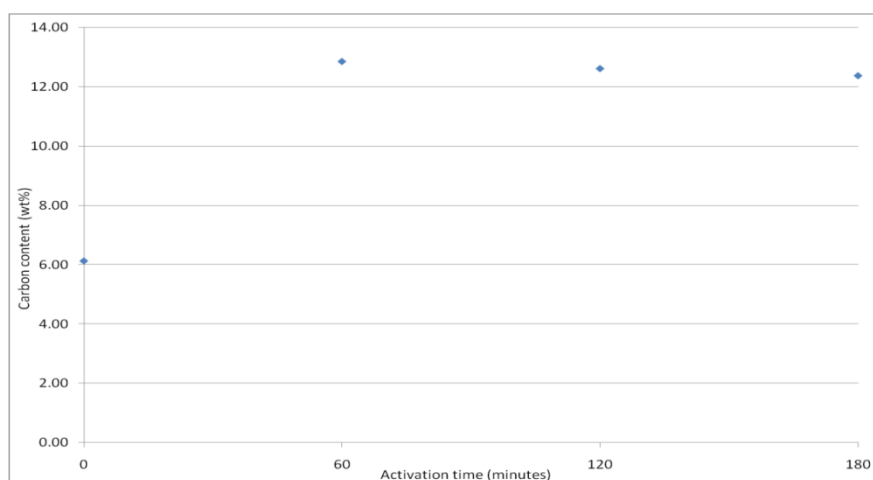


Figure 3.2.40: Carbon content of coked mordenite unactivated and activated at 500°C for different activation times, generated with methanol at 300°C for 300 minutes.

The carbon content and the H:C ratio is presented in Figure 3.2.40 and 3.2.41 for unactivated mordenite and mordenite activated at the various times employed. In Figure 3.2.40 it can be observed that an unactivated sample post-reaction had a carbon content of approximately 6.2wt%. When the mordenite was activated for 60 minutes it is apparent that the carbon content increased to approximately 12.8wt%. Increasing the activation time further to 120 and 180 minutes respectively had very little effect on the carbon content, yielding 12.6wt% for 120 minutes activation and 12.4wt% for 180 minutes activation.

In Figure 3.2.41 it can be seen that an unactivated sample had a H:C ratio of 2.9, whereas when the material was activated for 60 minutes it can be observed that the H:C ratio increased to 1.1. Increasing the activation time further to 120 and 180 minutes respectively

has very little effect if any on the H:C ratio which was found to be 1.3 for 120 minutes and 1.2 for 180 minutes activation time.

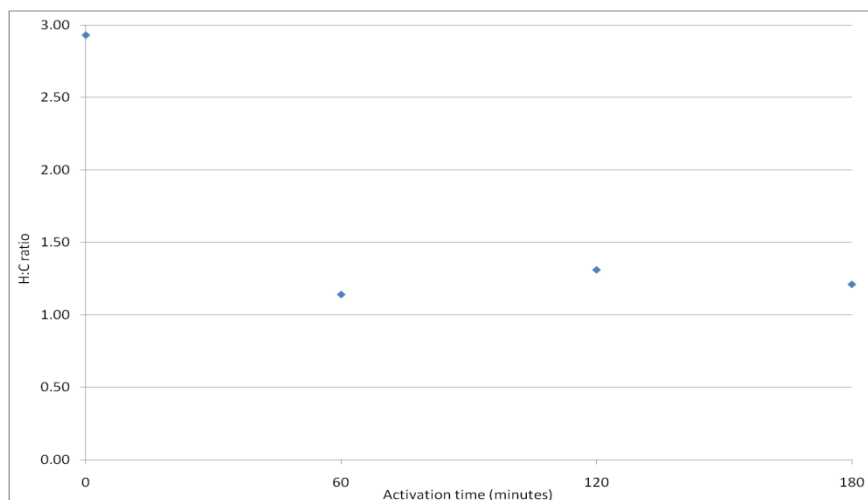


Figure 3.2.41: Atomic H:C ratio of coked mordenite unactivated and activated at 500°C for different activation times, generated with methanol at 300°C for 300 minutes (not corrected for the influence of adsorbed water).

It can be observed that the unactivated sample contains approximately 50% of the carbon and is less hydrogen deficient, compared to activated forms indicating that, as expected, fewer acid sites are present and retard the formation of the initial hydrocarbon pool. But during the reaction some of the weaker acid sites activate and become available for the formation of the carbonaceous deposits. Activated samples exhibit very similar carbon contents and hydrogen deficiencies, which indicates that beyond a certain minimum, activation time has a limited effect on activating additional acid sites.

Overlaid derivative TGA profiles are presented in Figure 3.2.42 for NH₄MOR20 and Figure 3.2.43 for the unactivated mordenite and mordenite activated at the various times employed. In Figure 3.2.54 the non-reacted NH₄MOR20 exhibits two first derivative TGA profile peaks appearing *ca.* 60°C and 450°C respectively. The peak at 60°C is attributed to adsorbed water, whereas the peak at approximately 450°C can be attributed to the decomposition of

ammonium ions resulting in the formation of the Brønsted acidic form of the zeolite upon the evolution of ammonia.

In Figure 3.2.43 it can be observed that the unactivated sample reacted at 300°C displays four first derivative TGA profile peaks at 60, 350, 450 and 650°C. The peak at 60°C is attributed to adsorbed water. The peaks at 350 and 450°C are believed to be associated with surface bound species such as alkylated aromatic and polycyclic species or species with a moderate combustion temperature. The species associated with peak observed centering around 650°C are the bulk of the deposits believed to reside in the pores of the zeolite on the form of alkylated aromatics and polycyclic species.

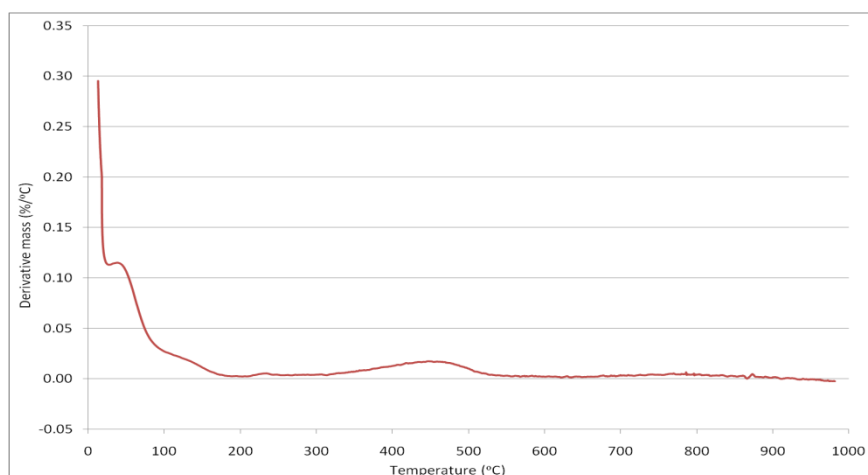


Figure 3.2.42: First derivative TGA profile attained under air of non-reacted NH₄MOR20.

The three activated samples exhibit four first derivative TGA profile peaks at approximately 80, 325, 425 and 625°C respectively. The peak at 80°C is attributed to adsorbed water. The peaks at 325 and 425°C are ascribed to surface bound species such as alkyl substituted aromatics and polycyclic compounds. The peak at 625°C is associated with the bulk of the species believed to be trapped within the pores of the zeolite in the form of alkyl substituted aromatic and polycyclic compounds.

Interestingly the unactivated mordenite has a relatively large peak at 450°C which is related at least in part, to the decomposition of the remaining ammonium ions. This may imply that due to the partial activation of the zeolite as a consequence of reaction temperature, fewer

acid sites are present on the internal surface of the mordenite hence restricting the initial growth of the hydrocarbon pool. Hence the weaker acid sites are present to a greater extent.

The activated samples produce nearly identical first derivative mass data, suggesting that the carbonaceous deposits formed are chemically identical in each case and as such longer activation times produce no observable difference in speciation and amount of deposit.

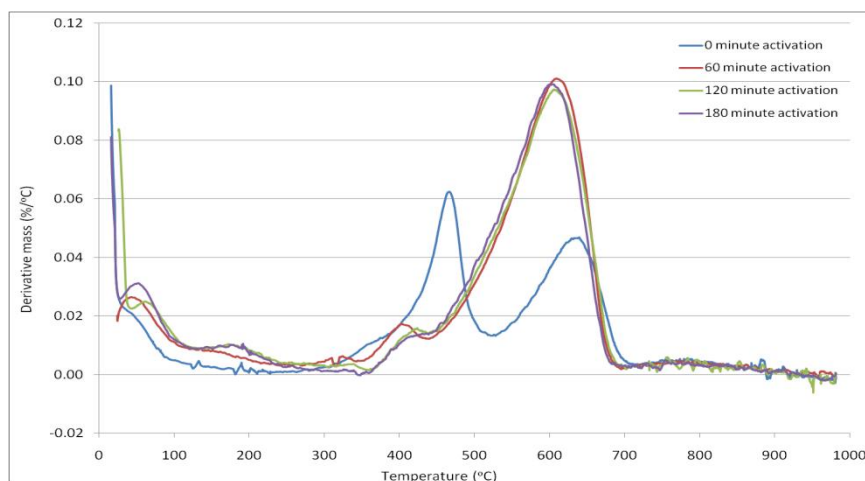


Figure 3.2.43: First derivative TGA profiles attained under air of coked mordenite unactivated and activated at 500°C for different activation times, generated with methanol at 300°C for 300 minutes.

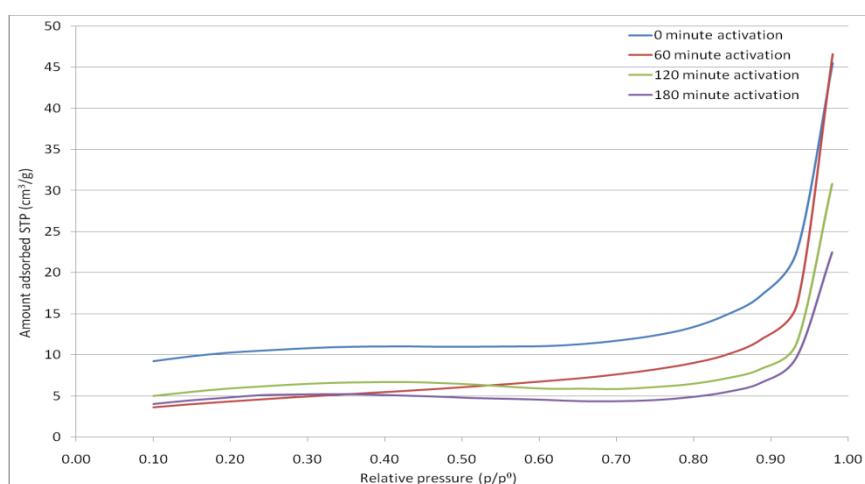


Figure 3.2.44: Nitrogen adsorption isotherms of coked mordenite unactivated and activated at 500°C for different activation times, generated with methanol at 300°C for 300 minutes.

Figure 3.2.44 presents stacked N₂ physisorption isotherms for the unactivated mordenite and materials activated at the various times employed. Post-reaction nitrogen adsorption isotherms were type IV for the unactivated coked mordenite and type II for all activated coked samples. BET surface areas along with single point surface area determination at $p/p^0 = 0.1$ are presented in Table 3.2.8.

Material	BET surface area (m ² g ⁻¹)	Single point surface area at $p/p^0 = 0.1$ (m ² g ⁻¹)	Isotherm
Unactivated	33	36	Type IV
60 minutes activation	16	14	Type II
120 minutes activation	20	20	Type II
180 minutes activation	17	16	Type II

Table 3.2.8: BET and single point surface areas and isotherm types for coked mordenite unactivated and activated at 500°C for different activation times, generated with methanol at 300°C for 300 minutes.

The surface area is constant regardless of activation time (at approximately 18m²g⁻¹) and displays no apparent microporosity indicating that the micropores are no longer accessible. The unactivated form has a surface area of 33m²g⁻¹ and still displays a small amount of porosity as indicated by the type IV isotherm. According to the carbon contents there is approximately 50% less carbon present on the unactivated mordenite compared to any of the activated forms. The thermal analysis shows a significant derivative mass peak which may be associated with external surface species, it is apparent that the carbonaceous deposits must be forming close to the pore openings and completely blocking off otherwise accessible internal micropore volume, while leaving a small amount of micropore volume accessible from the external surface.

Stacked XRD patterns are presented in Figure 3.2.45 for unactivated mordenite and materials activated at the various times employed. In Figure 3.2.45 it can be observed that the activated samples exhibit a shift from the unactivated sample. This indicates that there may be a deformation of the crystal lattice. On the basis of the isotherms presented, it can be hypothesised that a degree of strain may be exhibited upon the pore walls of the zeolite due to the formation of large bulky products such as alkyl substituted aromatic and polycyclic species.

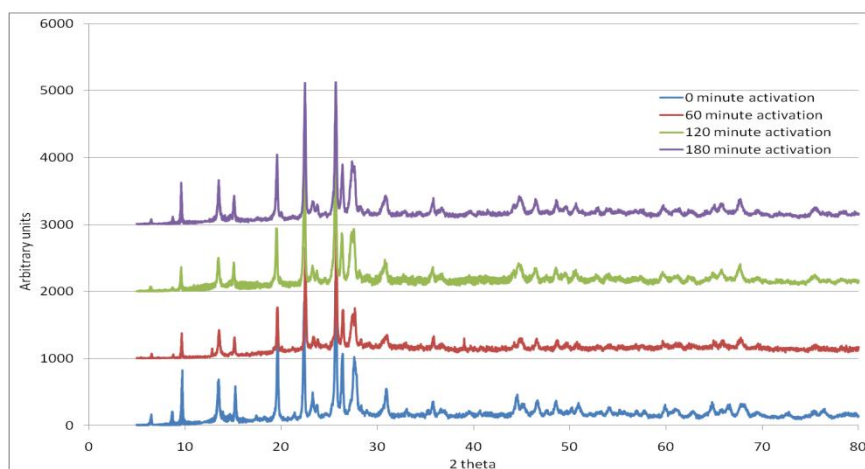


Figure 3.2.45: XRD patterns of coked mordenite unactivated and activated at 500°C for different activation times, generated with methanol at 300°C for 300 minutes.

3.2.6 Carbonaceous species generated by reaction of methanol with some materials other than mordenite

In order to determine whether other materials produce carbonaceous deposits of a similar nature to the mordenite sample discussed previously, Cu(55)MOR20, MCM-41 and γ -alumina were examined. Materials were activated at 500°C for 60 minutes under a 30ml min⁻¹ argon gas stream. They were then run at 300°C for 300 minutes in a 50% methanol feedstream with a GHSV of 3000hr⁻¹. Post-coking samples were allowed to cool to room temperature under argon.

The carbon content and the H:C ratios are presented in Table 3.2.5 for pre- and post-coking Cu(55)MOR20, MCM-41 aluminosilicate and γ -alumina.

Material	Cwt%	H:C ratio
Cu(55)MOR20	0	-
Coked Cu(55)MOR20	11.23	1.44
MCM-41	0	-
Coked MCM-41	3.10	3.17
γ -alumina	0	-
Coked γ -alumina	0.59	9.00

Table 3.2.9: Carbon content and atomic H:C ratio of materials and coked materials generated with methanol at 300°C for 300 minutes (Not corrected for the influence of adsorbed water).

It can be observed in Table 3.2.9 that none of the pre-reaction samples contain any carbon. The carbon content of coked Cu(55)MOR20 is approximately 11.2wt% which is a little lower than those observed in the case of its non-Cu containing counterpart. This indicates that through the influence of the copper species, less carbon may have accumulated on the material. This could be as a result of occlusion effects of the copper, or may arise from a direct effect of the copper particles. The atomic H:C ratio is approximately 1.4 indicating a similar distribution of species as those observed for samples generated at identical conditions discussed previously.

The post-coking carbon content of MCM-41 is approximately 3.1wt% which is significantly less than that observed for mordenite. This is consistent with the lower strength of acidity associated with MCM-41 as compared to zeolite systems [56]. The atomic H:C ratio is approximately 3.2 indicating the presence of a significant quantity of water adsorbed on the material.

The carbon content of coked γ -alumina is approximately 0.6wt%, indicating that comparatively little coking occurs over the material under the reaction conditions. The atomic H:C ratio is 9.0 indicating the presence of relatively large quantities of water and hydroxyl groups in the material.

Overlaid first derivative TGA profiles are presented in Figure 3.2.46 for Cu(55)MOR20 prior to and post-coking, Figure 3.2.47 for MCM-41 aluminosilicate prior to and post-coking and Figure 3.2.48 for γ -alumina prior to and post-coking.

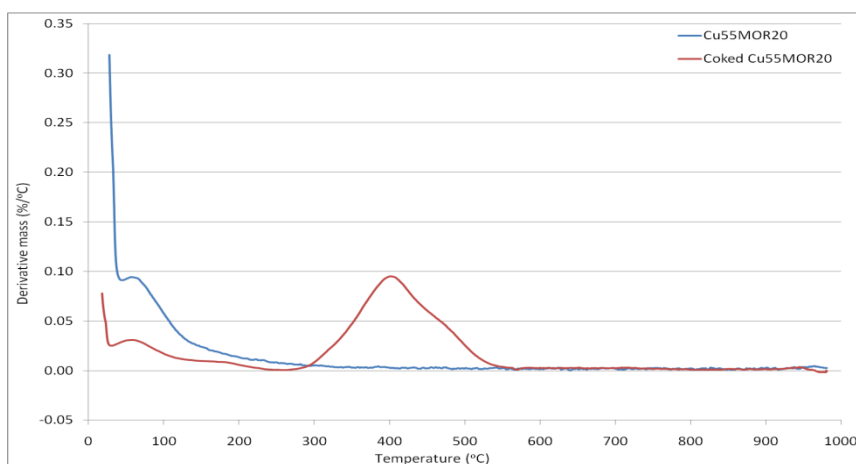


Figure 3.2.46: First derivative TGA profiles attained under air of Cu(55)MOR20 and coked Cu(55)MOR20 generated with methanol at 300°C for 300 minutes.

In Figure 3.2.46 it can be observed that the prior to and post-coking Cu(55)MOR20 samples exhibit very different first derivative TGA profiles. The pre-reaction sample exhibits a single first derivative TGA profile peak at approximately 80°C which is attributed to adsorbed water. This is elevated by 20°C compared to the first derivative TGA profile displayed previously for NH₄MOR20.

The coked sample exhibits a much more interesting first derivative TGA profile. Peaks are observed at 70 and 400°C. The peak at 70°C is associated with the adsorbed water present on the material. The broad peak at 400°C is attributed to the carbonaceous deposits in the ion exchanged zeolite. Due to the presence of the copper in the system the combustion of the carbonaceous deposits is catalysed reducing the previously observed combustion temperature of approximately 625°C for carbonaceous species present in the pores of the zeolite.

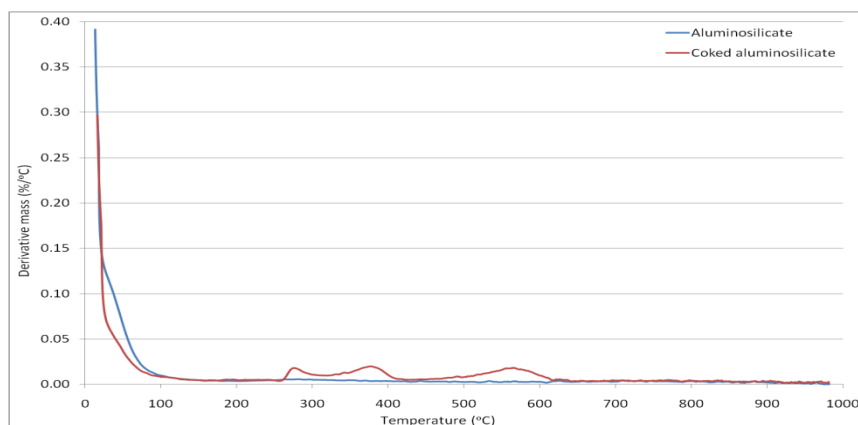


Figure 3.2.47: First derivative TGA profiles attained under air of MCM-41 and coked MCM-41 generated with methanol at 300°C for 300 minutes.

In Figure 3.2.47 it can be observed that pre- and post-reaction MCM-41 exhibit different first derivative TGA profiles. The pre-coking sample exhibits a single peak present at approximately 70°C and can be attributed to the presence of adsorbed water. The coked sample offers a slightly more interesting pattern with relatively small peaks present at 60, 280, 375 and 550°C.

The peak at 60°C is associated with adsorbed water. The peaks at 280, 375 and 550°C are associated with the small quantity of carbonaceous deposits present on the MCM-41. It may be expected that the lower temperatures are associated with surface bound species whereas the higher temperature is associated with species formed in the pores of the aluminosilicate. This would indicate a similar profile as those observed for the non-copper containing mordenite catalysts observed previously, but with reduced temperatures.

It can be observed in Figure 3.2.48 that the pre- and post-reaction γ -alumina display similar first derivative mass spectra. The non-coked sample exhibits a single peak associated with adsorbed water at approximately 70°C. The coked sample exhibits two small peaks at 60 and 400°C. The peak at 60°C is attributed to the presence of adsorbed water. The peak at 400°C is associated with the small quantity of carbonaceous deposit observed on the material post-coking.

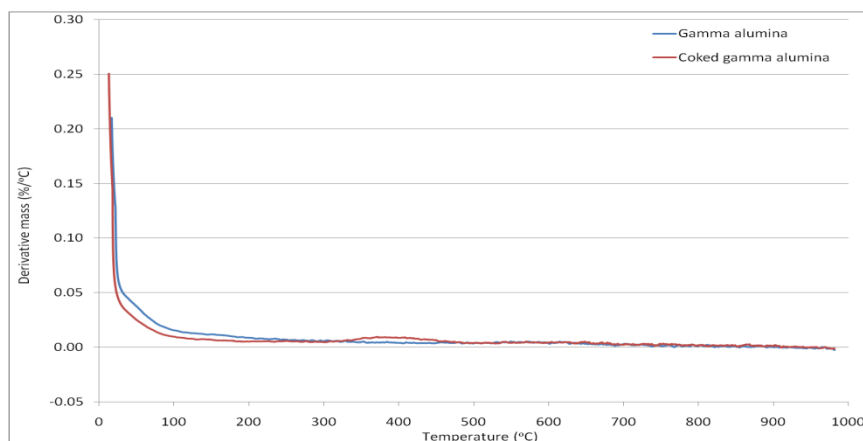


Figure 3.2.48: First derivative TGA profiles attained under air of γ -alumina and coked γ -alumina generated with methanol at 300°C for 300 minutes.

Stacked isotherms are presented in Figure 3.2.49 for Cu(55)MOR20 prior to and post-coking, Figure 3.2.50 for non-coked and coked MCM-41 and Figure 3.2.51 for γ -alumina prior to and post-coking.

In Figure 3.2.49 it can be observed that Cu(55)MOR20 exhibits a type IV isotherm and a type II isotherm for the coked sample. BET analysis gives a surface area of 217 m^2g^{-1} (single point surface area at $p/p^0 = 0.1$ of 274 m^2g^{-1}) prior to coking and 15 m^2g^{-1} (single point surface area at $p/p^0 = 0.1$ of 14 m^2g^{-1}) for the post-coking material. Comparing the surface area of the $\text{NH}_4\text{MOR20}$ (244 m^2g^{-1}) to the Cu(55)MOR20 (217 m^2g^{-1}) there appears to be a decrease in surface area due to the incorporation of the copper. This may be as a direct result of the presence of the copper within the pores of the material or as a result of dealumination of the framework, limiting pore accessibility. A significant decrease in the surface area is observed post-reaction and a change in the type of isotherm indicating the apparent loss of porosity due to the deposition of the carbonaceous material.

In Figure 3.2.50 it can be observed that both pre and post-reaction MCM-41 exhibit a type IV isotherm. The application of the BET relationship results in a surface area of 926 m^2g^{-1} (single point surface area at $p/p^0 = 0.1$ of 839 m^2g^{-1}) for the non-coked material and 760 m^2g^{-1} (single point surface area at $p/p^0 = 0.1$ of 658 m^2g^{-1}) for the coked sample.

A decrease in the surface area and no obvious change in the general shape of the isotherm are observed post-reaction. The decrease in the surface area is rather large indicating that the

carbonaceous deposits are present to a degree in the pores of the aluminosilicate, but do not block the network significantly to indicate a complete loss of the porosity.

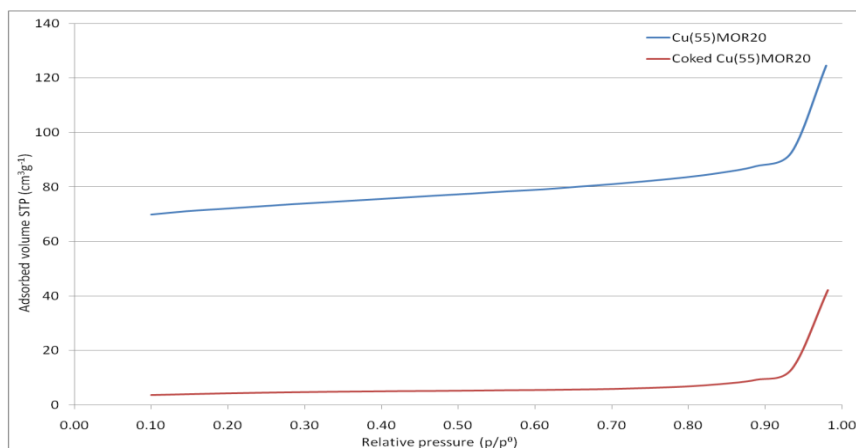


Figure 3.2.49: Nitrogen adsorption isotherms of Cu(55)MOR20 and coked Cu(55)MOR20 generated with methanol at 300°C for 300 minutes.

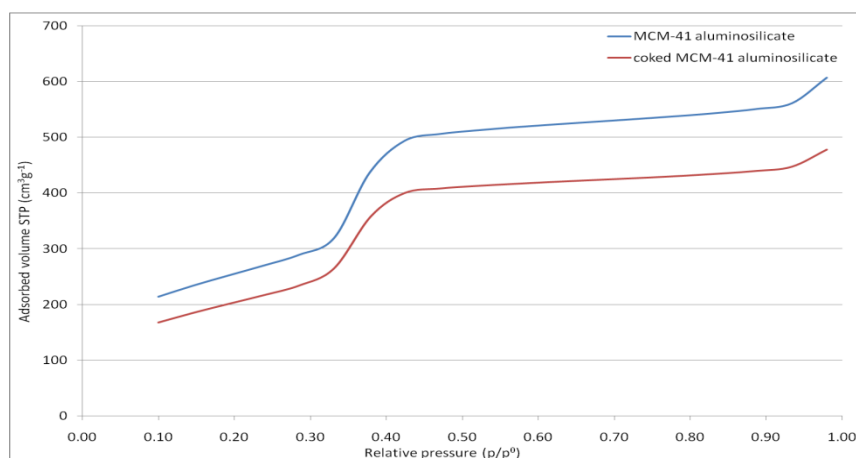


Figure 3.2.50: Nitrogen adsorption isotherms of MCM-41 and coked MCM-41 generated with methanol at 300°C for 300 minutes.

Both pre- and post-reaction γ -alumina exhibits a type IV isotherm. The BET method results in a surface area of 143 m²g⁻¹ (single point surface area at $p/p^0 = 0.1$ of 127 m²g⁻¹) prior to coking and 140 m²g⁻¹ (single point surface area at $p/p^0 = 0.1$ of 131 m²g⁻¹) for the post-reaction sample.

In Figure 3.2.51 it can be observed that no blockage of pores has occurred post-reaction for γ -alumina as the pre- and post-coking isotherms are almost identical when overlaid. The surface area indicates no apparent change pre and post-reaction, indicating that the small quantity of carbon observed in via elemental analysis must be well distributed on the surface of the alumina.

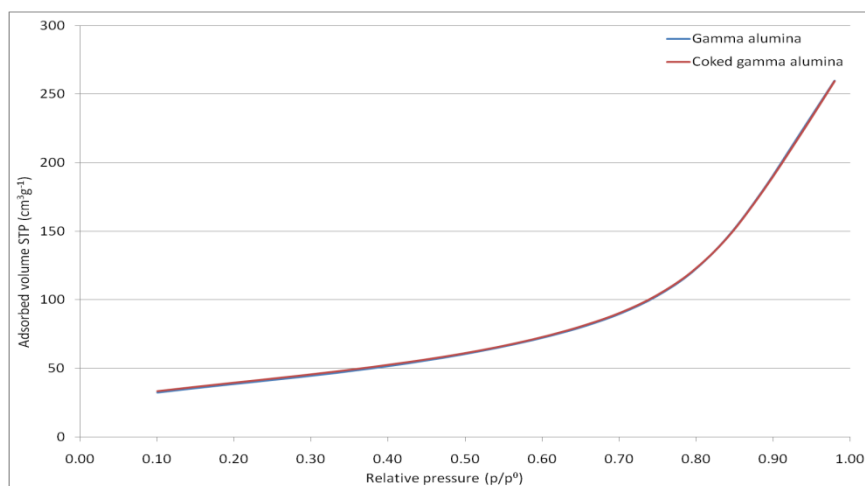


Figure 3.2.51: Nitrogen adsorption isotherms of γ -alumina and coked γ -alumina generated with methanol at 300°C for 300 minutes.

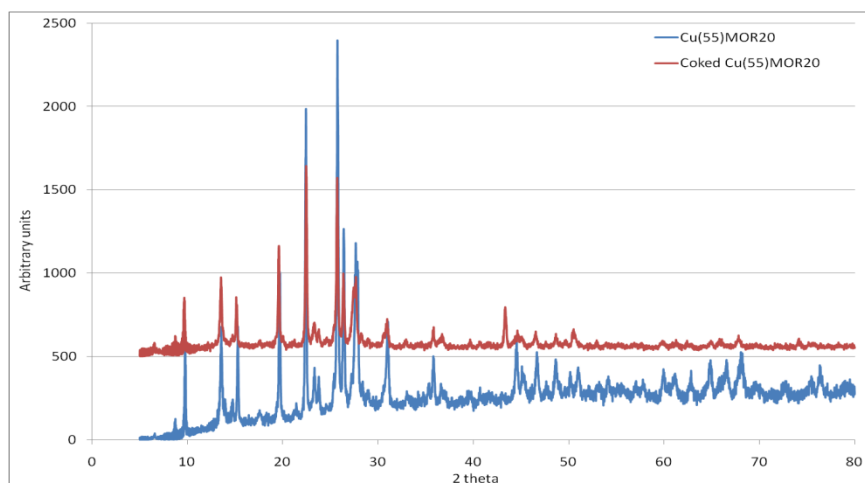


Figure 3.2.52: XRD patterns of Cu(55)MOR20 and coked Cu(55)MOR20 generated with methanol at 300°C for 300 minutes.

Stacked XRD patterns are presented in Figure 3.2.52 for Cu(55)MOR20 prior to and post-reaction, Figure 3.2.53 for MCM-41 aluminosilicate prior to and post-reaction and Figure 3.2.54 for γ -alumina prior to and post-reaction. In Figure 3.2.52 it can be observed that there is an increasing background in the pre-reaction sample due to the highly dispersed copper in the sample and hence no copper associated peaks are observed. During coking the copper sinters to a degree and diffraction peaks associated with copper become visible at approximately 43 and $74^\circ 2\theta$. It is also apparent that the post-reaction sample appears to have a shifted reflection (511) at approximately $28^\circ 2\theta$ which is attributed to lattice deformation. Given that the nitrogen adsorption isotherms presented in Figure 3.2.49 suggest that the pores of the zeolite are completely blocked, it could be hypothesised that the bulky carbonaceous residue results in strain occurring within the pores.

In Figure 3.2.53 it can be observed that there is no difference between the two XRD patterns of MCM-41 pre- and post-reaction. No shift in the peak at $2^\circ 2\theta$ is observed indicating that no deformation of the lattice occurs. The isotherms presented in Figure 3.2.50 support this as there is still a significant amount of porosity present within the post-reaction aluminosilicate.

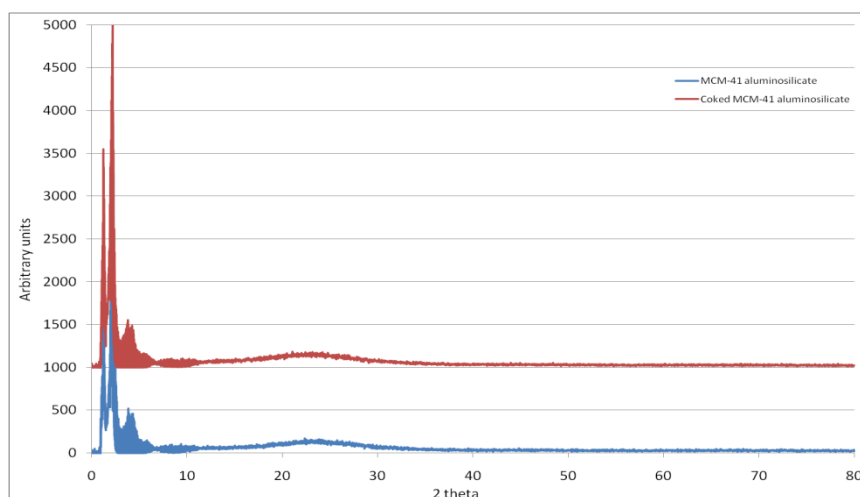


Figure 3.2.53: XRD patterns of MCM-41 and coked MCM-41 generated with methanol at 300°C for 300 minutes.

In Figure 3.2.54 it can be observed that there is no difference between the two γ -alumina XRD patterns pre- and post-reaction. As there was very little carbon observed over the material and no obvious change in the isotherms Figure 3.2.51, surface area and porosity this may be expected.

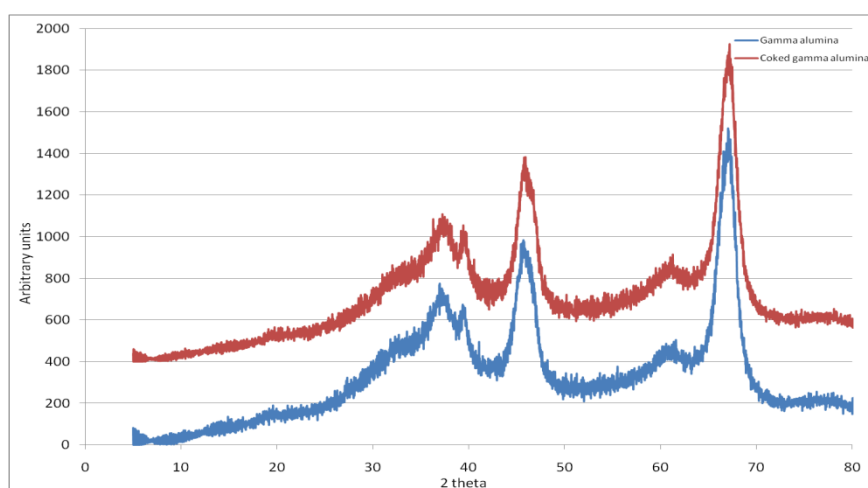


Figure 3.2.54: XRD patterns of γ -alumina and coked γ -alumina generated with methanol at 300°C for 300 minutes.

3.3 Conclusions

It was observed in general that as the reaction temperature was increased that the carbon content and hydrogen deficiency of the carbonaceous residue increased. This was further supported by the ^{13}C CP solid state NMR investigations which indicated that the carbonaceous residue underwent distinct changes from aromatic species at 150°C through methylated benzenes between 250-300°C to polycyclic aromatic species observed at 500°C. Between 350-450°C a plateau in carbon content was observed.

The reactivity of the carbonaceous deposits was probed by TGA, which indicated discrete regions of mass loss under an air atmosphere. Samples generated at 250-350°C exhibited unique, albeit relatively minor loss features at approximately 325 and 425°C. The sample generated at 400°C exhibited features at 425 and 525°C. Employing a lower oxygen concentration and mass spectrometry demonstrated that these lower temperature peaks undergo both cracking and combustion processes. An argon atmosphere showed that the

features at lower temperatures would readily crack at similar temperatures as those observed with a lower oxygen concentration. The samples generated 200 and 400°C show significantly more cracking products. However these materials were reanalysed under air after the argon treatment and it was found that all lower temperature features previously attributed to carbonaceous species were removed.

Thermal volatilisation analysis of the samples generated at 300 and 500°C further demonstrated the differences between the carbonaceous deposits formed. The sample generated at 300°C exhibited a whole host of species including a broad distribution of aromatic materials in a similar form to those known to exist as a hydrocarbon pool. The sample generated at 500°C exhibited no aromatic fraction and only methane and hydrogen evolution was observed, which suggests that the carbonaceous deposits are in an inactive form.

Nitrogen adsorption isotherms indicated a large change in the surface area for the sample generated at 150°C which contained a relatively small amount of carbon (4 wt%). Samples generated at 250-500°C exhibited complete loss of microporosity. By comparison the $p/p^0 = 0.1$ data gave the same trend as that observed for BET, with some small changes in the observed surface area. XRD analysis demonstrated that the zeolite framework remained intact after reaction. ^{27}Al DP solid state NMR spectroscopy, however, suggested that an increase in the amount of extra framework aluminium was observed after reaction for samples generated at 300 and 500°C.

In general, increasing the reaction time resulted in an increase in the carbon content and hydrogen deficiency of the carbonaceous residue. A plateau was observed across a 300 minute time period (120-420 minutes) possibly suggesting the formation of an active hydrocarbon pool. ^{13}C DP solid state NMR investigations demonstrated that polymethylbenzene species were formed rapidly over the mordenite. Materials coked at longer reaction times 60, 180 and 420 minutes exhibited similar ^{13}C CP solid state NMR spectra. The sample generated at 600 minutes however appeared to contain a larger fraction of polycyclic species.

The reactivity of the carbonaceous residue was quite similar regardless of reaction time. At longer time on stream 480-600 minutes a shoulder was observed at 525°C in the broad peak observed at approximately 625°C much like that observed for the sample generated at 400°C for 300 minutes.

At 2 and 5 minutes on stream a degree of porosity was retained, from 30 to 480 minutes the surface area remained constant and the isotherm (type II) indicated that the micropores were completely blocked. A further decrease in surface area was observed for samples generated at 540 and 600 minutes respectively. The same trend was observed employing the $p/p^0 = 0.1$ data set. XRD analysis indicated that the framework was retained after reaction, although some changes were observed at higher $^{\circ} 2\theta$ values. These changes are not believed to be related to the formation of extra-framework aluminium species as suggested by Boveri *et al.* [57], but rather may be a consequence of coking [58].

In general with increasing ethanol impurity, the carbon content and hydrogen deficiency of the deposited carbonaceous species do not change much. The sample generated with a 0.90 mol% impurity at 300°C for 300 minutes however exhibited a rather significant increase in carbon at 14.7 wt%.

The reactivity of the carbonaceous deposits was observed to be similar regardless of the ethanol impurity employed, though the sample generated with a 1.10 mol% impurity exhibited a first derivative TGA profile similar to that observed for higher temperatures with “pure” methanol-only coking. The materials all exhibited similar nitrogen adsorption isotherms and surface areas (BET and $p/p^0 = 0.1$). Post-reaction XRD analysis indicated that the framework remained unaffected with increasing ethanol impurity.

The addition of a 2.00 mol% methyl acetate impurity had no effect on carbon content, hydrogen deficiency or reactivity of the carbonaceous deposits. This is compared to studies undertaken with a methanol-only feedstream at the equivalent temperature for 300 minutes. Nitrogen adsorption isotherms and post-reaction XRD investigations indicated respectively that the micropores were completely blocked and that the framework was retained after reaction. Although some very small changes in the pattern were observed at larger $^{\circ} 2\theta$ values, which are believed to be phenomena related to coking [58]. Perhaps, interestingly, not all of the systems examined exhibited this hence further work would be required to verify this.

It was found that activated mordenite exhibited very similar carbonaceous species regardless of activation time. Carbon contents and hydrogen deficiency were found to be almost identical and the first derivative TGA profiles were almost identical when overlaid, indicating the similarity in the reactivity of the carbonaceous deposits. However the carbonaceous

species formed over the unactivated mordenite contained approximately 50% less carbon and was 50% less hydrogen deficient.

The first derivative TGA profile exhibited features coinciding with the formation of carbonaceous deposits similar in reactivity to deposits formed upon activated mordenite. The unactivated mordenite sample retained a small degree of microporosity, whereas the activated materials exhibited a complete loss. XRD patterns show that in all instances regardless of activation time the framework remains intact, though shifted for activated mordenites.

All of the other materials studied and coked with a methanol-only feedstream at 300°C for 300 minutes, contained carbon after reaction. Cu(55)MOR20 exhibited a comparable amount (11.2 wt%) to an activated ammonium mordenite (12.3 wt%). MCM-41 and γ -alumina exhibit significantly less (3.1 and 0.6 wt% respectively) due to lower acid strength compared to zeolite systems.

The reactivity of the carbonaceous deposits was observed to be higher for the copper mordenite, but this may have been in part due to the presence of copper which could have promoted the combustion of the carbonaceous residue. The sample completely lost microporosity upon coking and the resultant XRD pattern exhibited signs of copper sintering post-reaction and that the zeolite framework was retained.

MCM-41 and γ -alumina exhibited very little mass loss in their respective first derivative TGA profiles, due to carbonaceous deposits though they were observed in similar regions albeit lower temperature to those exhibited by ammonium mordenite. The MCM-41 sample exhibited an 18% loss in surface area post-reaction, but still retained a large degree of microporosity. Post-reaction γ -alumina has a very similar nitrogen adsorption isotherm to the pre-reaction sample, indicating no change in the pore volume or surface area. The XRD pattern shows that the pore structure is retained for the aluminosilicate and alumina samples.

From studies employing a methanol-only feedstream, it was found that the carbonaceous species deposited rapidly on mordenite (methyl aromatics were observed at two minutes time on stream). As the temperature was increased, the deposits became more graphitic like. Impurities (ethanol or methyl acetate) had little effect on the amount or reactivity of the carbonaceous deposits. Mordenite produced a unique distribution of species which are not formed with MCM-41 or γ -alumina. Additional activation time had no obvious effect on the amount or reactivity of the species.

Overall very little difference was observed between the surface areas determined from the BET equation and single point surface area determination at $p/p^0 = 0.1$, except in the case of the MCM-41 sample. Where a significantly lower surface area was observed for the data determined at $p/p^0 = 0.1$, which was lower than quoted by Sigma-Aldrich ($900-950 \text{ m}^2 \text{ g}^{-1}$). Perhaps, interestingly, no apparent enhancement was observed for the unactivated mordenite (composite type I/IV isotherm).

References

- [1] J. Haw, W. Song, D. Marcus, J. Nicholas, *Accounts of Chemical Research* 36 (2003) 317
- [2] C. Chang, A. Silvestri, *Journal of Catalysis* 47 (1977) 249
- [3] C. Chang, A. Silvestri, *Chemical technology* 10 (1987) 624
- [4] M. Bjorgen, S. Svelle, F. Joenson, J. Nerlov, S. Kolboe, F. Bonino, L. Palumbo, S. Brodiga, U. Olsbye, *Journal of Catalysis* 249 (2007) 195
- [5] M. Stocker, *Microporous and Mesoporous Materials* 29 (1999) 3
- [6] H. Zaidi, K. Pant, *Catalysis Today* 96 (2004) 155
- [7] J. Fougerit, N. Gnep, M. Guisnet, *Microporous and Mesoporous Materials* 29 (1999) 79
- [8] B. Arstad, S. Kolboe, *Catalysis Letters* 71 (2001) 209
- [9] W. Song, H. Fu, J. Haw, *Journal of the American Chemical Society* 123 (2001) 4744
- [10] G. Moradi, F. Yaripour, P. Vale-Sheyda, *Fuel Processing Technology* 91 (2010) 461
- [11] I. Dahl, S. Kolboe, *Catalysis Letters* 20 (1993) 329
- [12] I. Dahl, S. Kolboe, *Journal of Catalysis* 149 (1994) 458
- [13] B. Arstad, S. Kolboe, *Journal of the American Chemical Society* 123 (2001) 8137
- [14] M. Bjorgen, S. Akyalcin, U. Olsbye, S. Bernard, S. Kolboe, S. Svelle, *Journal of Catalysis* 275 (2010) 170
- [15] D. Lestaege, V. Van Speybroeck, M. Waraquier, *Physical Chemistry Chemical Physics* 11 (2009) 5222
- [16] S. Svelle, M. Bjorgen, S. Kolboe, D. Kuck, M. Letzel, U. Olsbye, O. Sekiguchi, E. Uggerud, *Catalysis Letters* 109 (2006) 25
- [17] S. Kolboe, S. Svelle, B. Arstad, *The Journal of Physical Chemistry A* 113 (2009) 917

- [18] T. Mole, G. Bett, D. Seddon, *Journal of Catalysis* 84 (1983) 435
- [19] A. Sassi, M. Wildman, H. Ahn, P. Prasad, J. Nicholas, J. Haw, *The Journal of Physical Chemistry B* 106 (2002) 2294
- [20] C. Li, P. Stair, *Studies in Surface Science and Catalysis* 105 (1997) 500
- [21] J. Park, S. Kim, M. Seo, S. Kim, Y. Sugi, G. Seo, *Applied Catalysis A: General* 349 (2008) 76
- [22] M. Bjorgen, U. Olsbye, S. Kolboe, *Journal of Catalysis* 215 (2003) 30
- [23] M. Bjorgen, U. Olsbye, D. Petersen, S. Kolboe, *Journal of Catalysis* 221 (2004) 1
- [24] J. Haw, D. Marcus, *Topics in Catalysis* 34 (2005) 41
- [25] Y. Chua, P. Chair, *Journal of Catalysis* 213 (2003) 39
- [26] M. Anderson, M. Ocelli, J. Klinowski, *The Journal of Physical Chemistry* 96 (1992) 388
- [27] Y. Jiang, M. Hunger, W. Wang, *Journal of the American Chemical Society* 128 (2006) 11679
- [28] W. Wang, A. Buchholz, M. Seiler, M. Hunger, *Journal of the American Chemical Society* 125 (2005) 15260
- [29] www.chem.wisc.edu/areas/reich/handouts/nmr-c13/cdata.htm (accessed on 31/03/2011)
- [30] M. Seiler, U. Schenk, M. Hunger, *Catalysis Letters* 62 (1999) 139
- [31] F. Oliver, E. Munson, J. Haw, *The Journal of Physical Chemistry* 96 (1992) 8106
- [32] A. Sassi, W. Song, M. Wildman, J. Haw, *Catalysis Letters* 81 (2002) 101
- [33] W. Kolodziejwski, A. Corma, K. Wozniak, J. Klinowski, *The Journal of Physical Chemistry* 100 (1996) 7345
- [34] H. Schulz, Z. Siwei, W. Baumgartner, *Studies in Surface Science and Catalysis* 34 (1987) 479
- [35] J. Xia, D. Mao, N. Xu, Q. Chen, Y. Zhang, Y. Tang, *Chemistry Letters* 33 (2004) 1456
- [36] G. Maurin, P. Senet, S. Devautour, P. Gaveau, F. Henn, V. Van Doren, J. Giuntini, *The Journal of Physical Chemistry B* 105 (2001) 9157
- [37] J. Kuhn, J. Gross, J. Jansen, F. Kapteijn, P. Jansens, From zeolites to porous MOF materials-The 40th anniversary of international zeolite conference. *170 A* (2007) 942
- [38] M. Hunger, *Catalysis Today* 97 (2004) 3

- [39] L. Carlson, P. Isbester, E. Munson, *Solid State Nuclear Magnetic Resonance* 16 (2000) 93
- [40] J. White, M. Truitt, *Progress in Nuclear Magnetic Resonance Spectroscopy* 51 (2007) 139
- [41] X. Han, Z. Yan, W. Zhang, X. Bao, *Current Organic Chemistry* 5 (2001) 1017
- [42] U. Olsbye, M. Bjorgen, S. Svelle, K. Lillerud, S. Kolboe, *Catalysis Today* 106 (2005) 108
- [43] B. Hereijgers, F. Bleken, M. Nilsen, S. Svelle, K. Lillerud, M. Bjorgen, B. Weckhuysen, U. Olsbye, *Journal of Catalysis* 264 (2009) 77
- [44] T. Mole, J. Whiteside, *Journal of Catalysis* 82 (1983) 261
- [45] S. Teketel, S. Svelle, K. Lillerud, U. Olsbye, *ChemCatChem* 1 (2009) 78
- [46] O. Mikkelsen, P. Ronning, S. Kolboe, *Microporous and Mesoporous Materials* 40 (2000) 95
- [47] B. Arstad, J. Nicholas, J. Haw, *Journal of the American Chemical Society* 126 (2004) 2991
- [48] D. McCann, D. Lesthaeghe, P. Kletnieks, D. Guenther, M. Hayman, V. Van Speybroeck, M. Waroquier, J. Haw, *Angewandte Chemie International Edition* 47 (2008) 5179
- [49] P. Magnoux, M. Guisnet, *Applied Catalysis* 38 (1988) 341
- [50] M. Vandichel, D. Lesthaeghe, J. Van der Mynsbrugge, M. Waroquier, V. Van Speybroeck, *Journal of Catalysis* 271 (2010) 67
- [51] R. Johansson, S. Hruby, J. Rass-Hansen, C. Christensen, *Catalysis Letters* 127 (2009) 1
- [52] A. Bhan, A. Allian, G. Sunley, D. Law, E. Iglesia, *Journal of the American Chemical Society* 129 (2007) 4919
- [53] M. Boronat, C. Martinez-Sanchez, D. Law, A. Corma, *Journal of the American Chemical Society* 130 (2008) 16316
- [54] G. Sunley, D. Watson, *Catalysis Today* 58 (2000) 293
- [55] P. Cheung, A. Bhan, G. Sunley, E. Iglesia, *Angewandte Chemie International Edition* 45 (2006) 1617
- [56] K. Madhusudan Reddy, C. Song, *Catalysis Today* 31 (1996) 137
- [57] M. Boveri, C. Marquez-Alvarez, M. Laborde, E. Sastre, *Catalysis Today* 114 (2006) 217
- [58] J. Zhang, H. Zhang, X. Yang, Z. Huang, W. Cao, *Natural Gas Chemistry* 20 (2011) 266

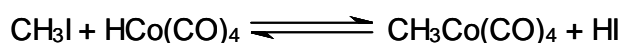
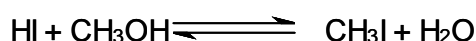
4 Carbonaceous species deposited from methanol carbonylation

4.1 Introduction

Methanol carbonylation was first developed in the 1950's by Walter Reppe at BASF [1, 2]. As a result of the development of new Mo-Ni alloys (hastelloye), reactors able to withstand the corrosion associated with the presence of iodide species were developed at the end of the 1950's enabling the development of an industrial scale process in the 1960's [3, 4].

The process developed by BASF involved reaction of methanol and or DME and water with carbon monoxide in the presence of CoI_2 in the liquid phase operating at 250°C at 600 bar [1, 2].

It was envisaged that the reaction proceeds as shown in Reaction Scheme 4.1.1, where the starting complex cobalt iodide initially reacts with water and carbon monoxide to produce tetracarbonyl-hydridocobalt and hydrogen iodide. Methanol and hydrogen iodide react to produce a mixture of water and methyl iodide. The methyl iodide then interacts with the tetracarbonyl-hydridocobalt complex regenerating the hydrogen iodide and producing the intermediate tetracarbonyl-methylcobalt. Carbon monoxide is inserted into the $\text{CH}_3\text{-Co}$ bond of the complex this then hydrolyzes producing acetic acid and regenerating tetracarbonyl-hydridocobalt [5].

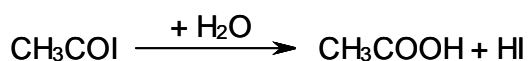
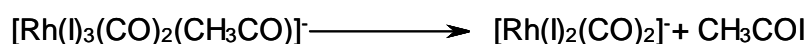
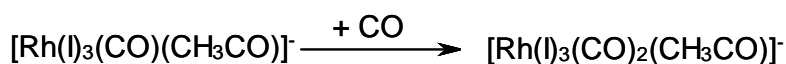
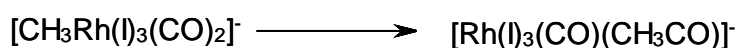
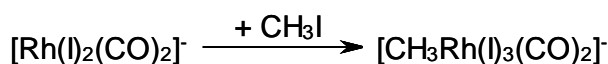
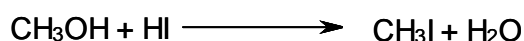


Reaction Scheme 4.1.1: The BASF methanol carbonylation process.

The selectivity of this process is 90% with respect to methanol and 70% with respect to carbon monoxide [6].

In 1968 Monsanto announced an improvement over the existing BASF process by employing a rhodium based catalyst [7]. However, methyl iodide was still required as a co-catalyst. The process employed milder conditions than those previously required, where methanol and carbon monoxide react continuously in the liquid phase at 180°C and 30 bar [6].

The process operates in a slightly different manner to the BASF process and the various steps are outlined in Reaction Scheme 4.1.2. The main differences are that the hydrogen iodide was not formed *in-situ* and that the rhodium based catalyst contains iodide, as opposed to just carbonyl, ligands.



Reaction Scheme 4.1.2: The Monsanto methanol carbonylation process [6, 8].

The selectivity of the process is 99% with respect to methanol and 85% with respect to carbon monoxide [9].

In 1996 BP unveiled their new methanol carbonylation technology, the Cativa process [9, 10] which employs iridium and iodide based catalysts [11] in conjunction with a ruthenium promoter [6]. The process operates at similar conditions to the Monsanto technology but offers a whole host of benefits including; higher reaction rates, cheaper catalysts and enhanced selectivity (most notably a reduction in the water-gas shift side reaction). Overall, Cativa has better CO utilisation than the Monsanto process (about 30% less CO₂ is emitted)

[6]. The rate determining step was found to be the carbonyl insertion [12]. Furthermore, the reaction of methyl iodide was found to be approximately 100 times faster than for the Monsanto process [6].

All of the above processes are homogeneous and require the catalyst to be dissolved in water to avoid precipitation of the complex. They also require the use of a very corrosive iodide compound which makes reactor builds expensive. Hence new technologies are currently being developed to remove the necessity of using a halide co-catalyst and the need for the presence of water, in a bid to reduce cost and significantly decrease the amount carbon dioxide being produced. Recently work involving BP describing the application of copper exchanged mordenite as a possible catalyst for a heterogeneous halide-free carbonylation process has been published [13].

Subsequent studies by Cheung et al [14] have shown that higher rates of reaction and/or lower temperatures of conversion can be achieved by using dimethylether rather than methanol as a reactant, possibly due to water binding competitively at CO binding sites. It has also been observed that the carbonylation on acidic zeolites proceeds concurrently with side reactions (such as methanol to hydrocarbons) [15] and significant deactivation [14].

This study is directed towards examining the carbonaceous deposits formed during methanol carbonylation reactions and determining the nature of the species present. Furthermore, mordenite samples, as opposed to copper mordenite samples, are the focus of attention since subsequent interest has become directed towards non-doped samples as catalysts for the heterogeneous halide-free process.

4.2 Results and discussion

4.2.1 Temperature dependence of the carbonaceous species deposited during carbonylation

To probe the effect of reaction temperature on the carbonaceous species formed on the zeolite during methanol carbonylation chemistry, materials were activated at 500°C for 60 minutes under a 50 ml min⁻¹ N₂ stream. Activated mordenite was run in the methanol carbonylation

reaction for 300 minutes in a 10% methanol feedstream consisting of CO:H₂ in a 4:1 ratio at a GHSV of 3000 hr⁻¹. Four reaction temperatures were employed: 150, 250, 300 and 500°C. Coked mordenite samples were cooled to room temperature under a nitrogen flow.

¹³C CP MAS NMR spectroscopy was performed on the post-reaction materials in an attempt to identify the nature of any carbonaceous residue. The data is presented in Figure 4.2.1.

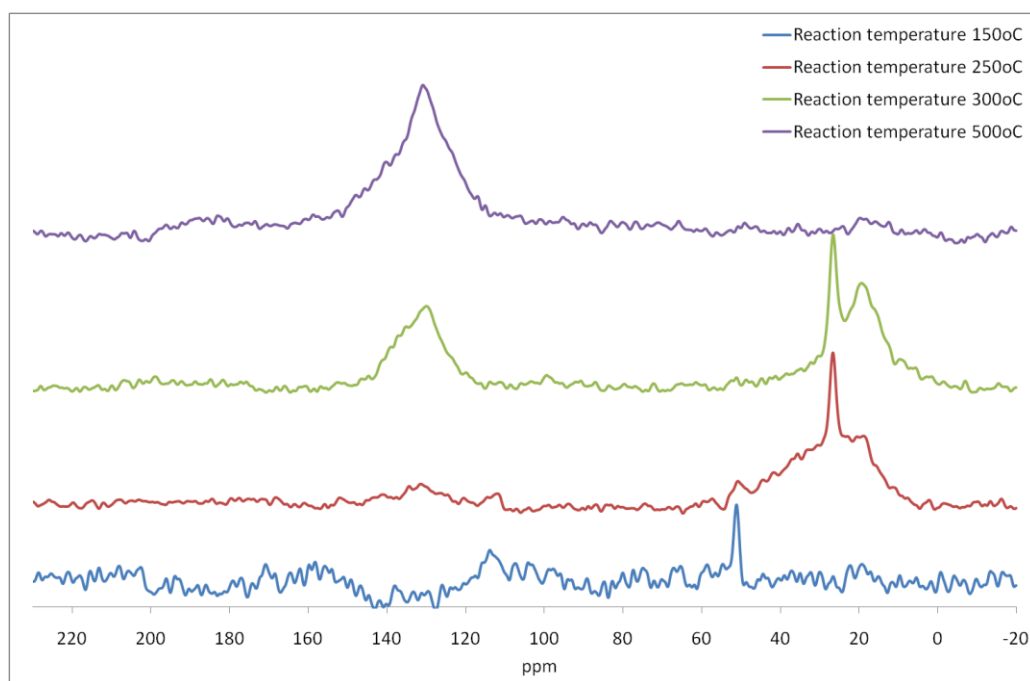


Figure 4.2.1: ¹³C CP MAS NMR spectrum of coked mordenite generated with methanol at different reaction temperatures for 300 minutes.

In Figure 4.2.1 for the sample generated at 150°C it can be observed that there is only a single sharp signal present *ca.* 51 ppm. The signal can be attributed to adsorbed methanol [16]. The lack of any other apparent carbon species over the coked mordenite indicates that at low reaction temperatures under carbonylation conditions methanol does not react to form other carbonaceous deposits such as dimethylether which would be expected to occur at *ca.* 60 ppm [17] or surface bound methoxy species which would be expected at *ca.* 56 ppm [17].

It can be observed that by increasing the reaction temperature to 250°C, carbonaceous deposits are formed. In this instance, a relatively large sharp signal is observed at 26 ppm. Other smaller signals are observed 18, 51 and 131 ppm. By increasing the reaction temperature, signals which can be attributed to methyl substituted aromatics at 18 and 131 ppm [18, 19, 20] are observed. The signal at 26 ppm can be attributed to trapped hydrocarbons [21] and methyl species attached to small polycyclic species [22]. Given that there is significant broadening between 5 and 45 ppm it is possible that a large range of additional aliphatic species may be present.

Upon increasing the temperature to 300°C, it can be seen that the signal observed at *ca.* 131 ppm has increased in intensity, as is also true for the signal at *ca.* 18 ppm. The signal at *ca.* 50 ppm is no longer apparent and there is no apparent change in the signal observed at 26 ppm. This indicates that by increasing the reaction temperature very little overall change occurs in the nature of the carbonaceous deposits, although it would appear that there has been a change in the distribution indicating an increase in the methylated aromatic species. The broadening is still apparent at 300°C suggesting that trapped aliphatic species may still be present.

It can be observed that upon increasing the reaction temperature to 500°C, that all associated methyl signals have been lost leaving a very large broad signal *ca.* 131 ppm. This signal suggests the presence of aromatic and polycyclic species [22]. Given the broadness of the signal a large distribution of species would be expected to be present.

It is interesting that the expected product of the carbonylation acetic acid was not observed under any of the conditions investigated (CH₃ at *ca.* 20 ppm and CO at *ca.* 170-180 ppm) [23, 24]. The presence of the potential by-product acetone was not observed (CH₃ at *ca.* 30 ppm and CO at *ca.* 206 ppm) [23, 24]. Therefore the NMR investigations suggest that the carbonaceous deposits formed over the zeolite in the first five hours of reaction for all temperatures except 150°C, are akin to the hydrocarbon pool found in methanol to hydrocarbon chemistry as discussed in the previous chapter. The sample generated at 300°C is representative of the target under which the process currently under development is operated. The sample generated at 150°C displays only adsorbed methanol suggesting that the temperature is insufficient under the conditions to generate hydrocarbon pool like species or undergo carbonylation. This is very different from the result reported in the case of the methanol-only feed of the same temperature for the same duration in the previous chapter.

Whilst the lower partial pressure of methanol should be born in mind in this respect, this result suggests an inhibiting effect of CO and/or the influence of H₂ present in the feedstream, although incomplete activation (as shown later) is also a possible contributing factor.

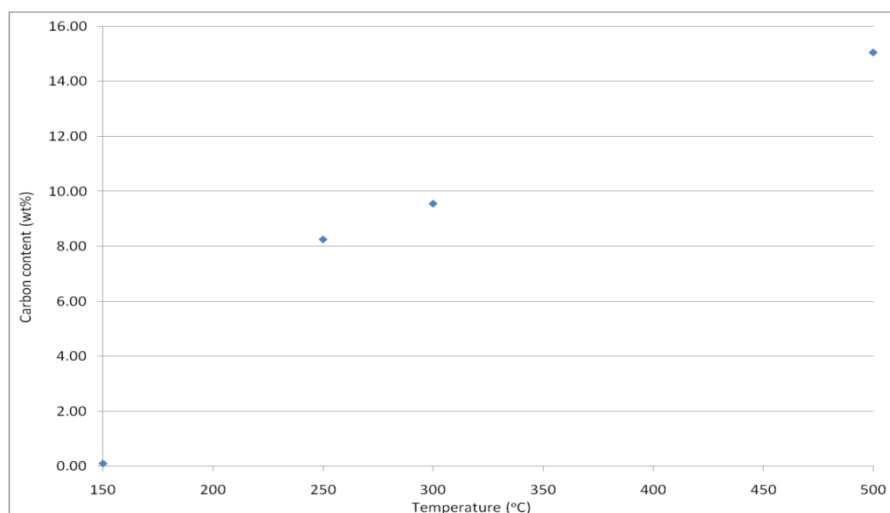


Figure 4.2.2: Carbon content of coked mordenite generated with methanol at different reaction temperatures for 300 minutes.

Elemental analysis was undertaken to determine the amount of carbon and hydrogen on the coked samples following reaction. The carbon content and the atomic H:C ratios are presented in Figures 4.2.2 and 4.2.3 for the various reaction temperatures employed. In Figure 4.2.2 it can be observed that post-150°C approximately 0.1 wt% carbon is deposited on the mordenite and the solid state NMR experiments demonstrated that this can be attributed to methanol. Increasing the temperature results in an increase in the carbon content observed on the post-reaction mordenite. The samples generated at 250 and 300°C show a small difference in carbon content of approximately 1.3 wt% with respect to each other. The sample generated at 500°C has a carbon content of approximately 15.1 wt%. In these reactions very little bed profile inhomogeneity was observed by visual inspection giving relatively good reproducibility between duplicate analyses (at least 97%).

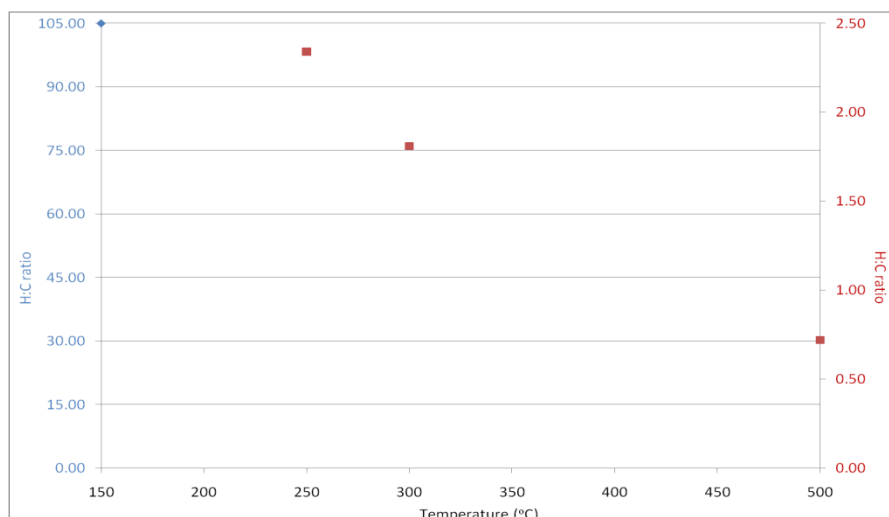


Figure 4.2.3: H:C atomic ratios of coked mordenite generated with methanol at different reaction temperatures for 300 minutes (not corrected for the influence of adsorbed water). The H:C ratio for the sample generated at 150°C should be measured against the left hand Y-axis, whereas 250, 300 and 500°C should be measured against the right Y-axis.

In Figure 4.2.3 it can be observed that post-150°C carbonylation that a large H:C atomic ratio is observed of approximately 105, indicating the lack of carbon present and a significant amount of water present on the material. Increasing the reaction temperature to 250 and 300°C results in post-reaction H:C atomic ratios of approximately 2.3 and 1.8 respectively. The sample generated at 500°C exhibits a H:C ratio of approximately 0.7, which indicates the increase in the hydrogen deficiency of the residue as the reaction temperature is increased. The solid state NMR spectra indicate the highly complex distribution of species formed at 250°C and above that make up the deposits and hence the atomic H:C ratios indicated are an average of all species. It would be expected that, due to the possible water content the H:C ratios are not close to the “real” ratio. A stark illustration of this point is the ratio for the sample generated at 150°C which should be approximately 4.0, as indicated by the solid state NMR and which is 105 by elemental analysis.

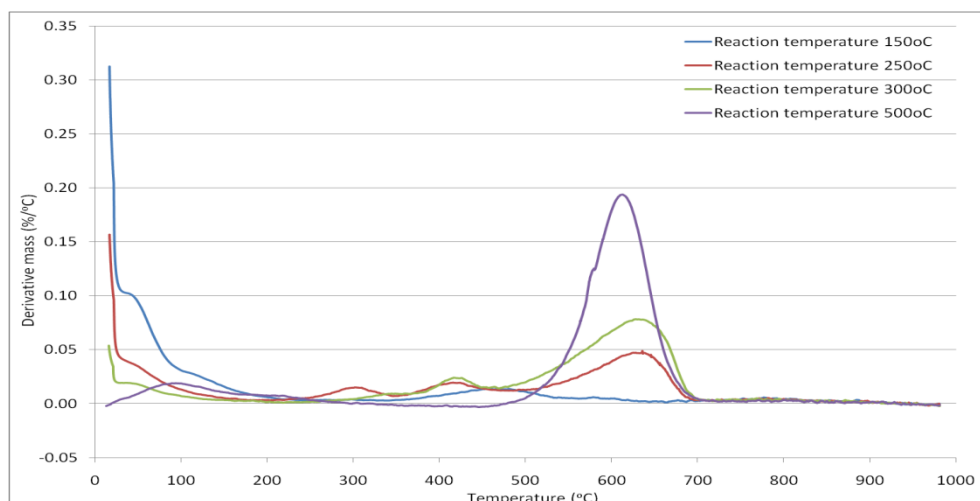


Figure 4.2.4: First derivative TGA profiles attained under air of coked mordenite generated with methanol at different reaction temperatures for 300 minutes.

Thermogravimetric analysis (TGA) was undertaken to probe the differences in the reactivity of the carbonaceous deposits. Overlaid first derivative TGA profiles for the various reaction temperatures employed are presented in Figure 4.2.4 (under air), Figure 4.2.5 (under 2% O₂/Ar) and Figure 4.2.6 (under argon). The same temperature ramp rate (10°C/min) was used in all cases.

In Figure 4.2.4 it can be observed that the sample generated at 150°C displays three first derivative TGA profile peaks occurring at 60°C attributed to water desorption, 120°C and at 475°C. As shown later, this latter feature may possibly relate to the decomposition of original ammonium ions in this sample. It should be noted that such features were not observed in the studies undertaken in the previous chapter. It should be noted that the studies outlined within this chapter were performed in a different reactor (at BP Chemicals' research laboratory) and that N₂ rather than Ar was used as carrier gas.

Post-250 and 300°C samples exhibit similar first derivative TGA profiles displaying peaks attributed to water desorption and the combustion of the carbonaceous residue. Peaks are observed at 300-325, 425 and 625°C indicating a difference in reactivity of the carbonaceous species formed. Solid state NMR studies suggest that these species are in the form of alkyl substituted aromatics and polycyclic compounds [25, 26]. Previous studies have suggested that the difference in temperatures may be an effect of the location of the carbonaceous

residue and hence the difference in the accessibility of oxygen [27], as discussed in the previous chapter.

The post-reaction mordenite generated at 500°C displays two first derivative TGA profile peaks at *ca.* 100 and 625°C. These can be attributed to water desorption as well as removal of the carbonaceous species which are, according to solid state NMR, polycyclic in nature. It can be observed that the peak attributed to water desorption has shifted to higher temperatures as the carbon content increases and as the reactivity of the residue decreases.

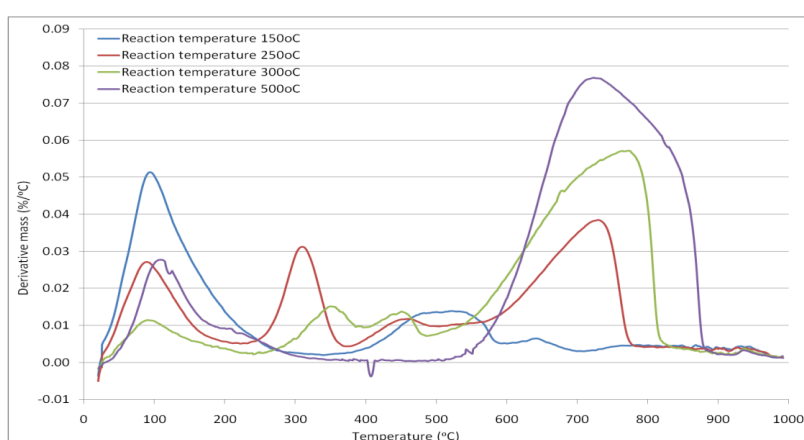


Figure 4.2.5: First derivative TGA profiles attained under 2% O₂/Ar of coked mordenite generated with methanol at different reaction temperatures for 300 minutes.

There is a degree of similarity between the profile observed in Figure 4.2.5 and that observed previously in Figure 4.2.4. Interestingly for the sample generated at 150°C, a new peak is observed *ca.* 650°C, which was not observed previously. In most cases the peaks observed between 20-600°C have shifted by approximately 25°C which was reported in the previous chapter and attributed to a systematic effect. The peaks previously observed at 625°C have shifted to varying degrees and have broadened significantly. This can be attributed to a change in the combustion kinetics created by a decrease in the partial pressure of oxygen.

What is most interesting is that the shifts in temperature are not the same regardless of the sample, as observed in the previous chapter, but appear to broaden more with an increase in reaction temperature.

Product	MeOH carb 150	Temp (°C)	MeOH carb 250	Temp (°C)	MeOH carb 300	Temp (°C)	MeOH carb 500	Temp (°C)
Hydrogen	N	N/A	Y	300	-	-	-	-
Water	Y	120 550	Y	120 450 725	Y	100 450 775	Y	125 600 825
Carbon monoxide	Y	550	Y	450 725	Y	450 775	Y	625
Carbon dioxide	Y	475 650	Y	450 725	Y	450 775	Y	725
Methane	N	N/A	Y	300	Y	350	N	N/A
Ethene	N	N/A	Y	300	Y	350	N	N/A
Ethane	N	N/A	Y	300	Y	350	N	N/A
Propene	N	N/A	Y	300	Y	350	N	N/A
Propane	N	N/A	Y	300	Y	350	N	N/A
Butene	N	N/A	Y	300	Y	350	N	N/A
Butane	N	N/A	Y	300	Y	350	N	N/A
Benzene	N	N/A	Y	300	N	N/A	N	N/A
Ammonia	Y	500	N	N/A	N	N/A	N	N/A

Table 4.2.1: Evolved gas mass spectrometry under 2% O₂/Ar for coked mordenite generated with methanol at 150, 250, 300 and 500°C for 300 minutes (products have been identified by examining unique fragments and fragment patterns).

Online mass spectrometry was undertaken to determine which gases were evolved from the sample during thermal analysis under different atmospheres. Mass spectrometry data is presented for the various reaction temperatures employed for 2% O₂/Ar in Table 4.2.1 and argon in Table 4.2.2. In some cases unique mass to charge ratios were scanned, whereas in others multiple fragments were used for the identification of products. The mass spectrometry data presented in Table 4.2.1 corresponds to the thermal analysis data performed under 2% O₂/Ar.

It is apparent when examining the evolved species from coked mordenite samples observed in Table 4.2.1 that under a 2% O₂/Ar atmosphere a variety of processes are occurring. The 150°C post-reaction sample exhibits products indicating the combustion of hydrocarbons at approximately 625°C which is perhaps a little unexpected due to the observation made in the ¹³C CP solid state NMR investigations indicating only the presence of methanol, which is expected to be removed at significantly lower temperatures. It is also apparent from the appearance of fragments relating to ammonia, that the zeolite has residual ammonium ions after the activation procedure.

The samples generated at 250 and 300°C exhibit a very broad distribution of species, indicating that the carbonaceous residues are undergoing cracking type processes at low temperatures (*ca.* 300-350°C) as well as combustion observed occurring at higher temperatures 450°C and above. It is interesting to note that there is a very distinct temperature division between the processes, and that there is no apparent overlap indicating combustion was occurring as hydrocarbons were being generated via cracking processes. Coked samples generated at higher temperatures only exhibit products indicative of combustion.

It can be observed in Figure 4.2.6 that the sample generated at 150°C exhibits three first derivative TGA profile peaks. Desorption of water and volatile material is suggested by the presence of a very broad peak *ca.* 100°C. A peak at approximately 500°C may indicate the decomposition of residual ammonium ions as suggested by the work performed under a 2% oxygen atmosphere, or the formation of hydrocarbons from the residual methanol. Finally a very broad peak is observed *ca.* 825°C suggesting the removal of carbonaceous material via high temperature cracking processes.

The mordenites coked at 250 and 300°C exhibit peaks attributed to water desorption at *ca.* 90-100°C. In addition, two moderate temperature peaks were observed at 325 and 450°C for the sample generated at 250°C, whereas for the sample generated at 300°C they were observed at 375 and 450°C. It is notable that they appear at temperatures significantly above the reaction temperature and are therefore considered real and not artefacts of reactor shut-down. As suggested previously for the lower temperature data, it is anticipated that an active form of the hydrocarbon pool remains. Therefore that the observation of peaks at these temperatures is due either to catalysed lower temperature cracking of the species, or conversion of the alkyl substituted aromatics to olefins, methane and a deactivated form of

the hydrocarbon pool, possibly as larger polycyclic molecules. A very broad peak is observed *ca.* 850°C for both samples, though the material generated at 250°C exhibits a decrease in mass loss after this temperature. At higher reaction temperatures only two first derivative temperature profile peaks are observed at *ca.* 125 and 825°C.

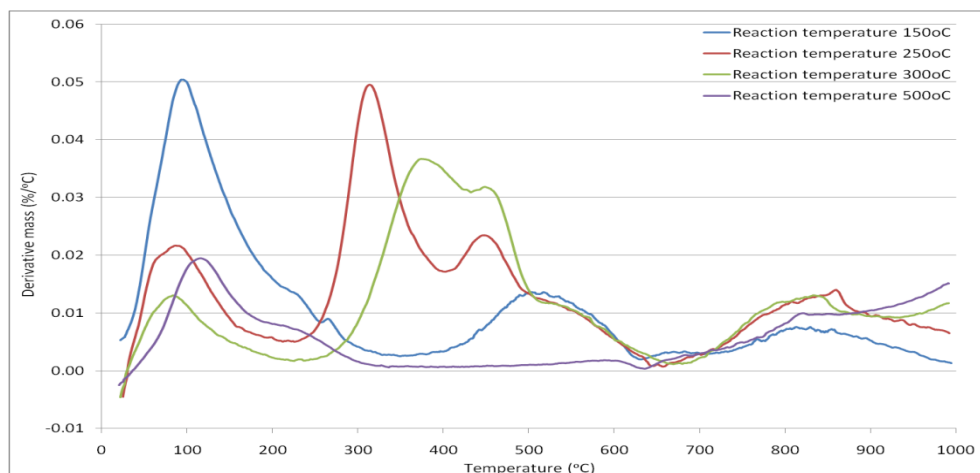


Figure 4.2.6: First derivative TGA profiles attained under argon of coked mordenite generated with methanol at different reaction temperatures for 300 minutes.

The mass spectrometry data presented in Table 4.2.2 corresponds to the thermal analysis data performed under argon. It can be observed in Table 4.2.2 that the distribution of products formed under an argon atmosphere for the samples generated at 250 and 300°C is similar to that observed for those observed under a 2% O₂/Ar atmosphere. The only differences are the lack of combustion products, the formation of ammonia, which is now apparent at *ca.* 525°C and the peak observed at 450°C previously undergoing combustion, undergoes cracking processes in the presence of argon. It is also noticeable that the formation of hydrogen occurs across a much broader range than under the 2% O₂/Ar atmosphere. The sample generated at 500°C evolves methane at higher temperatures *ca.* 600°C and hydrogen at 825°C. It is clearly highly inactive under cracking conditions.

Product	MeOH carb 150	Temp (°C)	MeOH carb 250	Temp (°C)	MeOH carb 300	Temp (°C)	MeOH carb 500	Temp (°C)
Hydrogen	Y	225 900	Y	300 850	Y	425 825	Y	825
Water	Y	125 450 725	Y	125	Y	125	Y	150
Carbon monoxide	N	N/A	N	N/A	N	N/A	N	N/A
Carbon dioxide	N	N/A	N	N/A	N	N/A	N	N/A
Methane	Y	225	Y	300 450	Y	350 450	Y	600
Ethene	N	N/A	Y	300 450	Y	350 450	N	N/A
Ethane	Y	550	Y	300 450	Y	525	N	N/A
Propene	Y	275 475	Y	300 450	Y	350 450	N	N/A
Propane	N	N/A	Y	300 450	Y	350 450	N	N/A
Butene	Y	275 475	Y	300 450	Y	350 450	N	N/A
Butane	N	N/A	Y	300 450	Y	350 450	N	N/A
Benzene	N	N/A	Y	325 450	Y	400	N	N/A
Ammonia	Y	525	Y	525	Y	525	N	N/A
Dimethyl ether	Y	225	N	N/A	N	N/A	N	N/A

Table 4.2.2: Evolved gas mass spectrometry under Ar for coked mordenite generated with methanol at 150, 250, 300 and 500°C for 300 minutes (products have been identified by examining unique fragments and fragment patterns).

The post-150°C reaction sample is very interesting because it possibly undergoes methanol to hydrocarbon chemistry in the TGA instrument, since only methanol was observed in the ¹³C MAS NMR spectrum of this sample, though care must be taken in this assumption, due to low levels of carbon (indicated by elemental analysis) and low signal to noise ratio. It is observed that methane and hydrogen are evolved at *ca.* 225°C presumably from the methanol observed in the solid state NMR study. Around the same temperature, dimethylether is observed presumably arising from dehydration of the methanol. Water is observed at approximately 325°C. At approximately 275 and 475°C fragments attributed to C₃-C₄ olefins are observed. Ammonia is observed at 525°C indicating the decomposition of the residual ammonium ions. The highest temperature hydrocarbon observed is ethane at 550°C, thereafter only the formation of hydrogen at approximately 900°C is observed.

Samples were retained after performing TGA under argon and reanalysed under air to determine how the carbonaceous material may have changed due to the argon treatment. Overlaid first derivative TGA profiles under air for post- Ar TGA treatment for the 150, 250, 300 and 500°C reaction temperature samples are presented in Figure 4.2.7.

It can be observed in Figure 4.2.7 that the argon treatment has been rather successful at removal of species for the samples generated at 150 and 250°C respectively. The sample generated at 150°C exhibits only a single peak at *ca.* 70°C indicating the presence of adsorbed water, whereas the sample generated at 250°C exhibits two first derivative TGA profile peaks at approximately 60 and 600°C. The peak observed at 600°C is attributed to carbonaceous deposits, but it can be seen that the peak is significantly less prominent than previously observed indicating the degree of removal.

It can be observed that the samples reacted at 300 and 500°C display two first derivative TGA profile peaks at *ca.* 70-80°C and 625°C. It is apparent that removal of carbonaceous deposits via argon treatment has been partially successful for the sample generated at 300°C, whereas there is very little difference post-argon treatment for the 500°C sample. This demonstrates the extent to which reactivities of the samples under argon vary as a function of temperature at which the carbonaceous species were laid down.

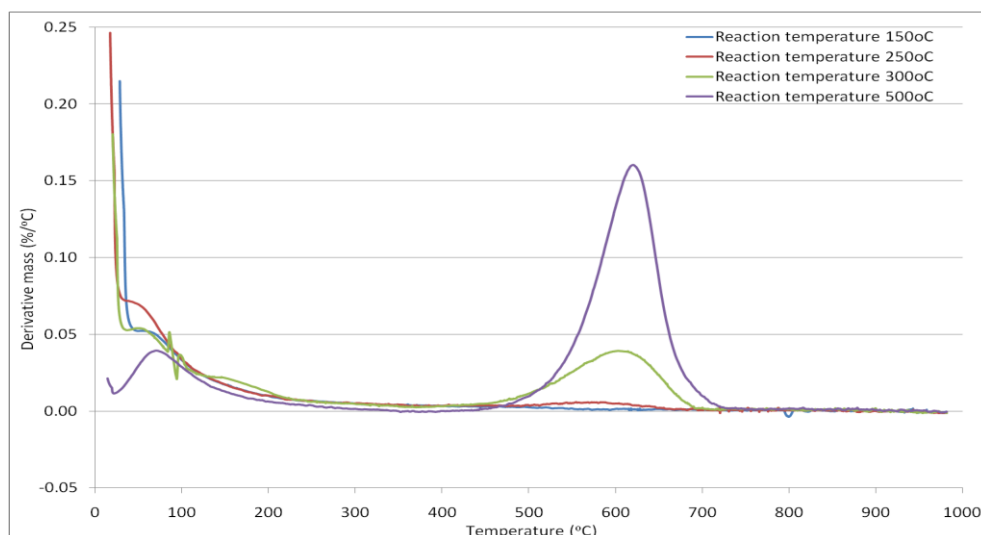


Figure 4.2.7: First derivative TGA profiles attained under air of post TGA argon of coked mordenite generated with methanol at different reaction temperatures for 300 minutes.

Nitrogen adsorption isotherms were examined to determine the location of the coke. Figure 4.2.8 presents the stacked isotherms for materials following reaction at various different temperatures. Post-reaction nitrogen adsorption isotherms were type IV for samples generated at 150 and 250°C, whereas for samples generated at 300 and 500°C respectively the isotherms were type II. BET surface areas and single point surface area determination at $p/p^0 = 0.1$ are presented in Table 4.2.3.

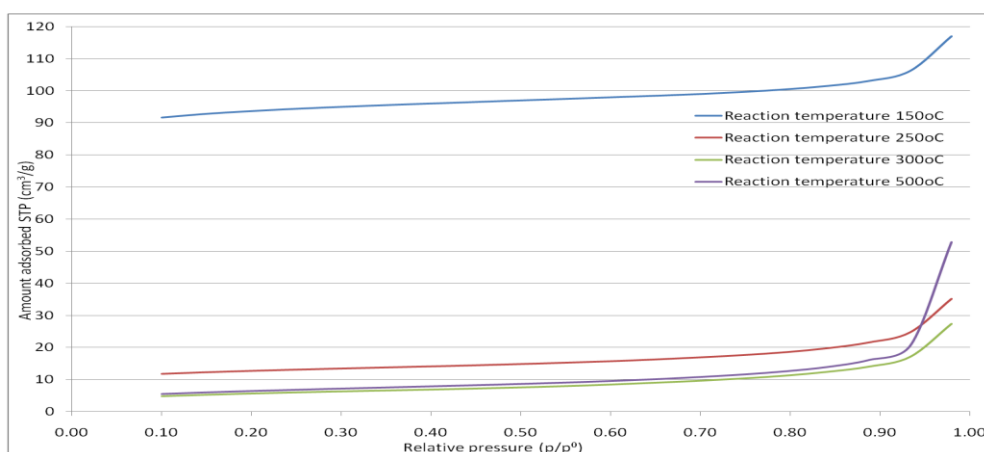


Figure 4.2.8: Nitrogen adsorption isotherms of coked mordenite generated with methanol at different reaction temperatures for 300 minutes.

Material	BET surface area (m ² g ⁻¹)	Single point surface area at p/p ₀ = 0.1 (m ² g ⁻¹)	Isotherm
Reaction temperature 150°C	278	359	Type IV
Reaction temperature 250°C	40	46	Type IV
Reaction temperature 300°C	20	19	Type II
Reaction temperature 500°C	22	21	Type II

Table 4.2.3: BET and single point surface areas and isotherm types for coked mordenite generated with methanol at different reaction temperatures for 300 minutes.

In Figure 4.2.8 and Table 4.2.3 it can be observed that the sample generated at 150°C exhibits a type IV isotherm and a surface area of approximately 278 m²g⁻¹. Increasing the reaction temperature to 250°C and above, results in a rapid loss of surface area indicating that the carbonaceous materials deposit in the pores of the zeolite.

The sample generated at 250°C exhibits a type IV isotherm indicating a degree of porosity has been retained. Increasing the reaction temperature to 300°C and above decreases the surface area to approximately 20 m²g⁻¹ and a type II isotherm is observed, which indicates total loss of accessible porosity. No apparent further change in the surface area for the samples generated at 300 and 500°C is observed. It is interesting that the sample generated at 250°C retains a degree of porosity, but it appears from the solid state NMR and the thermal analysis data that external surface species may be formed.

Powder x-ray diffraction investigations were undertaken to determine the influence that the reaction has upon the zeolite framework. Stacked patterns are presented in Figure 4.2.9 for the various reaction temperatures employed. In Figure 4.2.9 it can be observed that the sample generated at 500°C exhibits shifts in the generated XRD pattern-most notably the (150), (202) and (350) reflections at approximately 22, 26 and 27° 2θ respectively. In previous studies it was observed that samples that contained over 11 wt% of carbon exhibited shifts in the (511) reflection evident at 28° 2θ. The observed shifts may be as a consequence

of the relatively large carbon content (approximately 15 wt%) and the resultant deformation of the framework due to the strain induced by the bulky carbonaceous species. Some small structural changes are observed, much like those discussed on in the methanol only chapter. These are believed to be related to the coke, although further investigation would be required for a definitive answer.

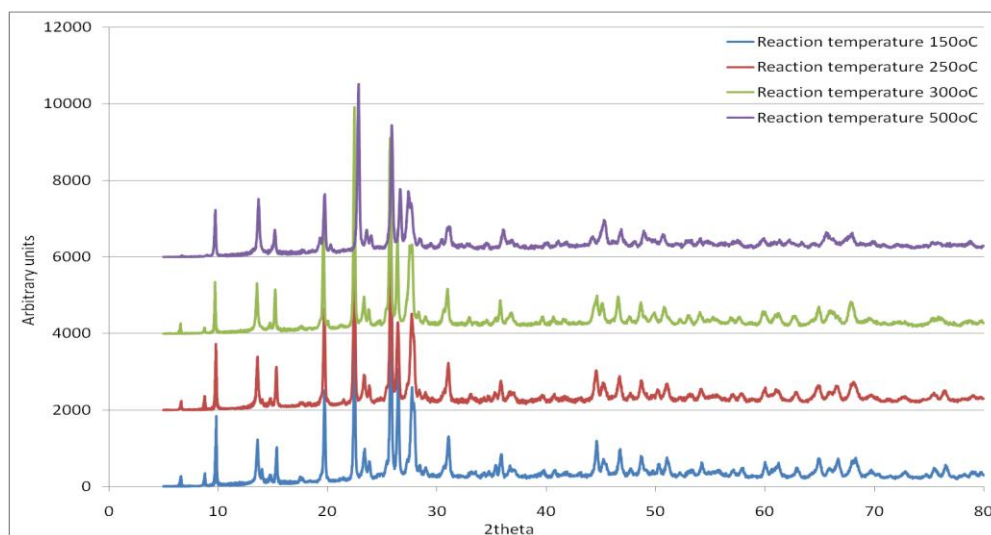


Figure 4.2.9: XRD patterns of coked mordenite generated with methanol at different reaction temperatures for 300 minutes.

4.2.2 Time on stream dependence of the carbonaceous species deposited during carbonylation

To probe the effect of reaction time on the carbonaceous species formed on the zeolite during methanol carbonylation chemistry, mordenite was activated as described in the methanol carbonylation temperature dependence section. Activated materials were run at 300°C in a 10% methanol feedstream consisting of CO:H₂ in a 4:1 ratio at a GHSV of 3000 hr⁻¹. Four reaction times 60, 180, 420 and 600 minutes-were employed. Post-reaction coked mordenite was cooled to room temperature under a nitrogen flow.

Solid state ^{13}C MAS NMR spectroscopy using cross polarisation was undertaken on four non-enriched post carbonylation reaction samples generated at 60, 180, 420 and 600 minutes reaction time at 300°C . The data is presented in Figure 4.2.10.

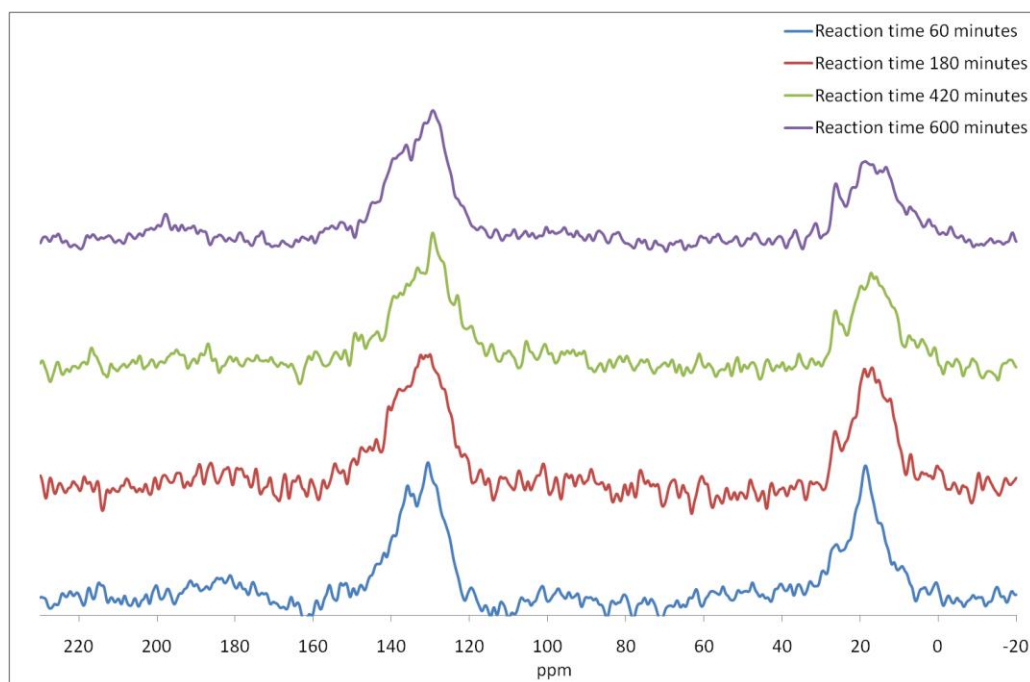


Figure 4.2.10: ^{13}C CP MAS NMR spectrum of coked mordenite generated with methanol at 300°C for different reaction times.

It can be observed in Figure 4.2.10 that after 60 minutes at least four broad signals are observed. The signals at 19 and 131 ppm are indicative of the presence of methyl substituted aromatics [19, 28], whereas the signals at 26 and 136 ppm indicate that the residue contains a polycyclic aromatic component [22, 29].

It can be observed in Figure 4.2.10 that as the reaction temperature is increased that there is no obvious change in the nature of the residue, as indicated by the solid state NMR spectra. As mentioned in the introduction to this chapter, it has been observed that carbonylation occurs concurrently with methanol to hydrocarbon chemistry. Given that the observed distribution of species is similar to those observed for coking in the presence of methanol-only feedstreams, it could suggest that the hydrocarbon pool has reached an approximate steady state (similar to that observed in methanol-only studies).

The carbon content and the H:C ratios are presented in Figures 4.2.11 and 4.2.12 for the various reaction times investigated. It can be observed in Figure 4.2.11 that the zeolite reacted for 60 minutes reaction time the carbon content was approximately 6.8 wt%. Thereafter increasing the reaction time increased the carbon content up to 420 minutes where the carbon content was approximately 10.8 wt%. Increasing the reaction time to 600 minutes resulted in a minimal further increase (approximately 0.2 wt%) beyond the value at 420 minutes on stream.

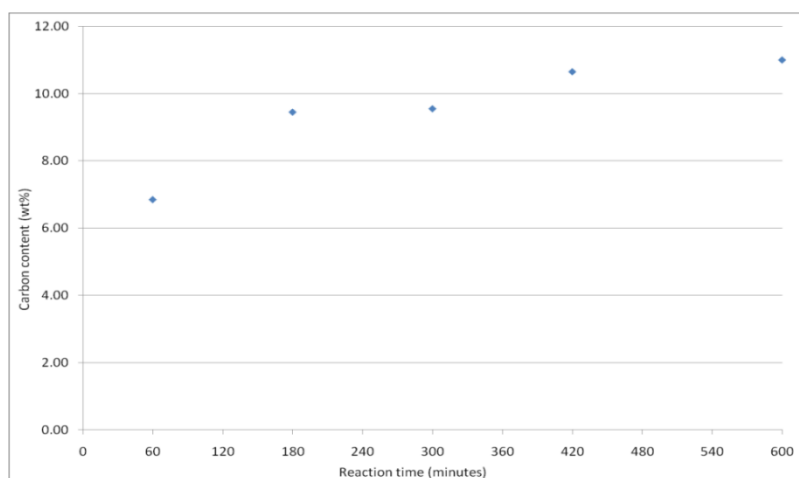


Figure 4.2.11: Carbon content of coked mordenite generated with methanol at 300°C for different reaction times.

The increase in the carbon contents of coked mordenite doesn't suggest that the hydrocarbon pool is in a steady state. Therefore it may be the case that the methanol to hydrocarbon process is competing with the carbonylation process. It would appear that at short reaction times the methanol to hydrocarbon reaction predominates suggested by the rapid lay down of carbon observed in the elemental analysis (much like that observed in the previous chapter at 5 minutes time on stream for a methanol-only feedstream) and the formation of a hydrocarbon pool like species observed in the solid state NMR measurements. When the reaction time was increased, the carbonylation appeared to become the dominate process based upon the decrease in the amount of carbon laid down at longer reaction times. The solid state NMR investigations suggest no further evolution of the carbonaceous species at

longer reaction times, unlike the case for the previous chapter, where it was documented for methanol-only feed.

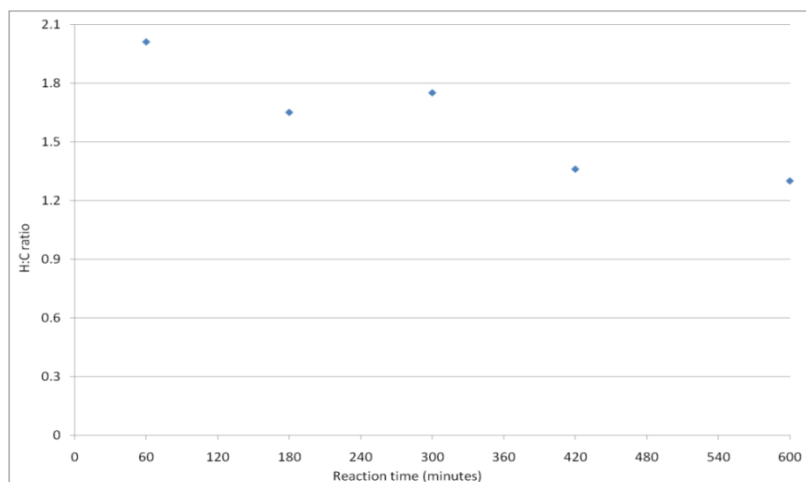


Figure 4.2.12: Atomic H:C ratio of coked mordenite generated with methanol at 300°C for different reaction times (not corrected for the effects of adsorbed water).

In Figure 4.2.12 it can be observed that the H:C ratio decreases as the reaction time increases in-line with the increase in the carbon content observed above. The solid state NMR investigations suggest that the nature of species does not change significantly, which indicates that there may be an increase in the more hydrogen deficient species already present over the mordenite as the reaction time increases. Unfortunately, due to the limitations inherent to cross polarisation techniques the peaks cannot be easily quantified and hence this proposal cannot be proved currently.

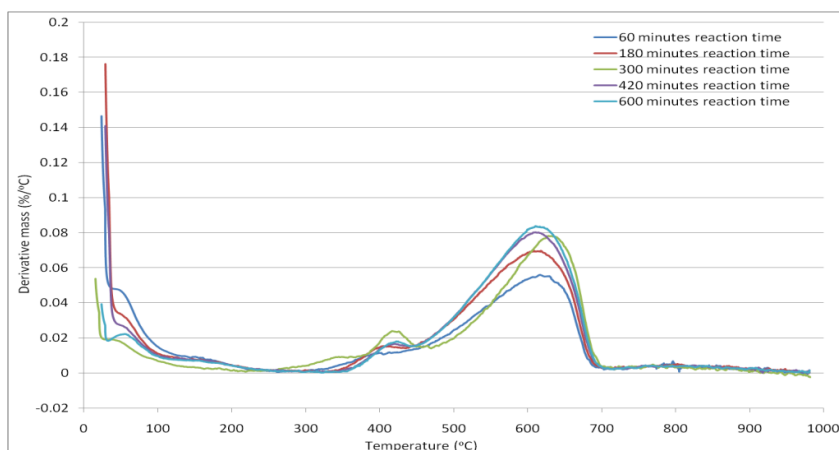


Figure 4.2.13: First derivative TGA profiles attained under air of coked mordenite generated with methanol at 300°C for different reaction times.

Overlaid first derivative TGA profiles undertaken in an air atmosphere are presented in Figure 4.2.13 for the various reaction times investigated. It can be observed in Figure 4.2.13 that all post-reaction samples exhibit a very similar first derivative TGA profile regardless of reaction time, as anticipated from the solid state NMR studies. A peak attributed to desorption of water is apparent at *ca.* 70°C. Peaks attributed to the removal of the carbonaceous deposits are observed at approximately 425 and 625°C. There is a peak evident at 325°C for the sample generated at 300 minutes reaction time.

Post-reaction nitrogen adsorption isotherms were type II for all reaction times and are presented in Figure 4.2.14. BET surface areas and single point surface area determination at $p/p^0 = 0.1$ are reported in Table 4.2.4.

As the reaction time increases, it can be observed that surface area remains the same at approximately 20 m²g⁻¹. This is interesting because even though no apparent change is observed in the surface area, the amount of carbon increases from approximately 6.8 wt% at 60 minutes to 11.0 wt% at 600 minutes. There is also no obvious change in the first derivative TGA profile, which may suggest the formation of additional surface bound species which can be assigned to moderate temperature peaks *ca.* 325 and 425°C respectively. This therefore implies that the additional carbonaceous residue must be formed within the pores of the zeolite and the initial formation of the carbonaceous residue must occur in the pore

mouths hence reducing the surface area significantly, but still leaving a significant void to allow gradual diffusion of bulky carbonaceous species over the course of the reaction.

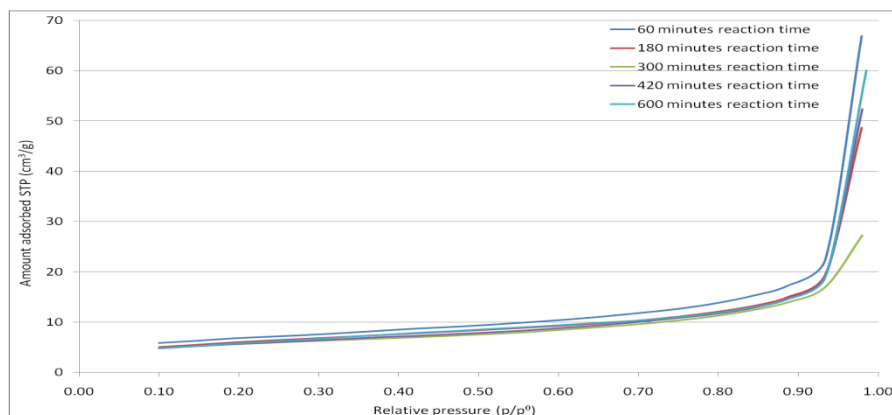


Figure 4.2.14: Nitrogen adsorption isotherms of coked mordenite generated with methanol at 300°C for different reaction times.

Material	BET surface area (m^2g^{-1})	Single point surface area at $p/p_0 = 0.1$ (m^2g^{-1})	Isotherm
Reaction time 60 minutes	23	19	Type II
Reaction time 180 minutes	22	23	Type II
Reaction time 300 minutes	20	20	Type II
Reaction time 420 minutes	20	19	Type II
Reaction time 600 minutes	21	19	Type II

Table 4.2.4: BET and single point surface areas and isotherm types for coked mordenite generated with methanol at 300°C for different reaction times.

Stacked post-reaction XRD patterns are presented in Figure 4.2.15 for the various reaction times investigated. It can be observed in Figure 4.2.15 that there are no apparent shifts in any of the XRD patterns at any time on stream. This is in-line with the previous discussion associating the shifts with the carbon content. The largest carbon content exhibited in this

study was observed for the sample generated at 600 minutes reaction time. As discussed previously, it appears that coked mordenites that contain more than 11 wt% of carbon exhibit shifts in the (150), (202) and (350) reflections possibly due to strain exerted internally on the zeolite structure.

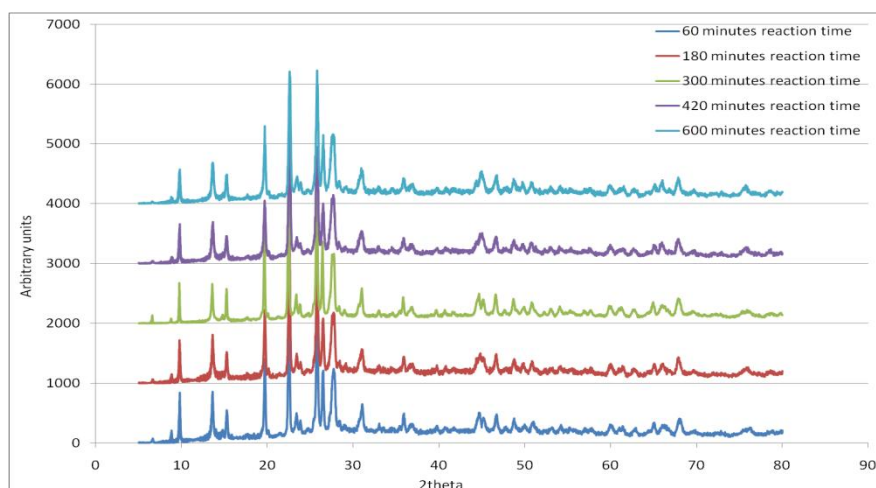


Figure 4.2.15: XRD patterns of coked mordenite generated with methanol at 300°C for different reaction times.

4.3 Conclusions

As the reaction temperature was increased it was found that the carbon content and hydrogen deficiency of the carbonaceous residue deposited under the methanol carbonylation feedstream increased significantly. This was further highlighted by the solid state NMR investigations which indicated the degree of change in the nature of the materials. The carbonaceous residue showed discrete regions of mass loss in TGA studies undertaken in an air atmosphere. Coked mordenites generated at 250 and 300°C showed a degree of similarity and were different from the other samples, exhibiting additional features at 300-350°C and *ca.* 425°C. These are believed to be associated with more reactive species deposited on the external surface of the zeolite, whereas the higher temperature peak at about 625°C can be attributed to less accessible species trapped within the pores.

Applying TGA studies using a 2% oxygen concentration and monitoring with mass spectrometry demonstrated that species attributed to these lower temperature peaks undergo a

mixture of cracking and combustion. Further studies employing an argon only atmosphere demonstrated that the adsorbed species would readily undergo cracking type reactions. These same samples were reanalysed under an air atmosphere after the argon treatment, which demonstrated the complete removal of these lower temperature features.

Nitrogen adsorption isotherms indicate that the sample generated at 250°C retains a degree of porosity which may account for the additional reactivity observed in the TGA experiments. No noticeable change is observed for the sample generated at 150°C, whereas the samples generated at 300 and 500°C respectively display a complete loss of microporosity. The data determined from $p/p^0 = 0.1$ exhibits an enhancement in surface area for the sample generated at 150°C ($359 \text{ m}^2 \text{ g}^{-1}$), whereas the other samples retain a similar surface area. The trend also remains the same as that observed employing the BET equation. The powder XRD pattern generated for the sample coked at 500°C shows a degree of shift for the (150), (202) and (350) reflections indicating a deformation of the framework, which may be as a direct consequence of the amount of carbon on the coked mordenite. The small structural observed may be attributed to the formation of coke and have been observed over other zeolites resulting in such small structural changes [30].

Increasing the reaction time results in an increase in the carbon content and hydrogen deficiency of the carbonaceous species deposited on the mordenite. Interestingly at longer reaction times, smaller incremental increases in carbon content were observed. Solid state NMR investigations indicate that at all times on stream beyond 60 minutes there is a degree of similarity in the nature of the material, indicating no obvious change in the nature of the carbonaceous deposits.

Probing the reactivity of the carbonaceous deposits under air supports the observations made in the solid state NMR studies. The only obvious difference in the first derivative TGA profiles is in the sample generated at 300 minutes which displayed an additional peak at 325°C. The nitrogen adsorption isotherms exhibit similar adsorption branches suggesting that the residue is forming in the pore mouths and gradually diffusing through the zeolite as the reaction proceeds. The surface areas determined from the measurements taken at $p/p^0 = 0.1$ offer very little difference in the determined surface area or observed trend. No reflection shifts are observed in the XRD patterns as the reaction time increases, which may be a result of insufficient carbon contents to apply strain to the zeolite framework.

From work undertaken employing methanol carbonylation feedstreams it has been found that as the reaction temperature is increased the carbonaceous deposits become more carbon rich and hydrogen deficient. It was also observed that a large proportion of the carbonaceous species (60-70%) observed after 300 minutes time on stream were deposited within 60 minutes and the speciation was found to be very similar at 60-600 minutes time on stream.

It is quite clear that there may indeed be a benefit in employing a single point surface area determination at $p/p^0 = 0.1$ for samples that exhibit a relatively large surface area and type IV isotherm.

References

- [1] W. Reppe, H. Friederich, N. von Kutepow, W. Morsch, US Patent 2729651 (to BASF) (1956)
- [2] W. Reppe, H. Friederich, US Patent 27289137 (to BASF) (1957)
- [3] N. Von Kutepow, W. Himmle, H. Hohenschutz, *Chemie. Ingenieur. Technik.* 37 (1965) 383
- [4] H. Hohenschutz, N. Von Kutepow, W. Himmle, *Hydrocarbon Processing* 45 (1966) 141
- [5] C. Thomas, G. Suiss-Fink, *Coordination Chemistry Reviews* 243 (2003) 125
- [6] A. Haynes, *Advances in Catalysis* 53 (2010) 1
- [7] F. Paulik, J. Roth, *Chemical Communications* 24 (1968) 1578
- [8] D. Forster, *Journal of the American Chemical Society* 98 (1976) 846
- [9] M. Howard, M. Jones, M. Roberts, S. Taylor, *Catalysis Today* 18 (1993) 325
- [10] G. Sunley, D. Watson, *Catalysis Today* 58 (2000) 293
- [11] A. Haynes, P. Maitilis, G. Morris, G. Sunley, H. Adams, P. Badger, C. Bowers, D. Cook, P. Elliott, T. Ghaffer, H. Green, T. Griffin, M. Payne, J. Pearson, M. Taylor, P. Vickers, R. Watt, *Journal of the American Chemical Society* 126 (2004) 2847
- [12] T. Kinnunen, K. Laasonen, *Journal of Molecular Structure* 542 (2001) 273

- [13] T. Blasco, M. Boronat, P. Concepcion, A. Corma, D. Law, J. Vidal-Moya, *Angewandte Chemie International Edition* 46 (2007) 3938
- [14] P. Cheung, A. Bhan, G. Sunley, E. Iglesia, *Angewandte Chemie International Edition* 45 (2006) 1617
- [15] A. Bhan, E. Iglesia, *Accounts of Chemical Research* 41 (2008) 559
- [16] F. Oliver, E. Munson, J. Haw, *The Journal of Physical Chemistry* 96 (1992) 8106
- [17] Y. Jiang, M. Hunger, W. Wang, *Journal of the American Chemical Society* 128 (2006) 11679
- [18] A. Sassi, W. Song, M. Wildman, J. Haw, *Catalysis Letters* 81 (2002) 101
- [19] L. Carlson, P. Ibester, E. Munson, *Solid State Nuclear Magnetic Resonance* 16 (2000) 93
- [20] X. Han, Z. Yan, W. Zhang, X. Bao, *Current Organic Chemistry* 5 (2001) 1017
- [21] M. Anderson, M. Ocelli, J. Klinowski, *The Journal of Physical Chemistry* 96 (1992) 388
- [22] www.chem.wis.edu/areas/reich/handouts/nmr-c13/cdata.htm (accessed on 31/03/2011)
- [23] G. Fulmer, A. Miller, N. Sherden, H. Gottlieb, A. Nudelman, B. Stoltz, J. Bercaw, K. Goldberg, *Organometallics* Article 29 (2010) 2176-2179
- [24] www.chem.ucla.edu/~webspectra/notesonsolvents.html (accessed on 31/03/2011)
- [25] M. Stocker, *Microporous and Mesoporous Materials* 29 (1999) 3
- [26] H. Schulz, Z. Siwei, W. Baumgartner, *Studies in Surface Science* 34 (1987) 479
- [27] P. Magnoux, M. Guisnet, *Applied Catalysis* 38 (1988) 341
- [28] J. Haw, W. Song, D. Marcus, J. Nicholas, *Accounts of Chemical Research* 36 (2003) 317
- [29] J. White, M. Truitt, *Progress in Nuclear Magnetic Resonance Spectroscopy* 51 (2007) 139

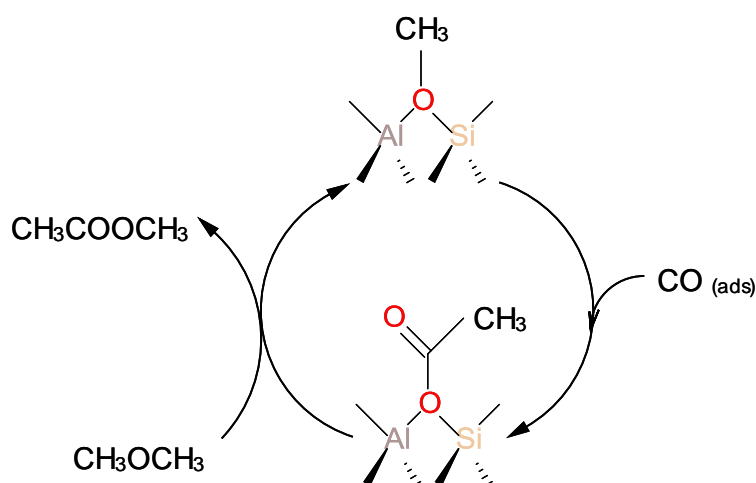
[30] J. Zhang, H. Zhang, X. Yang, Z. Huang, W. Cao, *Natural Gas Chemistry* 20 (2011) 266

5 Carbonaceous species deposited from dimethylcarbonate and mixed dimethylcarbonate, carbon monoxide and hydrogen feedstreams

5.1 Introduction

Recent research has been directed towards the use of dimethylether as opposed to methanol as the substrate for heterogeneous halide-free carbonylation [1-3]. Dehydration of methanol occurring during carbonylation results in the production of water which subsequently competes with carbon monoxide for adsorption on Lewis acid sites, inhibiting the reaction [3, 4].

A mechanism for dimethylether carbonylation was proposed by Cheung et al [2] (Reaction Scheme 5.1.1) whereby dimethylether interacts at Bronsted acid sites forming a surface bound methyl species and methanol. The surface bound methyl species combine with adsorbed carbon monoxide and produce acetyl moieties, further reaction of which with dimethylether yield methyl acetate and a new surface bound methyl species according to the cycle shown below.



Reaction Scheme 5.1.1: Proposed mechanism for the carbonylation of dimethylether (adapted from [2] and [5]).

However dimethylether can be difficult to handle due to its relatively low vaporisation temperature (normal boiling point -24.8°C). Therefore dimethylcarbonate which is a liquid at room temperature (normal boiling point 90.0°C) is sometimes employed as an alternative. Dimethylcarbonate is a product from oxidative carbonylation of methanol [6]. One of the problems associated with this process, however, is the decomposition of dimethylcarbonate to yield dimethylether and carbon dioxide, which can occur over residual acid sites on metal ion exchanged zeolites [6]. Therefore dimethylcarbonate can act as a suitable precursor feed to generate dimethylether and subsequently study the resultant coke formed.

This study was directed towards examining the carbonaceous deposits formed from dimethylcarbonate under three different sets of conditions. Initially a dimethylcarbonate, carbon monoxide and hydrogen containing feedstream was used employing a γ -alumina pre-bed to decompose dimethylcarbonate prior to interaction with the zeolite. Due to unforeseen effects created by the pre-bed, a set of experiments were designed employing the same feedstream without employing the pre-bed. Finally, experiments were undertaken to examine the effects of a dimethylcarbonate-only feedstream with no pre-bed.

5.2 Results and discussion

5.2.1 Dimethylcarbonate carbonylation (using a γ -alumina pre-bed) temperature dependence

To probe the effect of reaction temperature on the carbonaceous species formed on the zeolite during dimethylcarbonate carbonylation chemistry, materials were activated at 500°C for 60 minutes under a $50\text{ ml min}^{-1}\text{ N}_2$ stream. Activated mordenite was run in the dimethylcarbonate carbonylation reaction for 300 minutes in a 10% dimethylcarbonate feedstream consisting of $\text{CO}:\text{H}_2$ in a 4:1 ratio at a GHSV of 3000 hr^{-1} . Four reaction temperatures were employed: 150, 250, 300 and 500°C (a γ -alumina pre-bed was used to decompose dimethylcarbonate to dimethylether). Coked mordenite samples were cooled to room temperature under a nitrogen flow.

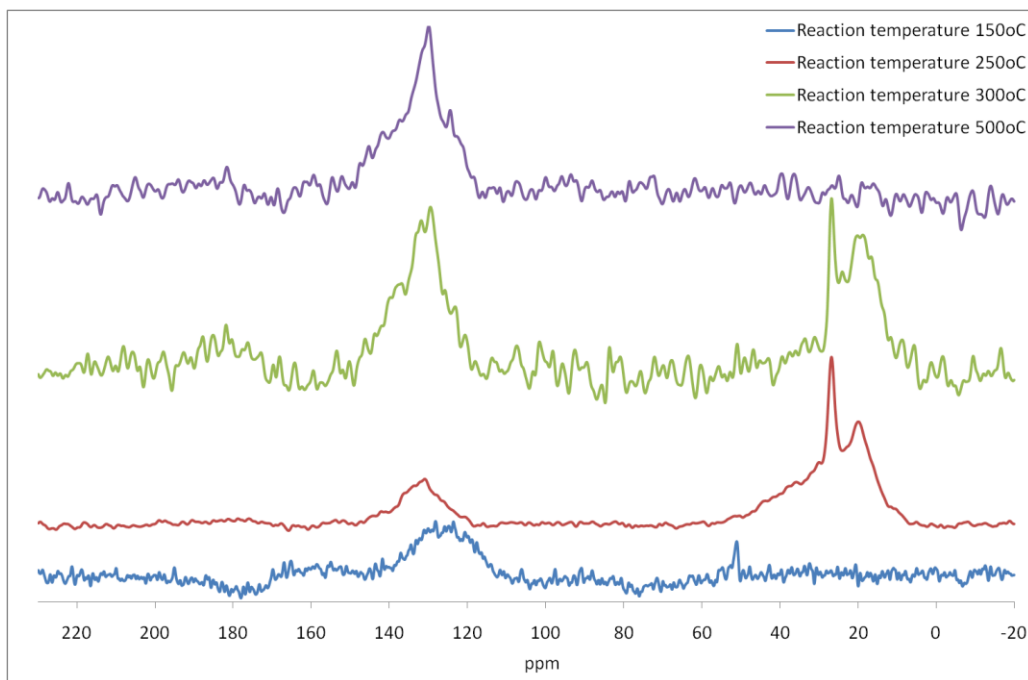


Figure 5.2.1: ^{13}C CP MAS NMR spectrum of coked mordenite generated with dimethylcarbonate using a pre-bed at different reaction temperatures for 300 minutes.

^{13}C CP MAS NMR spectroscopy was performed on coked mordenite in an attempt to identify the nature of the carbonaceous residues formed. The data is presented in Figure 5.2.1. In Figure 5.2.1 for the sample generated at 150°C it can be observed that there is a sharp signal evident at *ca.* 50 ppm indicating the presence of adsorbed methanol [7]. Another broad signal is evident at approximately 128 ppm which can be attributed to aromatic species [8, 9], although it occurs in a region of the spectrum where baseline effects may contribute.

Increasing the reaction temperature to 250°C resulted in a change in the carbonaceous residue. The signal previously observed at 50 ppm is no longer evident and the signal attributed to aromatic species has become more apparent. New signals are observable at *ca.* 19 ppm in conjunction with the broad signal observed at 130 ppm suggest the formation of alkyl substituted aromatic compounds [8, 9]. The signal at 26 ppm may indicate the presence of polycyclic species [10] (in conjunction with part of the broad signal at 130 ppm) and/ or trapped aliphatic hydrocarbons [11] (with a broad envelope being observed between 8 and 55 ppm).

The coked mordenite generated at 300°C displays a similar series of species as observed previously for the sample generated at 250°C, though an enhancement in the signal observed around 130 ppm is apparent and the broad envelope previously evident in the 8 to 55 ppm range shows a change. In the aromatic region, a shoulder is observed at *ca.* 132 ppm which also indicates the presence of alkyl substituted aromatics [12] and a pronounced shoulder at 138 ppm is present suggesting that polycyclic aromatic species have formed [10].

Upon further increasing the reaction temperature to 500°C, resonances in the aliphatic region are no longer apparent and a signal is observed at *ca.* 130 ppm with a very broad base encompassing 120-150 ppm, suggesting the presence of a broad distribution of polycyclic species [10, 12] and that no poly-methyl benzene species are observed at higher temperatures.

The carbon content and the atomic H:C ratios are presented in Figures 5.2.2 and 5.2.3 for the various reaction temperatures employed. In Figure 5.2.2 it can be observed that the coked mordenite generated at 150°C contains approximately 2.0 wt% carbon. The solid state NMR study suggests that methanol is present adsorbed on the post-reaction mordenite and that there may be some aromatic species. Increasing the temperature resulted in an increase in the post-reaction carbon content of the samples generated at 250°C (8.1 wt%) and 300°C (9.7 wt%). At moderate temperatures (250 and 300°C) it is interesting that the observed carbon contents are very similar to those observed generated with a “wet” methanol carbonylation feedstream (as detailed in Chapter 4), whereas at 150°C the amount of deposited carbon is significantly greater for the “dry” dimethylcarbonate carbonylation feed. Upon increasing the reaction temperature to 500°C, however, it was found that the carbon content of the coked mordenite decreased significantly to 4.6 wt%. The decrease in carbon content may be explained by the presence of the γ -alumina pre-bed which was included to facilitate the decomposition of dimethylcarbonate to dimethylether. At higher temperatures, the pre-bed may open new catalytic routes to species which do not react with the mordenite. If this is the case, as the alumina begins to deactivate it would be expected that the feed would contain a greater concentration of species that can be converted by mordenite.

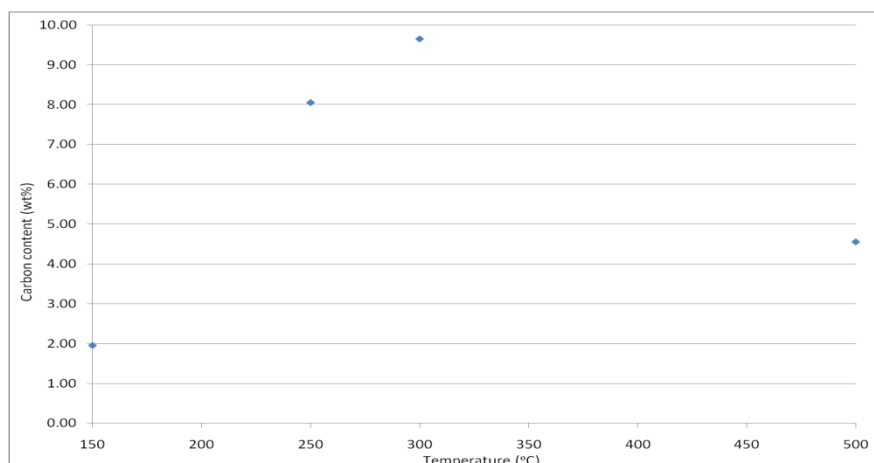


Figure 5.2.2: Carbon content of coked mordenite generated with dimethylcarbonate using a pre-bed at different reaction temperatures for 300 minutes.

In Figure 5.2.3 it can be observed that the coked mordenite generated at 150°C exhibits a significantly lower H:C ratio than that compared to the sample generated with a methanol carbonylation feedstream (H:C 105 as reported in Chapter 4). This could be a result of the observed increase in the carbon content and the subsequent decrease of water content in the sample due to using a dry feedstream, although there would invariably be an increase of water adsorbed in the material over time upon storage following reaction. The samples generated at 250 and 300°C have similar H:C ratios (2.3 and 1.8 respectively) and carbon contents (8.2 wt% and 9.7 wt% respectively) to those generated with a methanol carbonylation feedstream which seems to suggest that the same degree of hydration may have been achieved for both samples. The sample generated at 500°C exhibits a H:C ratio of approximately 2.4 which is similar to the ratio observed for the sample generated at 250°C, although the solid state NMR study suggests that the latter sample has species in the form of alkyl substituted aromatics and polycyclic aromatics deposited. This contrasts to that formed at 500°C in which there are no apparent aliphatic species, suggesting that the carbonaceous residue comprises of aromatic and polycyclic species.

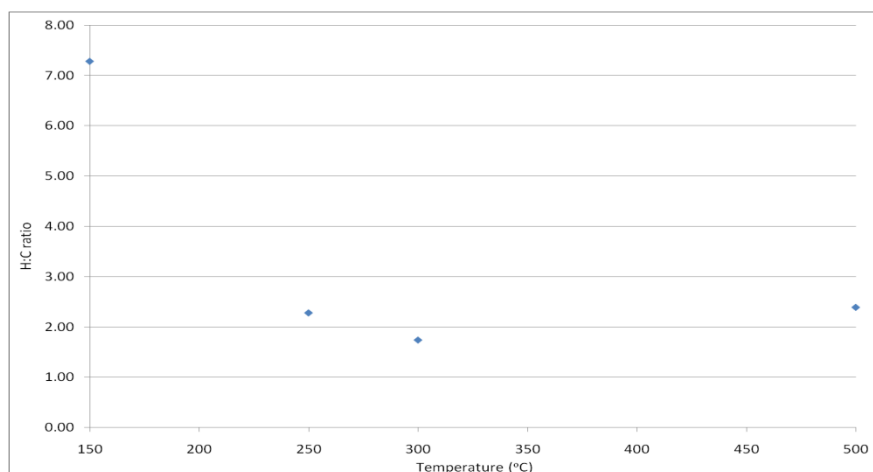


Figure 5.2.3: H:C atomic ratios of coked mordenite generated with dimethylcarbonate using a pre-bed at different reaction temperatures for 300 minutes (not corrected for the influence of adsorbed water).

Thermogravimetric analysis was undertaken to probe the differences in the reactivity of the carbonaceous deposits. Overlaid first derivative TGA profiles for the various reaction temperatures employed are presented in Figure 5.2.4 (under air), Figure 5.2.5 (under 2% O₂/Ar) and Figure 5.2.6 (under argon). The same temperature ramp rate (10°C/min) was used in all cases. It can be observed in Figure 5.2.4 that the sample generated at 150°C exhibits three first derivative TGA profile at *ca.* 70, 120 and 475°C, they can be assigned to desorption of water, the removal of volatiles (methanol) and the removal of the carbonaceous species (as indicated by the studies employing a reduced partial pressure of O₂ with corresponding mass spectrometry respectively). The sample generated at 150°C under dimethylcarbonate carbonylation conditions exhibits a similar first derivative TGA profile to the sample generated at the same temperature with a methanol carbonylation feedstream.

Coked mordenite samples generated at 250 and 300°C exhibit similar first derivative TGA profiles, corresponding to water desorption and the removal of carbonaceous species. It should be noted that the material generated at 300°C did not appear to display a first derivative TGA profile peak at approximately 325°C as exhibited in earlier chapters for coke generated at this temperature with different feedstreams.

Increasing the reaction temperature to 500°C resulted in a change in the first derivative TGA profile where now only two peaks are observed, one at *ca.* 70°C attributed to water

desorption and the other at 575°C attributed to the removal of carbonaceous species. It is apparent that the carbonaceous species are removed at a significantly lower temperature for the sample generated at 500°C than those exhibited in previous chapters.

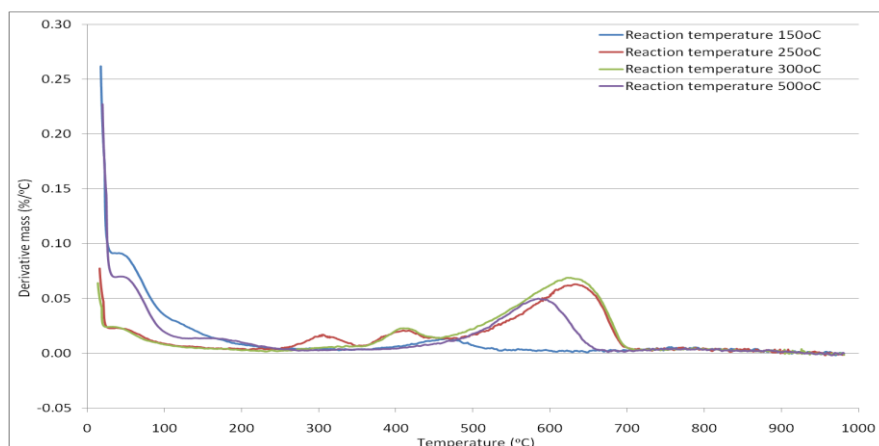


Figure 5.2.4: First derivative TGA profiles attained under air of coked mordenite generated with dimethylcarbonate using a pre-bed at different reaction temperatures for 300 minutes.

It can be observed in Figure 5.2.5 that similar first derivative TGA profiles are apparent for all samples under the 2% O₂/Ar atmosphere, although shifts are observed and a degree of peak broadening occurs. The coked mordenite generated at 150°C exhibits very little change in its first derivative profile with respect to that determined under air, except broadening of the initial peak which now overlaps with the temperature attributed to methanol desorption.

The samples generated at 250 and 300°C exhibit shifts in the peaks attributed to the removal of carbonaceous deposits. The peaks previously observed at 325 and 425°C have shifted by approximately 25°C, whereas the peaks at 625°C have shifted by 125°C. This can be attributed to the change in the oxygen concentration. For the coked mordenite generated at 500°C, it can be observed that a significant degree of broadening has occurred for the peak observed at lower temperature and an increase of 100°C is evident for the peak previously observed at 575°C.

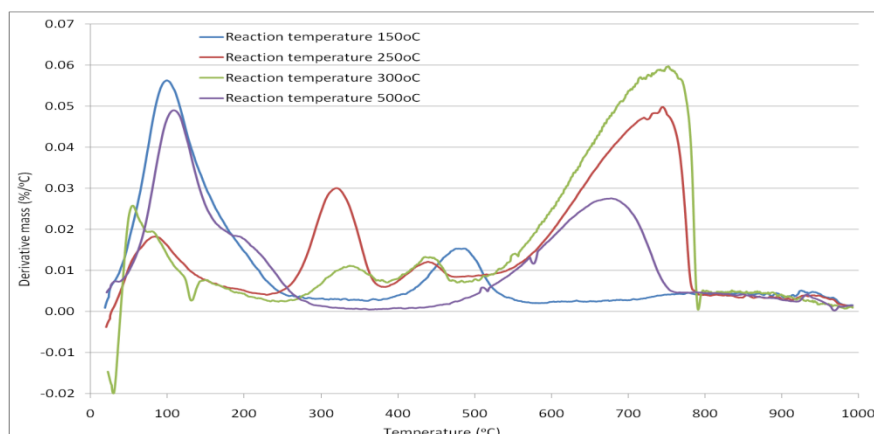


Figure 5.2.5: First derivative TGA profiles attained under 2% O₂/Ar of coked mordenite generated with dimethylcarbonate using a pre-bed at different reaction temperatures for 300 minutes.

Online mass spectrometry was undertaken to determine which gases were evolved from the sample during thermal analysis under different atmospheres. Mass spectrometry data is presented for the various samples using 2% O₂/Ar in Table 5.2.1. In some cases unique mass to charge ratios were scanned, whereas in others multiple fragments were used for the identification of products. The mass spectrometry data presented in Table 5.2.1 corresponds to the thermal analysis data performed under 2% O₂/Ar.

It can be observed in Table 5.2.1 that the sample generated at 150°C evolves a mixture of hydrogen, water, carbon monoxide, carbon dioxide and ethane upon heating under a 2% O₂/Ar atmosphere. This suggests that the sample undergoes combustion and cracking. As with previous studies, samples generated at 250 and 300°C display a wide range of evolved species, which reflects the broad distribution of carbonaceous species present on the mordenite. It is interesting that both samples exhibit cracking and combustion products simultaneously at the same temperature, unlike coked mordenites generated with methanol carbonylation feedstreams. The sample generated at 500°C only evolves water and carbon dioxide, suggesting that even though the material contained less carbon than observed for the same reaction temperature in previous studies with different feedstreams, the reactivity of the carbonaceous deposits was similar.

Product	DMC carb 150	Temp (°C)	DMC carb 250	Temp (°C)	DMC carb 300	Temp (°C)	DMC carb 500	Temp (°C)
Hydrogen	Y	500	Y	300	Y	375 450	-	-
Water	Y	50	Y	125 425 775	Y	90 150 375 450 775	Y	125 725
Carbon monoxide	Y	500	Y	325 425 675	Y	450	N	N/A
Carbon dioxide	Y	500	Y	325 425 725	Y	350 450 625 750	Y	675
Methane	N	N/A	Y	325	Y	350	N	N/A
Ethene	N	N/A	Y	325	Y	325	N	N/A
Ethane	Y	475	Y	325	N	N/A	N	N/A
Propene	N	N/A	Y	325	Y	325	N	N/A
Propane	N	N/A	Y	325	N	N/A	N	N/A
Butene	N	N/A	Y	325	Y	325	N	N/A
Butane	N	N/A	Y	325	Y	325	N	N/A
Benzene	N	N/A	Y	325	N	N/A	N	N/A
Ammonia	N	N/A	N	N/A	N	N/A	N	N/A

Table 5.2.1: Evolved gas mass spectrometry under 2% O₂/Ar for coked mordenite generated with dimethylcarbonate using a pre-bed at 150, 250, 300 and 500°C for 300 minutes (products have been identified by examining unique fragments and fragment patterns).

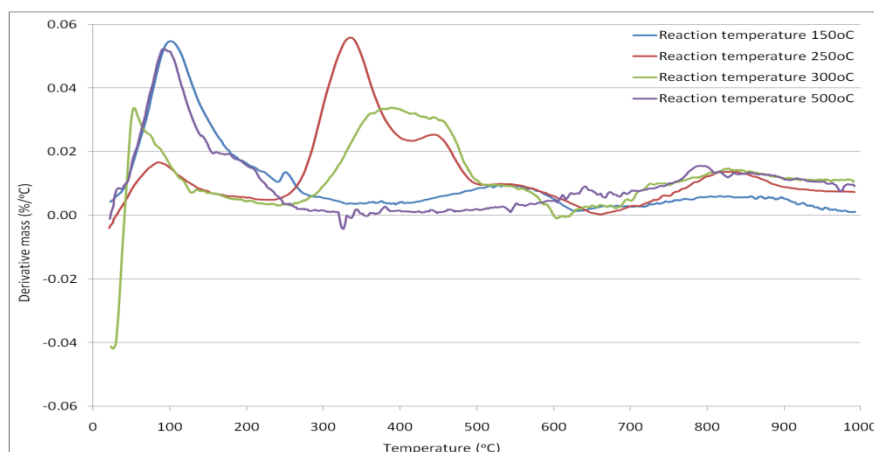


Figure 5.2.6: First derivative TGA profiles attained under argon of coked mordenite generated with dimethylcarbonate using a pre-bed at different reaction temperatures for 300 minutes.

It can be observed in Figure 5.2.6 that mordenite coked at 150°C displays a first derivative TGA profile under Ar exhibiting three peaks. A broad peak present at approximately 125°C related to the removal of a mixture of water and volatiles (methanol). The peak present at *ca.* 525°C is due to the decomposition of residual ammonium ions present in the mordenite. An additional higher temperature peak is also observed at approximately 850°C.

The coked mordenite samples generated at 250 and 300°C exhibit a degree of similarity in their first derivative TGA profiles. A peak attributed to desorption of water is apparent at approximately 70-80°C. Peaks are observed at *ca.* 325 and 450°C for the sample generated at 250°C whereas for the sample generated at 300°C a single broad peak is present at about 425°C, which appears to be a combination of two peaks occurring at around 375 and 450°C. The lower temperature peaks observed for both of the samples appear at temperatures 75°C above the reaction temperature in which these samples were generated, suggesting that they are materials indicative of the reaction and not artefacts generated upon cooling the reactor. The peaks are believed to be associated with removal of a proportion of the carbonaceous residue, which occurs via cracking type processes. A broad peak is observed in both instances at *ca.* 825°C, though the sample generated at 250°C exhibits a decrease and a subsequent levelling off of the peak above this temperature. The sample generated at 500°C however displays two peaks in the first derivative TGA profile at 125 and 825°C.

The similarity observed between the materials generated under dimethylcarbonate and methanol carbonylation conditions is clear, even with the effect of the alumina pre-bed for the sample generated at 500°C. First derivative TGA profiles under an argon atmosphere for samples generated at the same temperature in Chapter 4 appear almost identical, suggesting that the feed used has little bearing on the bulk aromatic and polycyclic species formed.

The mass spectrometry data presented in Table 5.2.2 corresponds to the thermal analysis data performed under Ar. In Table 5.2.2 it can be observed that the sample generated at 500°C only evolves water (adsorbed) when treated with an argon atmosphere, suggesting that the carbonaceous residue is unreactive in terms of cracking.

Samples generated at 250 and 300°C display an identical list of products indicating that the peaks observed at moderate temperatures (325-450°C) contain active species which readily crack at relatively low temperatures. Ammonia is observed suggesting that residual ammonium ions present prior to activation still remain after reaction. These are very similar to the observations made in the methanol carbonylation study.

The sample generated at 150°C appears to undergo methanol to hydrocarbon chemistry in the TGA instrument. This may be expected due to methanol being observed in the solid state NMR investigation and on the basis of the range of species observed in the TGA analysis.

Product	DMC carb 150	Temp (°C)	DMC carb 250	Temp (°C)	DMC carb 300	Temp (°C)	DMC carb 500	Temp (°C)
Hydrogen	N	N/A	Y	325 500 825	Y	475 800	-	-
Water	Y	150 375	Y	125 350	Y	90 125 375	Y	125
Carbon monoxide	N	N/A	N	N/A	N	N/A	N	N/A
Carbon dioxide	N	N/A	N	N/A	N	N/A	N	N/A
Methane	N	N/A	Y	325 450	Y	375 450	N	N/A
Ethene	Y	275 450	Y	325 450	Y	450	N	N/A
Ethane	N	N/A	Y	325	Y	400	N	N/A
Propene	Y	275 450	Y	325 450	Y	425	N	N/A
Propane	N	N/A	Y	325 450	Y	375	N	N/A
Butene	Y	275 450	Y	325 450	Y	400	N	N/A
Butane	Y	275	Y	325 450	Y	375	N	N/A
Benzene	N	N/A	Y	350	Y	400	N	N/A
Ammonia	Y	550	Y	550	Y	550	N	N/A
Dimethylether	Y	125 225	N	N/A	N	N/A	N	N/A

Table 5.2.2: Evolved gas mass spectrometry under Ar for coked mordenite generated with dimethylcarbonate using a pre-bed at 150, 250, 300 and 500°C for 300 minutes (products have been identified by examining unique fragments and fragment patterns).

Nitrogen adsorption isotherms were examined to determine the location of the coke. Figure 5.2.7 presents the stacked isotherms for materials following reaction at various different temperatures. Post-reaction nitrogen adsorption isotherms were type IV for samples generated at 150 and 500°C, whereas samples generated at 250 and 300°C respectively the isotherms were type II. BET surface areas along with single point surface area determination at $p/p^0 = 0.1$ are presented in Table 5.2.3.

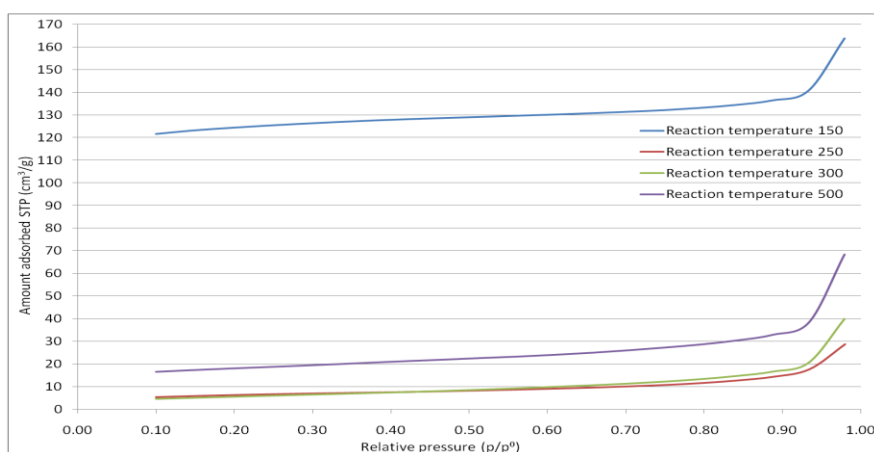


Figure 5.2.7: Nitrogen adsorption isotherms of coked mordenite generated with dimethylcarbonate using a pre-bed at different reaction temperatures for 300 minutes.

Material	BET surface area (m^2g^{-1})	Single point surface area at $p/p^0 = 0.1$ (m^2g^{-1})	Isotherm
Reaction temperature 150°C	370	476	Type IV
Reaction temperature 250°C	22	21	Type II
Reaction temperature 300°C	21	18	Type II
Reaction temperature 500°C	59	65	Type IV

Table 5.2.3: BET and single point surface areas and isotherm types for coked mordenite generated with dimethylcarbonate using a pre-bed at different reaction temperatures for 300 minutes.

It can be observed in Table 5.2.3 that the coked mordenite generated at 150°C exhibits a type IV isotherm and a surface area of approximately 370 m²g⁻¹, which corresponds to an increase upon reaction. As the reaction temperature is increased to 250 and 300°C the isotherm changes to type II and the surface area decreases significantly to approximately 22 m²g⁻¹ indicating the loss of microporosity after reaction. In the study employing methanol carbonylation conditions (reported in Chapter 4) it was observed that a small degree of porosity was retained after reaction for the sample generated at 250°C. This may suggest a difference in the position of the carbonaceous deposits in the pores where employing methanol results in a build-up within the pore structure whereas DMC results in a build-up at the pore mouth. As the reaction temperature is increased to 500°C, a degree of porosity is retained and surface area apparently increases with respect to the 250 and 300°C samples to *ca.* 59 m²g⁻¹. As mentioned previously in this study, this is believed to be an artefact caused by the presence of the alumina pre-bed which effects the formation of the carbonaceous deposits and which may be caused by the pre-bed altering the feedstream composition. This is supported in a study which employed no such pre-bed and resulted in a significant increase in the amount of carbon deposited over the zeolite and which is discussed later in this chapter.

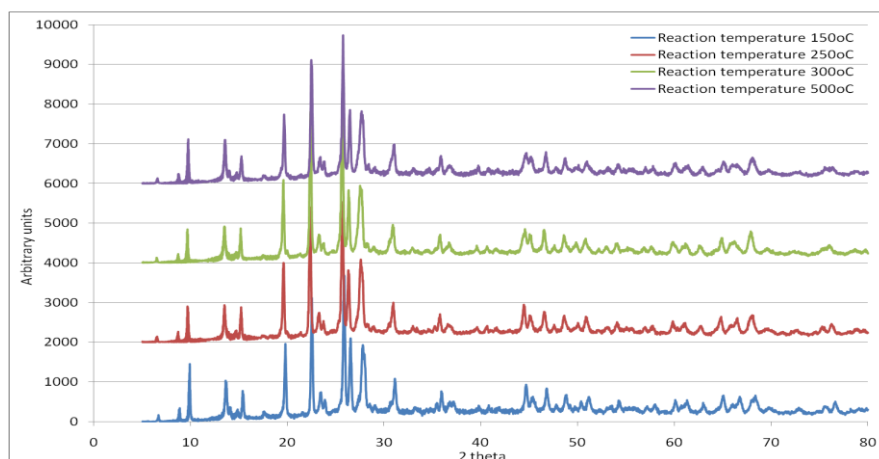


Figure 5.2.8: XRD patterns of coked mordenite generated with dimethylcarbonate using a pre-bed at different reaction temperatures for 300 minutes.

Powder x-ray diffraction investigations were undertaken to determine the influence that the reaction has upon the zeolite framework. Stacked patterns are presented in Figure 5.2.8 for

the various reaction temperatures employed. In Figure 5.2.8 it can be observed that all post-reaction samples exhibit XRD patterns indicating that the framework after reaction remained intact. The sample generated at 250 exhibits shifts in the (200), (330) and (150) reflections which occur at approximately 10, 20 and 22° 2 θ .

5.2.2 Dimethylcarbonate carbonylation (with no γ -alumina pre-bed) temperature dependence

Given the observations made in the previous study for coked mordenite generated at 500°C employing a γ -alumina pre-bed, a series of reactions were performed without the γ -alumina to probe the effect of temperature on the carbonaceous species formed on the zeolite during dimethylcarbonate carbonylation chemistry. Materials were activated as described in the materials section in Chapter 2 and reactions were run under the conditions described previously.

^{13}C CP MAS NMR spectroscopy was performed on coked mordenite in an attempt to identify the nature of any carbonaceous residue. The data is presented in Figure 5.2.9.

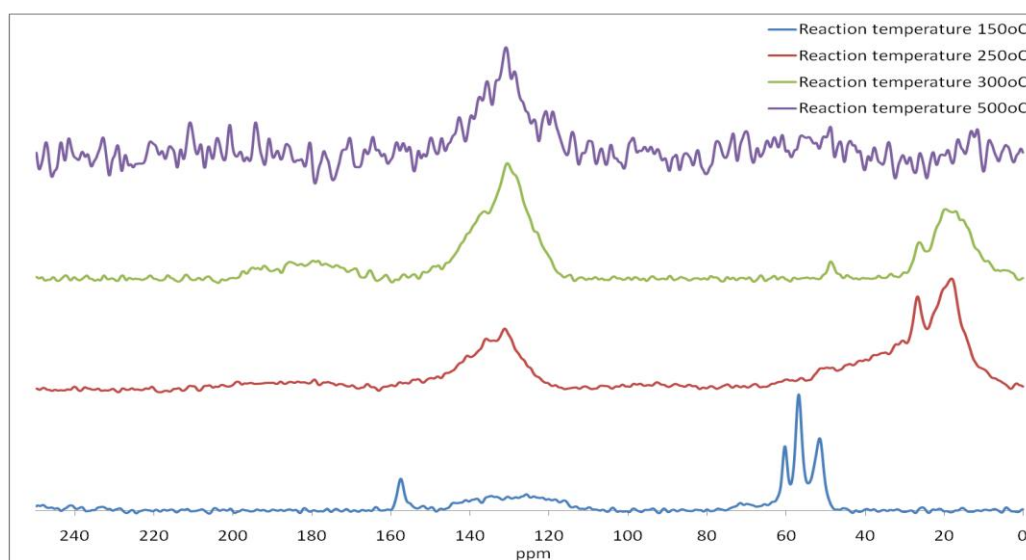


Figure 5.2.9: ^{13}C CP MAS NMR spectrum of coked mordenite generated with dimethylcarbonate at different reaction temperatures for 300 minutes.

It can be observed in Figure 5.2.9 that by removing the alumina pre-bed for the sample generated at 150°C, the solid state NMR spectrum changes significantly. Low field signals indicative of methanol [7] (51 ppm), surface bound methoxy species [7] and/or dimethylcarbonate methyl groups [13] (57 ppm) and dimethylether [7] and/or silanol bound methanol [14] (60 ppm) are observed. High field signals appearing at *ca.* 126 and 135 ppm suggest the formation of aromatic and polycyclic compounds [10, 15], whereas the signal at 158 ppm can be assigned to dimethylcarbonate carbonyl species [13]. This indicates that the zeolite readily converts dimethylcarbonate without the necessity of a pre-bed. It also suggests that the zeolite under “dry” carbonylation conditions will readily convert the feed to aromatic species which are similar to those observed at lower temperatures employed in comparable methanol only studies.

The sample generated at 250°C exhibits a very different solid state NMR spectrum. As with other feeds, signals suggesting the presence of a hydrocarbon pool consisting of alkyl substituted aromatic compounds [8, 9] (18 and 131 ppm) and substituted polycyclic aromatic compounds [10] (26 and 138 ppm) are observed. A very broad base is observed for the low field signals (18 and 26 ppm) suggesting that a broad distribution of trapped hydrocarbons may be present on the mordenite [11]

It can be observed that the sample generated at 300°C displays similar features to those observed previously for the mordenite coked at 250°C. The broad base observed at high field for the sample generated at 250°C has become significantly narrower encompassing the range between 3-30 ppm. The presence of methanol [7] is indicated by the signal present at 49 ppm, but perhaps most interesting of all is the appearance of a carbonyl species (180 ppm) and a significant increase in a signal at *ca.* 20 ppm which suggests the presence of acetic acid [13, 16] on the mordenite post-reaction. Given that the process currently under development by BP operates at 300°C this is perhaps not unexpected. It is however notable that no such observation was made when the alumina pre-bed was in place. However care must be taken with the assignment of the signal present at 180 ppm as it may also indicate the presence of adsorbed carbon monoxide [17].

The coked mordenite generated at 500°C has a similar solid state NMR spectrum to all of the other studies regardless of the feedstream employed. Signals indicating the presence of polycyclic compounds are observed (at 131 and 138 ppm) [10, 12].

The solid state NMR spectra generated for the samples employing no γ -alumina pre-bed have unique signals not observed previously with any feed. This indicates that the presence of the alumina may have more of an effect at lower temperatures than previously understood.

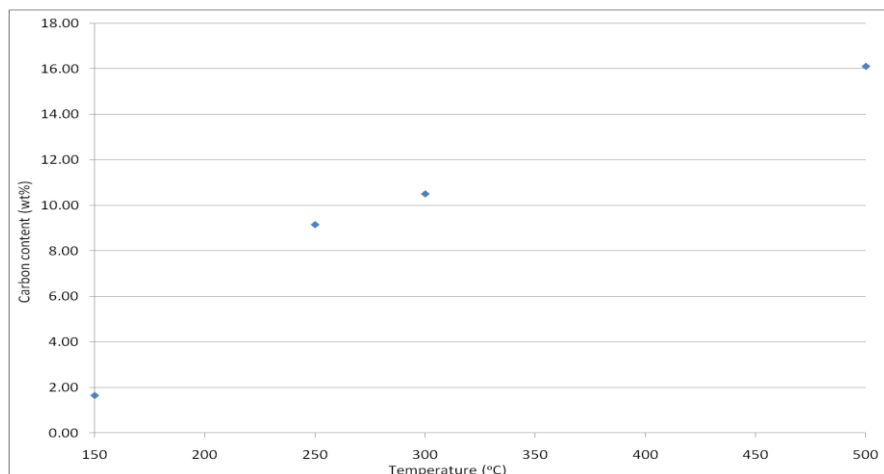


Figure 5.2.10: Carbon content of coked mordenite generated with dimethylcarbonate at different reaction temperatures for 300 minutes.

The carbon content and the atomic H:C ratios are presented in Figures 5.2.10 and 5.2.11 for the various reaction temperatures employed. It can be observed in Figure 5.2.10 that as the reaction temperature increased the carbon content of the post-reaction mordenite increased. This was observed for all temperature dependence studies except where the alumina pre-bed was used. Comparing the carbon contents of the samples generated with and without a pre-bed it was found that for the sample generated at 150°C very little change in the carbon content was observed, although the solid state NMR investigations show a significantly different distribution of species. The samples generated at higher temperatures exhibited an increase in the amount of carbon laid down on the mordenite. For the samples generated at 250 and 300°C, there was approximately a 1 wt% increase in the carbon content, whereas for the sample coked at 500°C the carbon content increased from 4.6 wt% (with pre-bed) to 16.1 wt% (without pre-bed). This indicates, with good agreement from the solid state NMR investigations, that the γ -alumina had an effect on not only the nature but also the amount of the carbon deposited upon the sample.

It can be observed in Figure 5.2.11 that the H:C ratio decreased as the reaction temperature increased. The carbonaceous residue (for samples generated at 250, 300 and 500°C) was more hydrogen deficient compared to those obtained for samples generated at the same temperature with a pre-bed. The sample generated at 150°C, however, exhibited a decrease in hydrogen deficiency compared to the sample generated with a pre-bed.

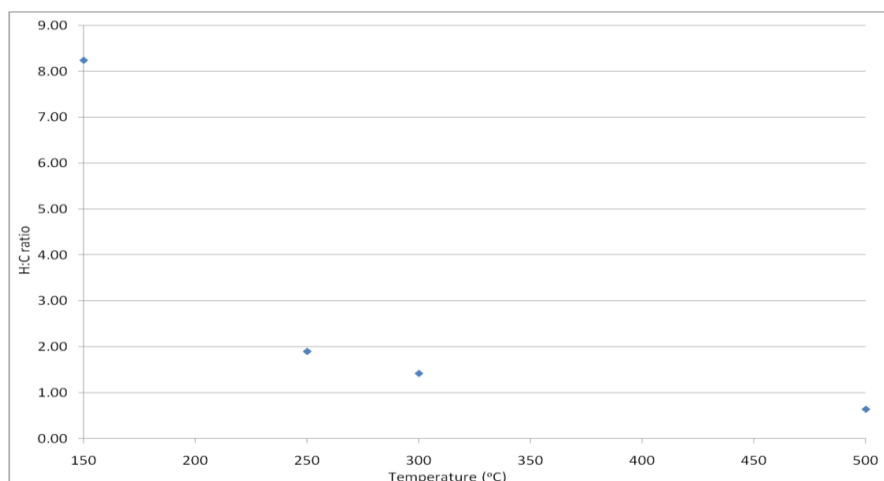


Figure 5.2.11: H:C atomic ratios of coked mordenite generated with dimethylcarbonate at different reaction temperatures for 300 minutes (not corrected for the influence of adsorbed water).

Thermogravimetric analysis was undertaken to probe the differences in the reactivity of the carbonaceous deposits. Overlaid first derivative TGA profiles determined under an air atmosphere for the various reaction temperatures employed are presented in Figure 5.2.12.

In Figure 5.2.12 it can be observed that a similar series of first derivative TGA profiles are observed for all samples compared to those for corresponding studies employing a pre-bed, although there is a degree of difference for the mordenite samples coked at 150 and 500°C respectively. The sample generated at 150°C exhibits additional peaks present at 170 and 225°C which may indicate the removal of the oxygenated species assigned in the solid state NMR investigations. As the peak at 450°C is present, again this may be attributed to the decomposition of residual ammonium ions and/or possibly the removal of the carbonaceous

residue associated with aromatic and polycyclic species. The coked mordenite reacted at 500°C exhibits a significant increase in the peak present at *ca.* 625°C, which in previous studies was attributed to the polycyclic aromatic species present in the zeolite, which may be expected based upon the significant increase in carbon content.

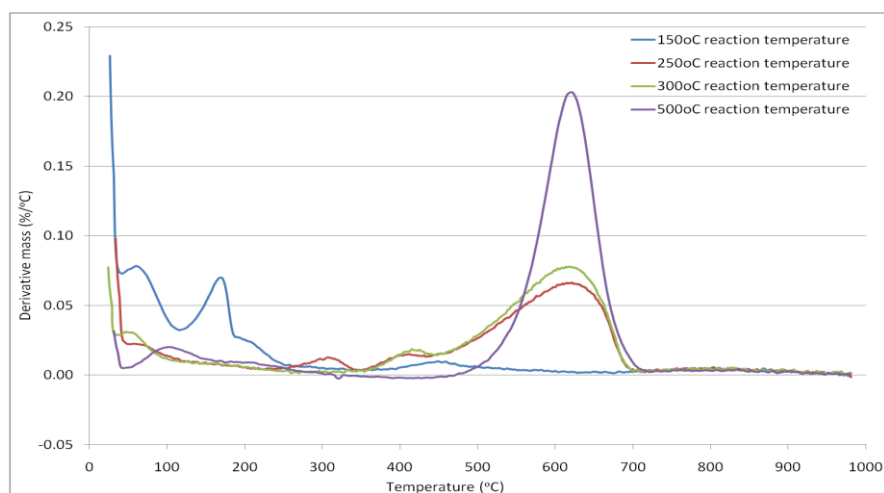


Figure 5.2.12: First derivative TGA profiles attained under air of coked mordenite generated with dimethylcarbonate at different reaction temperatures for 300 minutes.

Nitrogen adsorption isotherms were examined to determine the location of the coke. Figure 5.2.13 presents the stacked isotherms for materials following reaction at various different temperatures. Post-reaction nitrogen adsorption isotherms were type IV for the sample generated at 150, whereas for samples generated at 250, 300 and 500°C respectively the isotherms were type II. BET surface areas along with single point surface area determination at $p/p^0 = 0.1$ are presented in Table 5.2.4.

It can be observed in Figure 5.2.13 and Table 5.2.4 that, much like the sample generated at 150°C with a pre-bed, the corresponding sample generated without a pre-bed exhibited an apparent increase in the surface area although there may be limitations with this measurement. For samples generated at 250°C and above, the loss of microporosity is apparent indicating that the carbonaceous residues block the micropore system. The surface area has decreased significantly to approximately $20 \text{ m}^2\text{g}^{-1}$ and does not appear to change further as the reaction temperature is increased up to 500°C.

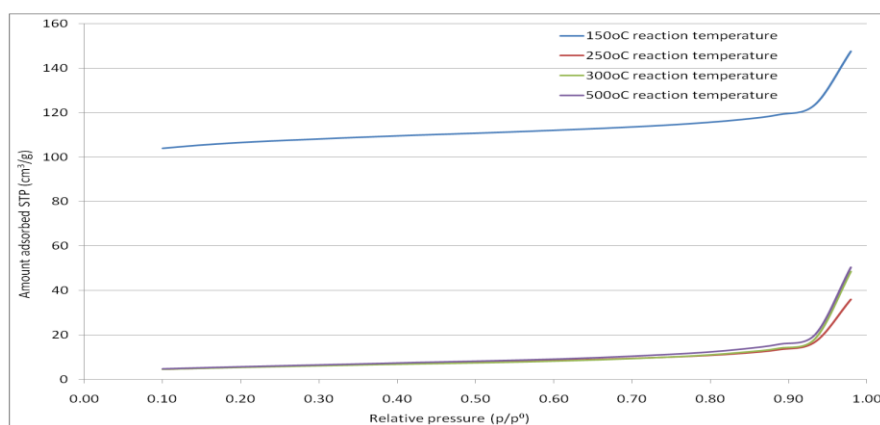


Figure 5.2.13: Nitrogen adsorption isotherms of coked mordenite generated with dimethylcarbonate at different reaction temperatures for 300 minutes.

Material	BET surface area (m^2g^{-1})	Single point surface area at $p/p_0 = 0.1$ (m^2g^{-1})	Isotherm
Reaction temperature 150°C	316	407	Type IV
Reaction temperature 250°C	20	18	Type II
Reaction temperature 300°C	19	18	Type II
Reaction temperature 500°C	21	19	Type II

Table 5.2.4: BET and single point surface areas and isotherm types for coked mordenite generated with dimethylcarbonate at different reaction temperatures for 300 minutes.

Stacked XRD patterns are presented in Figure 5.2.14 for the various reaction temperatures employed. It can be observed that the framework remains intact regardless of reaction temperature although post-reaction samples generated at 300 and 500°C exhibit shifts in the (330) and (150) reflections corresponding to approximately 20 and 22° 2 θ . The reflections at 44 and 45° 2 θ undergo a transformation for post-reaction mordenites generated at 300 and 500°C. Some structural changes are apparent at greater than 35° 2 θ which may be as a consequence of the carbonaceous deposits.

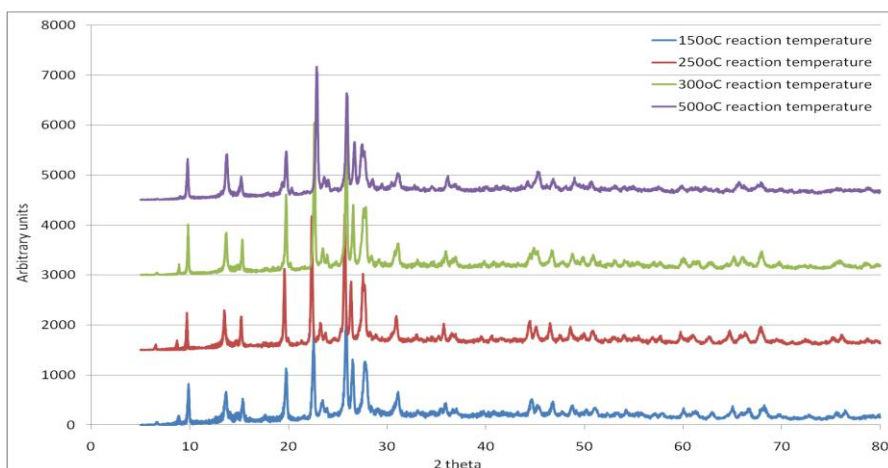


Figure 5.2.14: XRD patterns of coked mordenite generated with dimethylcarbonate at different reaction temperatures for 300 minutes.

5.2.3 Temperature dependence of the carbonaceous species deposited during dimethylcarbonate-only reactions

To investigate the effect of reaction temperature on the carbonaceous species deposited on the zeolite from a dimethylcarbonate only feedstream, materials were activated at 500°C for 60 minutes under 30 ml min⁻¹ of Ar. Activated mordenite was run in a 45% dimethylcarbonate feedstream at a GHSV of 3000 hr⁻¹ at reaction temperatures 250, 300 and 500°C. Coked mordenite samples were cooled to room temperature under an argon flow.

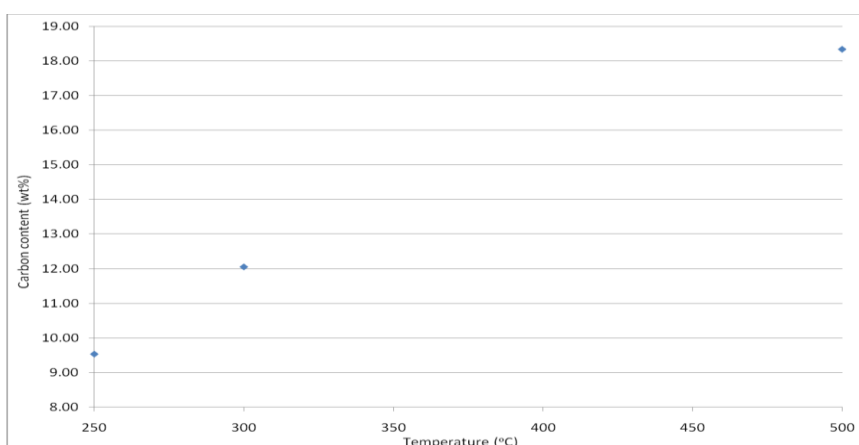


Figure 5.2.15: Carbon content of coked mordenite generated from dimethylcarbonate at different reaction temperatures for 300 minutes.

The carbon content and atomic H:C ratios are presented in Figures 5.2.15 and 5.2.16 for the reaction temperatures employed within this study. In Figure 5.2.15, it can be observed that feeding dimethylcarbonate over the mordenite at 250°C deposits approximately 9.5 wt% of carbon. Increasing the temperature results in an increase in the post-reaction carbon contents of the samples generated at 300°C (12.1 wt%) and 500°C (18.3 wt%) respectively. In particular the sample generated at 300°C is similar in some respects to the samples generated under a methanol only feedstream. Specific differences are observed in the samples generated at 250 and 500°C. Under a dimethylcarbonate only feedstream, less carbon is observed on the sample generated at 250°C (11.6 wt% under methanol only), whereas more carbon is observed for the sample generated at 500°C (17.6 wt% under methanol only). Good reproducibility was observed at all reaction temperatures (at least 96%).

In Figure 5.2.16, it can be observed that the H:C ratio decreases with increasing reaction temperature. Similar values are observed for samples generated under both methanol and dimethylcarbonate only feedstreams, suggesting that the reactant type in this instance has little influence on the amount and bulk nature of the carbonaceous deposits. This is rather interesting given that the carbon content was observed to be less for the sample generated at 250°C and more for 500°C, which indicates that the total amount of hydrogen present within the systems were different. This may be due to a change in the water content of the sample or due to a change in the speciation of carbonaceous deposits.

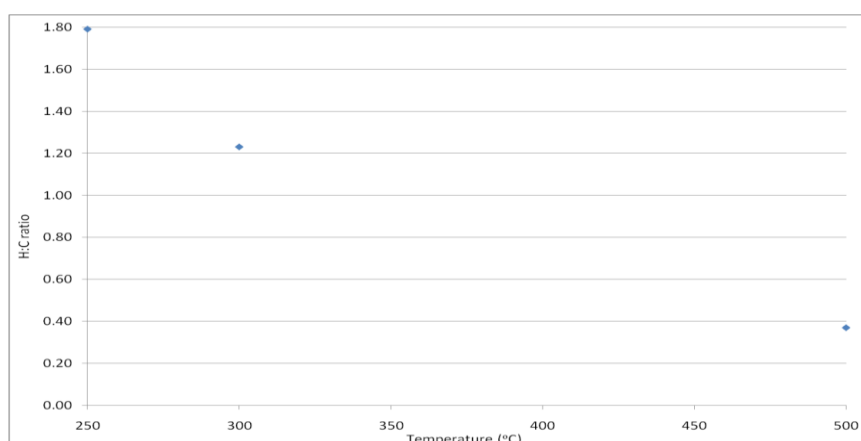


Figure 5.2.16: Atomic H:C ratio of coked mordenite generated from dimethylcarbonate at different reaction temperatures for 300 minutes (not corrected for the influence of adsorbed water).

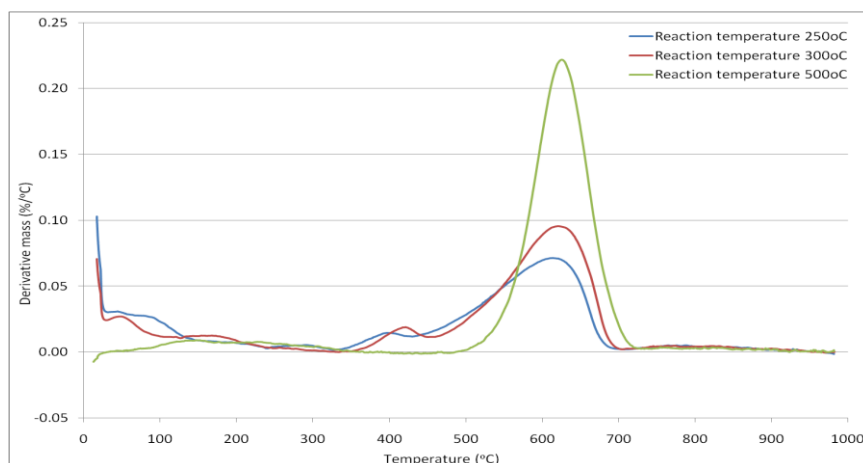


Figure 5.2.17: First derivative TGA profiles attained under air of coked mordenite generated with dimethylcarbonate at different reaction temperatures for 300 minutes.

Thermogravimetric analysis was undertaken to probe the differences in the reactivity of the carbonaceous deposits. Overlaid first derivative TGA profiles for the various reaction temperatures employed are presented in Figure 5.2.17 (under air). In Figure 5.2.17 it can be observed that the sample generated at 250°C displays four first derivative mass peaks, the first occurring at *ca.* 70°C which can be attributed to water desorption and the three other peaks at *ca.* 300, 400 and 625°C associated with the removal of carbonaceous species. The differences observed in temperatures attributed to the removal of carbonaceous species have been explained in previous chapters, detailing the possible existence of surface bound hydrocarbons, which would explain the observed difference in activity under an oxygen atmosphere. A similar first derivative TGA profile is observed for the sample generated at 300°C. The coked sample generated at 500°C displays two first derivative TGA profile peaks at approximately 125 and 625°C, attributed to water desorption and the removal of carbonaceous deposits respectively.

The first derivative TGA profiles observed for samples generated with a dimethylcarbonate-only feedstream are very similar to those observed for coked mordenites generated under methanol only conditions. This suggests that the use of dimethylcarbonate as feedstream has little if any, real effect on the reactivity of the carbonaceous deposits generated at comparable reaction temperatures when compared to the methanol only feed.

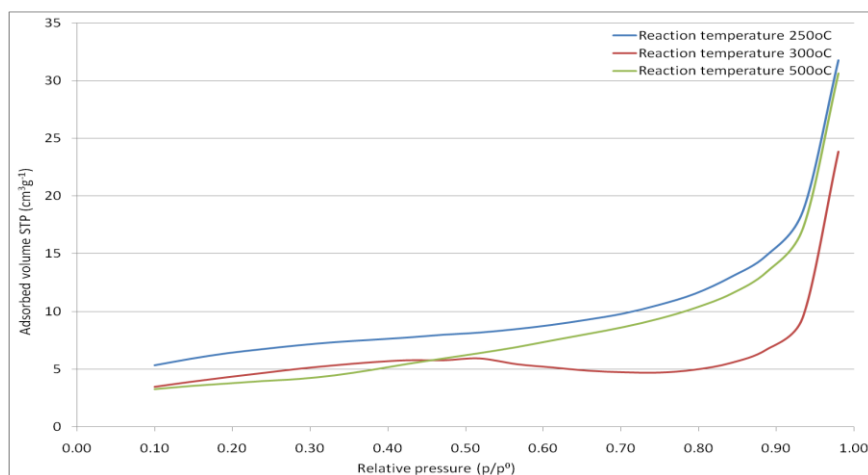


Figure 5.2.18: Nitrogen adsorption isotherms of coked mordenite generated with dimethylcarbonate at different reaction temperatures for 300 minutes (The isotherm for the sample generated at 300°C is problematic after approximately 0.4 P/P⁰ but is used to illustrate the relative pressure range used in the BET method. It was not possible to rerun this isotherm because a problem developed on the system).

Nitrogen adsorption isotherms were examined to determine the location of the coke. Figure 5.2.18 presents the stacked isotherms for materials following reaction at various different temperatures. Post-reaction nitrogen adsorption isotherms were type II in all instances. BET surface areas along with single point surface area determination at $p/p^0 = 0.1$ are presented in Table 5.2.5.

In Figure 5.2.18 and Table 5.2.5 it can be observed that at all reaction temperatures a total loss of microporosity occurs indicated by a type II isotherm present in all instances. As the reaction temperature is increased, the surface area decreases from 23 m²g⁻¹ after the 250°C reaction to 13 m²g⁻¹ after the 500°C reaction.

Materials	BET surface area (m^2g^{-1})	Single point surface area at $p/p_0 = 0.1$ (m^2g^{-1})	Isotherm
Reaction temperature 250°C	23	21	Type II
Reaction temperature 300°C	17	14	Type II
Reaction temperature 500°C	13	13	Type II

Table 5.2.5: BET and single point surface areas and isotherm types for coked mordenite generated with dimethylcarbonate at different reaction temperatures for 300 minutes.

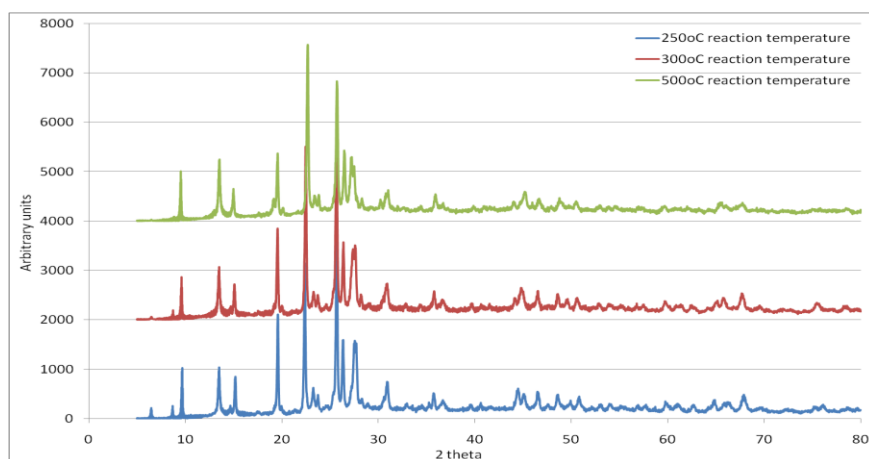


Figure 5.2.29: XRD patterns of coked mordenite generated at different reaction temperatures for 300 minutes.

Powder x-ray diffraction investigations were undertaken to determine the influence that the reaction has upon the post-reaction samples. Stacked patterns are presented in Figure 5.2.19 for the various reaction temperatures employed. It can be observed that the sample generated at 500°C displays a shift in the (150) reflection which occurs at approximately 22° 2θ. It is also apparent that a degree of structural change has occurred possibly due to the deposition of carbonaceous material on the zeolite.

5.3 Conclusions

Samples generated under a mixed dimethylcarbonate, CO and H₂ feedstream employing a γ -alumina pre-bed exhibited an increased carbon content and hydrogen deficiency as the temperature increased to 300°C. The sample generated at 500°C however had a significantly lower carbon content and hydrogen deficiency. The solid state NMR investigations indicated that even though there was significantly less carbon observed and an elevation in the H:C ratio, the residue was still of a similar nature to that observed in other studies. The samples generated at lower temperatures exhibited very similar first derivative TGA profiles to the coked mordenite generated with a methanol carbonylation feedstream. The thermal analysis undertaken under air, 2% O₂/Ar and Ar with corresponding mass spectrometry indicated the degree of similarity between the carbonaceous deposits formed under methanol and DMC carbonylation conditions at 150, 250 and 300°C. The sample generated at 500°C displayed peaks at lower temperatures for air and 2% O₂/Ar, suggesting that the carbonaceous deposits though similar may be more accessible and hence able to combust at lower temperatures.

This was also suggested by the nitrogen adsorption studies which indicated that the sample generated at 500°C retained a degree of porosity. No change is observed for the sample generated at 150°C, whereas the samples generated at 250 and 300°C display a complete loss of microporosity. Single point surface area determination at $p/p^0 = 0.1$ displayed an enhancement in surface area compared to the surface area determined via the BET equation, for the sample generated at 150°C (476 m² g⁻¹). However the other samples exhibited no substantial change in surface area. The framework is found to remain intact after reaction.

It was observed for coked mordenites generated with no γ -alumina pre-bed under a mixed dimethylcarbonate, CO and H₂ feedstream that as the reaction temperature increased the carbon content and hydrogen deficiency of the residue increased. Solid state NMR studies showed that samples generated at 250°C and 500°C exhibited species similar to those performed at corresponding temperatures in other studies. The sample coked at 150°C showed a very interesting spectrum of oxygenated species (methanol, surface bound methoxy, dimethylether and dimethylcarbonate) and an aromatic component was observed. The 300°C post-reaction sample exhibited similar features to those observed in the methanol carbonylation studies, but also indicated the possible presence of acetic acid.

Thermal analysis under air demonstrated that the samples generated with a dimethylcarbonate carbonylation feedstream exhibited very similar first derivative TGA profiles for samples generated at 250 and 300°C whether a pre-bed was present or not. The sample generated at 150°C exhibited additional peaks present at 170 and 225°C which may indicate the removal of the oxygenated species. The post-500°C reaction coked mordenite exhibits a significant increase in the loss at 625°C assigned to the removal of carbonaceous species.

The nitrogen adsorption isotherms indicated that no change had occurred in the material generated at 150°C. The samples generated at higher temperatures exhibited a complete loss of accessible microporosity and a surface area of approximately 20 m²g⁻¹. An enhancement was observed employing single point surface area determination at $p/p^0 = 0.1$ for the sample generated at 150°C (407 m² g⁻¹), whereas no apparent changes were observed for the other samples generated at higher temperatures. The zeolite framework was observed to remain intact post-reaction regardless of reaction temperature, with only a few minor framework changes present due to the carbonaceous deposits.

As the reaction temperature is increased for samples generated under a dimethylcarbonate feedstream, the carbon content and hydrogen deficiency of the carbonaceous residue increased. Samples generated at moderate reaction temperatures exhibited a similarity in the reactivity of the carbonaceous deposits, whereas for the post-500°C sample it was observed that the carbonaceous residue was significantly less reactive to air.

Nitrogen adsorption isotherms display a complete loss of microporosity, indicating that the carbonaceous species are trapped in the pores of the zeolite. No obvious advantage was seen employing the single point surface area determination at $p/p^0 = 0.1$ for any of the samples generated with a DMC-only feedstream. Post-reaction XRD indicates that the framework remains intact regardless of reaction temperature, but some alteration of the framework has occurred possibly an effect of the carbonaceous deposits.

It is of interest to mention that the observed framework alterations observed throughout this work only occur when the effects of reaction temperature are examined, which at higher temperatures result in relatively harder coke fractions deposited over mordenite.

References

- [1] T. Blasco, M. Boronat, P. Concepcion, A. Corma, D. Law, J. Vial-Moya, *Angewandte Chemie International Edition* 46 (2007) 3938
- [2] P. Cheung, A. Bhan, G. Sunley, E. Iglesia, *Angewandte Chemie International Edition* 45 (2006) 1617
- [3] A. Bhan, E. Iglesia., *Accounts of Chemical Research*. 41 (2008) 559
- [4] P. Cheung, A. Bhan, G. Sunley, D. Law, E. Iglesia, *Journal of Catalysis*. 245 (2007) 110
- [5] A. Haynes, *Advances in Catalysis*. 53 (2010) 1
- [6] S. Anderson, S. Manthata, T. Root, *Applied Catalysis A: General*. 280 (2005) 117
- [7] Y. Jiang, M. Hunger, W. Wang, *Journal of the American Chemical Society* 128 (2006) 11679
- [8] J. Haw, W. Song, D. Marcus, J. Nicholas. *Accounts of Chemical Research* 36 (2003) 317
- [9] W. Wang, A. Buchholz, M. Seiler, M. Hunger, *Journal of the American Chemical Society* 125 (2005) 15260
- [10] www.chem.wis.edu/areas/reich/handouts/nmr-c13/cdata.htm (accessed on 31/03/2011)
- [11] M. Anderson, M. Ocelli, J. Klinowski, *The Journal of Physical Chemistry* 96 (1992) 388
- [12] A. Sassi, W. Song, M. Wildman, J. Haw, *Catalysis Letters* 81 (2002) 101
- [13] H. Gottlieb, V. Kotlyar, A. Nudelman, *The Journal of Organic Chemistry* 62 (1997) 7512
- [14] L. Carlson, P. Isbester, E. Munson, *Solid State Nuclear Magnetic Resonance* 16 (2000) 92
- [15] F. Oliver, E. Munson, J. Haw, *The Journal of Physical Chemistry* 96 (1992) 8106
- [16] www.chem.ucla.edu/~webspectra/notesonsolvents.html (accessed on 31/03/2011)
- [17] K. Zamaraev, V. Mastikhin, *Colloids and Surfaces* 12 (1984) 401

6 Conclusions

6.1 Comparative conclusions

Throughout this project two main objectives were focused upon, firstly, understanding the nature and composition of the carbonaceous species deposited over mordenite employing different sets of conditions and secondly, the removal of the deposits in TGA based experiments. Up until now each chapter has focused upon the use of a single feedstream type and as such the results have been dealt with this in mind although a degree of comparison has been made. Within this chapter select data sets (^{13}C CP MAS NMR, elemental analysis and TGA employing different atmospheres) are compared for materials coked with methanol only, mixed methanol, carbon monoxide and hydrogen and mixed dimethylcarbonate, carbon monoxide and hydrogen feedstreams.

The basis for these comparisons stems from the carbonylation process currently under development at BP Chemicals which operates at 300°C and approximately 30 bar employing a methanol and syn-gas (4:1 $\text{CO}:\text{H}_2$) feedstream. Very recently methanol has been substituted for dimethylether for reasons mentioned in the Introduction to Chapter 4.

From the reaction temperatures employed, four were examined more extensively than others 150, 250, 300 and 500°C . Out of these, it was found that samples generated at 150°C in all instances did not have significant carbon contents and was found to have very different ^{13}C CP solid state NMR spectra compared to the other samples. The sample generated at 500°C , however, had large quantities of carbon deposited on the mordenite (except when employing a pre-bed in the case dimethylcarbonate carbonylation feedstream) and a product distribution consisting of primarily polycyclic species (which in terms of MTH chemistry are associated with deactivated hydrocarbon pool species). Samples generated at 250°C , which appears to be a break through temperature for the formation of methylated aromatic species (Figure 6.1.1), and 300°C (BP Chemicals process temperature) (Figure 6.1.5) however exhibited a very interesting distribution of carbonaceous species consisting of alkyl substituted aromatics and polycyclic species and this was apparent for both reaction temperatures under any feedstream regardless of carbon content (Tables 6.1.1 and 6.1.2). In all cases the very broad feature attributed to the presence of methylated aromatics was found to be more significant for the sample generated at 300°C . Examining the effect of time on stream at 300°C exhibited no appreciable difference between the distribution of species observed between 60 and 420

minutes regardless of the feedstream used (Figures 6.1.9, 6.1.11 and 6.1.13) although differences were observed in the carbon contents of the post-reaction zeolites (Tables 6.1.3-6.1.6). For samples generated at 600 minutes, however, some deviation is observed (Figure 6.1.15). Studies undertaken within this thesis showed that the carbonaceous species are formed very rapidly with complex mixtures if methylated aromatics and polycyclic species present at 5 minutes time on stream.

It has been observed that coking of mordenite is an essential phase of the process, whereby as the surface area of the mordenite decreases the hydrocarbon pool reaction rate decreases and the carbonylation selectivity and rate increases. This only occurs up to a certain maximum, which to date has not been established. After this maximum however, rapid deactivation of the catalyst has been found. Studies have been undertaken by BP Chemicals in potential regeneration procedures to reactivate the coked catalyst. Initial studies were performed under air and it was observed that heating the material to 500°C (standard activation temperature) decreased the catalytic activity sufficiently due to partial destruction of the framework as to be of no further use within the process. Studies undertaken within this thesis on samples generated at 250 (Figure 6.1.2) and 300°C (Figure 6.1.6) have indicated that under air most of the carbonaceous deposits are removed by approximately 700°C. (Work not presented within this thesis has indicated that the mordenite framework is completely destroyed at this point). Carbonaceous residues deposited over the coked mordenite generated at 300°C for 60-600 minutes have exhibited similar reactivities regardless of time on stream. Work employing a lower partial pressure of oxygen (2%) has shown an increase in the temperature of removal of the bulk of the carbonaceous deposits on average approximately 800°C (Figures 6.1.3 and 6.1.7) though in some instances up to 900°C. This clearly is not a viable method for the removal of carbonaceous deposits.

Studies were undertaken employing an argon atmosphere and it was found that a small proportion (on average about 30%) of the carbonaceous residue was removed (Figures 6.1.4 and 6.1.8) via cracking processes. Mass spectrometry of the studies undertaken on the evolved gases from argon treatment for samples generated at 250 and 300°C exhibited a multitude of aliphatic and olefinic species and also benzene (which is an unusual species to observe). As mentioned previously the coking of the mordenite and subsequent blockage of the microporous network was essential for carbonylation to proceed. Work undertaken by Ellis *et al.* [1] indicated that mordenite began to deactivate after maximum selectivity to

acetyls was achieved, which may indicate that a small amount of deposited carbonaceous materials formed from MTH chemistry could have been responsible.

From the work presented within this thesis five key conclusions can be drawn from this project;

1. Mordenite coked with methanol only feedstreams provides a good speciation model for materials coked during methanol carbonylation.
2. Carbonaceous materials are deposited very rapidly, methylated aromatics and polycyclic species are evident after only 5 minutes.
3. Caution must be exercised when applying the methanol only coking model to materials coked during dimethylcarbonate carbonylation employing a γ -alumina pre-bed.
4. Treatment with an oxygen containing atmosphere completely removes the carbonaceous materials as indicated by elemental analysis (0.0 wt% carbon), but the zeolite is damaged (shown in Figure 7.3.1 in Appendices).
5. A small but reactive fraction of the carbonaceous residue is removed from coked materials treated with an argon atmosphere.

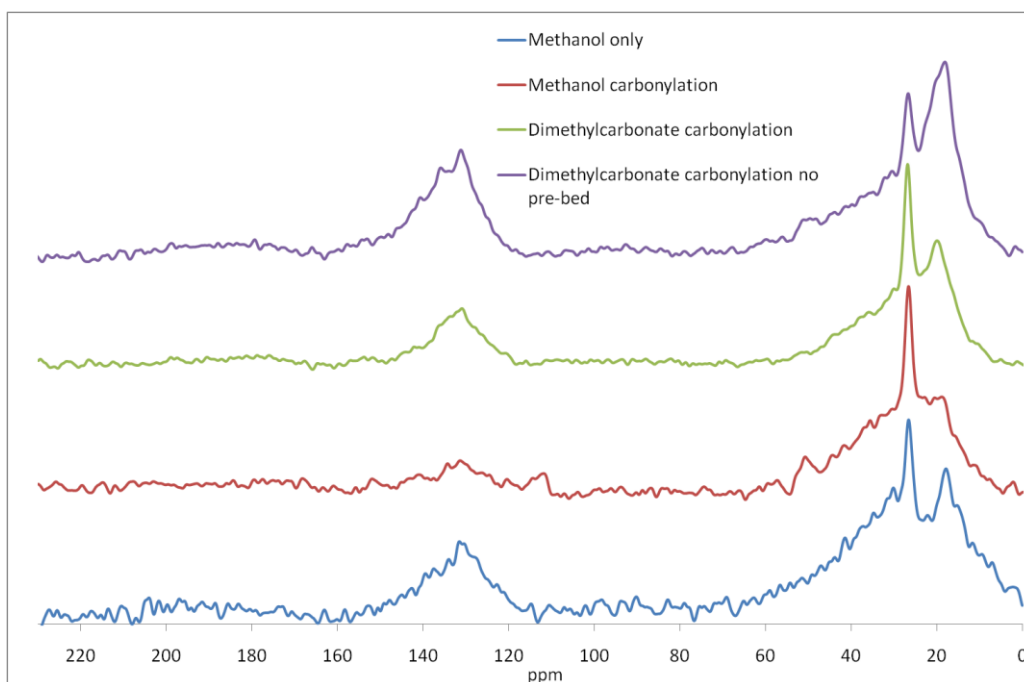


Figure 6.1.1: ^{13}C CP MAS NMR spectra of coked mordenite generated with different feedstreams at 250°C for 300 minutes.

250°C reaction	Cwt%	H:C ratio
Methanol-only	11.61	1.68
Methanol carbonylation	8.25	2.34
Dimethylcarbonate carbonylation with pre-bed	8.05	2.28
Dimethylcarbonate carbonylation no pre-bed	9.15	1.90

Table 6.1.1: Carbon contents and H:C ratios of coked mordenite generated with different feedstreams at 250°C for 300 minutes.

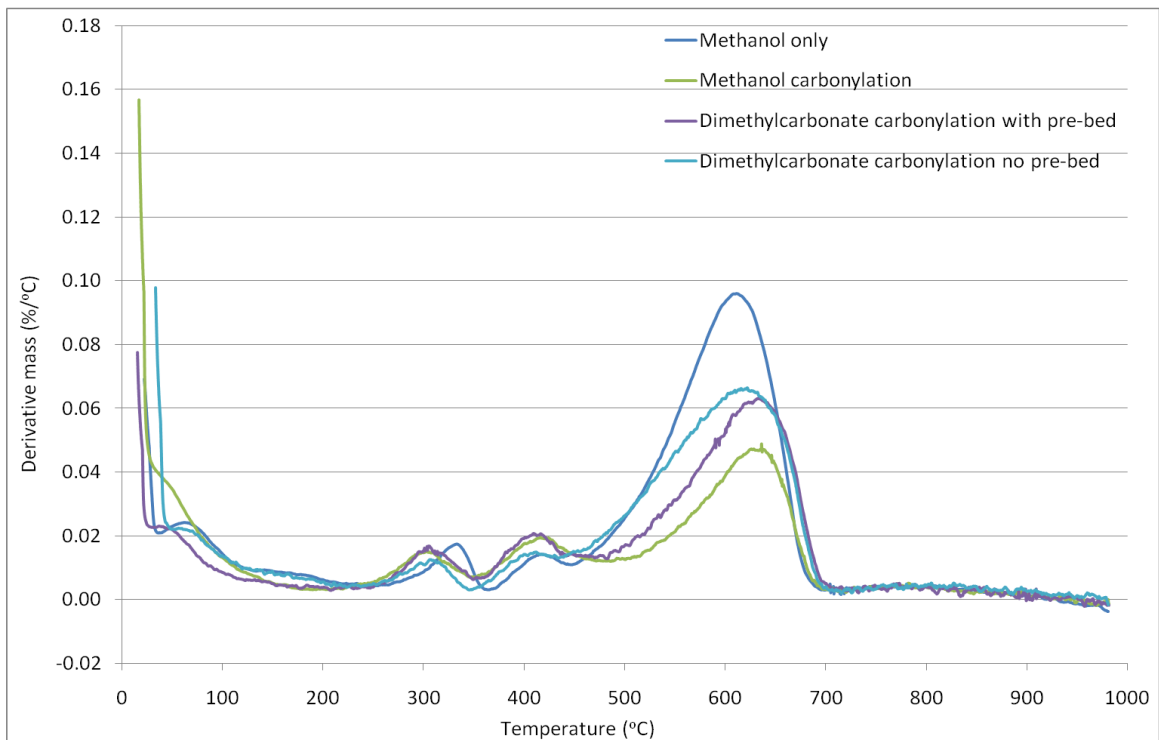


Figure 6.1.2: First derivative TGA profiles attained under air of coked mordenite generated with different feedstreams at 250°C for 300 minutes.

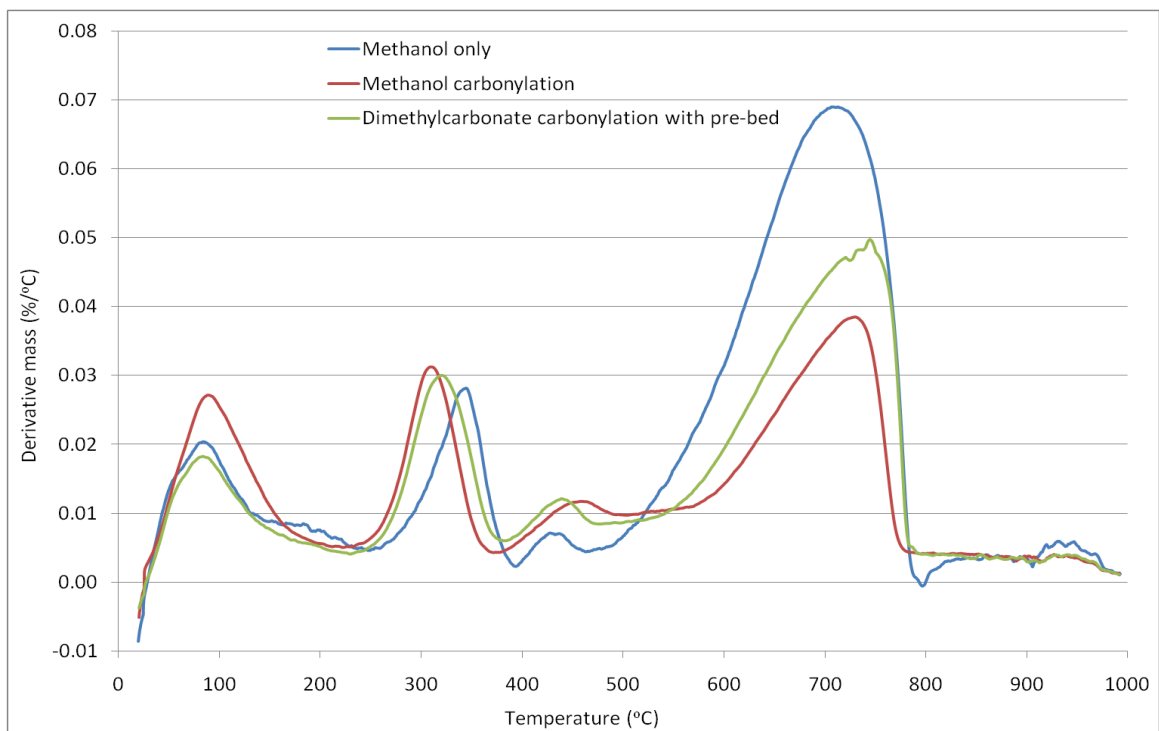


Figure 6.1.3: First derivative TGA profiles attained under 2% O₂/Ar of coked mordenite generated with different feedstreams at different 250°C for 300 minutes.

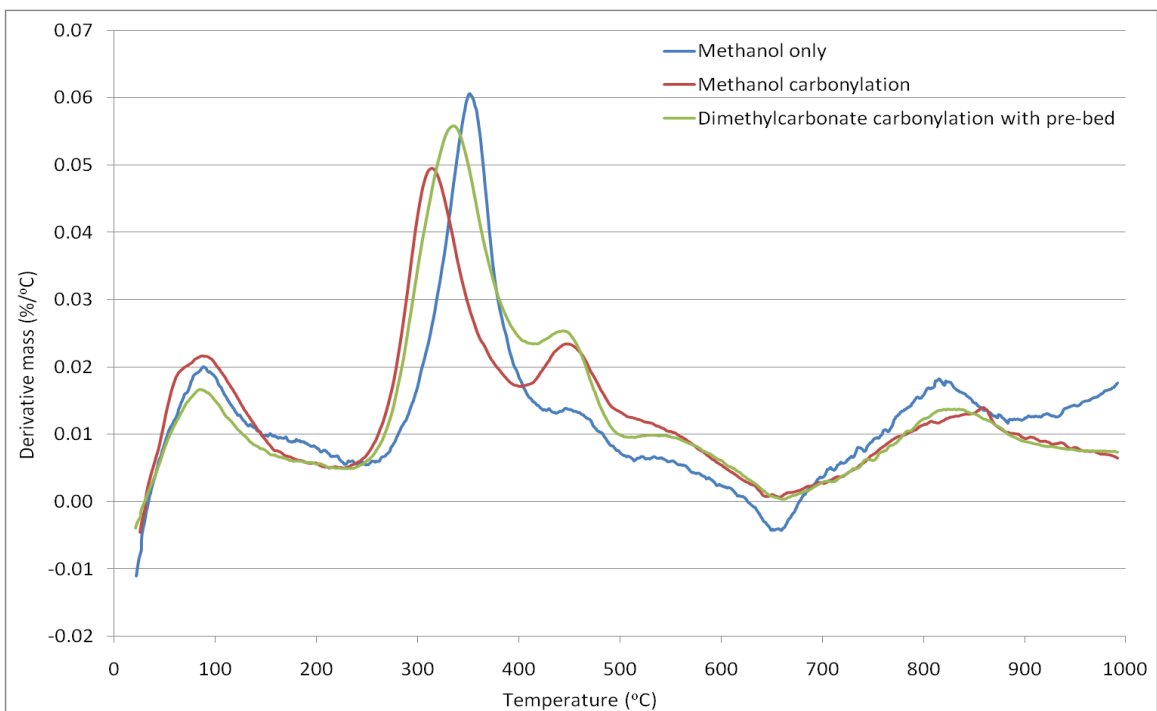


Figure 6.1.4: First derivative TGA profiles attained under argon of coked mordenite generated with different feedstreams at 250°C for 300 minutes.

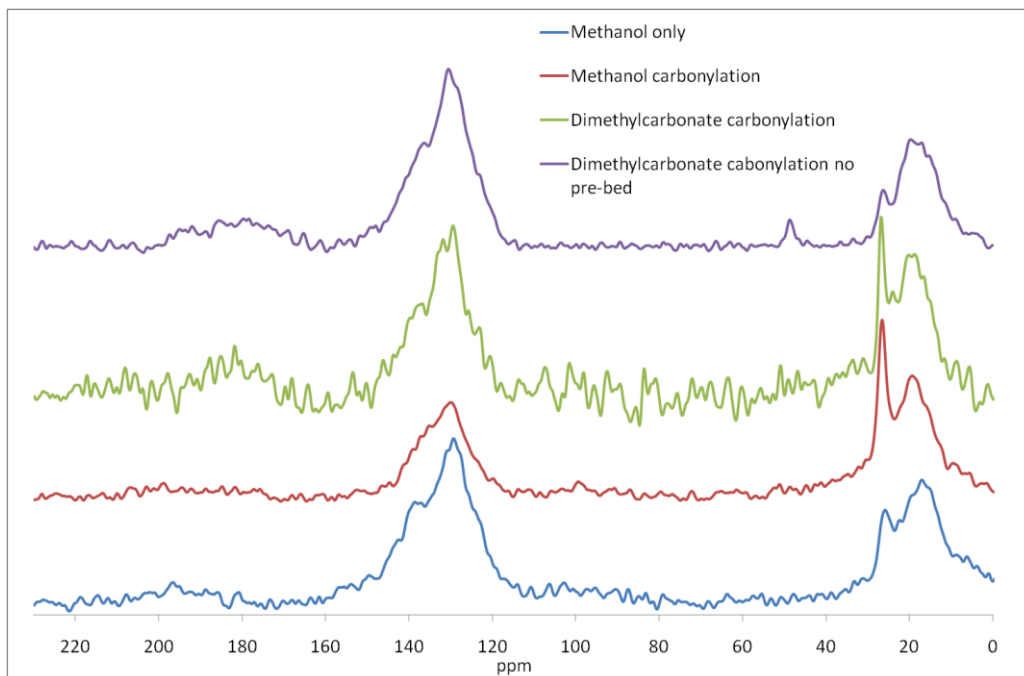


Figure 6.1.5: ^{13}C CP MAS NMR spectra of coked mordenite generated with different feedstreams at 300°C for 300 minutes.

300°C reaction	Cwt%	H:C ratio
Methanol-only	12.61	1.24
Methanol carbonylation	9.55	1.81
Dimethylcarbonate carbonylation with pre-bed	9.65	1.74
Dimethylcarbonate carbonylation no pre-bed	10.50	1.42

Table 6.1.2: Carbon contents and H:C ratios of coked mordenite generated with different feedstreams at 300°C for 300 minutes.

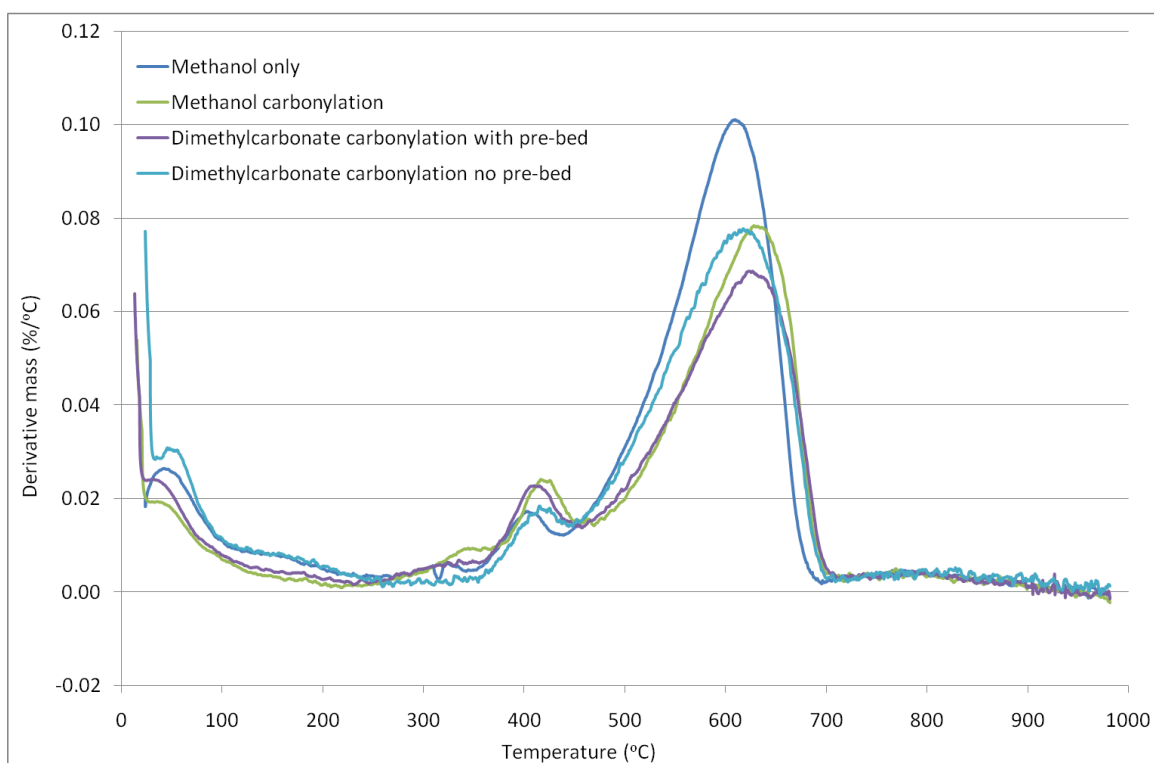


Figure 6.1.6: First derivative TGA profiles attained under air of coked mordenite generated with different feedstreams at 300°C for 300 minutes.

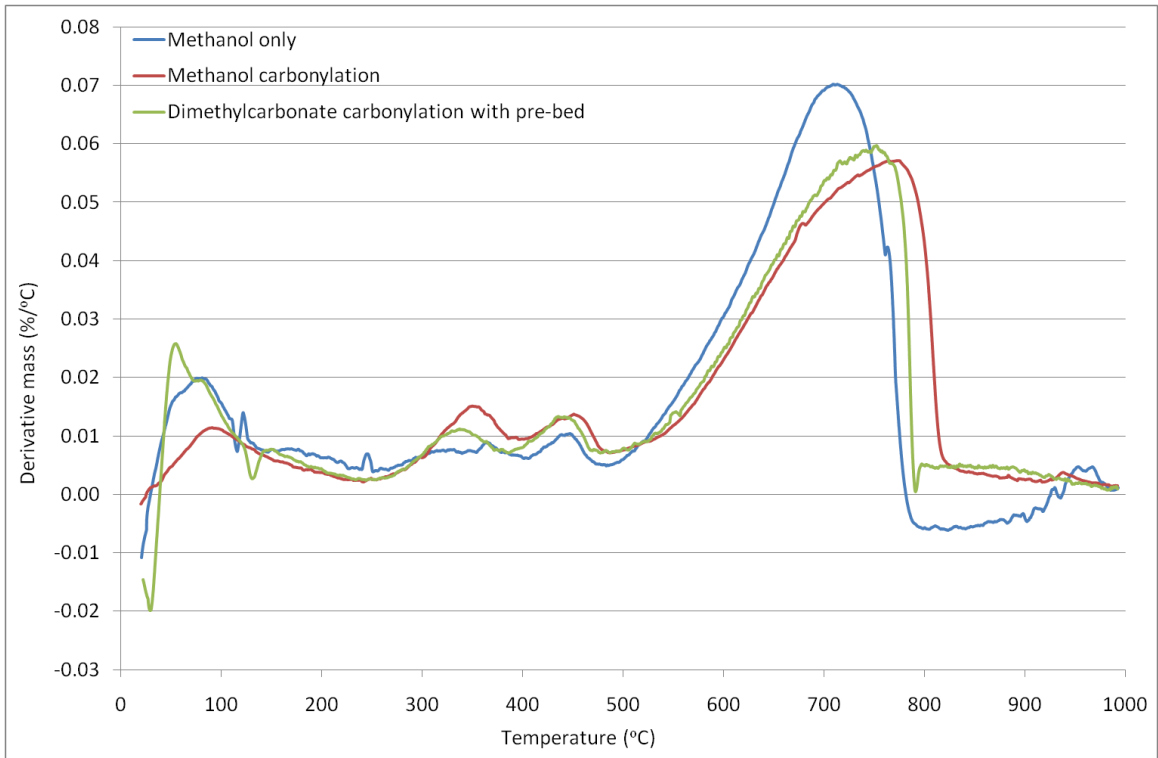


Figure 6.1.7: First derivative TGA profiles attained under 2% O₂/Ar of coked mordenite generated with different feedstreams at different 300°C for 300 minutes.

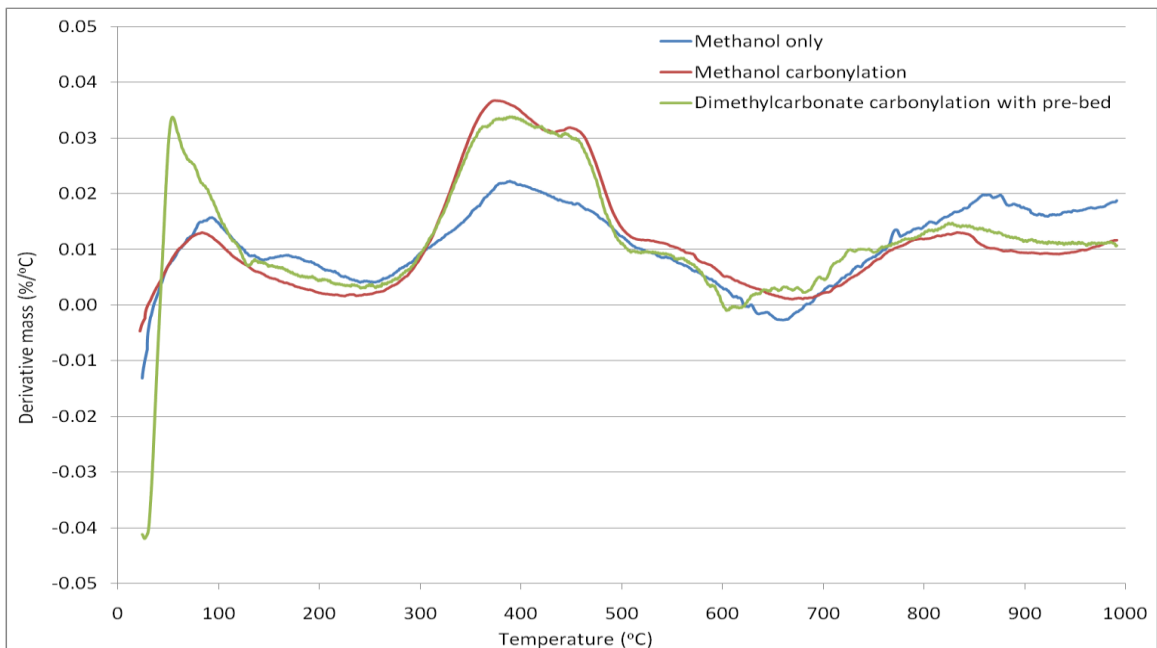


Figure 6.1.8: First derivative TGA profiles attained under argon of coked mordenite generated with different feedstreams at 300°C for 300 minutes.

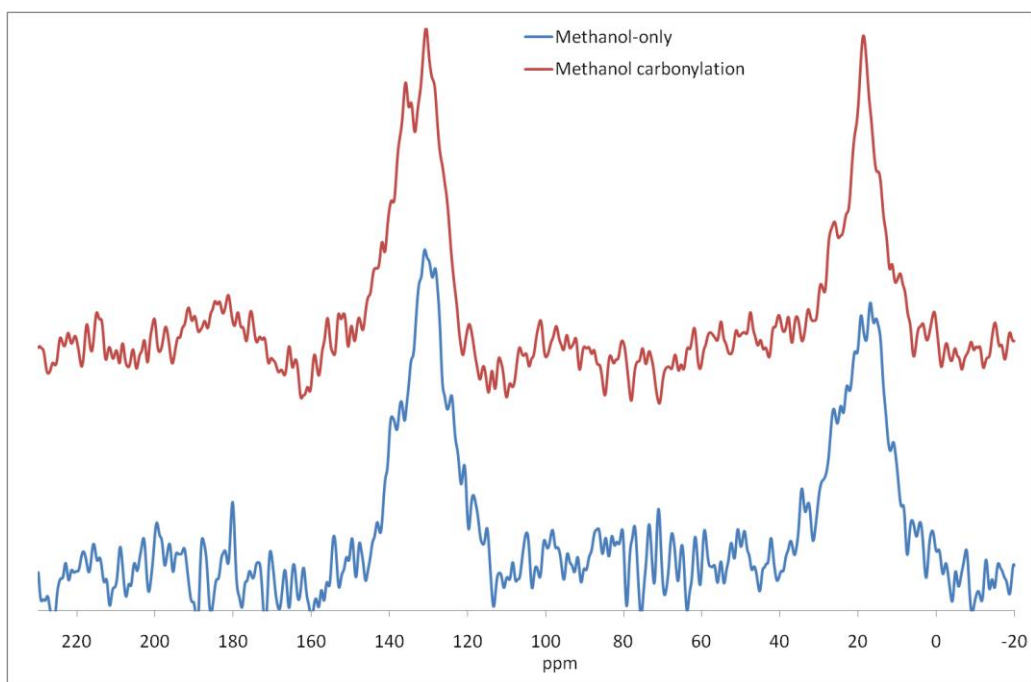


Figure 6.1.9: ^{13}C CP MAS NMR spectrum of coked mordenite generated with methanol containing feedstreams at 300°C for 60 minutes.

60 minute reaction	Cwt%	H:C ratio
Methanol-only	10.82	1.54
Methanol carbonylation	6.85	2.01

Table 6.1.3: Carbon contents and H:C ratios of coked mordenite generated with methanol containing feedstreams at 300°C for 60 minutes.

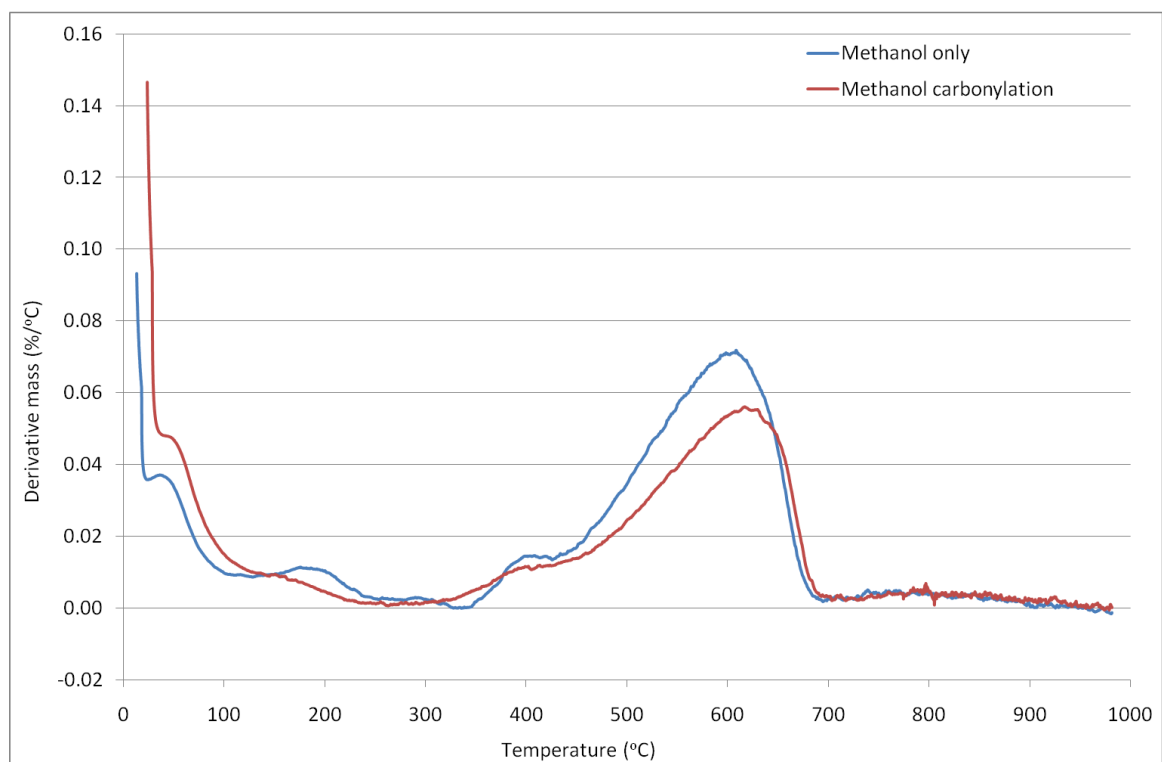


Figure 6.1.10: First derivative TGA profiles attained under air of coked mordenite generated with methanol containing feedstreams at 300°C for 60 minutes.

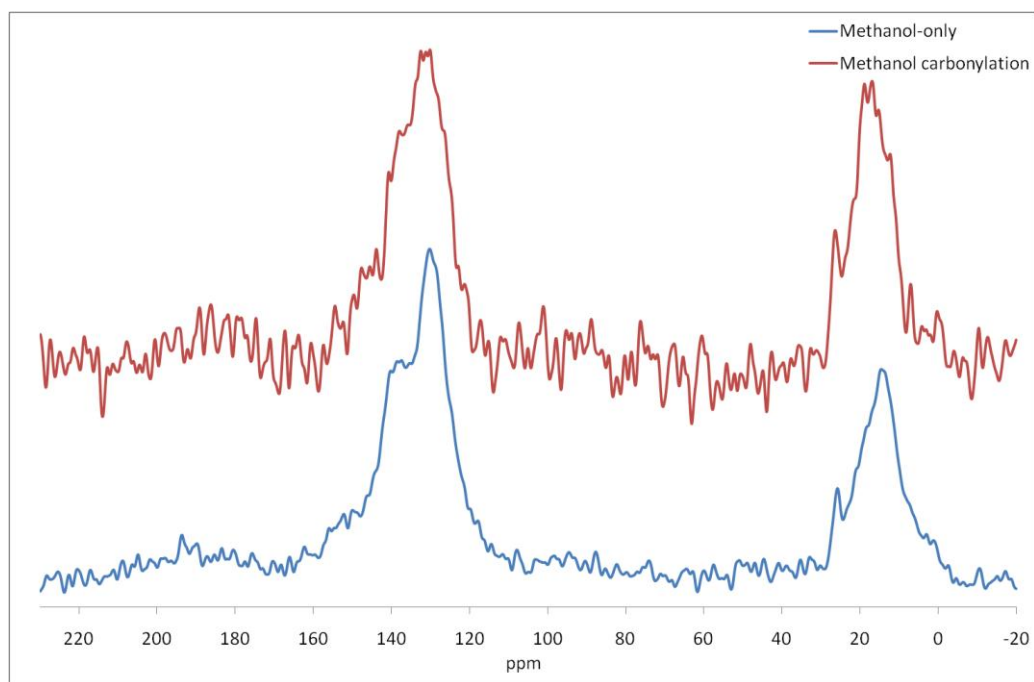


Figure 6.1.11: ^{13}C CP MAS NMR spectrum of coked mordenite generated with methanol containing feedstreams at 300°C for 180 minutes.

180 minute reaction	Cwt%	H:C ratio
Methanol-only	12.94	1.14
Methanol carbonylation	9.45	1.65

Table 6.1.4: Carbon contents and H:C ratios of coked mordenite generated with methanol containing feedstreams at 300°C for 180 minutes.

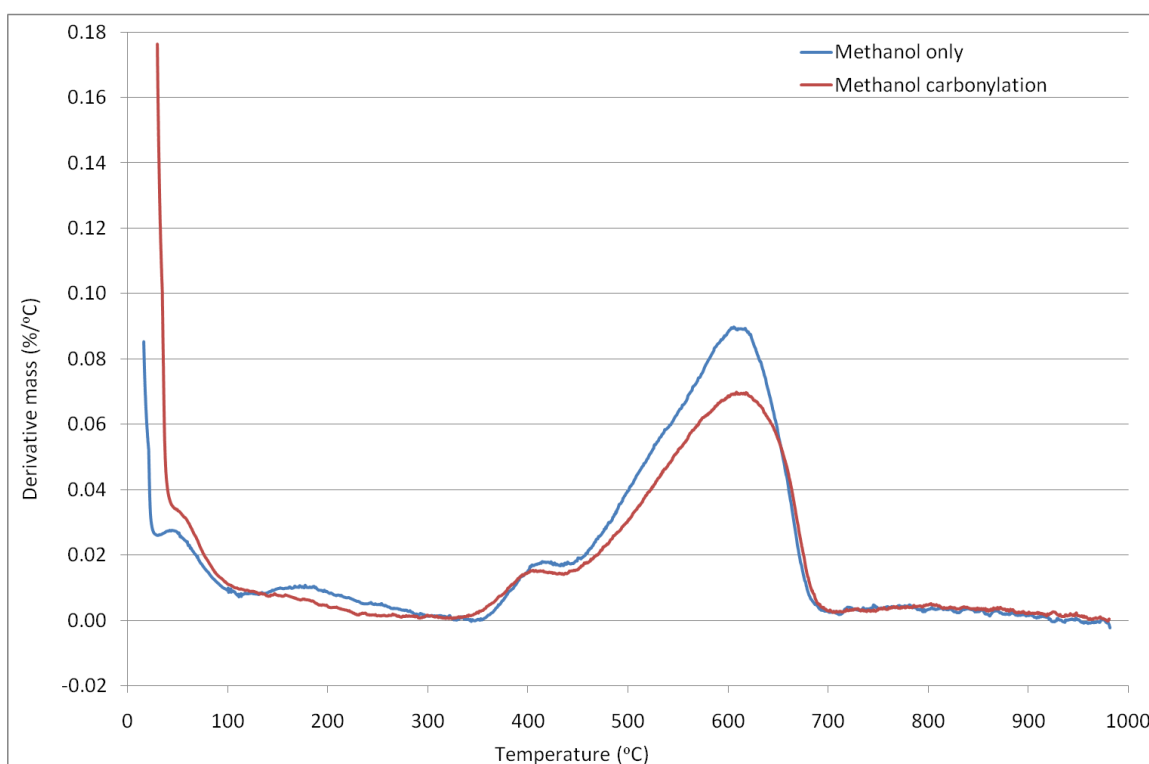


Figure 6.1.12: First derivative TGA profiles attained under air of coked mordenite generated with methanol containing feedstreams at 300°C for 180 minutes.

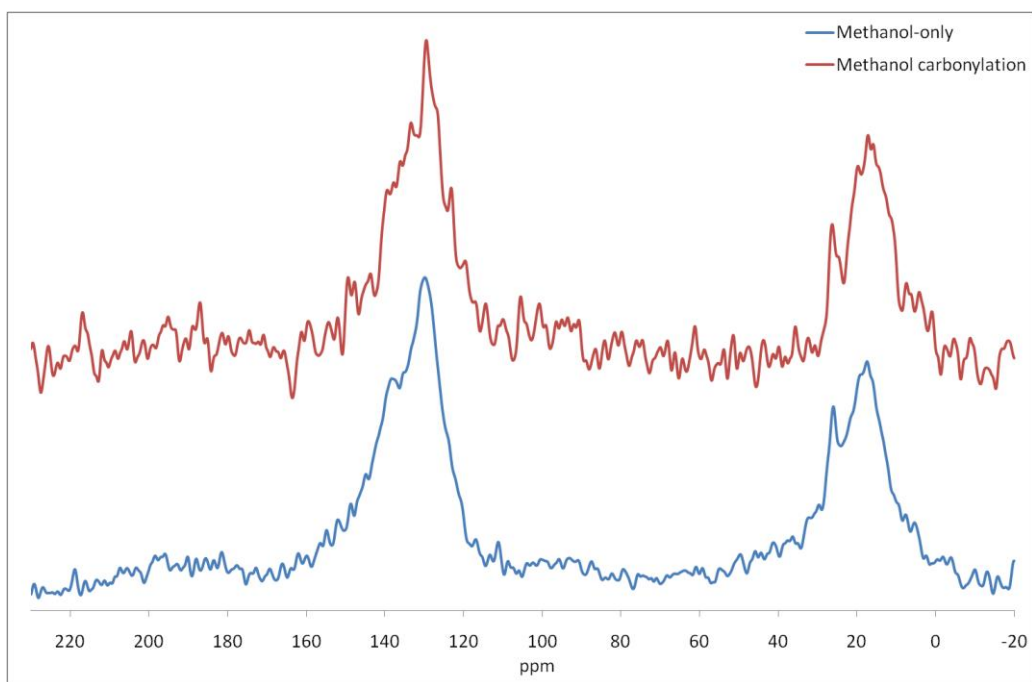


Figure 6.1.13: ^{13}C CP MAS NMR spectrum of coked mordenite generated with methanol containing feedstreams at 300°C for 420 minutes.

420 minute reaction	Cwt%	H:C ratio
Methanol only	12.02	1.32
Methanol carbonylation	10.65	1.36

Table 6.1.5: Carbon contents and H:C ratios of coked mordenite generated with methanol containing feedstreams at 300°C for 420 minutes.

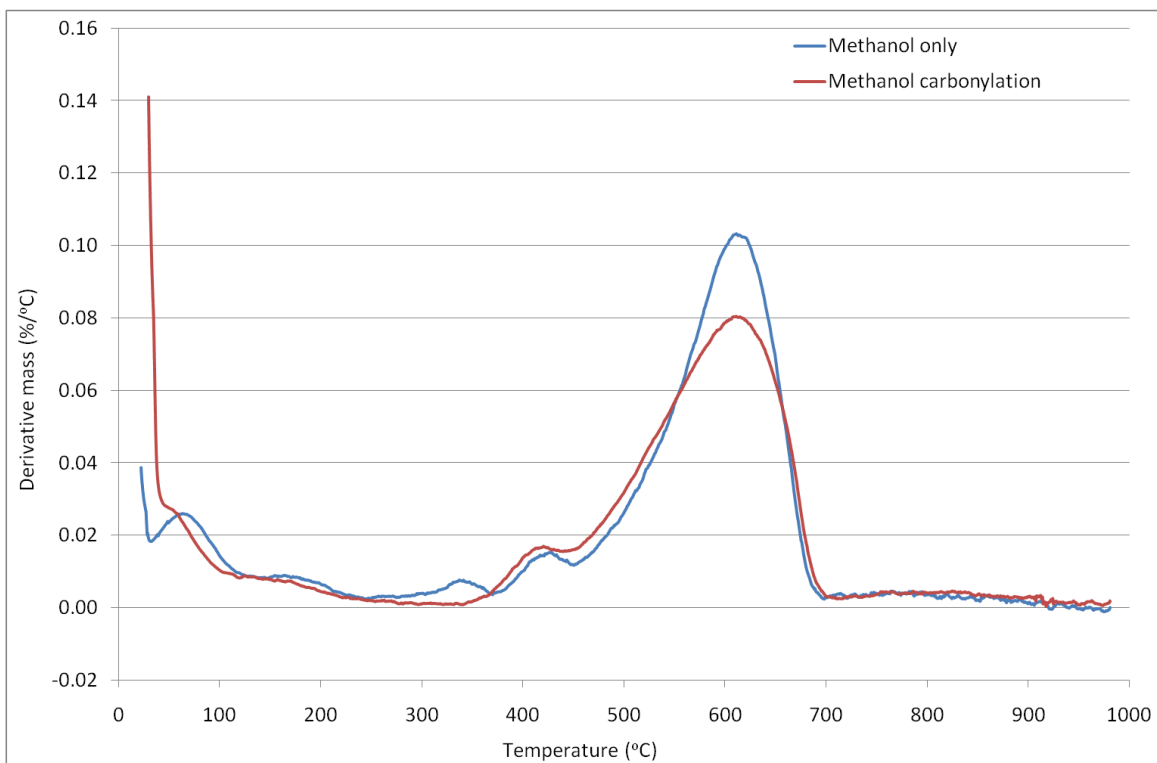


Figure 6.1.14: First derivative TGA profiles attained under air of coked mordenite generated with methanol containing feedstreams at 300°C for 420 minutes.

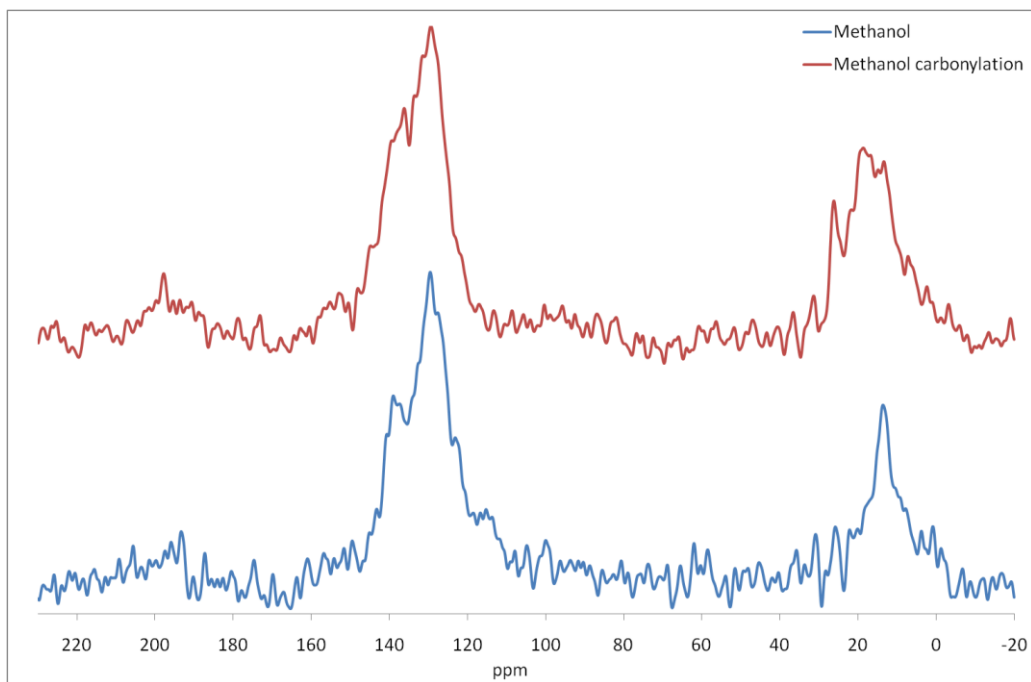


Figure 6.1.15: ^{13}C CP MAS NMR spectrum of coked mordenite generated with methanol containing feedstreams at 300°C for 600 minutes.

600 minute reaction	Cwt%	H:C ratio
Methanol to Hydrocarbons	15.64	0.99
Methanol carbonylation	11.00	1.30

Table 6.1.6: Carbon contents and H:C ratios of coked mordenite generated with methanol containing feedstreams at 300°C for 600 minutes.

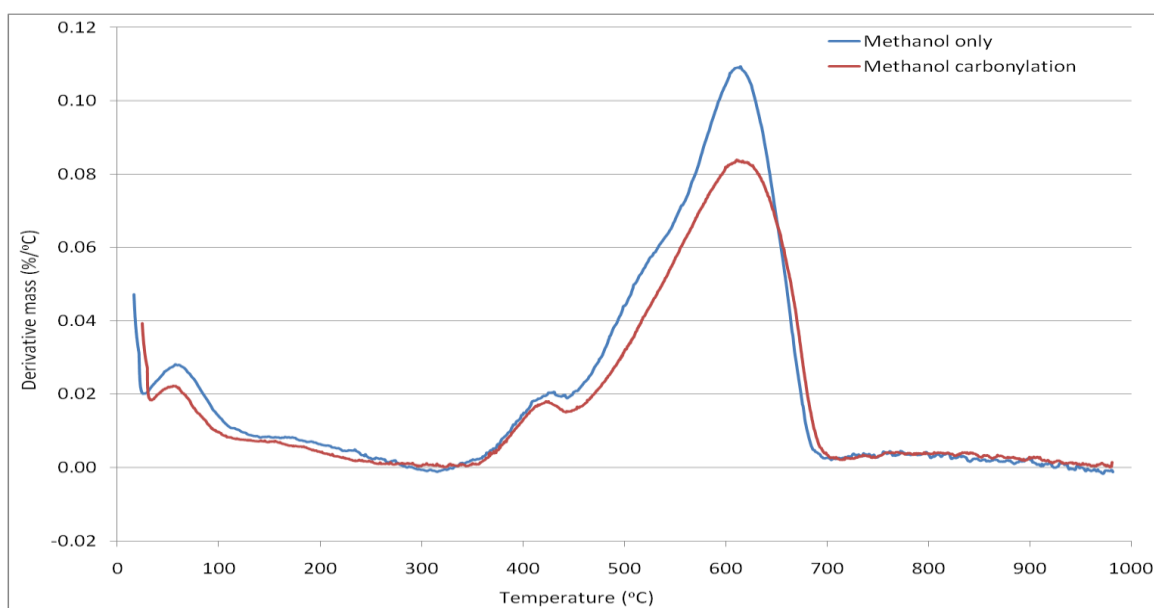


Figure 6.1.16: First derivative TGA profiles attained under air of coked mordenite generated with methanol containing feedstreams at 300°C for 600 minutes.

6.2 Preliminary further work

6.2.1 Steaming of coked mordenite

On the basis of removal of carbonaceous deposits, experiments were designed to examine the use of a water saturated argon feedstream as a potential removal technique. As such experiments using coked samples generated with a methanol-only feedstream at 300°C for 300 minutes were examined. Two steaming temperatures were employed 350 and 750°C using 60 ml min⁻¹ of argon for 18 hours.

Reaction	Post-reaction C wt%	Post-350°C steaming C wt%	Post-750°C steaming C wt%
300°C methanol-only	12.52	10.21	0.46

Table 6.2.1: Carbon contents of coked mordenite generated with methanol at 300°C for 300 minutes prior to and post-steaming at different temperatures for 18 hours.

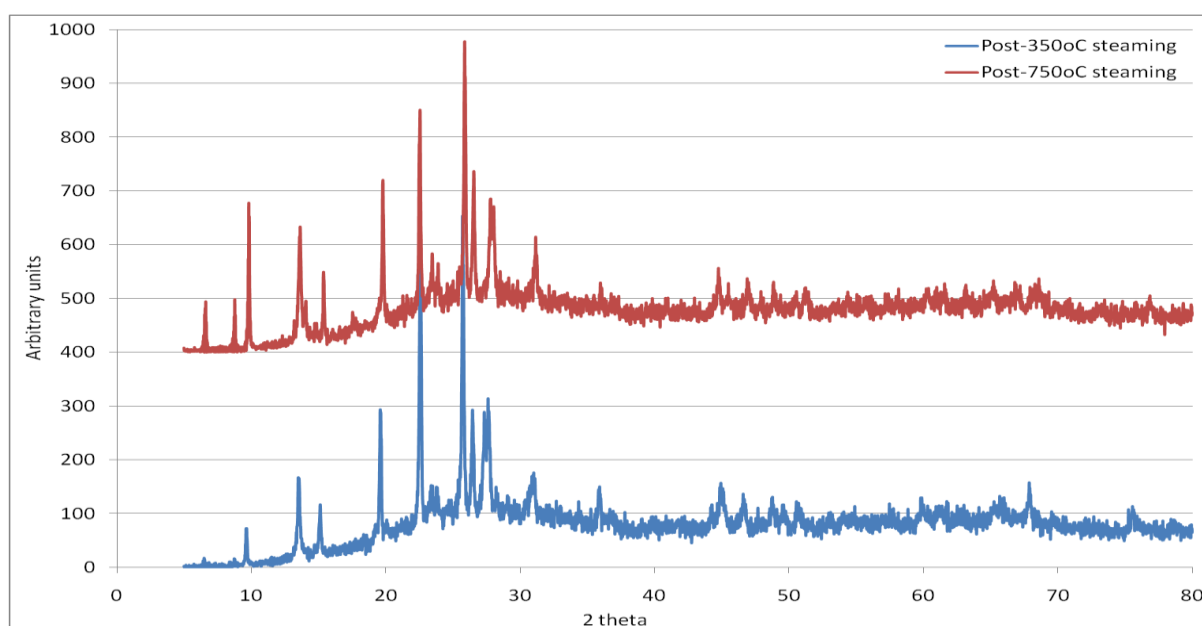


Figure 6.2.1: XRD patterns of coked mordenite generated with methanol at 300°C for 300 minutes post-steaming at different temperatures for 18 hours.

It can be observed in Table 6.2.1 that a small portion of the carbonaceous deposits are removed at 350°C. After treatment at 750°C most of the deposit is removed though a relatively small fraction still remains. Figure 6.2.1 shows that the framework is still intact for both mordenite samples after steaming treatment regardless of temperature. The observed background is an effect caused by the sample holder employed in this study.

6.2.2 TGA employing dilute H₂ and H₂/CO atmospheres

It has been observed that the use of oxygen for the removal of coke destroys the framework, therefore TGA experiments employing gases that can potentially remove coke endothermically were proposed. As the carbonylation feedstream consists of carbon monoxide and hydrogen (4:1 respectively) preliminary TGA investigations employing dilute hydrogen (5% H₂/N₂) and a dilute syn gas mixture (1:1:98, CO:H₂:Ar) at 50 ml min⁻¹, were undertaken to probe the reactivity of the carbonaceous deposits under hydrogen containing atmospheres for materials generated with a methanol only feedstream at 300°C for 300 minutes respectively. They were run from 20°C-1000°C at a ramp rate of 1°C min⁻¹.

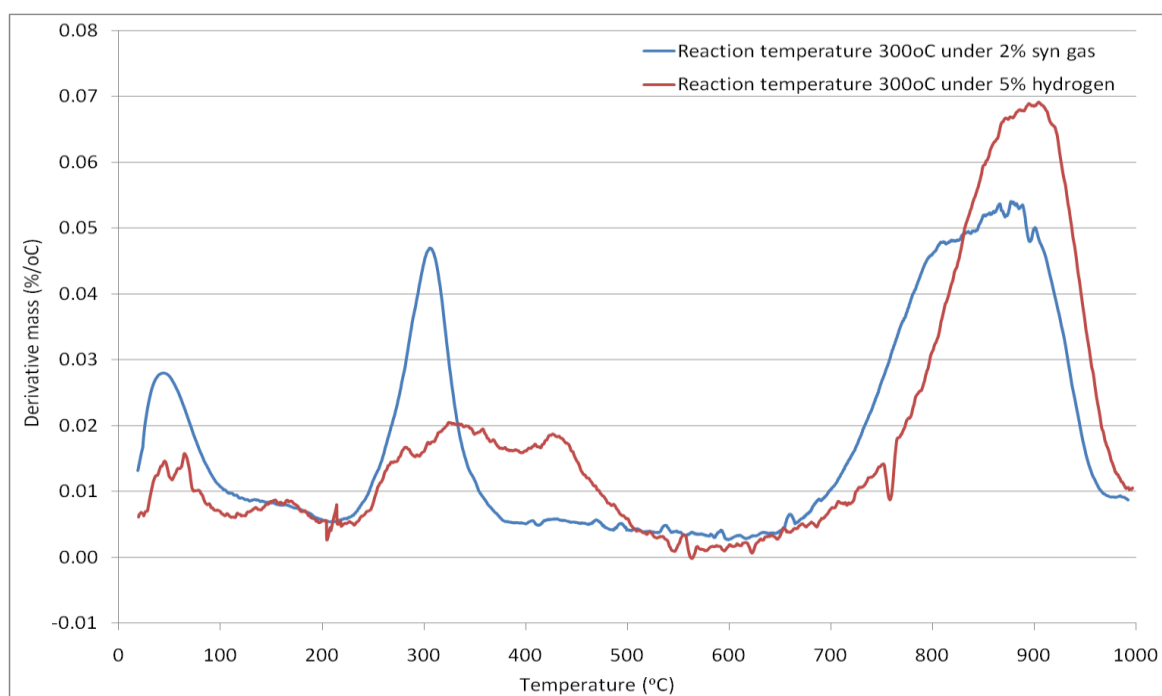


Figure 6.2.2: First derivative TGA profiles attained under 2% syn gas and 5% hydrogen of coked mordenite generated with methanol containing feedstreams at 300°C for 300 minutes.

Preliminary results observed in Figure 6.2.2 show the first derivative TGA profiles for sample generated at 300°C. It can be observed that under a dilute hydrogen atmosphere that the sample exhibits a broad feature at *ca.* 375°C is similar to that observed under an argon only atmosphere. Under a hydrogen atmosphere the large feature observed under an air atmosphere at approximately 625°C has shifted to higher temperatures. Applying the syn gas atmosphere the broad signal observed previously is now a relatively sharp feature around 300°C which is the temperature in which the sample was generated. The broad feature observed at high temperature under dilute hydrogen has shifted to a slightly lower temperature under the dilute syn gas.

The preliminary work detailed above offers some rather interesting alternatives to treatment methods for coked materials. With further development of the steaming experiments and TGA experiments detailed within, a potential multi-stage regeneration model could be developed for materials coked with methanol based feedstreams.

6.3 Future work

The results of this project demonstrate that carbonaceous deposits formed over mordenite at shorter times on stream (10 hours or less) are very similar in nature regardless of the feed employed. It would therefore be rather interesting to examine if the deposited carbonaceous species deviates above 10 hours on stream.

It was observed when employing a methanol only atmosphere that reaction temperatures 250-350°C exhibited some very interesting moderate temperature features in TGA investigations. Examination of this temperature range from 225-375°C in 25°C increments may reveal previously unobserved features.

As experiments were performed under methanol only, dimethylcarbonate only and mixed carbonylation feedstreams, experiments probing the effect of methanol with carbon monoxide and methanol with hydrogen would be of interest in an attempt to understand the individual role these gases play in the development of the carbonaceous deposits.

The experiments were undertaken at atmospheric pressure, which in reality doesn't model the conditions that the working mordenite may see in carbonylation experiments. Therefore it

could be of interest to examine the effect on the carbonaceous deposits caused by increasing pressure from ambient to 30 bar.

Further investigations into the relevance of the effect of impurities such as acetone should be considered for both methanol only and mixed feedstreams.

References

[1] B. Ellis, M. Howard, R. Joyner, N. Reddy, M. Padley, W. Smith *Studies in Surface Science and Catalysis* 101 (1996) 771

7 Appendices

7.1 Reproducibility

The carbon content (wt%) and H:C data presented throughout this thesis are mean values based upon duplicate samples (in most cases two samples in others as many as five). The reproducibility of the data sets are displayed as follows where (value = the value furthest out from the mean value).

$$100 \pm \left(\left(\frac{\text{Mean value} - \text{Value}}{\text{Mean value}} \right) * 100 \right)$$

7.2 Mass spectrometry fragments

Product	m/z	m/z	m/z
Hydrogen	2	-	-
Water	17	18	-
Carbon monoxide	16	28	-
Carbon dioxide	16	28	44
Methane	15	16	-
Ethene	26	27	28
Ethane	27	28	30
Propene	39	41	42
Propane	27	28	29
Butene	39	41	56
Butane	22	29	43
Benzene	77	78	-
Ammonia	15	16	17
Dimethyl ether	45	26	-

The mass spectrometry data was interpreted based upon the above fragments for each corresponding product.

7.3 Supplementary information

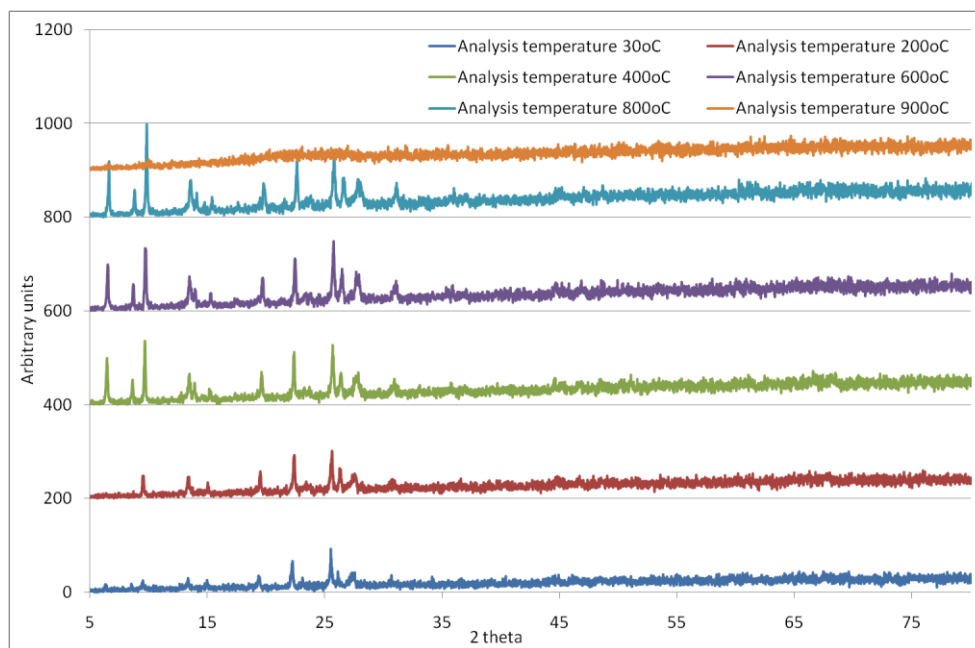


Figure 7.3.1: Variable temperature XRD analysis from 30°C - 900°C (10°C min⁻¹ ramp rate) under 2% O₂/Ar of coked mordenite generated under methanol carbonylation conditions at 300°C for 360 minutes reaction time.